

Transcriptomic and functional genomics of russeting on apple

Von der Naturwissenschaftlichen Fakultät der
Gottfried Wilhelm Leibniz Universität Hannover

zur Erlangung des Grades
Doktor der Naturwissenschaften (Dr. rer. nat.)

genehmigte Dissertation

von

Jannis Straube, M. Sc.

2023

Referent: Prof. Dr. rer. nat. Thomas Debener

Korreferent: Prof. Dr. agr. Moritz Knoche

Tag der Promotion: 22.09.2023

Abstract

Russetting is a common, economically important fruit skin disorder that occurs in many fruit crops, including apples (*Malus x domestica*, Borkh.). This skin disorder is caused by environmental factors such as high humidity, prolonged periods of surface moisture, and wounding. While previous studies have focused on the later stages of russetting, the initiation sequence of this disorder remains unclear. To address this knowledge gap, this dissertation aimed to: (1) establish an induction system for russetting in apple fruit using prolonged periods of surface moisture, (2) determine the sequence of russet formation on a histological level under prolonged periods of surface moisture, (3) investigate the behavior of candidate genes involved in periderm and cuticle-related processes on the gene expression as well as metabolic changes, (4) compare the sequence of wound- and moisture-induced russetting, (5) provide a transcriptomic resource for the initial processes during russet formation in apples, and (6) to provide preliminary data on potential candidate genes involved in russetting.

Application of surface moisture using a fixed polyethylene tube to developing apple fruit was found to induce microcracks in the fruit skin during early fruit development, and an increase in water vapor permeance was observed in microcracked compared to non-microcracked fruit skins. Microcracked fruit surfaces developed russetting. Histological, gene expression, and metabolic analyses revealed a biphasic behavior during the formation of russetting in response to surface moisture. In Phase I, microcracks appeared within 2 d of moisture treatment and expanded over time, accompanied by a decrease in cuticle-related genes and cutin- and wax-specific metabolites. In Phase II, microcracking decreased after moisture removal, and periderm formation was observed starting 4 d after moisture removal, accompanied by an increase in periderm related genes and suberin specific metabolites. Russetting was observed during Phase II only after at least 6 d of moisture exposure in Phase I. Histological, gene expression, and metabolic analyses showed that the sequence of russetting initiation during Phase II induced by surface moisture was similar to that induced by skin wounding. Transcriptomic analyses revealed that Phase I was characterized by a decrease in cell cycle, cell wall, and cuticle-related genes and an increase in stress-related genes, whereas Phase II was characterized by an increase in meristematic activity, followed by an increase in abscisic acid, lignin, and suberin-related genes.

Overall, the studies of this dissertation provide for the first time information on the initial processes of russetting in apple fruit skin and are a valuable resource for future research on the molecular mechanisms underlying this phenomenon.

Keywords: *Malus x domestica*, russet, periderm, cuticle, fruit skin, transcriptomics, histology, suberin, cutin, wax, lignin

Zusammenfassung

Berostung ist eine weitverbreitete, wirtschaftlich wichtige Fruchthauterkrankung vieler Obstarten, darunter auch bei Äpfeln (*Malus x domestica*, Borkh.). Berostung wird durch Umweltfaktoren wie hohe Luftfeuchtigkeit, längere Perioden von Oberflächenfeuchtigkeit und Verwundung verursacht. Während vorangegangene Studien Prozesse während späteren Stadien der Berostung analysiert haben, ist die Entstehungssequenz dieser Erkrankung nach wie vor unklar. Um diese Wissenslücke zu schließen, hatte diese Dissertation folgende Ziele: (1) ein Induktionssystem für die Berostung an Apfelfrüchten unter Verwendung von Oberflächenfeuchtigkeit zu etablieren, (2) die Sequenz der durch Oberflächenfeuchtigkeit entstehenden Berostung auf histologischer Ebene, (3) sowie auf Genexpressionsebene und Stoffwechselebene zu untersuchen, (4) die Abfolge von wund- und feuchtigkeitsinduzierter Berostung zu vergleichen, (5) eine transkriptomische Ressource für die anfänglichen Prozesse während der Berostungsbildung bei Äpfeln bereitzustellen und (6) vorläufige Daten hinsichtlich der funktionellen Charakterisierung von potentiellen Kandidatengenen zu zeigen.

Es wurde festgestellt, dass die Anwendung von Oberflächenfeuchtigkeit mit Hilfe eines fixierten Polyethylengefäßes auf sich entwickelnde Apfelfrüchte während der frühen Fruchtentwicklung Mikrorisse in der Fruchtschale hervorruft. Mikrorissige Fruchtschalen zeigten eine erhöhte Wasserdampfdurchlässigkeit im Vergleich zu intakten Fruchtschalen. Mikrorissige Früchte entwickelten Berostung. Die Reaktion auf Oberflächenfeuchtigkeit verlief in zwei Phasen. In Phase I traten Mikrorisse innerhalb von 2 Tagen auf, begleitet von einer Verringerung der Genexpression und Metaboliten, die mit der Cuticula in Verbindung stehen. In Phase II verringerten sich die Mikrorisse nach dem Entfernen der Feuchtigkeit und es bildete ein Periderm, begleitet von einer erhöhten Expression von Periderm assoziierten Genen und Metaboliten. Die Berostung trat erst nach mindestens 6 Tagen Feuchtigkeitseinwirkung in Phase I auf. Die Sequenz der Berostung in Phase II, die durch Oberflächenfeuchtigkeit verursacht wurde, ist dieselbe wie nach Verwundung. Die transkriptomische Analyse ergab, dass die Phase I durch eine Abnahme der Expression von Zellzyklus-, Zellwand- und Cuticula-assoziierten Genen und einen Anstieg der stressbezogenen Gene gekennzeichnet war, während Phase II durch einen Anstieg der meristematischen Aktivität, gefolgt von einem Anstieg der Abscisinsäure-, Lignin- und Suberin-assoziierte Gene, gekennzeichnet war.

Zusammenfassend liefern die Studien dieser Dissertation erstmals Einblicke in die anfänglichen Prozesse der Berostung in Apfelfrüchten und dient als wertvolle Ressource für zukünftige Forschungen zu den zugrunde liegenden molekularen Mechanismen.

Schlagwörter: *Malus x domestica*, Berostung, Periderm, Cuticula, Fruchtoberfläche, Transkriptomik, Histologie, Suberin, Cutin, Wachs, Lignin

Content

Abstract	I
Zusammenfassung	II
Content	III
Abbreviations	V
1. General introduction	1
1.1. Russeting: A significant fruit skin disorder	1
1.2. The molecular basis of plant cuticle structure and synthesis	4
1.3. Molecular processes in periderm formation	8
1.4. Genetic and metabolic factors associated with russeting in apple	16
1.5. Transcriptomics in horticultural crops with a focus on apple	17
1.6. Objectives	19
2. Surface moisture increases microcracking and water vapour permeance of apple fruit skin	20
3. Russeting in apple is initiated after exposure to moisture ends—I. Histological evidence	30
3.1. Supplementary data Chapter 3.....	49
4. Russeting in apple is initiated after exposure to moisture ends. Molecular and biochemical evidence	50
4.1. Supplementary data Chapter 4.....	74
5. Apple fruit periderms (russeting) induced by wounding or by moisture have the same histologies, chemistries and gene expressions	79
5.1. Supplementary data Chapter 5.....	100
6. Time course of changes in the transcriptome during russet induction in apple fruit	102
6.1 Supplementary data Chapter 6.....	122
7. Functional analysis of candidate genes potentially involved in apple fruit russeting	141
7.1 Supplementary data Chapter 7.....	159
8. General discussion	162
8.1. Russet induction: Exploring opportunities for future study and advancement	163
8.1.1. Uncovering the mechanisms behind russet induction: Insights from Phase I studies and future perspectives	163
8.1.2. Unraveling the mechanism of russet induction in Phase II: Insights into the underlying processes	165
8.2. Advancing functional characterization models for russeting in apple	167
8.3. Conclusion	169
References	170

Electronic appendix	205
Acknowledgements	207
<i>Curriculum vitae</i>	208
List of publications	209

Abbreviations

A

AA1	ABA Antagonist1
ABA	abscisic acid
ABC	ATP-binding cassette
ARF	auxin responsive factors
ASFT	aliphatic suberin feruloyl-transfere

B

BP	bark of the trunk
BDG	BODYGUARD

C

CCoAOMT	caffeoyl-CoA-O-methyltransferase
cDNA	complementary DNA
CDS	coding sequence
C3'H	<i>p</i> -coumaroyl-quinat/shikimate 3'-hydroxylase
CER	ECERIFERUM
CL	cuticle layer
CLE	clavate 3 (CLV3)/embryo surrounding region (ESR)-related
CM	cuticular membranes
CO	complementation
CoA	coenzyme A
COMT	caffeic acid O-methyltransferase
CP	cuticle proper
CUS	cutin synthase
CYPs	cytochrome P450
C4H	cinnamate 4-hydroxylase
C757	C757pGFPU10-35s-ocs-LH

D

DAFB	days after full bloom
DEG	differentially expressed gene
DFG	German Research Foundation
DNA	deoxyribonucleic acid
GDSL	Gly-Asp-Ser-Leu
GELPs	GDSL-type esterase/lipase proteins

E

ECR	enoyl-CoA reductase
ER	endoplasmic reticulum
ES	epidermal skin samples
ESTs	expressed sequence tags

F

FAE	fatty acid elongation complex
FAR	fatty acid reductase
FDR	false discovery rate
F5H	ferulate 5-hydroxylase
FHT	fatty ω -hydroxyacid/fatty alcohol hydroxycinnamoyl transferase
4CL	4-coumarate-CoA ligase

G

GC-MS	gas chromatography–mass spectrometry
GDR	Genome Database for <i>Rosaceae</i>
GFP	green fluorescent protein
GPAT	glycerol-3-phosphate acyltransferase

H

HCD	β -hydroxyacyl-CoA dehydratase
HCT	hydroxycinnamoyl-CoA transferase

K

KCR	β -ketoacyl-CoA reductase
KCS	β -ketoacyl-CoA synthase
KNAT	KNOTTED-like from <i>Arabidopsis thaliana</i>

L

LACS	long-chain acyl-CoA synthetases
LCFA	long-chain fatty acids
LCFA-CoA	long-chain fatty acyl-CoA
lncRNA-Seq	long non-coding RNA sequencing
LOB	LOB domain-containing protein
log ₂ FC	log ₂ Fold Change
LTP	lipid transfer protein

M

microcracks	microscopic cracks
MYB	myeloblastosis

N

ANAC/NAC	NAC domain containing protein
nd	not detected
NGS	next-generation sequencing

O

OE	over expression
----	-----------------

P

PM	periderm membranes
PPO	polyphenol oxidase
PS	peridermal skin samples
PTL	Petal loss
PXI	phloem intercalated with xylem

Q

qPCR	quantitative real-time PCR
QTLs	quantitative trait loci

R

RAS	response to ABA and salt
RNA	ribonucleic acid
RNA-Seq	RNA sequencing

S

SAND	sand family protein
SHN	SHINE
SE	standard error
SEM	scanning electron microscopy
SPAD	suberin poly(aliphatic) domain
SPPD	suberin poly(phenolic) domain
SVP	short vegetative phase

T

TDIF	tracheary element differentiation inhibitory factor
TPM	transcripts per million

U

UK	uridylate kinase
----	------------------

V

VCS	vascular cambium-specific
VIGS	virus-induced gene silencing
VLCFAs	very long chain fatty acids
VLCFA-CoA	very long-chain fatty acyl-CoA

W

WGCNA	weighted correlation network analysis
WOX	WUSCHEL-related homeobox
WSD	wax ester synthase/acyl-coenzyme A: diacylglycerol acyltransferase

1. General introduction

The fruit skin is an important protective barrier that shields the inside of the fruit from various abiotic and biotic stresses during development. Apples (*Malus x domestica*, Borkh.), which are the third most produced fruit in the world (93 million tons in 2021), with China as the leading producer (46 million tons in 2021), are of immense economic importance (FAOSTAT, www.fao.org/faostat). The global market for apples and apple products is worth billions of dollars annually, with a wide range of value-added products such as apple juice and cider produced in addition to fresh apples. The *Rosaceae* family, to which apples belong, also includes other important fruit crops such as pear (*Pyrus communis*), cherry (*Prunus avium*), strawberry (*Fragaria x ananassa*), plum (*Prunus domestica*) and almond (*Prunus dulcis*).

However, in apple production, skin disorders such as skin spot (Grimm et al., 2012; Winkler et al., 2014), scarf skin (Byers, 1977), and russetting (Faust and Shear, 1972b) can have a significant economic impact on pre- and postharvest performance (Lara et al., 2014; Lara et al., 2019; Khanal et al., 2019; Fernández-Muñoz et al., 2022). While the exact causes of russetting are not fully understood, this dissertation will focus on investigating the initial steps that lead to the induction of russetting on apple fruit skins. Understanding the triggers of russetting is critical to mitigating its impact on fruit appearance and performance.

1.1. Russetting: A significant fruit skin disorder

Russetting, which refers to the replacement of the waxy cuticle by a corky periderm on fruit skins, is a common skin disorder in various fruits such as apples (Skene, 1982), grapes (Goffinet and Pearson, 1991), prunes (Michailides, 1991), pears (Scharwies et al., 2014), and mangoes (Athoo et al., 2020) (Figure 1A). Russetting is an economically important trait because it negatively affects postharvest performance and consumer appeal due to the dull unattractive appearance of brownish corky fruit skins. Russeted fruit surfaces have higher water vapour permeability compared to intact fruit surfaces covered by a cuticle, resulting in increased water loss and higher mass loss during storage (Khanal et al., 2019).

Russetting can result from biotic stressors such as mechanical wounding (Simons and Aubertin, 1959), pathogenic infections caused by fungi such as yeasts (Gildemacher et al., 2004; Gildemacher et al., 2006) and powdery mildew (Daines, 1984), viruses (Welsh and May, 1967; Wood, 1972; Li et al., 2020), or insect infestations such as mites (Easterbrook and Fuller, 1986; Duso et al., 2010). Abiotic stresses such as high humidity (Tukey, 1959; Knoche and Grimm, 2008) or prolonged surface moisture (Knoche and Grimm, 2008; Winkler et al., 2014; Khanal et al., 2020a; Chen et al., 2020; Straube et al., 2020) can also induce russetting.

In apples, russeting is particularly prevalent during early fruit development in fruits with larger and more variably sized epidermal and hypodermal cells (Faust and Shear, 1972b; Taylor, 1975, 1978; Simons and Chu, 1978; Wertheim, 1982; Khanal et al., 2020b; Chen et al., 2020) . During this developmental stage, rapid surface area expansion rates can lead to increased growth strain (Knoche et al., 2011; Knoche and Lang, 2017). Combined with low cuticle deposition rates, this can lead to the formation of microscopic cracks, known as microcracks, in the fruit cuticle (Lai et al., 2016) (Figure 1B). Apple fruit skins are prone to microcracking, especially when exposed to surface moisture (Knoche and Grimm, 2008) . Hereby, the pattern of microcracks has been shown to follow the anticlinal cell walls (ridges) of the epidermal cell layer (Curry, 2009; Curry, 2012; Knoche et al., 2018).

Studies have shown that apples have the ability to repair microcracks through two mechanisms. The first is the deposition of wax as described by Curry (2009). The second is the formation of a periderm in the hypodermis in close proximity to microcracks that traverse the cuticle (Meyer, 1944; Pratt, 1972) (Figure 1C,D). These microcracks are essential for the development of a russeted fruit skin (Faust and Shear, 1972a, 1972b; Curry, 2009). In fact, these changes in the fruit skin have been found to partially restore the functionality of a microcracked cuticle, such as reducing water loss rates (Khanal et al., 2019). However, the underlying cause of microcracking remains unclear, as do the triggers for the subsequent repair mechanisms. Unfortunately, studying the initiation of these processes is challenging due to the nature of woody perennials such as apple, which only flower once a year. In addition, russeting can only be induced during early fruit development, further limiting the window of opportunity. In addition, environmental factors strongly influence the russeting trait, making it difficult to control the onset of russeting under natural conditions. As a result, researchers need specific induction techniques to minimize the impact of random factors that can influence russeting during this critical period.

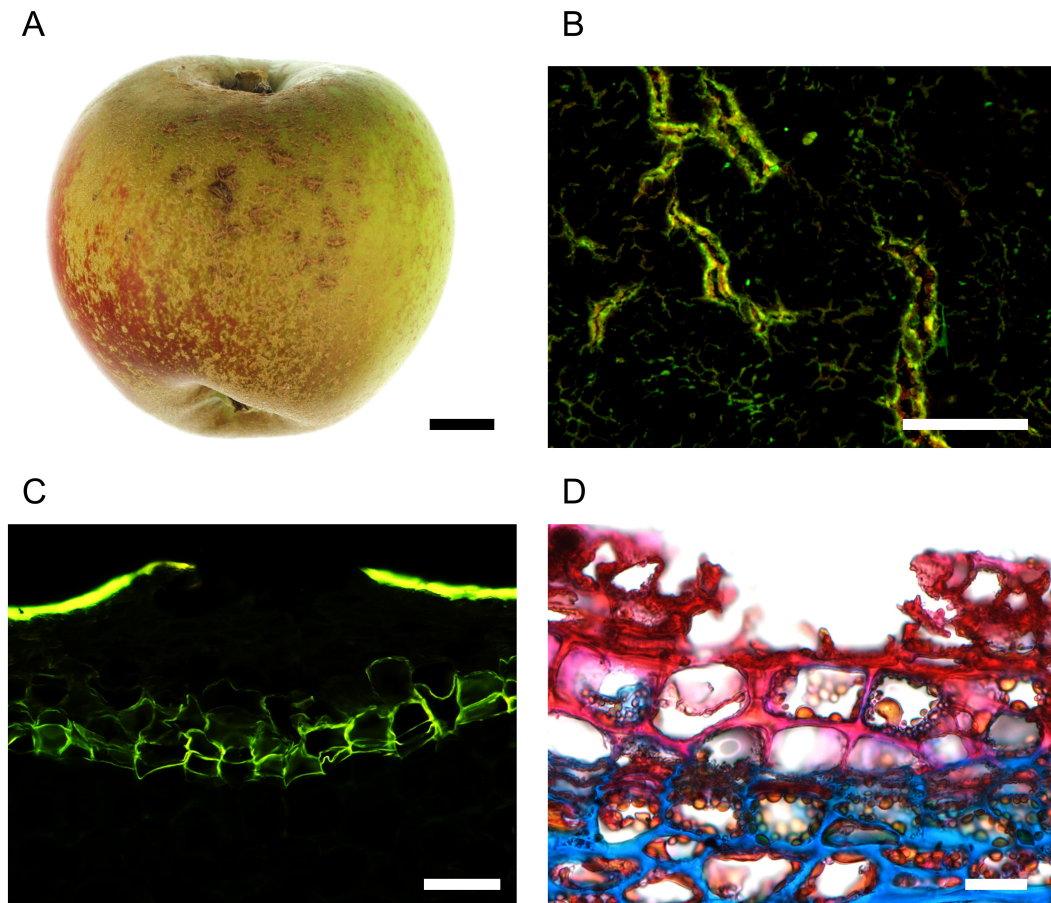


Figure 1. Phenotypic characteristics of russeted apple fruit skins. (A) Fully russeted fruit of the susceptible cultivar 'Karmijn' at maturity. (B) Microcracks in the cuticle are visualized by the accumulation of acridine orange stain. (C) The use of Fluorol Yellow 088 stain allows visualization of a sectioned, microcracked surface that has been sealed with periderm. The stain highlights the microcracks within the cuticle, as well as the suberin-containing cell walls of the phellem, both of which appear yellow after staining. (D) A bright light image capturing the initial phases of russet formation. Samples were stained with rodamin B, acriflavine, and astral blue. The blue staining indicates the presence of non-suberized cell walls, while the pink staining indicates the presence of suberized phellem cell walls. In addition, the pink stain shows the presence of the plant cuticle. Lignified cell walls appear as a deep red color. The scale bars for each image are: (A) 1 cm, (B) 200 nm, (C) 50 μm , (D) 20 μm .

Several horticultural management strategies have been developed to address the problem of russeting in apple. Research has shown that the growth regulator gibberellin A_{4+7} can reduce russeting symptoms in apple (Taylor, 1975). This is likely due to gibberellin A_{4+7} reducing the size of epidermal cells (Curry, 2012) and the extent of cuticular microcracking (Knoche et al., 2011). In addition, protective measures such as bagging the fruit with paper bags or rain shelters during early fruit development have been shown to reduce russet symptoms (Tukey, 1959; Creasy and Swartz, 1981; Yuan et al., 2019). Furthermore, application of chlorogenic

acid at 30 DAFB has been shown to inhibit russeting (Wang et al., 2014) . To prevent russeting by breeding less susceptible cultivars, it is imperative to understand the underlying molecular mechanisms and/or genetic loci associated with russet susceptibility.

1.2. The molecular basis of plant cuticle structure and synthesis

The cuticle plays a crucial role in protecting and regulating the aerial parts of terrestrial plants. It is a hydrophobic lipid layer covering the epidermal cell layer that forms early during embryonic development (Szczuka and Szczuka, 2003) . Its primary functions include regulating water movement in and out of plant tissues (Riederer and Schreiber, 2001; Schreiber, 2010), controlling gas exchange (O₂, CO₂) (Yeats and Rose, 2013), and providing protection against UV light (Krauss et al., 1997; Yeats and Rose, 2013) and pathogens (Serrano et al., 2014).

Cuticular waxes determine the barrier function of the cuticle in terms of water permeability (Schönherr, 1976) . In addition, the cuticle prevents the fusion of organs during plant development (Sieber et al., 2000; Takahashi et al., 2010; Ingram and Nawrath, 2017). The outer layer of the cuticle, known as epicuticular waxes, allows self-cleaning of the plant surface from debris and dust based on the so-called lotus effect (Barthlott and Neinhuis, 1997) . A cuticle-like cell wall structure plays a crucial role in protecting the root meristem from abiotic stresses during seedling establishment and lateral root formation, facilitating proper root development (Berhin et al., 2019).

Plant cuticles are primarily composed of a polymerized matrix of cutin, together with organic solvent-soluble lipids, commonly known as waxes, and a smaller portion of polysaccharides (Yeats and Rose, 2013) . Cuticles can have either an amorphous or lamellar structure (Kolattukudy, 1980; Heumann, 1990) . Plant cuticles undergo two stages of ontogeny: the formation of the “cuticle proper” (CP), followed by the underlying thicker “cuticle layer” (CL) (Jeffree, 2006) (Figure 2). The CP consists primarily of waxes, whereas the CL is rich in cutin embedded with polysaccharides and intracuticular waxes (Yeats and Rose, 2013) . The thickest part of the cuticle is typically found above the anticlinal epidermal cell walls (Jeffree, 2006) . The composition of monomers and components present in plant cuticles varies between species and even organs (Espelie et al., 1979; Marga et al., 2001; Jeffree, 2006; Kallio et al., 2006).

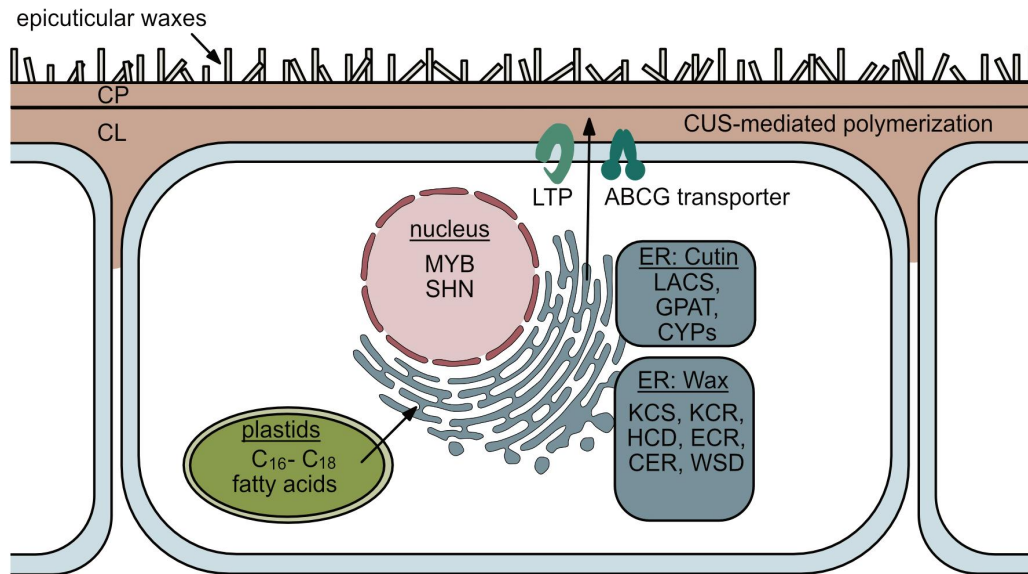


Figure 2. Schematic illustration of plant cuticle structure and associated molecular pathways. The cuticle consists of two major structures: the cuticle layer (CL) and the cuticle proper (CP). The synthetic pathways responsible for cuticle formation originate from two crucial cellular compartments, namely the plastids and the endoplasmic reticulum (ER). CER = ECERIFERUM, CUS = cutin synthase, CYPs = cytochrome P450, ECR = enoyl-CoA reductase, GPAT = glycerol-3-phosphate acyltransferase, HCD = β -hydroxyacyl-CoA dehydratase, KCS = β -ketoacyl-CoA synthase, KCR = β -ketoacyl-CoA reductase, LACS = laccase, LTP = lipid transfer protein, MYB = myeloblastosis transcription factor, SHN = SHINE, WSD = wax ester synthase/acyl-coenzyme A: diacylglycerol acyltransferase.

The cutin polymer is typically composed of hydroxylated or epoxy-hydroxylated fatty acids (predominantly C_{16} and C_{18}), that are crosslinked by esterification (Espelie et al., 1979; Kolattukudy, 1981, 1996; Kolattukudy, 2001). The major C_{16} cutin monomers are 9- or 10,16-dihydroxyhexadecanoic acid and 16-hydroxyhexadecanoic acid. Major C_{18} cutin monomers are 18-hydroxy-9,10-epoxyoctadecanoic acid and 9,10,18-trihydroxyoctadecanoic acid and their monosaturated homologs (Heredia, 2003; Fich et al., 2016). The cuticles covering fast-growing plant organs such as apple flowers and leaves tend to have higher C_{16} family monomers (Kolattukudy and Walton, 1972; Holloway, 1973; Espelie et al., 1979; Kolattukudy, 2001), whereas cuticles covering the apple fruit are dominated by C_{18} fatty acid-based cutin monomers (Holloway, 1973; Espelie et al., 1979). According to Si et al. (2021), the deposition of cutin monomers typically occurs on the inner surface of the cuticle.

Waxes in plant cuticles are based on a mixture of very long chain fatty acids (VLCFAs; mainly C_{20} - C_{40}) including alcohols, alkanes, aldehydes, ketones and esters as well as flavonoids, sterols and triterpenes (Kunst and Samuels, 2003; Jetter et al., 2006; Yeats and

Rose, 2013). In apple cuticles the major constituents are n-nonacosane (C₂₉) and ursolic acid (Morice and Shorland, 1973; Belding et al., 1998; Dong et al., 2012). Specifically in apple fruit cuticles, triterpenes and triterpenoids are major components of the wax fraction, such as ursolic acid and oleanolic acid (André et al., 2012; Legay et al., 2017). Waxes are deposited in the inner matrix of the cutin polymer (intracuticular waxes) and on the outer part of the cuticle (epicuticular waxes). In many plants, triterpenes and triterpenoids are exclusively deposited in the intracuticular wax layer (Buschhaus and Jetter, 2011). Flavonoids that have been found in plant cuticles are e.g. chalconaringenin or naringenin (Hunt and Baker, 1980; Domínguez et al., 2011b).

Polysaccharides in plant cuticles are specifically located in inner matrix adjacent to the epidermal cell walls and are mainly composed of cellulose, hemicellulose, and pectins (Norris and Bukovac, 1968; López-Casado et al., 2007; Domínguez et al., 2011a; Domínguez et al., 2011b; Fernández et al., 2016).

Another polymer found in cuticles is cutan, which is composed mainly of alkyl moieties with a carbon chain length of C₂₂ to C₃₂ (Villena et al., 1999; Schouten et al., 1998; van Bergen et al., 2004; Deshmukh et al., 2005; Bargel et al., 2006). To date, there is no evidence for cutan in apple cuticles.

Studies in *Arabidopsis* (*Arabidopsis thaliana*) and tomato (*Solanum lycopersicum*) have identified important parts of the synthesis pathway of plant cuticles. Genes involved in the synthesis, transport and polymerization of cuticular lipids and in the regulation of their synthesis have been identified.

The cutin monomer synthesis pathway begins with *de novo* synthesis of C₁₆ and C₁₈ fatty acids in plastids (Figure 2). These fatty acids are transported to the endoplasmic reticulum (ER), where they are modified into various oxygenated monoacylglycerols. Three steps are involved: First, esterification of coenzyme A (CoA) to a fatty acid; second, ω - or mid-chain hydroxylation; and third, linkage of the fatty acid-CoA to glycerol (Yeats and Rose, 2013; Fich et al., 2016).

In the first step, CoA is esterified to a fatty acid by long-chain acyl-CoA synthetases (LACS). In the second step, proteins of the cytochrome P450 family hydroxylate these fatty acids. CYP86 enzymes perform the ω -hydroxylation (Wellesen et al., 2001; Xiao et al., 2004; Li-Beisson et al., 2009), while mid-chain hydroxylation is performed by members of the CYP77 subfamily (Li-Beisson et al., 2009; Sauveplane et al., 2009). Finally, glycerol-3-phosphate acyltransferases (GPAT) transfer the fatty acid-CoA to glycerol-3-phosphate. GPAT4, GPAT6 and GPAT8 are widely recognized for their role in this process (Li et al., 2007; Li-Beisson et al., 2009; Petit et al., 2016).

The early steps of wax synthesis overlap with those of the cutin synthesis pathway. This includes the *de novo* synthesis of C₁₆ and C₁₈ fatty acids and esterification of CoA to fatty acids (Yeats and Rose, 2013). In the next step fatty acids, are elongated to a chain length >C₂₀ (VLCFAs) by the fatty acid elongation complex (FAE). The FAE consists of four different enzymes: β -ketoacyl-CoA synthase (KCS), β -ketoacyl-CoA reductase (KCR), β -hydroxyacyl-CoA dehydratase (HCD), and enoyl-CoA reductase (ECR) (Kunst and Samuels, 2009; Yeats and Rose, 2013). After synthesis, VLCFAs are modified by two pathways: The acyl reduction pathway and the decarbonylation pathway (Kunst and Samuels, 2009). In the former, primary alcohols and wax esters are formed, and the enzymes ECERIFERUM 4 (CER4) (Wang et al., 2018) and wax ester synthase/acyl-coenzyme A: diacylglycerol acyltransferase 1 (WSD1) (Li et al., 2008) have been shown to be active in this process. The latter pathway produces aldehydes, alkanes, secondary alcohols, and ketones, and specific enzymes such as CER1 (Hannoufa et al., 1993; McNevin et al., 1993; Aarts et al., 1995) have been well characterized for their involvement in this step.

Our current understanding of the transport of cutin monomers and wax moieties is limited. The transport processes that have been extensively studied rely on ATP-binding cassette (ABC) transporters that are located in the plasma membrane of the cell. In Arabidopsis the transporters ABCG11 (Bird et al., 2007; Panikashvili et al., 2010), ABCG13 (Panikashvili et al., 2011) and ABCG32 (Bessire et al., 2011) as well as their orthologs *SIABCG36* and *SIABCG42* in tomato (Elejalde-Palmett et al., 2021) have been shown to transport cuticular lipids. In addition, the transport of waxes to the cuticle by the lipid transfer proteins (LTP) LTPG1 and LTPG2 has been reported (Debono et al., 2009; Lee et al., 2009a; Kim et al., 2012). Transport of cutin monomers by LTP's has not been demonstrated.

Few enzymes have been characterized for the polymerization of cutin monomers. Cutin synthase 1 (CUS1) has been shown to transesterify major cutin monomers in tomato (Girard et al., 2012; Yeats et al., 2012). Recent research has demonstrated a function of cutinsomes (self-assembled cutin monomers) during early cuticle formation and *CUS1* activity from the onset of cell expansion in tomato fruit (Segado et al., 2020). Analysis of CUS family proteins in evolutionarily diverse plant species revealed a conserved function in catalyzing cutin polymerization (Yeats et al., 2014). *CUS2*, an ortholog of *CUS1*, is required for the maintenance of sepal cuticular ridges in Arabidopsis, but its direct relationship to cuticle synthesis and polymerization remains unclear (Hong et al., 2017). Moreover, it has been suggested that the *BODYGUARD* (*BDG*) gene family in Arabidopsis, which encodes α/β hydrolases, may function in cutin polymerization (Kurdyukov et al., 2006a). The epidermis-specific *bdg1* shows a possible role in polymerization of C₁₈ cutin monomers (Jakobson et al.,

2016) , while observations on *bdg3* knockout lines show possible functions in nanoridge formation in petals (Shi et al., 2011).

Several transcription factors have been identified in regulatory processes of plant cuticle synthesis. Most of them belong to the MYB (myeloblastosis) family, such as MYB16 (Oshima et al., 2013; Oshima and Mitsuda, 2013), MYB41 (Cominelli et al., 2008), MYB94 (Lee and Suh, 2015; Lee et al., 2016), MYB96 (Lee et al., 2016), and MYB106 (Oshima et al., 2013). Other transcription factor families have also been implicated in the regulation of cuticle synthesis. Examples include the AP2/ERF family, especially the SHINE (SHN) clade (Aharoni et al., 2004). *SHN1*, *SHN2* and *SHN3* have been shown to be important regulators of cuticle formation and cuticular lipid synthesis (Aharoni et al., 2004; Shi et al., 2011; Shi et al., 2013).

Finally, cuticular lipid synthesis in fruits appears to be related to the levels of the phytohormones abscisic acid (ABA) and ethylene. In cucumber, gene expression of cuticular alkane synthesis was increased by ABA (Wang, W. et al., 2015a; Wang, W. et al., 2015b). In orange, a correlation between cuticular wax synthesis and ABA levels was suggested (Wang et al., 2016). A positive relationship between ethylene and cuticular wax synthesis has been demonstrated in orange and apple fruit (Ju and Bramlage, 2001; Cajuste et al., 2010; Li et al., 2017).

1.3. Molecular processes in periderm formation

The periderm is a protective tissue in plants that develops in response to biotic and abiotic stresses. It is an adaptation of plants to survive in harsh environmental conditions in terms of regulation of gas exchange (Lendzian, 2006), water loss (Khanal et al., 2019), and acts as a protective layer against pathogens (Thangavel et al., 2016). Peridermal structures form after the disruption of primary barriers and are found in stems (Graça and Pereira, 2004), roots (Wunderling et al., 2018), and fruits (Macnee et al., 2020) of angiosperms and gymnosperms. Anatomically, a periderm consists of three distinct cell tissues: The phelloderm, the phellogen, and the phellem (Figure 3A). The phelloderm, which is the innermost layer of the periderm, shows morphological similarities to the underlying parenchyma cells. The phellogen is a unicellular layer with meristematic activity. The phellem is a multilayered cell layer composed mainly of dead cells with suberized cell walls (Evert, 2006; Serra et al., 2022). It is generally characterized by its stacked cell structure, which is formed as new phellem layers are produced by the phellogen over time.

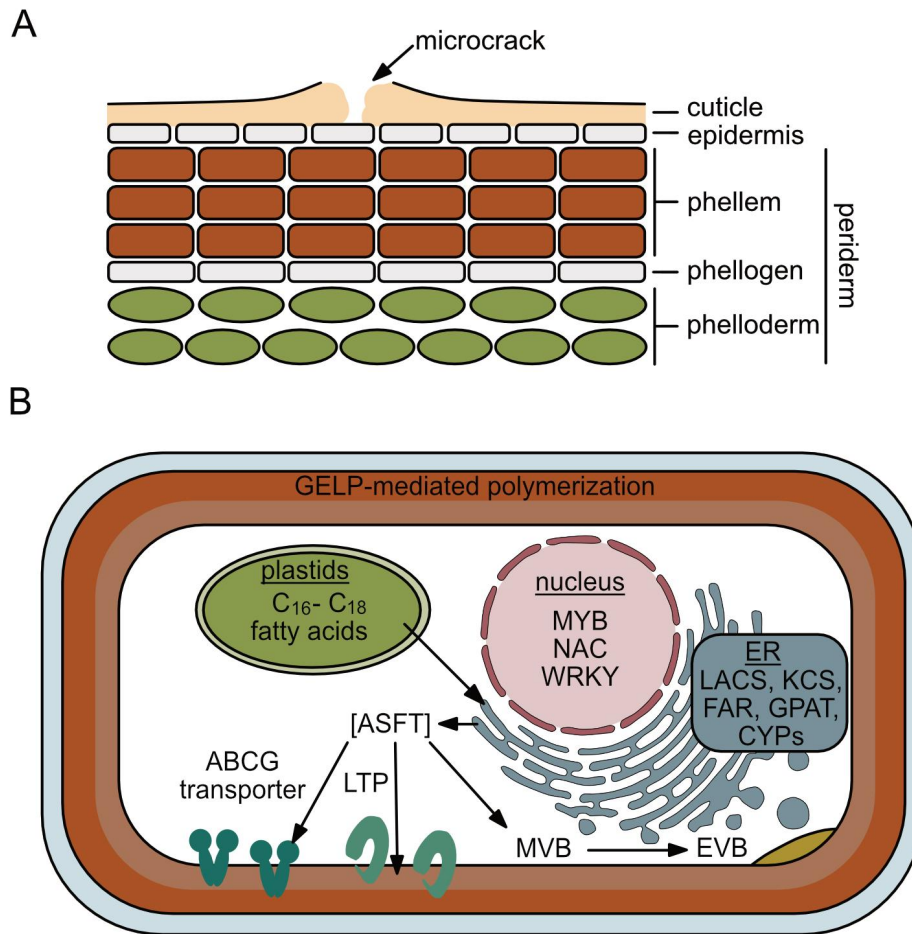


Figure 3. Schematic representation of periderm structure and aliphatic suberin impregnation in cell walls. (A) The periderm is composed of three distinct cell types: phelloderm, phellogen, and phellem. Periderm formation occurs in the hypodermis, specifically during russet formation beneath microcracks. (B) The scheme shows the molecular pathways involved in the formation of phellem cell walls impregnated with aliphatic suberin. Before being exported to the cell wall, the ω -hydroxy acids and primary alcohols can undergo feruloylation through the action of cytosolic ASFT. ASFT = aliphatic suberin feruloyl transferase; CYPs = cytochrome P450; ER = endoplasmic reticulum; EVB = extra vesicular bodies; FAR = fatty acid reductase; GELP = Gly-Asp-Ser-Leu (GDSL)-type esterase/lipase proteins; GPAT = glycerol-3-phosphate acyltransferase; KCS = β -ketoacyl-CoA synthase; LACS = laccase; LTP = lipid transfer protein; MVB = multivesicular body; MYB = myeloblastosis transcription factor; NAC = NAC domain containing protein.

The main component of the periderm is the phellem, which consists of both insoluble and soluble fractions. The insoluble fraction includes suberin, lignin, and polysaccharides such as cellulose and hemicellulose. On the other hand, the soluble fraction includes waxy constituents and phenolic compounds (Serra et al., 2022).

Suberin has been identified as the major component of the phellem cell wall, accounting for up to 50% of the total composition (Silva et al., 2005). Previous studies have characterized suberin as a heteropolymer consisting of two distinct domains: the suberin poly(aliphatic) domain (SPAD) and the suberin poly(phenolic) domain (SPPD) (Bernards, 2002). The inclusion of both domains within the suberin polymer itself remains a subject of debate (Woolfson et al., 2022). Some researchers suggest that only the chemically distinct SPAD is truly part of the suberin polymer (Serra and Geldner, 2022). The SPPD domain has more similarities with lignin or lignin-like polymers and is often found in association with suberin (Serra and Geldner, 2022). Recent research has shown that the SPPD domain is critical for suberin impregnation in cell walls and that both domains are interconnected (Andersen et al., 2021). The connection between the lignin of the primary cell wall and the suberin lamellae is proposed to be achieved by ferulic acid, a major compound found in the SPAD and SPPD domains (Bernards, 2002; Graça and Santos, 2007; Graça, 2010). Although there is an ongoing debate, this section will emphasize the composition of the SPAD domain as an important component of suberin, as opposed to SPPD. Aliphatic suberin is a complex biopolymer composed mainly of oxygenated fatty acid derivatives, with monomers dominated by ω -hydroxy fatty acids and α,β -dicarboxylic acids with a carbon chain length ranging from C₁₆ to C₃₀ as well as glycerol (Schreiber et al., 1999; Graça and Pereira, 2000; Franke and Schreiber, 2007). In particular, C₂₀, C₂₂, C₂₄ ω -hydroxy fatty acids are both major and unique compounds found in suberin polymers (Franke et al., 2005). The suberin found in apple fruit skins is primarily composed of primary alcohols, fatty acids, ω -hydroxy fatty acids, and α,β -dicarboxylic acids with carbon chain lengths ranging from C₂₀ to C₂₄ (Legay et al., 2017).

The lignin found in phellem cells is mainly composed of guaiacyl (G) units and, to a lesser extent, syringyl (S) monolignol units (Marques and Pereira, 2013; Fagerstedt et al., 2015; Lourenço et al., 2016; Dou et al., 2018). Commonly found are hydroxycinnamic acids such as coumaric acid, caffeic acid, ferulic acid and sinapic acid and their derivatives (Woolfson et al., 2022). Ferulic acid is a major component found in apple periderm (Legay et al., 2017).

The waxes found in the periderm consist mainly of alkanes, fatty alcohols (C₁₈-C₂₆), fatty acids (C₁₄-C₂₄), glycerol, triglycerides, and up to 50% of triterpenes belonging to the fridein and lupine families (Castola et al., 2002; Silva et al., 2005). The wax constituents present in the peridermal structures of apple fruit skins are a combination of lupine-type triterpenoids, C₁₆-C₂₀ carboxylic acids, C₂₄-C₃₀ primary alcohols, and several alkyl hydroxycinnamates (Legay et al., 2017). The water barrier properties of the periderm are determined by the waxes present (Soliday et al., 1979). It has been shown that ferulic acid esters appear to be a key factor in maintaining the water barrier of the periderm (Serra et al., 2010).

The synthesis of the SPAD domain, particularly aliphatic suberin, which is chemically very similar to cutin, begins with the use of C₁₆ and C₁₈ long-chain fatty acids (LCFAs) as a starting point (Serra and Geldner, 2022) (Figure 3B). In the ER, LCFAs are modified by LACS to form acyl-CoA thioesters. Among the LACS enzymes, LACS2 has been identified as suberin-specific (Ayaz et al., 2021; Renard et al., 2021). In addition, in the ER, long-chain fatty acyl-CoA (LCFA-CoA) are elongated into very long-chain fatty acyl-CoA (VLCFA-CoA) of various chain lengths by FAE, primarily through the action of the enzyme KCS. Suberin-specific enzymes involved in this process include KCS2 (Franke et al., 2009), KCS6 (Serra et al., 2009a), KCS20 (Lee et al., 2009b), and possibly KCS1 (Todd et al., 1999). During suberin synthesis, two pathways have been identified to follow up: First, the reduction of the VLCFA-CoA; second, the hydroxylation of unmodified fatty acids or primary alcohols. Specific enzymes associated with the first step are the fatty acyl reductases FAR1, FAR4 and FAR5 to produce fatty alcohols (Domergue et al., 2010; Vishwanath et al., 2013; Wang et al., 2021), while the latter step is mediated by enzymes of the CYP86A, CYP86B and CYP94B monooxygenase families that ω -hydroxylate fatty acids (Höfer et al., 2008; Compagnon et al., 2009; Molina et al., 2009; Serra et al., 2009b; Krishnamurthy et al., 2020; Krishnamurthy et al., 2021). The ω -hydroxy fatty acids can be used to synthesize α,β -dicarboxylic acids (Agrawal and Kolattukudy, 1977). However, it remains unclear whether suberin-specific enzymes are involved in this step. During cutin synthesis, the enzyme HOTHEAD is responsible for the synthesis of α,β -dicarboxylic acids from ω -hydroxy fatty acids (Kurdyukov et al., 2006b). This function may also occur during suberin synthesis.

ω -hydroxy acids and primary alcohols can be esterified with feruloyl-CoA from the phenylpropanoid pathway via aliphatic suberin feruloyl-transferase (ASFT) (Gou et al., 2009; Molina et al., 2009) or fatty ω -hydroxy acid/fatty alcohol hydroxycinnamoyl transferase (FHT) to generate feruloylated suberin precursors (Serra et al., 2010; Boher et al., 2013). Another crucial step in suberin synthesis is the transfer of glycerol to fatty acyl-CoA derivatives, which is facilitated by suberin-specific glycerol-3-phosphate transferases such as GPAT5 (Beisson et al., 2007) and possibly GPAT7 (Yang et al., 2012). This transfer occurs at the 2-*sn* position, resulting in the formation of 2-monoacylglycerol. After formation, the feruloylated and glycerylated suberin precursors are transported to the cell wall.

Several ABCG transporters have been identified as suberin monomer transporters in plants, including *ABCG1* in *Solanum tuberosum* and its ortholog in *Arabidopsis* (Landgraf et al., 2014; Shanmugarajah et al., 2019), *ABCG2*, *ABCG6*, *ABCG11*, and *ABCG20* in *Arabidopsis* (Panikashvili et al., 2010; Yadav et al., 2014), and *RCN1/ABCG5* in rice (*Oryza sativa*) (Shiono et al., 2014). In addition, lipid transfer proteins (LTP) have also been shown to play a role in suberin transport. In *Arabidopsis*, *LTPI-4* (Deeken et al., 2016) and *LTPG15* (Lee and

Suh, 2018) have been identified in suberin transport. Recent evidence suggests that extracellular vesiculo-tubular structures play a critical role in suberin monomer transport via an exocytosis pathway (Bellis et al., 2022).

Gly-Asp-Ser-Leu (GDSE)-type esterase/lipase proteins (GELPs) are the primary mediators of suberin polymerization in the cell wall. Recent work by Ursache et al. (2021) has identified several GELPs involved in suberin polymerization Arabidopsis roots. In addition to GELPs, suberin lamellae in the cell wall are likely to form to a lesser extent by self-assembly between ferulic acid or sinapic acid, ω -hydroxy fatty acids, and glycerol (Kligman et al., 2022).

The incrustation of cell walls with suberin is regulated by several transcription factors, including primarily members of the MYB, NAC, and WRKY families. Table 1 lists the currently known transcriptional regulators involved in the process of suberin synthesis.

Table 1. List of transcriptional regulators associated with the suberin synthesis pathway.

Gene	Description of function	Species	Reference
<i>MYB1</i>	Phellem specific activity, activator of lignin and suberin synthesis	<i>Quercus suber</i>	(Capote et al., 2018)
<i>MYB9</i>	Activator of suberin synthesis	<i>A. thaliana</i>	(Lashbrooke et al., 2016)
<i>MYB39</i>	Activator of suberin synthesis	<i>A. thaliana</i>	(Cohen et al., 2020)
<i>MYB41</i>	Activator of suberin synthesis	<i>A. thaliana</i> , <i>Actinidia chinensis</i>	(Kosma et al., 2014; Wei et al., 2020; Shukla et al., 2021)
<i>MYB53</i>	Activator of suberin synthesis	<i>A. thaliana</i>	(Shukla et al., 2021)
<i>MYB70</i>	Repressor of suberin synthesis	<i>A. thaliana</i>	(Wan et al., 2021)
<i>MYB74</i>	Activator of suberin synthesis	<i>Solanum tuberosum</i>	(Wahrenburg et al., 2021)
<i>MYB78</i>	Activator of suberin synthesis	<i>Saccharum officinarum</i>	(Figueiredo et al., 2020)
<i>MYB92</i>	Activator of suberin synthesis	<i>A. thaliana</i>	(Shukla et al., 2021)
<i>MYB93</i>	Activator of suberin synthesis	<i>Malus x domestica</i> , <i>A. thaliana</i>	(Legay et al., 2016; Shukla et al., 2021)
<i>MYB102</i>	Activator of suberin synthesis	<i>S. tuberosum</i>	(Wahrenburg et al., 2021)
<i>MYB107</i>	Activator of suberin synthesis	<i>A. thaliana</i> , <i>A. chinensis</i>	(Lashbrooke et al., 2016; Gou et al., 2017; Wei et al., 2020)
<i>MYC2</i>	Activation of <i>FAR</i> , ABA-mediated wound suberization	<i>A. chinensis</i>	(Wei et al., 2020)
<i>ANAC046</i>	Activator of suberin synthesis	<i>A. thaliana</i>	(Mahmood et al., 2019)
<i>ANAC103</i>	Repressor of suberin synthesis	<i>S. tuberosum</i>	(Verdaguer et al., 2016)
<i>WRKY1</i>	Regulation of phenylpropanoid synthesis	<i>S. tuberosum</i>	(Yogendra et al., 2015)
<i>WRKY9</i>	Activator of suberin synthesis	<i>A. thaliana</i>	(Krishnamurthy et al., 2021)
<i>WRKY33</i>	Activator of suberin synthesis	<i>Avicennia officinalis</i>	(Krishnamurthy et al., 2020)

Similar to cuticle lipid biosynthesis, phytohormones also play a role in suberin deposition in response to various stresses. An increase in ABA induced by salt stress has been observed to promote suberization in *Arabidopsis* roots (Barberon et al., 2016). Upon wounding, increased levels of ABA mediate the accumulation of primary fatty alcohol in the suberin of kiwi fruit (*Actinidia chinensis*) (Wei et al., 2020). Recent research has shown that ABA levels directly regulate several transcription factors associated with suberization in *Arabidopsis* (Xu, H. et al., 2022). Conversely, ethylene-based signaling was found to decrease suberization levels during iron deficiency (Barberon et al., 2016). In addition, Lu et al. (2022) highlighted that increased serotonin (5-hydroxytryptamine) levels are associated with a reduction in root suberization in both rice and *Arabidopsis*.

The synthesis of the SPPD domain, especially lignin, occurs via the phenylpropanoid pathway. The phenylpropanoid pathway begins with the enzyme phenylalanine ammonia-lyase, which catalyzes the conversion of the shikimate pathway derived phenylalanine to cinnamate (Havir and Hanson, 1970). Cinnamate is then hydroxylated to 4-hydroxy cinnamate (*p*-coumaric acid) by cinnamate 4-hydroxylase (C4H) (Russell and Conn, 1967; Russell, 1971; Mizutani et al., 1997), followed by conversion to *p*-coumaroyl-CoA by the enzyme 4-coumarate-CoA ligase (4CL) (Schneider et al., 2003). *p*-Coumaroyl-CoA serves as a precursor for flavonoid synthesis or for the synthesis of other common hydroxycinnamic acids such as caffeoyl-CoA, ferulic acid, and sinapic acid. Caffeoyl-CoA is derived through the enzymatic activity of *p*-coumaroyl-quininate/shikimate 3'-hydroxylase (C3'H) (Knollenberg et al., 2018) and hydroxycinnamoyl-CoA transferase (HCT) (Hoffmann et al., 2003), ferulic acid by methylation of caffeoyl-CoA by caffeoyl-CoA-O-methyltransferase (CCoAOMT) (Do et al., 2007), and sinapic acid by ferulate 5-hydroxylase (F5H) (Meyer et al., 1996), along with caffeic acid O-methyltransferase (COMT) (Humphreys et al., 1999).

The mechanism by which monolignols are transported to the cell wall is not fully understood, although three potential pathways have been proposed: First, passive diffusion across the plasma membrane; second, exocytosis facilitated by vesicles derived from the ER and Golgi apparatus; and third, active export mediated by ABC transporters (Miao and Liu, 2010; Liu et al., 2011; Liu, 2012; Perkins et al., 2019; Vermaas et al., 2019). To date, only ABCG29 has been identified as a transporter in this process (Alejandro et al., 2012).

Polymerization of lignin and the SPPD domain is thought to be mediated by peroxidases and H₂O₂ (Espelie et al., 1986). In potato, an anionic peroxidase has been implicated in the polymerization of hydroxycinnamic acids present in the SPPD domain of suberin (Bernards et al., 1999). Peroxidase 64 (PER64) and a dirigent-like protein (ESB1) were found to significantly contribute to lignin polymerization during observations of Casparian strip lignification (Hosmani et al., 2013; Lee et al., 2013). The peroxidase TPX1 was found to be

involved in the polymerization of suberin and lignin in tomato (Quiroga et al., 2000). Recent research using *Arabidopsis* loss-of-function mutants has shown that peroxidases, but not laccases, play critical role in lignin polymerization (Rojas-Murcia et al., 2020).

The transcriptional regulation of lignin synthesis has been extensively studied in several plant species, revealing a complex network of interactions. Among the transcription factors involved in this process, members of the MYB and NAC family have been found to play a primary role. Table 2 provides an overview of the known transcriptional regulators in this pathway.

Table 2. List of transcriptional regulators associated with the lignin synthesis.

Gene	Description of function	Species	Reference
BP	Repressor of lignin synthesis	<i>A. thaliana</i>	(Mele et al., 2003)
LIM1	Activator of lignin synthesis	<i>Nicotiana tabacum</i>	(Kawaoka et al., 2000)
LTF1	Repressor of lignin synthesis	<i>Populus deltoides x Populus euramericana</i>	(Gui et al., 2019)
PAP1	Activator of lignin synthesis	<i>A. thaliana</i>	(Borevitz et al., 2000)
MYBJS1	Activator of lignin synthesis	<i>N. tabacum</i>	(Gális et al., 2006)
MYB1	Activator of lignin synthesis	<i>Pinus taeda</i>	(Patzlaff et al., 2003b)
MYB2	Activator of lignin synthesis	<i>Eucalyptus gunnii</i>	(Goicoechea et al., 2005)
MYB3	Activator of lignin synthesis	<i>Populus trichocarpa</i>	(McCarthy et al., 2010)
MYB4	Repressor of lignin synthesis in <i>Arabidopsis</i> , activator of lignin synthesis in <i>P. taeda</i>	<i>A. thaliana, Pinus taeda</i>	(Jin et al., 2000; Patzlaff et al., 2003a)
MYB5a	Repressor of lignin synthesis	<i>Vitis vinifera</i>	(Deluc et al., 2006)
MYB8	Activator of lignin synthesis	<i>P. taeda</i>	(Bomal et al., 2008)
MYB11	Repressor of lignin synthesis	<i>Zea mays</i>	(Vélez-Bermúdez et al., 2015)
MYB20	Activator of lignin synthesis	<i>Populus trichocarpa, A. thaliana</i>	(McCarthy et al., 2010; Geng et al., 2020)
MYB21a	Repressor of lignin synthesis	<i>Populus tremula x tremuloides</i>	(Karpinska et al., 2004)
MYB26	Activator of lignin synthesis	<i>A. thaliana</i>	(Yang et al., 2007)
MYB31	Repressor of lignin synthesis	<i>Z. mays</i>	(Fornalé et al., 2006)
MYB32	Repressor of lignin synthesis	<i>A. thaliana</i>	(Preston et al., 2004)
MYB42	Activator of lignin synthesis in <i>Arabidopsis</i> , Repressor of lignin synthesis in <i>Zea mays</i>	<i>A. thaliana, Z. mays</i>	(Fornalé et al., 2006; Zhong et al., 2008; Sonbol et al., 2009; Geng et al., 2020)
MYB43	Activator of lignin synthesis	<i>A. thaliana</i>	(Geng et al., 2020)
MYB46	Activator of cellulose, xylan, and lignin synthesis	<i>A. thaliana</i>	(Zhong et al., 2007)
MYB52	Activator of lignin synthesis	<i>Malus x domestica</i>	(Xu, X. et al., 2022)
MYB58	Activator of lignin synthesis	<i>A. thaliana</i>	(Zhou et al., 2009)

Table 2 continued

<i>MYB61</i>	Activator of lignin synthesis	<i>A. thaliana</i>	(Newman et al., 2004)
<i>MYB63</i>	Activator of lignin synthesis	<i>A. thaliana</i>	(Zhou et al., 2009)
<i>MYB83</i>	Activator of lignin synthesis	<i>A. thaliana</i>	(McCarthy et al., 2009)
<i>MYB85</i>	Activator of lignin synthesis	<i>A. thaliana</i>	(Zhong et al., 2008; Geng et al., 2020)
<i>MYB103</i>	Activator of lignin synthesis	<i>A. thaliana</i>	(Öhman et al., 2013)
<i>MYB156</i>	Repressor of lignin synthesis	<i>Populus tomentosa</i>	(Yang et al., 2017)
<i>MYB308</i>	Repressor of lignin synthesis	<i>Antirrhinum majus</i>	(Tamagnone et al., 1998)
<i>MYB330</i>	Repressor of lignin synthesis	<i>A. majus</i>	(Tamagnone et al., 1998)
<i>NST1</i>	Activator of lignin synthesis	<i>A. thaliana</i>	(Mitsuda et al., 2007)
<i>NST2</i>	Activator of lignin synthesis	<i>A. thaliana</i>	(Mitsuda et al., 2005)
<i>NST3</i>	Activator of lignin synthesis	<i>A. thaliana</i>	(Mitsuda et al., 2007)

While the synthesis of waxes was introduced in Section 1.1, it will not further be elaborated on in this section in relation to the periderm.

Periderm formation parallels the vascular cambium, where several transcriptional regulators have been identified as important for cambial activity. These regulators include AINTEGUMENTA (Randall et al., 2015), several auxin responsive factors (ARF) (Brackmann et al., 2018; Smetana et al., 2019), ethylene response factor 018 (ERF18) and ERF109 (Etchells et al., 2012), WUSCHEL-related homeobox 4 (WOX4) (Hirakawa et al., 2010; Ji et al., 2010; Suer et al., 2011), and WOX14 (Etchells et al., 2013). In a recent study by Zhang, J. et al. (2019), a large number of additional transcription factors were found to be active in the vascular cambium. Among them, WOX4, WOX14, KNOTTED-like from *Arabidopsis thaliana* 1 (KNAT1), NAC domain-containing protein 15 (ANAC015), and LOB domain-containing protein 3 (LBD3) were found to promote cambial activity. Conversely, petal loss (PTL), response to ABA and salt 1 (RAS1), short vegetative phase (SVP), and MYB domain 87 (MYB87) were found to inhibit cambial activity. The study also identified WOX4 and KNAT1 as master regulators of cambial activity. In poplar, regulation of cambial cell division and radial growth is mediated by WOX4 downstream of *tracheary element differentiation inhibitory factor* and *phloem intercalated with xylem (TDIF-PXI)* signaling through *clavate 3 (CLV3)/embryo surrounding region (ESR)-related 41 (CLE41)* genes (Hirakawa et al., 2010; Kucukoglu et al., 2017). Recent research has shown that the zinc finger transcription factor vascular cambium-specific 2 (VCS2) regulates the proliferation rate of cambial cells in poplar by modulating the acetylation status of the *WOX4* promoter (Dai et al., 2023). In addition, MYB84 has been identified as a potential regulator of cambial activity. In cork oak (*Quercus suber*), its ortholog *MYB1* showed specific expression in phellem cells (Almeida et al., 2013a; Almeida et al., 2013b), whereas in *Arabidopsis*, *MYB84* was found to be active in phellogen and phellem (Wunderling et al., 2018). Leal et al. (2022) showed that *MYB84* was less

expressed in the phellem-specific transcriptome, compared to the whole root transcriptome. This suggests a possible involvement of MYB84 in the phellogen. While the phellem-specific transcriptome revealed several additional transcriptional regulators, these are primarily associated with suberin formation rather than periderm initiation processes. Vulavala et al. (2019) examined a phellogen-specific transcriptome and identified several genes associated with cell division and differentiation processes, providing insights into the molecular mechanisms underlying periderm development. Although significant progress has been made in understanding peridermal structures, there is still a need for further investigation to fully understand the complex network of factors that regulate periderm associated processes.

1.4. Genetic and metabolic factors associated with russetting in apple

Russet susceptibility in fruit has a genetic basis that varies among cultivars (Khanal et al., 2013a), mutants (Falginella et al., 2021), and segregating populations (Falginella et al., 2015; Lashbrooke et al., 2015; Macnee et al., 2021; Jiang et al., 2022). Investigations on segregating apple populations have identified several quantitative trait loci (QTLs) associated with this trait. Studies by Falginella et al. (2015) and Lashbrooke et al. (2015) found three major QTLs on linkage group 12 and chromosome 2 and 15. More recently, Powell et al. (2023) identified seven QTLs associated with russetting on linkage groups 2, 6, 7, 9, 12, 13, and 15. Genes involved in cuticle formation and epidermal patterning, such as *SHN3* and *ABCG11*, have been found to be associated with the russetting trait (Falginella et al., 2015; Lashbrooke et al., 2015). Specifically, *SHN3* shows distinctive gene expression patterns that correlate with russetting susceptibility (Lashbrooke et al., 2015). Legay et al. (2015) conducted an RNA-Seq study on mature apple fruit skins, which revealed that genes involved in cuticle-related functions were downregulated, while genes in the suberin and phenylpropanoid pathways were upregulated. To demonstrate the regulatory role of MYB93 in suberin synthesis, Legay et al. (2016) performed heterologous overexpression in *N. benthamiana* leaves, confirming its importance as a major regulator. Further research has identified additional transcriptional regulators involved in suberin deposition in angiosperms. Lashbrooke et al. (2016) showed that MYB9 and MYB107 from *Solanum lycopersicum*, as well as their homologs in apple, have regulatory functions in suberin deposition. In addition, *MdOSC5* was found to be involved in triterpene synthesis on russeted apple fruit skins, and promoter binding assays indicate that MdMYB52 and MdMYB66 activate *MdOSC5* (Falginella et al., 2021). In their recent research, Xu, X. et al. (2022) identified *MdMYB52* as a positive regulator of G-unit lignin monomers, while *MdMYB68* plays a critical role as a master regulator of suberin, as well as regulating modifications in hemicelluloses and pectins (Xu et al., 2023). In addition, using transcriptomic and proteomic approaches, Yuan et al.

(2019) identified two peroxidases, a shikimate O-hydroxycinnamoyl transferase, and a cinnamyl alcohol dehydrogenase associated with lignification of russeted surfaces. André et al. (2022) discovered a lipid transfer protein (LTP3) critical for maintain the cuticle integrity in apple fruit skins, as well as several BAHD (HXXD-motif) acyltransferases associated with triterpene hydroxycinnamate synthesis in russet fruit skins using a systems biology approach involving metabolomics, proteomics, and transcriptomics.

Legay et al. (2017) compared the metabolic composition of mature russeted and waxy apple skins of the semi-russeted 'Cox Orange Pippin' and found a shift in cutin, suberin, triterpene, and wax content. Russeted fruit skins contained higher levels of C₂₀, C₂₂, and C₂₄ fatty acids, alkyl hydroxycinnamates, and betulinic acid, and lower levels of C₁₆ and C₁₈ fatty acids, oleanolic acid and ursolic acid. Additionally, Gutierrez et al. (2018) found higher phloridzin content in the fruit skins of russeted apple sports compared to low-russeted apple sports at maturity. When comparing a subset of russeted and non-russeted sports of 'Golden Delicious' apples, it was found that phloroidzin content in the peel was higher during the vegetative phase of the fruit compared to the mature stage, especially in the former (Gutierrez et al., 2018).

Despite these advances, the earliest steps in the development of russeting in apple fruit remain poorly understood. This knowledge gap can be attributed to the fact that most studies have focused primarily on the later stages of russeting, highlighting the need for further research in this area.

1.5. Transcriptomics in horticultural crops with a focus on apple

The transcriptome refers to the complete set of RNA molecules expressed by a cell or tissue at a given time. In the 1980s, researchers began using Sanger sequencing as a method to identify expressed sequence tags (ESTs) (Sutcliffe et al., 1982; Putney et al., 1983). Later on, cDNA microarrays were introduced by Schena et al. (1995) as a tool for studying gene expression levels. However, these methods were limited in their ability to efficiently generate large amounts of data. Today, next-generation sequencing (NGS) is the preferred method for generating transcriptomic datasets due its higher throughput and cost efficiency. Popular NGS platforms include Roche 454, Ion Torrent, PacBio, Oxford Nanopore, SOLiD, and Illumina, which is currently the most widely used platform for transcriptomics (Ravisankar and Mathew, 2022). Through the development of several bioinformatics algorithms, researchers now have the ability to comprehensively explore the nuances of transcriptomic dynamics. This includes assembly of reference genomes and transcriptomes (Kim et al., 2013; Pertea et al., 2015), mapping reads to them (Dobin et al., 2013; Kim et al., 2019), counting reads

(Anders et al., 2015), and using software to explore expression data (Robinson et al., 2010; Love et al., 2014).

RNA sequencing (RNA-Seq) analysis involves three primary tasks: First, to identify gene structure, including intron-exon boundaries; second, to identify expressed and non-expressed regions of the genome; and third, to detect differences in expression profiles between genotypes, tissues, external factors, or developmental stages. To achieve these goals, various approaches have been developed over time to generate reliable transcriptomic data. Two popular methods for investigating these tasks are bulk transcriptomics and single-cell transcriptomics, with the latter gaining traction in recent years (Kulkarni et al., 2019; Kaur et al., 2023).

The increasing accessibility of genome sequences for horticultural crops has greatly improved the detection and analysis of genes important in various biological processes. For example, the first report of the apple (*Malus x domestica*) reference genome for 'Golden Delicious' was published by Velasco et al. (2010). In subsequent years, the apple genome has undergone significant improvements, and currently genome sequences for numerous cultivars are readily available (Daccord et al., 2017; Zhang, L. et al., 2019; Sun et al., 2020; Khan et al., 2022). Furthermore, the genomes of several wild relatives have been sequenced in recent years, including *Malus baccata* (Chen, X. et al., 2019), *Malus sieversii*, *Malus sylvestris* (Sun et al., 2020) and *Malus prunifolia* (Li et al., 2022). By incorporating these genomes, a pan-genome for apple was constructed (Sun et al., 2020), which may facilitate the identification of genes related to fruit quality traits. For example, a similar approach was taken for tomato, where pan-genome analysis led to the discovery of several genes associated with fruit flavor (Gao et al., 2019).

Transcriptomic approaches were used to study developmental and quality-related traits of apple fruits. Red coloration of apple fruits was found to be regulated by MYB10 (El-Sharkawy et al., 2015) and MYB114 (Jiang, S.-H. et al., 2019) through investigations using transcriptomics. Wang, N. et al. (2015) used transcriptomic profiling of a segregating F1 population to identify molecular processes and genes associated with the red-fleshed phenotype in apples. Using long non-coding RNA sequencing (lncRNA-Seq) analysis of apple fruit peels, lncRNAs were found to play a role in the anthocyanin pathway (Yang et al., 2019). Moreover, a combination of transcriptomics and metabolomics was recently used to study the pre-harvest browning of fruit skin and revealed that the major regulator of this undesirable trait is WRKY31, which regulates *LACS7* (Wang et al., 2023). An investigation of the transcriptional networks associated with pre- and post-ripening has highlighted the potential of ABA, in addition to ethylene, in the ripening process (Onik et al., 2018).

These findings demonstrate the utility of transcriptomic approaches in identifying key genes for important horticultural traits, particularly in apple.

1.6. Objectives

The aim of this dissertation is to identify the genetic and molecular mechanisms involved in the initiation of russeting in apple fruit skins using a combination of morphological, transcriptomic and metabolomic analyses. By unraveling the complexity of this trait, this research aims to provide valuable insights for the development of apple cultivars with increased resistance to russeting. Previous studies have focused on the analysis of naturally russeted fruit without a clear starting point. In contrast, our research provides detailed information on the early stages of russeting, which are currently unknown.

Therefore, this dissertation will highlight new findings on the following major objectives:

- **Chapter 2:** Establishment of a system for inducing russeting in apple fruit.
- **Chapter 3:** Characterization of the sequence of morphological changes that occur on the apple fruit skin during the formation of russeting.
- **Chapter 4:** Investigation of changes in gene expression of candidate genes identified from the literature, along with compositional changes that occur during the process of russet formation.
- **Chapter 5:** Investigate and contrast the morphology, gene expressions, and metabolic constitution of the periderm (russeting) induced by moisture and wounding.
- **Chapter 6:** Identification of transcriptomic events that occur during microcracking and initiation of russet formation in apple fruit skins.
- **Chapter 7:** Functional characterization of candidate genes identified by transcriptomic analyses.

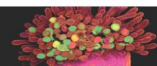
2. Surface moisture increases microcracking and water vapour permeance of apple fruit skin

Bishnu P. Khanal¹, Yahaya Imoro¹, Yun-Hao Chen¹, Jannis Straube² and Moritz Knoche¹

¹Institute of Horticultural Production Systems, Fruit Science Section, Leibniz University Hannover, Herrenhäuser Straße 2, 30419 Hannover, Germany



²Institute of Plant Genetics, Molecular Plant Breeding Section, Leibniz University Hannover, Herrenhäuser Straße 2, 30419 Hannover, Germany

Type of authorship:	Co-author
Type of article:	Research article
Contribution to the article:	Involved in conducting time course experiments to investigate water loss, permeance, infiltrated area, and microscopic observations during a 12 d application of water to the skin of apple fruit. In addition, J. Straube performed validation of the split fruit system by comparing fruits covered with water-filled tubes to those without.
Contribution of other authors:	B.P. Khanal participated in the study design, experimental investigation, data analysis and writing the manuscript. Y. Imoro performed the experiments and analyzed the data. Y.-H. Chen performed some of the experiments related to the time course experiments after water application and validation of the induction system. M. Knoche designed the experiments, analyzed the data, and was involved in writing the manuscript.
Journal	Plant Biology
Date of publication:	02.09.2020
Impact factor:	3.877 (2021)
DOI:	10.1111/plb.13178



RESEARCH PAPER

Surface moisture increases microcracking and water vapour permeance of apple fruit skin

B. P. Khanal¹ , Y. Imoro¹, Y. H. Chen¹, J. Straube² & M. Knoche¹ 

¹ Institute of Horticultural Production Systems, Fruit Science Section, Leibniz University Hanover, Hanover, Germany

² Institute of Plant Genetics, Leibniz University Hanover, Hanover, Germany

Keywords

cuticle; *Malus × domestica*; microcrack; moisture; transpiration.

Correspondence

M. Knoche, Institute of Horticultural Production Systems, Fruit Science Section, Leibniz University Hanover, Herrenhäuser Straße 2, 30419 Hanover, Germany.
E-mail: moritz.knoche@obst.uni-hannover.de

Editor

M. Riederer

Received: 10 July 2020; Accepted: 14 August 2020

doi:10.1111/plb.13178

ABSTRACT

- Surface moisture induces microcracking in the cuticle of fruit skins. Our objective was to study the effects of surface moisture on cuticular microcracking, the permeance to water vapour and russetting in developing ‘Pinova’ apple fruit.
- Surface moisture was applied by fixing to the fruit a plastic tube containing deionized water. Microcracking was quantified by fluorescence microscopy and image analysis following infiltration with acridine orange. Water vapour permeance was determined gravimetrically using skin segments (ES) mounted in diffusion cells.
- Cumulative water loss through the ES increased linearly with time. Throughout development, surface moisture significantly increased skin permeance. The effect was largest during early development and decreased towards maturity. Recovery time courses revealed that following moisture treatment of young fruit for 12 days, skin permeance continued to increase until about 14 days after terminating the moisture treatment. Thereafter, skin permeance decreased over the next 28 days, then approaching the control level. This behaviour indicates gradual healing of the impaired cuticular barrier. Nevertheless, permeance still remained significantly higher compared with the untreated control. Similar patterns of permeance change were observed following moisture treatments at later stages of development. The early moisture treatment beginning at 23 DAFB resulted in russetting of the exposed surfaces. There was no russet in control fruit without a tube or in control fruit with a tube mounted for 12 days without water.
- The data demonstrate that surface moisture increases microcracking and water vapour permeance. This may lead to the formation of a periderm and, hence, a russeted fruit surface.

INTRODUCTION

The cuticle is a biopolymer that envelopes all primary surfaces of terrestrial plants. It covers the fruits of most species and all leaf surfaces. The cuticle performs important functions as a barrier to pathogen invasion (Yeats & Rose 2013; Guan *et al.* 2015) and in regulating the passage of water and other substances across the surface. Depending on organ, circumstances and chemistry of the penetrant, the transcuticular movements can be either inwards or outwards (Kerstiens 1996; Schreiber & Schönherr 2009; Dominguez *et al.* 2011; Yeats & Rose 2013). Obviously, the maintenance of an appropriate level of regulatory function throughout fruit development requires the cuticle to remain intact. Compared with a leaf, maintenance of cuticular integrity in a fruit is particularly challenging. This is because fruits differ from leaves in that fruit expansion commonly occurs over a lengthy period – commonly around 5 months (Knoche & Lang 2017). The ongoing growth subjects the fruit cuticle and its subtending dermal layers (which together make up the skin) to continuous tangential strain (Skene 1982). The epidermal and hypodermal cell layers can accommodate this strain by ongoing anticlinal cell divisions and by gradual changes in cell anticlinal aspect ratio, from

portrait to landscape (Tukey & Young 1942). The polymeric cuticle, however, is not ‘alive’ in the same sense and so must sustain the ongoing strain, which sometimes leads to thinning as the surface area increases (Lai *et al.* 2016). If critical thresholds in the rate of strain are exceeded, cuticular failure occurs; microcracks develop that compromise the cuticle’s barrier function. Moreover, exposure of the strained cuticle to surface moisture, or even just to high humidity, can exacerbate microcracking in a number of fruit crop species, including apple (Knoche & Grimm 2008; Knoche *et al.* 2011) and sweet cherry (Knoche & Peschel 2006). Incidentally, extended periods of surface wetness or high humidity are also conducive to this russetting (Tukey 1959; Creasy 1980; Winkler *et al.* 2014).

Microcracking of the cuticle is the first step in the development of a number of fruit skin disorders, including shrivelling (Knoche *et al.* 2019), macrocracking (Schumann *et al.* 2019), russetting (Faust & Shear, 1972a,b; Winkler *et al.* 2014) and skin spotting (Grimm *et al.* 2012; Winkler *et al.* 2014). Taken together, these skin disorders are of considerable commercial importance. Although in most cases they do not affect the nutritional quality of the fruit or the taste, etc., they do affect fruit appearance and so compromise fruit value at the point of sale.

Many fruit crop species are capable of repair processes that restore the functionality of the damaged cuticle barrier (Knoche & Lang 2017). For example, in russetting, a periderm is formed in the subtending hypodermal layer when the cuticular surface is breached by multiple microcracks (Meyer 1944; Faust & Shear, 1972a,b). The phellogen divides and produces stacks of cork cells that replace the barrier function of the primary surface. From a biological perspective, the formation of a periderm is beneficial as it restores (in part at least) the lost barrier functions of the primary surface in respect to the passage of water (Khanal *et al.* 2019). Unfortunately, the rough, brownish appearance of a russeted fruit usually leads to its downgrading and even rejection in high-end markets.

A second repair process is the deposition of wax in the microcracks. The filling of cracks with wax has been documented using scanning electron microscopy (SEM) for apple fruit surfaces on a number of occasions (Roy *et al.* 1999; Curry 2009; Curry & Arey 2010). In contrast to russetting, such wax deposition does not involve a morphological change in skin structure. Hence, this process is more rapid than the formation of a periderm. In addition, wax deposition in the strained cutin polymer alleviates stress by strain fixation (Khanal *et al.* 2013a). It is known that microcracks increase the water vapour permeance of the apple fruit surface (Maguire *et al.* 1999), but whether this secondary wax deposition and filling of microcracks completely restores the barrier properties of the fruit skin is not known. Also, it is not known, whether a filling of wax alters the subsequent susceptibility of the fruit surface to russetting.

The objectives of this study were: (a) to establish the effect of surface moisture on the formation of microcracks and the permeance of the skin to water vapour in developing apple fruit, and (b) to identify the effects of repair processes thereon. Because of the significance of russetting in commercial apple fruit production, (c) the relationship between microcracking and russetting was also quantified.

MATERIAL AND METHODS

Plant material

'Pinova' apple (*Malus × domestica* Borkh.) grafted on M9 rootstocks were grown in the experimental orchards of the Horticultural Research Station of Leibniz University in Ruthe, Germany (52° 14' N, 09° 49' E). Trees were cultivated according to the current regulations for integrated fruit production.

Fruit growth measurement

Fruits were sampled at 1- to 3-week intervals between full bloom and maturity (two fruits per tree, one from each side, for a total of 15 trees). Fruit mass was determined using a digital balance and fruit diameter was calculated from fruit mass, assuming a spherical shape and a density of 1. A sigmoidal regression model was fitted through the plot of fruit surface area *versus* time. Surface area growth rate ($\text{cm}^2 \cdot \text{day}^{-1}$) was calculated as the first derivative of this regression model. The relative growth rate at any time ($\text{cm}^2 \cdot \text{cm}^{-2} \cdot \text{day}^{-1}$) was obtained by dividing the growth rate at that time by the surface area at that time.

Moisture treatment

Fruits, free of visual defects, were selected and tagged at representative stages of development. For the moisture treatment, a polyethylene tube (8-mm inner diameter) was cut from the tip of a disposable Eppendorf reaction tube and glued to the fruit surface in the equatorial plane using fast-curing silicone rubber (Silicone RTV; Dow Toray, Tokyo, Japan).

After curing, tubes were filled with 1 ml deionized water using a disposable syringe. The hole in the tip of the tube was then sealed with silicone rubber. The tubes were inspected every 2 days and resealed when necessary. A untreated area in the equatorial region – usually opposite the tube – was left unprotected (without tube) on the same fruit and served as control.

To assure that water and not the tube was causal in inducing microcracking and subsequent russetting, an independent control experiment was conducted with three treatments: untreated control (no tube, no water), control with tube attached without water (with tube, no water), moisture treatment (with tube, with water). To prevent the accumulation of high humidity or rainwater inside the tube, the tube was cut in half and the cylindrical, non-tapered portion was glued to the equatorial surface of the fruit at 28 days after full blooming (DAFB). The tube was left open. After 12 days, the tubes were removed. Digital photographs of the surface of developing fruits were taken at 105 DAFB to document the presence or absence of a periderm.

The time course of moisture-induced microcracking was studied beginning at 29 DAFB. The duration of moisture exposure was 0, 2, 4, 8 or 12 days. Thereafter, the tubes were removed from the surface. The tubes detached very easily, there was no physical stress or damage to the fruit surface associated with tube removal. The effect of development stage on moisture-induced microcracking was studied beginning at 23, 44, 73 or 100 DAFB over 12-day periods of moisture exposure. Moisture-treated fruits were either harvested immediately after treatment or left on the tree to monitor the progress of any repair processes of the microcracked surfaces or to assess the extent of russetting at maturity. The fruits were processed immediately on the day of harvest or held overnight at 2 °C and 95% RH.

Water vapour permeance

The loss of water vapour through excised skin segments (ES) was quantified using stainless steel diffusion cells similar to those described by Geyer & Schönherr (1988). The ES (1.0- to 1.5-mm thick) were excised from the moisture-treated area or a untreated control area in the equatorial plane of the fruit. The cut surface of the ES was carefully blotted using soft tissue paper. The ES were then mounted on the diffusion cells using high-vacuum grease (Korasilon-Paste; Kurt Obermeier, Bad Berleburg, Germany). Diffusion cells were filled with deionized water through a port in the base and then sealed using clear transparent tape (Tesa film; Beiersdorf, Norderstedt, Germany). Following equilibration overnight, diffusion cells were incubated in a polyethylene box containing freshly dried silica gel at 24 °C. The diffusion cells in the polyethylene box were placed upside down on a metal grid such that the ES faced the silica gel. The amount of water loss from the diffusion cells was

quantified gravimetrically by weighing cells at regular intervals up to 4.5 h or 8.0 h. The rate of water loss (F in $\text{g}\cdot\text{h}^{-1}$) was obtained as the slope of a linear regression line fitted through a plot of cumulative transpiration *versus* time. The permeance (P ; $\text{m}\cdot\text{s}^{-1}$) of the ES was calculated using the following equation:

$$\text{Permeance}(P) = \frac{F}{(\Delta C \times A)}$$

In this equation, F represented the flow rate ($\text{g}\cdot\text{h}^{-1}/3600$) of water vapour, A the area of the transpiring surface of the ES (m^2) and ΔC the difference in water vapour concentration between the inside and the outside of the diffusion cells ($\text{g}\cdot\text{m}^{-3}$). Because the water vapour concentration above dry silica gel is close to zero (Geyer & Schönherr 1988), the water vapour concentration at saturation at 24 °C ($21.8 \text{ g}\cdot\text{m}^{-3}$; Nobel 1999) represents the driving force for transpiration.

Microcracks

Microcracking of the cuticle was followed using the fluorescent tracer acridine orange. Fruits were dipped in a 0.1% (w/w) aqueous solution of acridine orange (Carl Roth, Karlsruhe, Germany) for 10 min. Subsequently, fruits were removed from the solution, rinsed with deionized water and blotted using soft tissue paper. Fruits were viewed under a fluorescence binocular microscope (MZ10F; Leica Microsystems, Wetzlar, Germany). Calibrated images of the moisture-exposed and of the untreated control regions were prepared under incident fluorescence light (Camera DP71; GFP-plus filter, 480–440 nm excitation, ≥ 510 nm emission wavelength). Three to four images per fruit and per treatment (control *versus* moisture treatment) were taken on a total of seven to ten fruits. The area infiltrated by the acridine orange solution was quantified using image analysis (Cell^P; Olympus Europa, Hamburg, Germany). Under the above-mentioned conditions, tissue infiltrated with acridine orange exhibits yellow and green fluorescence. Following setting of appropriate colour thresholds, all images were processed using the same thresholds. The areas exhibiting yellow and green fluorescence were quantified.

Using the experimental setup described above, the time course for different moisture exposure durations at 29 DAFB, the developmental time course of a 12-day moisture exposure period imposed at 23, 44, 73 or 100 DAFB and the recovery time courses following a 12-day moisture exposure that began at 23, 44, 73 or 100 DAFB were studied.

Russetting

Developing fruits exposed to moisture were tagged and harvested at 159 DAFB, when the fruit was fully mature. To identify the region treated with surface moisture through until harvest, the area of skin included within the tube was marked when the tube was removed by applying four dots on the fruit surface at approximately equal intervals around the perimeter using a black permanent marker. Calibrated images of the portion of the fruit surface that was exposed to moisture were taken (Canon EOS 550D, lens: EF-S 18-55 mm, Canon Germany, Krefeld, Germany). Images of the untreated surface on

the same fruit served as control. The proportion of russeted area was quantified with image analysis (software package Cell^P; Olympus).

Statistical analysis

Data are presented as means \pm SE. Where error bars are not visible, they were smaller than the data symbols. Pairwise *t*-tests and regression analyses were carried out using the statistical software package SAS (version 9.1.3; SAS Institute, Cary, NC, USA). Significance of the coefficient of determination at 0.05, 0.01 and 0.001 is indicated by *, ** and ***, respectively.

RESULTS

Fruit mass and surface area increased in a sigmoidal pattern with time (Fig. 1). The growth rate in surface area reached a maximum of $1.6 \text{ cm}^2\cdot\text{day}^{-1}$ at about 77 DAFB (Fig. 1 upper left inset). The relative area growth rate (the rate of expansion per unit surface area) was maximal at the start of fruit development and decreased thereafter (Fig. 1 lower right inset).

The cumulative water loss through the ES exposed to moisture for up to 12 days increased linearly with time, indicating a constant rate of water loss (Fig. 2). The rate of water loss from an ES after 12 days of exposure to surface moisture was five-times higher than from a untreated control (Fig. 2).

When exposed to moisture at 29 DAFB, skin permeance increased rapidly, whereas the skin permeance of a untreated control surface on the same fruit decreased only slightly. After 2 days of moisture exposure (31 DAFB), the permeance increase was significant compared to the untreated control. After 8 days of moisture exposure (37 DAFB), the permeance reached a maximum and remained constant thereafter up to 12 days (41 DAFB), when the moisture treatment was terminated (Fig. 3a).

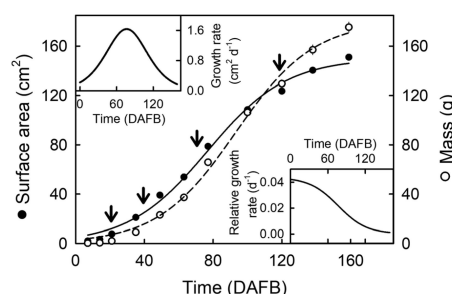


Fig. 1. Time course of changes in surface area and mass in developing 'Pinova' apple (main graph). The equations for the sigmoidal regression models were: Surface area (cm^2) = $180.26/(1 + \exp(-(\text{time}(\text{DAFB}) - 93.19)/22.77))$; $R^2 = 0.99$, Mass (g) = $150.12/(1 + \exp(-(\text{time}(\text{DAFB}) - 76.80)/22.96))$; $R^2 = 0.99$. Insets: Surface area growth rate (inset upper left corner) and relative surface area growth rate (inset lower right corner) in developing fruit. Arrows indicate the development stages when moisture treatments were imposed. Data represent mean \pm SE, $n = 30$, x-axis scale in days after full bloom (DAFB).

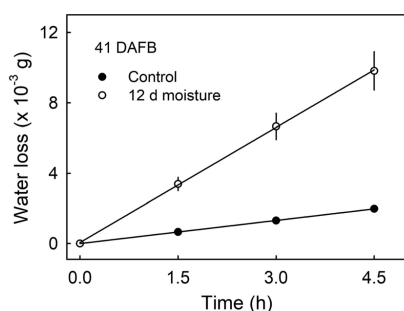


Fig. 2. Time course of water loss through excised skin segments (ES) of apple fruit exposed to moisture for 12 days, beginning at 29 days after full bloom (DAFB) until 41 DAFB. ES from the untreated surface of the same fruit served as control. Data represent mean \pm SE of 15 fruits.

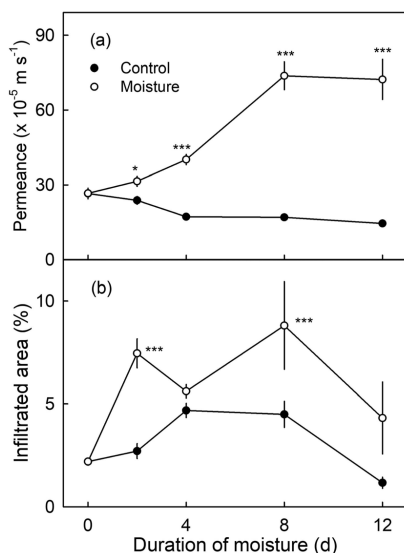


Fig. 3. Permeance (a) and acridine orange infiltrated area (b) as affected by the duration of exposure of the fruit surface to moisture. The surface was exposed to moisture beginning at 29 days after full bloom (DAFB) until 41 DAFB. Untreated surface of the same fruits served as control. Values represent mean \pm SE, $n = 12$ –15 (a) or 7–10 (b). * and *** indicate significant difference between control and moisture treatment at $P < 0.05$ and 0.001, respectively.

Moisture treatment increased the area infiltrated by acridine orange, indicating increased microcracking of the fruit surface. After 2 days of moisture treatment (31 DAFB), numerous, small, spot-like microcracks appeared (Fig. 4a–d). After 8 days, networks of long, wide microcracks had formed which were all infiltrated by the acridine orange (Fig. 4e,f). After 12 days, the area of infiltration of microcracks with acridine orange was reduced; many microcracks were visible, but they were not infiltrated by acridine

orange (Fig. 4g–j). Quantifying the areas infiltrated by acridine orange indicates that the extent of infiltration varied markedly with time. At all times, the infiltrated areas were larger for moisture-treated fruit than for untreated control fruit (Fig. 3b).

When fruits were treated with moisture for 12 days at later stages of development (44 to 56 DAFB, 73 to 85 DAFB and 100 to 112 DAFB), the increases in permeance due to moisture treatment were markedly smaller, but they were still significant relative to the controls, even between 100 and 112 DAFB (Fig. 5a). Also, the area infiltrated by acridine orange was largest when young fruits (from 23 to 35 DAFB) were treated with moisture. At later stages of development (44 to 56 DAFB, 73 to 85 DAFB or 100 to 112 DAFB), the effect of moisture was smaller and not significant (Fig. 5b).

Interestingly, following the moisture treatment of young fruit from 23 to 35 DAFB, skin permeance continued to increase and peaked at about 49 DAFB; this was 14 days after termination of the moisture treatment. Thereafter, permeance decreased rapidly within 28 days, but remained significantly higher than the untreated controls (Fig. 6a). The change in area infiltrated by acridine orange essentially mirrored the change in permeance (Fig. 6b).

Performing the same experiment, but at later stages of fruit development, resulted in similar qualitative changes, *i.e.* decreases in permeance, but at markedly reduced levels following termination of the moisture treatment (Fig. 6a inset, b inset). Recovery of permeance was complete when microcracks were induced by moisture treatments between 73 to 85 DAFB and 100 to 112 DAFB, but not between 44 and 56 DAFB. As during early microcrack induction, the permeance remained higher in the moisture-treated fruits than in the untreated controls.

Monitoring infiltration of the ES with acridine orange revealed the same general trends – a transient increase in the infiltrated area up to about 49 DAFB (Fig. 7a,b). At this time, a dense network of open cracks had formed (Fig. 7c,d); the infiltrated area then decreased (Fig. 6b). The microcracks remained visible but they were not infiltrated by acridine orange (Fig. 7e–h). The fruits which were treated with moisture at 23 to 35 DAFB developed a significant amount of russet (Table 1, Fig. 8). There was no russet in the two control treatments regardless of the presence of the tube on the fruit surface, indicating that water exposure and not the tube was causal in russet formation (Fig. 8). Fruits which were treated at later stages of development (44 to 56 DAFB, 73 to 85 DAFB and 100 to 112 DAFB) did not produce russet at maturity (Table 1).

Across all development stages, permeances of fruit skins and the areas infiltrated by the fluorescent tracer acridine orange were positively related (Fig. 9). The regression equation for the relationships was:

$$\text{Permeance (} \times 10^{-5} \text{ m} \cdot \text{s}^{-1}\text{)} = 8.3 (\pm 0.7) \times \text{Area (\%)} - 4.6 (\pm 2.4); R^2 = 0.78***, n = 40.$$

DISCUSSION

The most important findings of our study were:

- 1 A rapid increase in apple fruit skin microcracking and a corresponding increase in water vapour permeance in response to surface moisture.

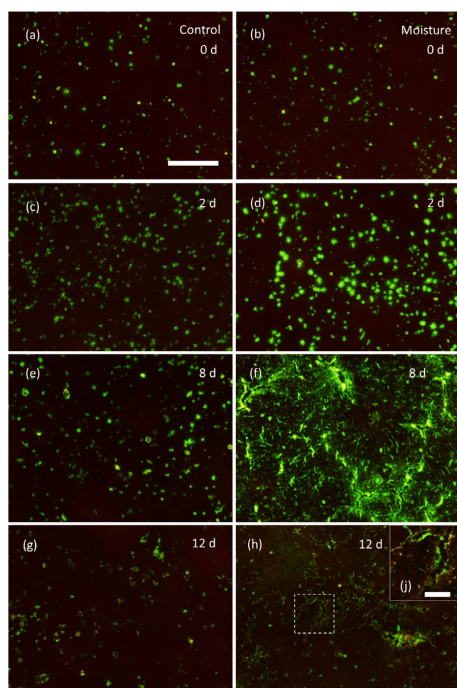


Fig. 4. Microscope images of fruit surfaces prepared after 10 min infiltration with a 0.1% aqueous solution of acridine orange. The surface was exposed to moisture beginning at 29 days after full bloom (DAFB) for 0 (b), 2 (d), 8 (f) or 12 (h) days. An untreated surface of the same fruit served as control (a, c, e, g). The image in (i) represents the magnified view of the area in (h) enclosed by the dotted rectangle. The scale bar (400 μm) in (a) is representative of images (b) to (f) of the composite. Scale bar in (i) = 100 μm .

- 2 A marked decrease (with some delay) in both microcracking and permeance following the termination of a moisture treatment; both values gradually approaching the control values.
- 3 A consistent effect of development stage on skin responses to exposure to moisture in terms of microcracking, of water vapour permeance and of russetting.

Microcracking and permeance to water vapour increase rapidly during and beyond the period of exposure to surface moisture

The effect of surface moisture observed in our *in vivo* study confirms earlier reports obtained *in vitro* using excised skin segments (Knoche & Grimm 2008; Knoche *et al.* 2011). As in earlier studies, the extent of moisture-induced microcracking depended markedly on the stage of fruit development (Knoche *et al.* 2011). Whole fruits and ES were most sensitive during early development (Wertheim 1982). During this stage, the growth strains are high as determined by the high relative area growth rates (Skene 1980; Lai *et al.* 2016).

Further indirect evidence for a relationship between russet and growth strain comes from studies in European pear (*Pyrus communis*), where a higher incidence of russet on the cheek as compared to the neck has been attributed to higher growth rates (Scharwies *et al.* 2014). Earlier studies established that the cuticle suffers from lower fracture strains compared to the underlying cellular layers of the dermis (Khanal & Knoche 2014), and that the fracture pattern of the cuticle is determined by the underlying cellular layers (Knoche *et al.* 2018). This is because the epidermal and hypodermal cell layers, and not the cuticle, represent the structural backbone of the apple fruit skin (Khanal & Knoche 2014). These arguments further suggest that microcracking, and the effect of surface moisture thereon, are also affected by the underlying cellular layers. It may be speculated that a swelling of anticlinal cell walls facilitates cell-to-cell separation along the abutting anticlinal walls as cell shape changes during growth from 'portrait' to 'landscape' (Meyer 1944; Maguire *et al.* 1999; Knoche *et al.* 2018). In sweet cherry, the swelling of cell walls reduces cell-to-cell adhesion, causing epidermal cells to partially separate at low rates of strain (Brüggenwirth & Knoche 2017). Whether this also applies for moisture-induced microcracking of apple fruit skin remains to be shown. The effect of moisture may be further exacerbated by decreases in the cuticle's fracture force and fracture strain due to hydration; this has often been reported for isolated cuticles (Knoche & Peschel, 2006; Khanal *et al.*, 2013b). In addition, surface wetness and high RH both decrease the biosynthesis and deposition of wax (Shepherd & Griffiths, 2006) and possibly also of cutin; this may lead to a thinner and mechanically weaker cuticle. However, direct evidence for effects of surface wetness and/or humidity on cutin and/or wax deposition in apple is lacking.

The changes in permeance observed in skins exposed to surface moisture throughout our study were a linear function of the extent of microcracking, as recorded by the areas infiltrated by acridine orange. This confirms an earlier report for Braeburn apples (Maguire *et al.* 1999).

It is interesting to note that the increase in microcracking and in water vapour permeance induced by surface moisture extended, and even increased further, well beyond the time when the surface moisture treatment was terminated. This observation is probably due to the ongoing growth strains causing gaping of the microcracks, before the cuticular repair processes were sufficiently active.

It could be argued that the moisture-induced russet is an artefact caused by the silicone and/or the Eppendorf tube. However, the following considerations make this possibility highly unlikely. First, when developing this technique, we also applied surface moisture using wet paper towels or wet tissue paper, or medical patches soaked and filled with water. All these rested loosely onto the fruit surface. These techniques were all equally effective in inducing russetting. However, these approaches were abandoned here because they were unreliable under field conditions. Second, natural moisture-induced microcracking and russetting can be seen in the stem cavity of most apple cultivars. During rain, the stem cavity fills with water. The area of skin beneath the 'puddle' so formed, remains wet for an extended period after the rain has stopped. Third, moisture-induced russetting has often been observed under field conditions (Tukey 1959; Creasy 1980); this is consistent with the findings reported herein. Fourth, we also

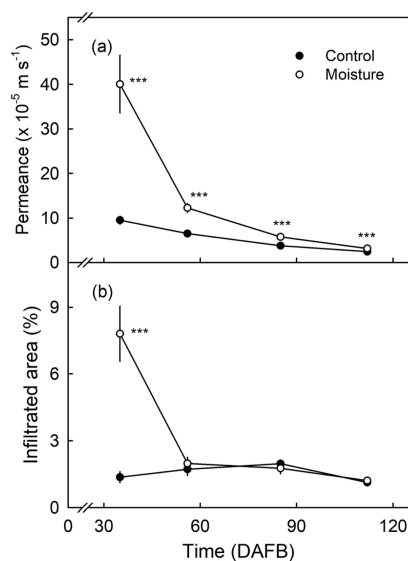


Fig. 5. Effect of surface moisture on permeance (a) and microcracking as shown by the area infiltrated by acridine orange (b) during fruit development. A selected area of the surface of a developing fruit was exposed to moisture for 12 days at four different stages of fruit development (from 23 to 35 days after full bloom (DAFB), 44 to 56 DAFB, 73 to 85 DAFB or 100 to 112 DAFB). The water vapour permeances and the surface areas infiltrated by acridine orange were quantified immediately after termination of the moisture treatment. Values represent mean \pm SE of 18–20 (a) and 7–10 fruits (b). *** indicates significant difference between control and moisture treatment at $P < 0.001$.

observed moisture-induced microcracking of the cuticle in earlier studies using excised epidermal segments of the apple fruit skin (Knoche & Grimm 2008). Fifth, if the silicone and/or the Eppendorf tube restricted growth, the fruit would be visibly deformed – it was not. Also, it would not be necessary to repeatedly reseal the tube to maintain surface wetness. The silicone we used attaches only very loosely to the fruit surface; it is thus very easily removed, without physical stress or damage to the fruit skin. Sixth, an empty tube (cylindrical, cut to only half length and left open) glued on the fruit did not produce any russet. Last, neither the silicone used nor the polyethylene Eppendorf tube release any chemicals that are phytotoxic. These arguments exclude possible artefacts due either to the silicone or to the Eppendorf tube.

For routine experimentation, we preferred to not mount empty tubes as control treatments. An empty tube may result in elevated humidity inside the tube and this would likely have induced microcracking and russetting (Knoche & Grimm 2008). Furthermore, condensation would likely have formed on the enclosed skin area due to the widely fluctuating temperatures in the field. Thus, unprotected exposure to the atmosphere (no tube) was selected as the most appropriate control.

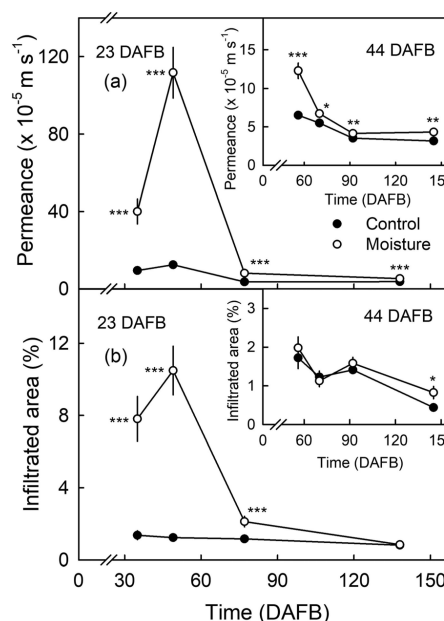


Fig. 6. Change in the permeances (a) main and inset) and acridine orange infiltrated areas (b) main and inset) of moisture-treated surfaces of developing fruits with time after termination of the moisture treatment. A selected portion of the fruit surface was exposed to moisture for 12 days, from 23 days after full bloom (DAFB) to 35 DAFB (main graphs) and from 44 DAFB to 56 DAFB (insets). Fruits were sampled at various stages of fruit development and the permeances and acridine orange-infiltrated areas of the fruit surface were quantified. Values represent mean \pm SE of 18–20 (a, a inset) and 7–10 fruits (b, b inset). *, **, *** indicate significant difference between control and moisture treatment at $P < 0.05$, 0.01 and 0.001, respectively.

Microcracking and permeance to water vapour decrease after removal of surface moisture

Our results demonstrate that following microcracking, fruit surface integrity recovers as demonstrated by parallel decreases in acridine orange infiltration and in water vapour permeance. Within 4 weeks of exposure to surface moisture, the barrier function was largely restored. Nevertheless, water vapour permeance remained slightly and significantly higher than in control fruit. Some microcracks remained visible but were not infiltrated by acridine orange. The decrease in the area of skin infiltrated by acridine orange was proportional to the decrease in skin permeance. The basis of this recovery effect may be twofold, as described below.

First, a likely candidate process is the deposition of wax in the microcracks. Indirect evidence comes from SEM images that show microcracks filled with wax crystals (Roy *et al.* 1999; Curry 2009; Curry & Arey 2010; Konarska 2013). Unfortunately, an attempt to gain direct quantification of microcrack infilling by wax crystals using interferometry was not successful

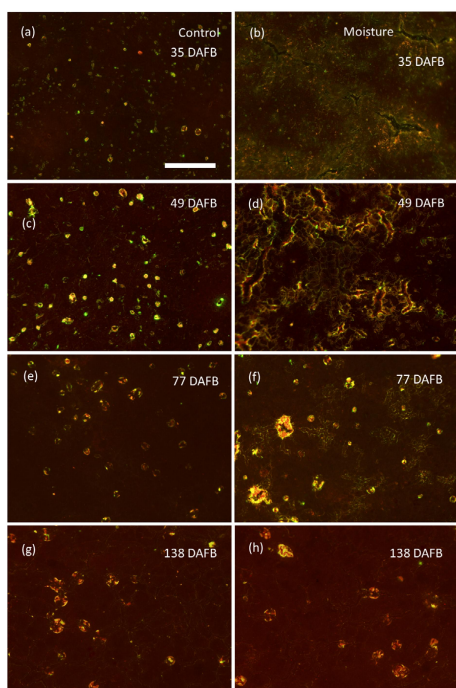


Fig. 7. Time course of changes in microcracking as recorded by acridine orange infiltration of the surface of developing apple fruit. Fruits were exposed to moisture for 12 days from 23 days after full bloom (DAFB) to 35 DAFB. Images were prepared from moisture-treated (b, d, f, h) and untreated (a, c, e, g) surfaces of the same fruit. The scale bar (400 μm) in (a) is representative of all images of the composite figure.

due to the high variability of microcracking over the apple fruit surface (B.P. Khanal, unpublished data). The wax that fills the microcracks in the cuticle surface is not necessarily derived from *de novo* synthesis in the epidermis and subsequent diffusion to the surface. Instead, wax deposition in microcracks is thought more likely derived from a redistribution of wax already within the cuticle. This view is based on the observation that wax is a highly dynamic structure that re-assembles itself if

Table 1. Effect of fruit development on surface moisture-induced russetting in 'Pinova' apple. Surface moisture was applied for 12 days at four stages of fruit development. The areas of russetting on the treated and untreated surfaces were quantified at harvest maturity. $n = 21$, DAFB = days after full bloom.

Stage of development (DAFB)	Frequency of fruit with russet (%)	Russeted area (% of treated area)	
		Moisture	Control
23 to 35	100	37.1 \pm 7.3	0
44 to 56	0	0	0
73 to 85	0	0	0
100 to 112	0	0	0

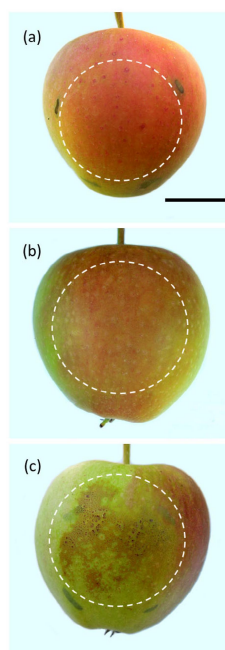


Fig. 8. Russet formation in 'Pinova' apple 105 days after full bloom (DAFB). (a) Untreated control fruit without tube and without water; (b) untreated control fruit with tube, but without water; (c) moisture-treated fruit with tube and with water. The tubes were mounted 28 DAFB, left on the fruit for 12 days and then removed. The dashed circle marks the original footprint of the tube. The moisture treatment, but neither of the two controls revealed marked russetting. The scale bar (2 cm) in (a) is representative of all images of the composite picture. For details see the Material and methods.

its structure is disturbed – either mechanically or by heat (Neinhuus *et al.* 2001; Koch *et al.* 2004). Also, the decrease in water vapour permeance of cuticles during storage has

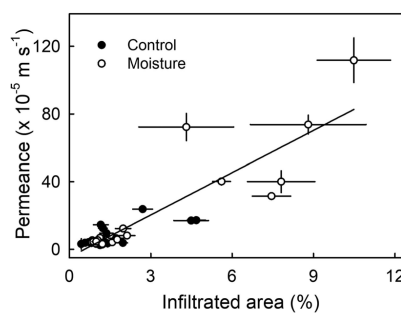


Fig. 9. Relationship between permeances and acridine orange infiltrations of the surface of apple fruits at various stages of development. Open circles are for moisture-treated skins, closed circles for untreated skins. Values represent mean \pm SE of 12–20 (permeance) and 7–10 (infiltrated area) fruits.

previously been attributed to a recrystallization of pre-existing wax (Geyer & Schönherr 1990). This behaviour is also consistent with its function during growth as a filler in the cutin polymer (Knoche *et al.* 2018).

Second, the formation of a subtending periderm in response to cuticular microcracking may also contribute to a decrease in microcracking and in water vapour permeance. However, the water vapour permeance of the periderm remains significantly higher than that of the cuticle on the primary surface (Khanal *et al.* 2019).

Effect of fruit development on microcracking, water vapour permeance and russetting

The effect of surface moisture on cuticular microcracking, skin permeance and russetting is consistent with the view that microcracking is the first visible symptom of cuticular damage, with increased permeance being the immediate consequence and this the probable trigger for russetting. Because surface moisture-induced microcracking is substantially limited to the early stages of fruit development, so susceptibility to russetting is also highest during the early stages of fruit development (Wertheim 1982). In the later stages of fruit development, apple fruit skin does not respond to the presence of surface moisture to nearly the same extent – in respect either to microcracking or to russetting.

The decrease in the response to surface moisture with increasing fruit maturity may be a characteristic of the cultivar 'Pinova' fruit investigated here. We note that in 'Elstar'

apples, late-season exposure to surface moisture results in a skin spot disorder and this is also a consequence of surface-moisture-induced microcracking (Grimm *et al.* 2012; Winkler *et al.* 2014).

The relationship between exposure to surface moisture and microcracking of apple fruit skin is important from a practical point of view. Because of their high capital and maintenance costs, the provision of rain shelters for apples is uneconomic. Instead, the method of choice to decrease the duration of surface moisture and, hence, the incidence of microcracking is to train the apple orchard to an open canopy structure. This could be augmented by a typical gibberellin (GA₃ or GA₄₊₇) spray application programme that works to minimize cuticular microcracking (Knoche *et al.* 2011) and russetting (Wertheim 1982).

ACKNOWLEDGEMENTS

We thank Friederike Schroeder and Simon Sitzenstock for technical support, and Andreas Winkler and Sandy Lang for helpful comments on an earlier version of this manuscript. This research was funded in part by a grant from the Deutsche Forschungsgemeinschaft.

AUTHOR CONTRIBUTIONS

M.K. and B.P.K. designed the research, Y.I., B.P.K., Y.H.C. and J.S. performed the experiments. B.P.K., Y.I. and M.K. analysed the data. B.P.K. and M.K. wrote the manuscript.

REFERENCES

- Brüggenwirth M., Knoche M. (2017) Cell wall swelling, fracture mode, and the mechanical properties of cherry fruit skins are closely related. *Planta*, **245**, 765–777.
- Creasy L.L. (1980) The correlation of weather parameters with russet of 'Golden Delicious' apples under orchard conditions. *Journal of the American Society for Horticultural Science*, **105**, 735–738.
- Curry E.A. (2009) Growth-induced microcracking and repair mechanism of fruit cuticles. Proceedings of the SEM Annual Conference, June 1–4. Albuquerque, New Mexico, USA. 18. December 2019 <https://stud.yres.com/doc/22675171/growth-induced-microcracking-and-repair-mechanisms-of-fruit>
- Curry E., Arey B. (2010) Apple cuticle – The perfect interface. In: Postek M.T., Newbury D.E., Platek S.F., Joy D.C. (Eds), *Scanning Microscopy*. Proceedings of SPIE 7729:77291P-1-77291P-11. <https://doi.org/10.1117/12.853913>
- Dominguez E., Heredia-Guerrero J.A., Heredia A. (2011) The biophysical design of plant cuticles: an overview. *New Phytologist*, **189**, 938–949.
- Faust M., Shear C.B. (1972a) Russetting of apples, an interpretive review. *HortScience*, **7**, 233–235.
- Faust M., Shear C.B. (1972b) Fine structure of the fruit surface of three apple cultivars. *Journal of the American Society for Horticultural Science*, **97**, 351–355.
- Geyer U., Schönherr J. (1988) In vitro test for effects of surfactants and formulations on permeability of plant cuticles. In: Cros B., Scher H. B. (Eds), *Pesticide Formulations: Innovations and Developments*. American Chemical Society, Washington, USA 22–33.
- Geyer U., Schönherr J. (1990) The effect of the environment on the permeability and composition of citrus leaf cuticles. I. Water permeability of isolated cuticular membranes. *Planta*, **180**, 147–153.
- Grimm E., Khanal B.P., Winkler A., Knoche M., Köpcke D. (2012) Structural and physiological changes associated with the skin spot disorder in apple. *Postharvest Biology and Technology*, **64**, 111–118.
- Guan Y., Chang R., Liu G., Wang Y., Wu T., Han Z., Zhang X. (2015) Role of lenticels and microcracks on susceptibility of apple fruit to *Botryosphaeria dothidea*. *European Journal of Plant Pathology*, **143**, 317–330.
- Kerstiens G. (1996) Cuticular water permeability and its physiological significance. *Journal of Experimental Botany*, **47**, 1813–1832.
- Khanal B.P., Grimm E., Finger S., Blume A., Knoche M. (2013a) Intracuticular wax fixes and restricts strain in leaf and fruit cuticles. *New Phytologist*, **200**, 134–143.
- Khanal B.P., Grimm E., Knoche M. (2013b) Russetting in apple and pear: a plastic periderm replaces a stiff cuticle. *AoB PLANTS*, **5**, pls048. <https://doi.org/10.1093/aobpla/pls048>
- Khanal B.P., Ikigu G.M., Knoche M. (2019) Russetting partially restores apple skin permeability to water vapour. *Planta*, **249**, 849–860.
- Khanal B.P., Knoche M. (2014) Mechanical properties of apple skin are determined by epidermis and hypodermis. *Journal of the American Society for Horticultural Science*, **139**, 139–148.
- Knoche M., Grimm E. (2008) Surface moisture induces microcracks in the cuticle of 'Golden Delicious' apple. *HortScience*, **43**, 1929–1931.
- Knoche M., Grimm E., Winkler A., Alkio M., Lorenz J. (2019) Characterizing neck shrivel in European plum. *Journal of the American Society for Horticultural Science*, **144**, 38–44.
- Knoche M., Khanal B.P., Brüggewirth M., Thapa S. (2018) Patterns of microcracking in apple fruit skin reflect those of the cuticular ridges and of the epidermal cell walls. *Planta*, **248**, 293–306.
- Knoche M., Khanal B.P., Stopar M. (2011) Russetting and microcracking of 'Golden Delicious' apple fruit concomitantly decline due to Gibberellin A₄₊₇ application. *Journal of the American Society for Horticultural Science*, **136**, 159–164.
- Knoche M., Lang A. (2017) Ongoing growth challenges fruit-skin integrity. *Critical Reviews in Plant Sciences*, **36**, 190–215.
- Knoche M., Peschel S. (2006) Water on the surface aggravates microscopic cracking of the sweet cherry fruit cuticle. *Journal of the American Society for Horticultural Science*, **131**, 192–200.
- Koch K., Neinhuis C., Ensikat H.J., Barthlott W. (2004) Self-assembly of epicuticular waxes on living plant surfaces imaged by atomic force microscopy (AFM). *Journal of Experimental Botany*, **55**, 711–718.
- Konarska A. (2013) The structure of the fruit peel in two varieties of *Malus domestica* Borkh. (Rosaceae) before and after storage. *Protoplasma*, **250**, 701–714.
- Lai X., Khanal B.P., Knoche M. (2016) Mismatch between cuticle deposition and area expansion in

- fruit skins allows potentially catastrophic buildup of elastic strain. *Planta*, **244**, 1145–1156.
- Maguire K.M., Lang A., Banks N.H., Hall A., Hopcroft D., Bennett R. (1999) Relationship between water vapour permeance of apples and microcracking of the cuticle. *Postharvest Biology and Technology*, **17**, 89–96.
- Meyer A. (1944) A study of the skin structure of 'Golden Delicious' apples. *Proceedings of the American Society for Horticultural Science*, **45**, 105–110.
- Neinhuis C., Koch K., Barthlott W. (2001) Movement and regeneration of epicuticular waxes through plant cuticles. *Planta*, **213**, 427–434.
- Nobel P.S. (1999) *Physicochemical & Environmental Plant Physiology*. Academic Press, San Diego, CA, USA.
- Roy S., Conway W.S., Watada A.E., Sams C.E., Erbe E.F., Wergin W.P. (1999) Changes in the ultrastructure of the epicuticular wax and postharvest calcium uptake in apples. *HortScience*, **34**, 121–124.
- Scharwies J.D., Grimm E., Knoche M. (2014) Russeting and relative growth rate are positively related in 'Conference' and 'Condo' pear. *HortScience*, **49**, 746–749.
- Schreiber L., Schönherr J. (2009) *Water and solute permeability of plant cuticles – Measurement and data analysis*. Springer, Berlin, Germany.
- Schumann C., Winkler A., Brüggewirth M., Köpcke K., Knoche M. (2019) Crack initiation and propagation in sweet cherry skin: a simple chain reaction causes the crack to 'run'. *PLoS One*, **14**, e0219794. <https://doi.org/10.1371/journal.pone.0219794>
- Shepherd T., Griffiths D.W. (2006) The effects of stress on plant cuticular waxes. *New Phytologist*, **171**, 469–499. <https://doi.org/10.1111/j.1469-8137.2006.01826.x>
- Skene D.S. (1980) Growth stresses during fruit development in Cox's Orange Pippin apples. *Journal of Horticultural Science*, **55**, 27–32.
- Skene D.S. (1982) The development of russet, rough russet and cracks on the fruit of the apple Cox's Orange Pippin during the course of the season. *Journal of Horticultural Science*, **57**, 165–174.
- Tukey L.D. (1959) Observations on the russeting of apples growing in plastic bags. *Proceedings of the American Society for Horticultural Science*, **74**, 30–39.
- Tukey H.B., Young J.O. (1942) Gross morphology and histology of developing fruit of the apple. *Botanical Gazette*, **104**, 3–25.
- Wertheim S.J. (1982) Fruit russeting in apple as affected by various gibberellins. *Journal of Horticultural Science*, **57**, 283–288.
- Winkler A., Grimm E., Knoche M., Lindstaedt J., Köpcke D. (2014) Late season surface water induces skin spot in apple. *HortScience*, **49**, 1324–1327.
- Yeats T.H., Rose J.K.C. (2013) The formation and function of plant cuticles. *Plant Physiology*, **163**, 5–20.

3. Russeting in apple is initiated after exposure to moisture ends—I. Histological evidence

Yun-Hao Chen¹, Jannis Straube², Bishnu P. Khanal¹, Moritz Knoche¹, Thomas Debener²




¹Institute of Horticultural Production Systems, Fruit Science Section, Leibniz University Hannover, Herrenhäuser Straße 2, 30419 Hannover, Germany

²Institute of Plant Genetics, Molecular Plant Breeding Section, Leibniz University Hannover, Herrenhäuser Straße 2, 30419 Hannover, Germany

Type of authorship:	Co-author
Type of article:	Research article
Contribution to the article:	J. Straube was involved in experimental design, field experiments, microscopic analysis and cuticle thickness measurements. In addition, J. Straube contributed to the analysis of the data and preparation of the figures.
Contribution of other authors:	Y.-H. Chen studied the histological changes that occur during russet formation, performed strain analysis, and contributed to writing, reviewing, and editing the manuscript. B.P. Khanal designed some of the experiments, observed microcrack formation, and contributed to writing, reviewing, and editing the manuscript. M. Knoche contributed to the conceptualization of the study and to writing, reviewing, and editing the manuscript. T. Debener supervised the experiments and contributed to conception of the study.
Journal	Plants
Date of publication:	30.09.2020
Impact factor:	4.658 (2021)
DOI:	10.3390/plants9101293

Article

Russeting in Apple Is Initiated After Exposure to Moisture Ends—I. Histological Evidence

Yun-Hao Chen ¹, Jannis Straube ², Bishnu P. Khanal ^{1,*} , Moritz Knoche ¹  and Thomas Debener ² 

¹ Institute of Horticultural Production Systems, Fruit Science Section, Leibniz University Hannover, Herrenhäuser Straße 2, 30419 Hannover, Germany; chen@obst.uni-hannover.de (Y.-H.C.); moritz.knoche@obst.uni-hannover.de (M.K.)

² Institute of Plant Genetics, Molecular Plant Breeding Section, Leibniz University Hannover, Herrenhäuser Straße 2, 30419 Hannover, Germany; straube@genetik.uni-hannover.de (J.S.); debener@genetik.uni-hannover.de (T.D.)

* Correspondence: khanal@obst.uni-hannover.de; Tel.: +49-511-762-9004

Received: 13 September 2020; Accepted: 28 September 2020; Published: 30 September 2020



Abstract: Russeting (periderm formation) is a critical fruit-surface disorder in apple (*Malus × domestica* Borkh.). The first symptom of insipient russeting is cuticular microcracking. Humid and rainy weather increases russeting. The aim was to determine the ontogeny of moisture-induced russeting in ‘Pinova’ apple. We recorded the effects of duration of exposure to water and the stage of fruit development at exposure on microcracking, periderm formation and cuticle deposition. Early on (21 or 31 days after full bloom; DAFB) short periods (2 to 12 d) of moisture exposure induced cuticular microcracking—but not later on (66 or 93 DAFB). A periderm was not formed during moisture exposure but 4 d after exposure ended. A periderm was formed in the hypodermis beneath a microcrack. Russeting frequency and severity were low for up to 4 d of moisture exposure but increased after 6 d. Cuticle thickness was not affected by moisture for up to 8 d but decreased for longer exposures. Cuticular ridge thickness decreased around a microcrack. In general, moisture did not affect cuticular strain release. We conclude that a hypodermal periderm forms after termination of moisture exposure and after microcrack formation. Reduced cuticle deposition may cause moisture-induced microcracking and, thus, russeting.

Keywords: russeting; periderm; *Malus × domestica*; surface moisture; cuticle; strain

1. Introduction

Russeting is a commercially important surface disorder of many fruit crop species, worldwide. Among other species affected are: apple [1], pear [2], grape [3] and prune [4]. The rough, brownish appearance of russeting renders a fruit unattractive to the consumer. Russeting also increases rates of postharvest moisture loss that lead to shriveling (fruit lose their fresh glossiness, so look old) and to higher rates of mass loss during storage, transport and retail (fruit are priced to the consumer on a per-kg basis) [5].

In anatomical terms, russeting represents a periderm comprising the phellem, a phellogen and a phelloderm [6,7]. The phellem cells (also referred to as cork cells) have suberized cell walls that are responsible for the dull and brownish color of a russeted fruit. These cork cells typically occur in stacks, resulting from division of the phellogen cells [8].

Information on how such a periderm is initiated in apple fruit skin is limited. Empirical evidence indicates that a range of factors may be involved. These include mechanical wounding [9], certain agrochemicals [10–12], epiphytic microorganism [13], insects (rust mites) [14] and diseases [15].

Of particular interest here is the effect of moisture on russeting in apple. Numerous studies indicate that exposure to surface wetness [16–18] or to high humidities [19] can be the cause of russeting in apple. Surface moisture, applied either as liquid-phase water or as vapor-phase water, induces microcracking in a number of fruit crop species, including apple [16]. Microcracks in the apple fruit skin are the first visible symptom of insipient russeting [20–22]. The mechanism of water-induced microcracking is not clear. It is possible that one of the factors is modification of the mechanical properties of the cuticle induced through changes in hydration [23].

We recently developed a system that reliably induces microcracking and russeting by local exposure of patches of the apple fruit surface to moisture [24]. Briefly, a length of tube is attached to the fruit surface using a non-phytotoxic silicone rubber. The tube is filled with water and periodically resealed to the fruit surface. The patch of skin included within the tube footprint first develops microcracks and, later, displays symptoms of russeting. These symptoms are microscopically identical to those observed on a fruit naturally exposed to surface moisture in the field. This system may be helpful in studying the mechanistic basis of russeting. It also avoids confusions associated with comparisons of different fruit genotypes or of different individual fruit or of different regions on the fruit surface. It allows critical comparisons to be made by imposing a moisture treatment to a defined patch of fruit skin, while an untreated (control) patch is defined in an equivalent region on the surface of the same fruit. It thereby allows standardization for a range of potential sources of response variability including stage of fruit development, differences in micro-environment, in orientation and in management (tree center vs. periphery etc.).

The specific objectives here were to identify the sequence of events that culminate in moisture-induced russeting. We were particularly interested to determine when and where a periderm is formed in relation to the location of moisture exposure. We focused on apple because apples are an important fruit crop species in both the northern and southern hemispheres and because russeting presents a problem to producers of this fruit crop.

2. Results

Following a 12 d exposure to moisture, a periderm had developed after an additional 8 d without moisture as indexed by stacks of fluorescing phellem cells visible in cross-sections of the skin (Figure 1). Furthermore, the typical russeting symptoms were visible at the fruit surface. There was no periderm and no russet visible in either of the moisture controls, regardless of the presence (or not) of the tube. Hence, we conclude that the periderm resulted from moisture exposure and not from the mounting of the tube. Because of this finding, there was no need to mount an empty tube as a control in subsequent experiments.

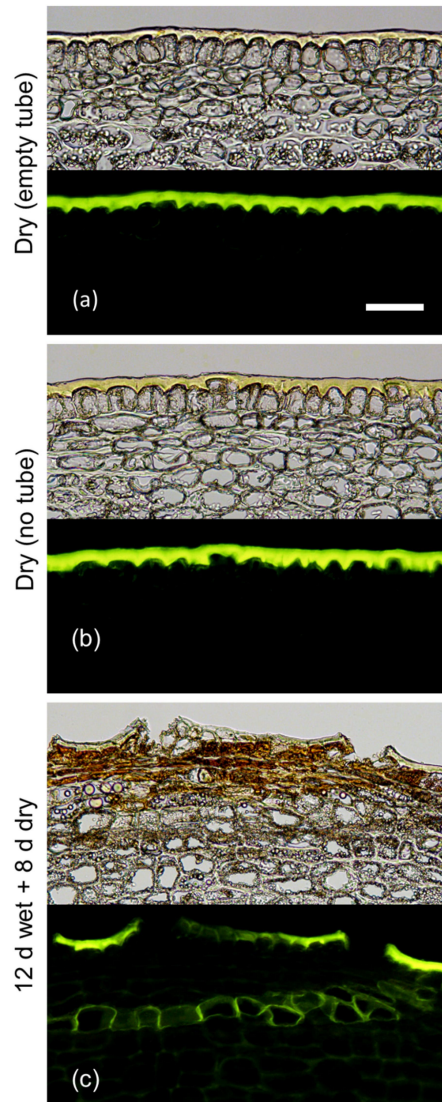


Figure 1. Effects of mounting tubes on the fruit surface without and with added moisture for 12 d, on the formation of periderm 8 d after removal of the tubes. (a) control that had a tube without water mounted for 12 d. (b) control without tube. (c) moisture treatment that had a tube containing water mounted for 12 d. The experiment comprised two phases: Phase I consisted of mounting the tube without or with water and Phase II marks the period after termination of moisture treatment. Micrographs taken under transmitted white light (upper) or incident fluorescent light (lower) (filter module U-MWB) following staining with Fluorol Yellow 088. The scale bar in (a) is 50 μm long and representative of all images in the composite ($n = 3$).

Moisture exposure of the fruit surface at the young stage induced microcracks in the cuticle as indexed by increased infiltration of the fluorescent tracer acridine orange (Figure 2). Moisture exposure periods of 2 to 12 d resulted in significantly higher acridine orange infiltration as compared to the non-exposed control (Phase I, Figure 2). When the moisture exposure was terminated, the area infiltrated with acridine orange decreased to a level similar to that of the non-treated control (Phase II). The only exception was at 8 d after termination of the moisture treatment. By this time, rainfall had occurred in the orchard (Phase II, Figure 2).

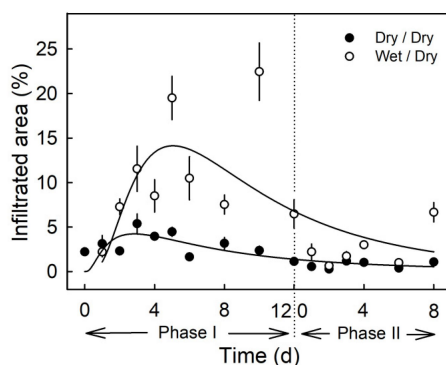


Figure 2. Time course of moisture-induced microcracking. Microcracking of the cuticle was indexed by quantifying the percentage of treated area infiltrated with acridine orange. The experiment comprised two phases: The first period of moisture exposure (Phase I) and the second period after termination of moisture exposure (Phase II). The end of Phase I and the beginning of Phase II is indicated by the dashed vertical line. The moisture treatment is referred to as ‘wet/dry’ and the control as ‘dry/dry.’ Data symbols present means \pm SE ($n = 6$ to 20).

During exposure to moisture (Phase I), there was no indication of periderm formation from microscopy of cross-sections stained with Fluorol Yellow 088, regardless of exposure duration (6 or 12 d; Figure 3). Microcracks had formed that traversed the cuticle. Following termination of moisture exposure (Phase II), a periderm developed by 4 d below the epidermis in the hypodermal cell layers. Periderm formation was indexed by stacks of cells that stained with Fluorol Yellow 088. These cells represented the typical cork cells (phellem) that originate from an underlying phellogen. There was no apparent difference between the periderms that formed after a 6 d or a 12 d period of moisture exposure.

Varying the duration of moisture exposure (Phase I) revealed that a minimum moisture period of 6 d was needed to induce a periderm within 4 d after moisture termination (Phase II). As in the previous experiment, there were no detectable changes in the fruit skin during moisture exposure except for the formation of microcracks. These were observed after 4 d of moisture exposure (Figure 4).

The frequency of russeted fruit and the percentage of russeted area were low for moisture exposures up to 4 d (Phase I) at the young stage (from 31 DAFB onwards) but increased markedly for moisture exposures of 6 d or longer. There was little difference in frequency of russeted fruit beyond 6 d moisture exposure (Figure 5a). However, the russeted areas continued to increase from 6 to 16 d of moisture exposure (Figure 5b). There was no moisture-induced russeting at maturity (156 DAFB), when surfaces were exposed to moisture for 12 d at 66 DAFB or at 93 DAFB ($n = 10$ –15; data not shown).

Fruit exposed to moisture for 12 d beginning at 31 DAFB had developed russet at maturity (156 DAFB) and a multistack phellem typical for russeted apples was visible (Figure 6). By maturity, the cuticle and the remains of the epidermis and hypodermis had sloughed off and the brown color of the periderm was fully exposed at the surface. Furthermore, the micromorphology of the

skin of moisture-treated fruit was identical to that of naturally russeted fruit of the same cultivar (data not shown).

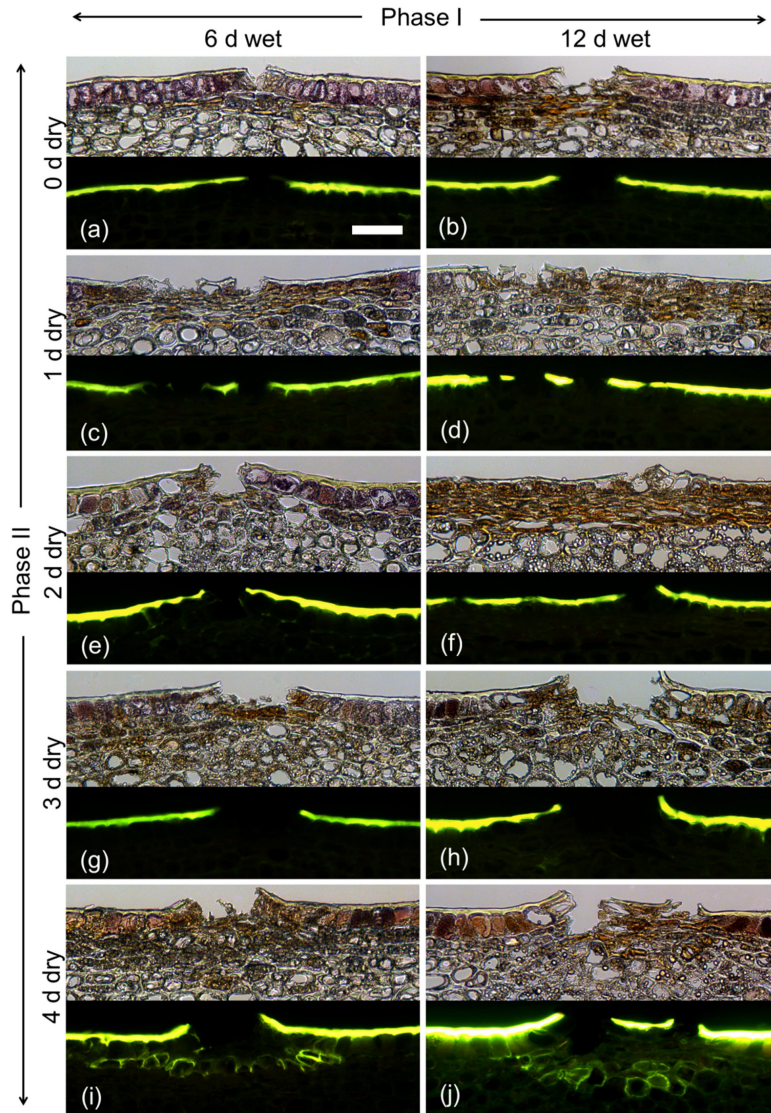


Figure 3. Effect of moisture exposure for 6 d (a,c,e,g,i) or for 12 d (b,d,f,h,j) on the time course of periderm development established at 0 d (a,b), 1 d (c,d), 2 d (e,f), 3 d (g,h) or 4 d (i,j) after termination of moisture exposure. The experiment comprised two phases: Phase I of moisture exposure and Phase II after termination of moisture exposure. Micrographs taken under transmitted white light (upper) or incident fluorescent light (lower) (filter module U-MWB) following staining with Fluorol Yellow 088. The scale bar in (a) is 50 μm long and representative of all images in the composite ($n = 3$).

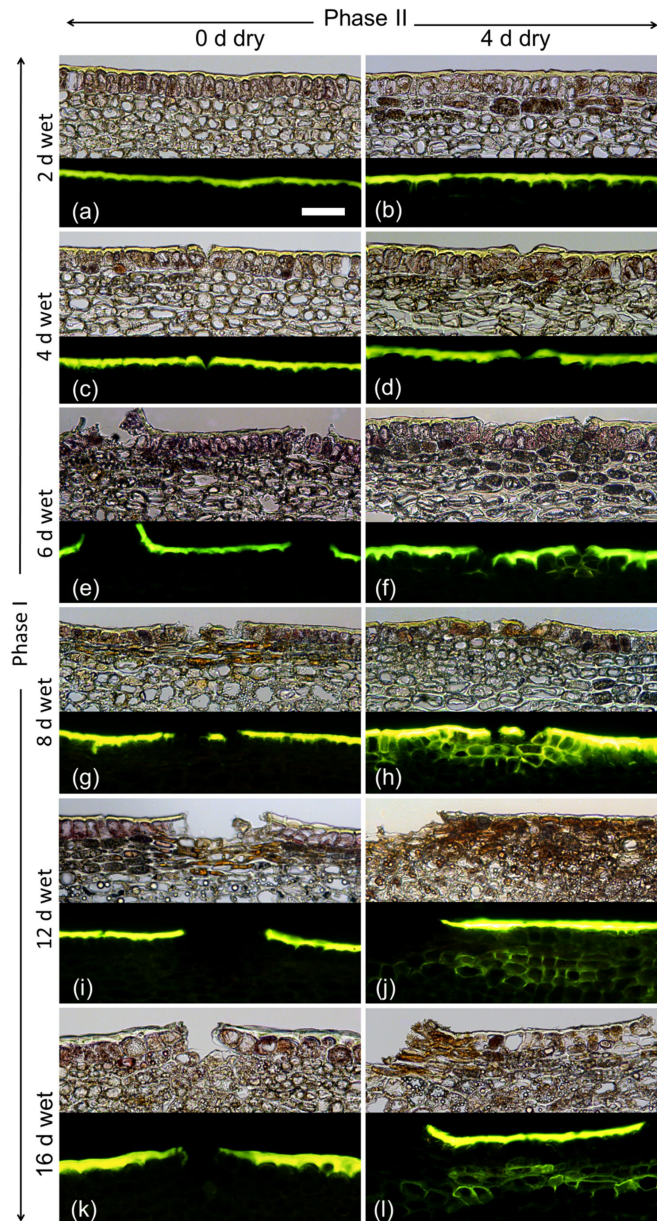


Figure 4. Effect of moisture exposure for 2 d (a,b), 4 d (c,d), 6 d (e,f), 8 d (g,h), 12 d (i,j) or 16 d (k,l) on periderm formation. The experiment comprised two phases: Phase I—time of moisture exposure and Phase II—time after termination of moisture exposure. Phase I was recorded immediately after termination of moisture exposure (0 d) (a,c,e,g,i,k). Phase II was recorded 4 d after termination of moisture exposure (b,d,f,h,j,l). Micrographs taken under transmitted white light (upper) or incident fluorescent light (lower) (filter module U-MWB) after being stained with Fluorol Yellow 088. The scale bar in (a) is 50 μ m long and representative of all images in the composite ($n = 3$).

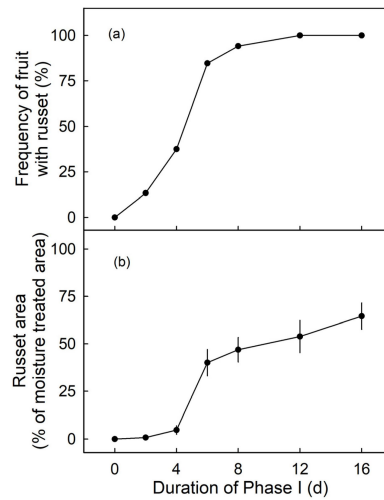


Figure 5. Effect of duration of moisture exposure (Phase I) on the frequency of russeted fruit (a) and the percentage of the moisture-exposed area that is russeted at maturity (156 days after full bloom; DAFB) (b). Fruits were exposed to moisture starting from 31 DAFB for 0, 2, 4, 6, 8, 12 or 16 d. Data represent means \pm SE ($n = 9-31$).

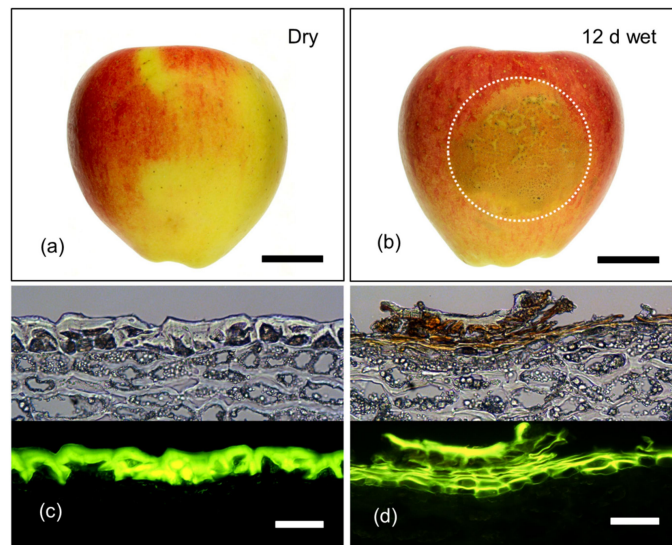


Figure 6. Macrographs (a,b) and micrographs (c,d) of mature (156 days after full bloom; DAFB) 'Pinova' apple fruit following exposure to surface moisture for 12 d at 31 DAFB (wet). Fruit without moisture-exposure, served as controls (dry). Micrographs represent cross-sections of the fruit skin in the moisture-exposed region and the dry region. Micrographs were taken under transmitted white light (upper) or incident fluorescent light (lower) (filter module U-MWB) after being stained with Fluorol Yellow 088. The area enclosed by the dotted circle represents the footprint of the moisture-treated patch of skin that subsequently developed russet. Scale bar in (a) and (b) is 2 cm long and that in (c) and (d) is 50 μ m long.

The developmental time course revealed that 12 d moisture exposure induced periderm at 31 DAFB but not at 66 or 93 DAFB (Figure 7). Interestingly, microcracks were observed only following moisture exposure at 31 DAFB but not at 66 or 93 DAFB (Figure 7).

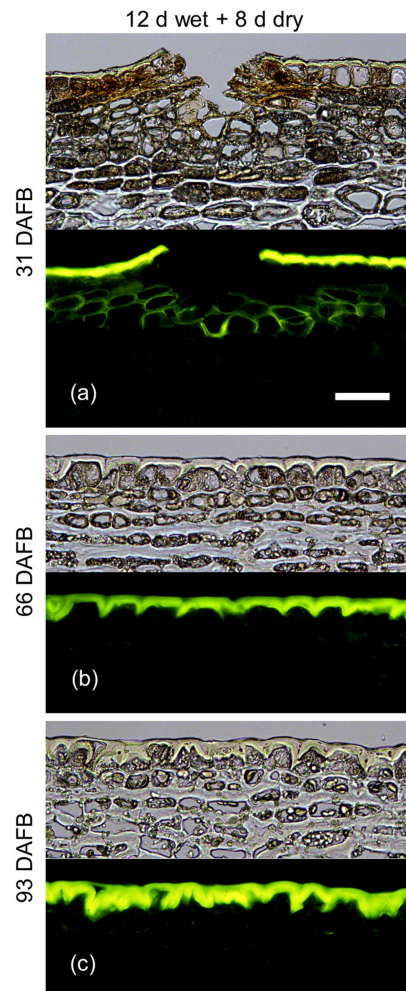


Figure 7. Effect of a 12 d moisture exposure (wet; Phase I) on periderm development in the skin of apple fruit. Cross-sections were prepared 8 d after termination of moisture exposure (dry; Phase II). The fruit surface was exposed to moisture starting at 31 days after full bloom (DAFB) (a) or 66 DAFB (b) or 93 DAFB (c). Cross-sections were prepared from the moisture-treated surface of the fruit. Images were taken under transmitted white light (upper) or incident fluorescent light (lower) (filter module U-MWB) after being stained with Fluorol Yellow 088. The scale bar in (a) is 50 μm long and representative of all images in the composite ($n = 3$).

Moisture had no effect on cuticle thickness during the first 8 d of exposure, nor on the ridges of the cuticular membrane (CM) above the anticlinal cell walls, nor on the lamellae above the periclinal cell walls (Phase I, Figure 8). From the day of moisture removal onwards, the thickness of the cuticle of the previously exposed patch increased at a lower rate comparable to that of the non-exposed control patch (Phase II, Figure 8).

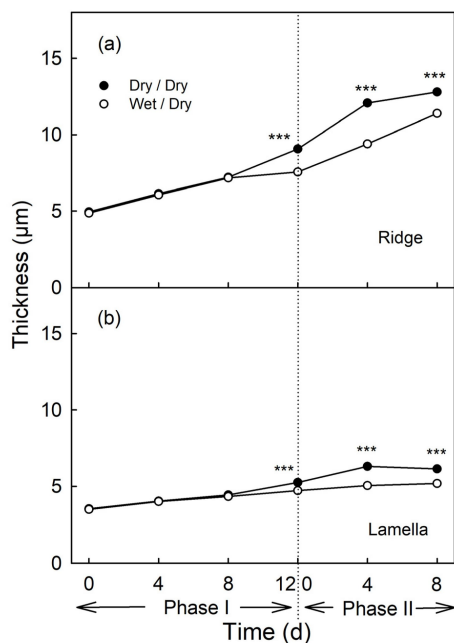


Figure 8. Effect of moisture exposure on the thickness of the cuticle above the anticlinal cell walls (ridge) (a) and above the periclinal cell walls (lamella) (b) of the apple fruit skin. In Phase I, the fruit was exposed to moisture for 12 d. Phase II began following termination of moisture exposure (indicated by the dotted vertical line) and the surface remained dry thereafter (wet/dry). Fruit surface without moisture exposure served as control (dry/dry). *** indicate significant difference between ‘dry/dry’ and ‘wet/dry’ treatment at $p < 0.001$. Data represent means \pm SE ($n = 6$).

The thicknesses of the CM ridges were lowest in the immediate vicinity of a microcrack. As distance increased, the CM thickness increased and approached the mean thickness averaged across the micrograph. This was also the case 4 d and 8 d after termination of the moisture treatment (Phase II, Figure 9).

Neither moisture exposure (Phase I) and nor the termination of moisture exposure (Phase II) had an effect on strain release following preparation of the excised skin segments (ES) and isolation of the CM (Figure 10a). However, the strain release after wax extraction was higher during Phase I and after exposure to moisture (Phase II) than of the non-exposed control (Figure 10b). The difference in strain release between exposed and non-exposed CM increased up to about 6 d after the beginning of exposure and then remained approximately constant (Figure 10b). Calculating total strain from the two component strains revealed that the ϵ_{tot} increased during moisture exposure (Phase I). The rate of increase was somewhat higher for the ϵ_{tot} from the moisture treatment than for the control. The difference in ϵ_{tot} decreased slightly when moisture exposure was terminated (Phase II; Figure 10c).

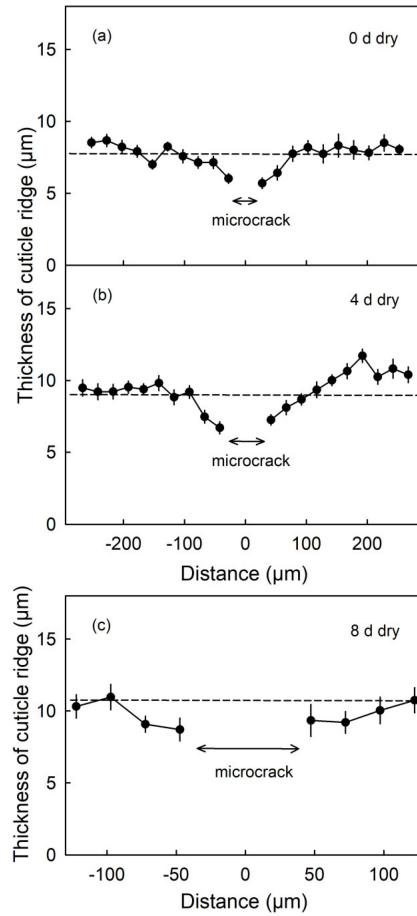


Figure 9. Thickness of the cuticle above the anticlinal cell walls (ridge) as affected by the distance from a moisture induced microcrack. Microcracks were induced by 12 d of moisture exposure. Thickness was measured on cross-sections of the fruit skin prepared from fruit sampled on the day of termination of moisture exposure (0 d (a) and 4 d (b) and 8 d (c) after moisture termination (during Phase II). The distance '0' represents the center of the microcrack. Thickness was measured in both directions from the microcrack. The dashed line is the grand mean thickness of all cuticle ridges within the micrograph. The arrows indicate the mean width of the microcrack. Data represent means \pm SE of 14 to 19 microcracks on a total of six fruits.

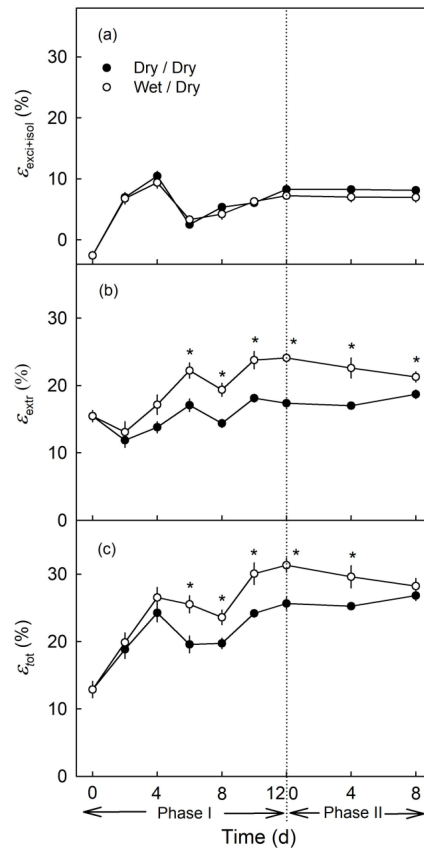


Figure 10. Effect of 12 d of moisture exposure (Phase I) on the elastic strain of the cuticular membrane (CM). Strain was quantified as the strain release during excision and isolation of the CM ($\epsilon_{exc+isol}$; **a**) and following wax extraction of the CM (ϵ_{extr} ; **b**) and the sum of $\epsilon_{exc+isol}$ plus ϵ_{extr} (ϵ_{tot} ; **c**). Phase I represents the period of moisture exposure (wet). Phase II represents the period after moisture termination (dry). The dotted line indicates the end of Phase I and the beginning of Phase II. * indicates a significant difference between dry/dry and wet/dry treatment at $p < 0.05$. Data represent means \pm SE ($n = 8$ to 20).

3. Discussion

Our results establish two important findings—(1) Periderm formation in young ‘Pinova’ apple fruit is not induced during moisture exposure but after termination of moisture exposure and (2) decreased rate of cuticle deposition contributes to moisture-induced microcracking.

3.1. Periderm Formation in Young Fruit Is not Induced During Moisture Exposure but After Termination of Moisture Exposure

Our study is consistent with earlier observations [20]. First, microcracks traversing the cuticle are the first visible symptom in moisture-induced russeting. We have not found a single instance where russet formation was not preceded by microcracking. Second, the periderm formed in the hypodermis, beneath the cuticle and epidermis was as described by Meyer [22] and Pratt [25]. Third,

early stages of fruit development were most susceptible to russet [1,20,26,27]. Indeed, no russeting occurred following exposure to moisture at later stages of fruit development. Fourth, our experimental approach provides conclusive evidence that surface moisture is the cause of russeting. A role of surface moisture in russeting has been suggested previously [18,19,24,28].

Our results consistently show that periderm formation is triggered following termination of the moisture treatment—not during it. This conclusion is based on the observation that increased durations of exposure to moisture beyond a minimum of 4 d had no effect on periderm formation. Regardless of the duration of moisture exposure, a periderm always formed about 4 d after moisture termination. This implies (1) that it is not microcracking per se that triggers russet formation and (2) that some sort of signal must be involved that has its source at the site of microcracking (the cuticle) and travels through two or three cell layers to the subtending hypodermis where the periderm is initiated. Whatever the nature of this signal, it triggers the process involved in the formation of a periderm. This process involves the dedifferentiation of a layer of cells in the hypodermis and their subsequent differentiation into a phellogen which divides repeatedly to produce a stack of suberized phellem cells [7].

Candidates for this signal could include mechanical stimuli, such as the one associated with the release of reversible strain (i.e., elastic and viscoelastic strains) when a microcrack forms in the cuticle. However, several arguments suggest this is unlikely to be the stimulus. First, there was little strain release on excision of an ES and on the isolation of the CM, thus indicating the absence of significant elastic strain in the apple fruit cuticle. This observation is consistent with an earlier one of Lai et al. [29]. Second, the contribution of the cuticle to the overall mechanical properties of the skin is small [30]. It is the epidermis and the hypodermis that together represent the structural backbone of the skin of an apple fruit. Third, if strain relaxation were a factor, one would expect periderm formation to begin after microcrack formation, that is, during moisture exposure (Phase I), not after a fixed time following termination of moisture exposure. We conclude that a mechanical signal is unlikely to be the cause.

An alternative signal candidate may be the change in the barrier properties of the microcracked cuticle. This type of signal could account for a response induced after removal of the tube. Furthermore, the remote response would also be accounted for. Changes in the chemical potential of substances for which the cuticle forms a primary barrier are probably candidates for such a signal. Following the formation of a microcrack, these substances will now move more freely across the skin. Such substances include the chemical potential of both liquid and vapor-phase water (the water potential) and the chemical potentials (partial pressures, concentrations) of dissolved moieties such as O₂, CO₂ and C₂H₄. The consequences of a suddenly less-restricted movement of water would be a change in water potential and thus of turgor. For a change of the chemical potential of the respiratory gases, for example, a decrease in [CO₂] or an increase in [O₂], there would likely be a change in pH. Whether these are the changes that trigger periderm formation is not known.

3.2. Moisture Exposure Increases Microcracking by Decreasing Cuticle Deposition

A causal role for moisture in microcracking has been documented for a number of fruit crop species including sweet cherry [31], apple [18,24], grapes [32], mango [33]. Several factors are involved in formation of microcracks. First, a mismatch of surface expansion rate and cuticle deposition rate causes increased elastic strain [29,34] leading to failure of the cuticle [35]. Second, moisture may exacerbate microcracking by altering the mechanical properties of the cuticle [23,31]. Third, our results suggest that cuticle deposition is reduced as a consequence of moisture exposure and this will likely increase microcracking. The CMs isolated from moisture-exposed regions showed a higher elastic strain than CMs from the control surfaces that remained dry. This could well have been due to decreased deposition of cuticle (cutin and wax) due to moisture exposure. That wax plays an important role, is inferred from the marked differences in strain release on extraction between the moisture treatment and the control. Earlier studies established that depositions of wax in the expanding cutin network on a growing fruit surface substantially reduce build-up of elastic strain by converting the elastic strain into a plastic strain [36]. Further, deposition of new layers of cutin underneath the existing old layers

fixes the elastic strain of the CM [37]. Continuing cutin and wax deposition will therefore fix the elastic strain in the dry control skins but to a lesser extent in the skins exposed to moisture. This would result in greater strain release upon wax extraction in the control, as compared to the conditions found in the moisture treatment. Further molecular and biochemical evidence is needed to draw a firmer conclusion on this point.

3.3. Conclusions

The exposure of discrete patches of the fruit skin of an apple to moisture induces the formation of a periderm after termination of the moisture treatment and after the formation of microcracks. The search for a signal that links the formation of cuticular microcracks, on the fruit surface, to the initiation of dedifferentiation and redifferentiation in the hypodermis, several cell layers below, must focus on this time slot. Our results provide indirect evidence that reduced cuticle deposition and, in particular, reduced wax deposition, is the result of moisture exposure and contributes to the formation of microcracks.

4. Materials and Methods

4.1. Plant Materials

'Pinova' apple trees (*Malus × domestica*, Borkh.) grafted on M9 rootstocks were cultivated at the Horticultural Research Station of the Leibniz University Hanover at Ruthe, Germany (52°14' N, 9°49' E) according to current regulations for integrated crop production. The planting year was 1999, the experiments were conducted in the 2016, 2018 and 2019 growing seasons. Mean daily temperatures, mean daily precipitation and the daily radiation are provided as a supplemental file (Table S1). 'Pinova' was selected because it responded consistently to moisture exposure by russeting (Khanal, unpublished data). Vigorous flower clusters were selected randomly from a total of 125 trees at full bloom (0 days after full bloom; DAFB) and thinned to one flower, so that only the king flower remained. Fruitlets without visual defects and of uniform size and color were selected for the experiments.

4.2. General Experimental Procedures

4.2.1. Moisture Treatment

Moisture was applied locally to a defined patch on the fruit surface [24]. Briefly, a polyethylene tube (8 mm inside diameter; Sarstedt, Nümbrecht, Germany) was cut to a 17 mm length and mounted on the fruit surface in the equatorial region using a non-phytotoxic, fast-curing silicone rubber (Dowsil™ SE 9186 Clear Sealant, Dow Toray, Tokyo, Japan). Deionized water was introduced through the open end of the tube and this open end was then sealed with silicone rubber. In this way, the patch of skin exposed to liquid water was limited to that enclosed within the tube (ca. 50 mm²). To avoid leakage, the silicone seal between tube and fruit was renewed every 2 d until the moisture treatment was terminated. An equivalent patch of skin was identified on the opposite face of the same fruit to serve as the control. Unless specified otherwise, no tube was mounted over the control patch. Earlier experiments established that russeting was due to moisture exposure and not to the mounting of the tube [24]. On the day moisture exposure was terminated, the tube was removed and the fruit surface dried with a soft paper tissue. The tube detached very easily from the epidermis, so that no significant physical force was needed and the fruit surface displayed no visible sign of injury. The footprints of the treated and control patches on each fruit were delineated using a permanent marker. A particular fruit was either sampled immediately or left on the tree for later evaluation. Following sampling, a fruit was transferred to the laboratory within 3 h. Intact fruit (21 or 31 DAFB) or sections of the fruit (66 or 93 DAFB) were stored in Karnovsky fixative [38] or immediately processed fresh, as described below.

4.2.2. Microcracks

Microcracks were quantified in both the 2018 and 2019 growing seasons following the procedure described earlier [24,35]. Briefly, whole fruit were dipped in a 0.1% (*w/v*) aqueous acridine orange solution (Carl Roth, Karlsruhe, Germany) for 10 min, rinsed with distilled water and carefully blotted dry using a soft paper tissue. The treated and the control patches of the skin were inspected using fluorescence microscopy (MZ10F; GFP-plus filter, 440–480 nm excitation, ≥ 510 nm emission wavelength; Leica Microsystems, Wetzlar, Germany) and imaged with a DP71 camera (Olympus Europa, Hamburg, Germany). Three or four images were recorded from different locations within each treated or control patch, on each of a total of six to ten fruit per sampling date. The areas (mm^2) infiltrated by acridine orange were quantified using image analysis (CellP, Olympus, Hamburg, Germany). The total fluorescing area within each treated (or control) patch, in each image, was calculated and was expressed as a percentage of the whole treated (or control) patch to which it referred.

4.2.3. Cross-Section of Fruit Skin

Tissue blocks (ca. 3 mm thick) comprising the fruit skin and some subtending parenchyma cells were excised from the treated or the control patches of the fixed fruit using a scalpel. The blocks were rinsed in distilled water and immersed in 70% (*v/v*) aqueous ethanol for 16 h. The blocks were then dehydrated in an ascending series of ethanol (80%, 90% and 96% *v/v*; 30 min each) under a partial vacuum (pressure 10.8 kPa). Subsequently, the blocks were transferred to 100% isopropanol for 40 min (twice) and a xylene substitute (AppliClear; AppliChem, Münster, Germany) for 40 min (twice) to displace the ethanol in the tissues, under the same partial vacuum. The dehydrated blocks were then infiltrated with a 1:1 (*v/v*) paraffin/xylene substitute mixture (Carl Roth) for 40 min (once) and paraffin alone for 40 min (twice). Finally, the blocks were embedded in paraffin. The paraffin blocks so obtained were cooled and stored at 4 °C pending later sectioning.

Thin sections (10 μm) were cut using a rotary microtome (Hyrax M 55, Zeiss, Germany). Sections were transferred to microscope slides, dried in an oven for 16 h at 38 °C and rehydrated as follows: xylene substitute (2 \times 10 min); descending series of ethanol (96%, 80%, 70% and 60% for 10 min each) and finally for 2 \times 5 min in distilled water.

4.2.4. Microscopy

Sections were stained for 1 h with 0.005% Fluorol Yellow 088 (Santa Cruz Biotechnology, Texas, USA) [39] dissolved in 90% glycerol and melted polyethylene glycol 4000 (SERVA Electrophoresis, Heidelberg, Germany). The sections were transferred to the stage of a fluorescence microscope (BX-60 equipped with a DP 73 digital camera; Olympus and viewed in transmitted white light or under incident fluorescent light (filter U-MWB; 450–480 nm excitation; ≥ 520 nm emission wavelength; Olympus, Hamburg, Germany). The minimum number of biological replicates was three. To confirm the occurrence of a periderm, a minimum of 50 sections through the whole block were examined.

4.2.5. Cuticle Thickness Measurement

Cross-sections of the skin from the moisture treated and the control patches were inspected at $\times 200$ in white light using a fluorescence microscope (BX-60; Olympus, Hamburg, Germany). The thickness of the CM above the anticlinal cell walls (ridge) or above the periclinal cell walls (lamella) were measured in two sets of images using image analysis (CellSens; Olympus, Hamburg, Germany). The first set comprised images selected for the absence of cuticular cracks. The thickness of the lamella and ridge were measured in a 350 μm long transect. For this, four images per fruit from a total of six fruits were used. For the second set, images were selected which had a single cuticular crack. Here, the width of the crack and the thickness of the cuticular ridges were measured in a 275 μm (0 d and 4 d) or 125 μm (8 d) long transect from the center of the crack to either side. A total of 14 to 19 images on six fruits were used.

4.2.6. Russet Quantification

Mature fruit were harvested at 156 DAFB. Digital calibrated images (Canon EOS 550D, lens: EF-S 18-55 mm, Canon Germany, Krefeld, Germany) were taken from the moisture treated and control patches on the fruit surface. The areas (mm²) of the russeted spots on the fruit surface (as indexed by their brownish, rough, corky appearance) were quantified (CellP; Olympus, Hamburg, Germany) and summed within each patch of skin enclosed by the tube. The area of russet is expressed as a percentage of the area of the patch. The number of replicates ranged from 9 to 31.

4.2.7. Cuticle Isolation and Strain Analysis

The ES were punched from the treated and control patches using a biopsy punch (8 mm diameter; Kai Europe, Solingen, Germany; 10 and 12 mm diameter; Acuderm, Terrace, FL, USA). The CMs were isolated enzymatically by incubating the ES in an isolation medium containing pectinase (9%, *v/v*; Panzym Super E flüssig; Novozymes A/S, Krogshoejvej, Bagsvaerd, Denmark) and cellulase (0.5% *v/v*; Cellubrix L.; Novozymes A/S) in a 50 mM citric acid buffer at pH 4.0 at ambient temperature [40]. NaN₃ was added at a final concentration of 30 mM to prevent microbial growth. Enzyme solutions were replaced periodically until CM separated from adhering cellular debris (about 4 weeks). The isolated CMs were carefully cleaned using a soft camel-hair brush. The CM were rinsed in distilled water, dried at 40 °C for a minimum period of 16 h and stored in multi-well cell culture plates held in polyethylene boxes above dry silica gel. For determination of the wax mass, the CM discs were extracted for 2 h using CHCl₃/MeOH (1:1, *v/v*; Carl Roth) in a Soxhlet apparatus. The dewaxed CMs are referred to as DCMs.

The elastic strain was quantified using the procedure described in Lai et al. [29] with minor modifications. The CMs were rehydrated, placed on a microscope slide, flattened by placing a coverslip on top and then imaged under a dissecting microscope (Wild M10; Leica Microsystems; camera DP71). For the DCMs, the discs were transferred from the CHCl₃/MeOH to MeOH and then directly to water, before being positioned on a microscope slide and flattened as described above. The areas of the CM and DCM discs were quantified by image analysis (CellP; Olympus, Hamburg, Germany).

The strains released following excision of the ES and isolation of the CM ($\epsilon_{exci+isol}$) and following wax extraction (ϵ_{extr}) were calculated as follows:

$$\epsilon_{exci+isol} = \frac{A - A_{CM}}{A_{DCM}} \times 100 \quad (1)$$

$$\epsilon_{extr} = \frac{A_{CM} - A_{DCM}}{A_{DCM}} \times 100 \quad (2)$$

$$\epsilon_{tot} = \epsilon_{exci+isol} + \epsilon_{extr}. \quad (3)$$

In this equation, A represents the area of the disc on the fruit surface before excision, that is, the cross-sectional area of the biopsy punch corrected for curvature of the disc. The A_{CM} and A_{DCM} represent the areas of the isolated CM and the extracted DCM. Because the $\epsilon_{exci+isol}$ and the ϵ_{extr} are additive, the total strain ϵ_{tot} equals the sum of the two component strains. The number of replicates ranged from 8 to 20.

4.3. Experiments

All experiments were conducted in two phases: the moisture treatment was imposed during Phase I. The moisture treatment was then terminated, the tube removed and the treated patch now opened up to the natural atmosphere of the orchard—this second period was Phase II. The following experiments were conducted:

(1) The first experiment established that moisture exposure was the cause of periderm formation (and not the mounting of a polyethylene tube using silicone sealant). The experiment was conducted at 28 DAFB and comprised a control (without tube, without water) and the following two treatments:

(i) an empty 8.5 mm long tube (no added water) with its distal end left open to the atmosphere and (ii) a moisture treatment in which an attached 17 mm long tube was filled with water and its distal end sealed with silicone sealant. The tube in (i) was half length so as to minimise any increase in humidity in the tube—earlier experiments showed that microcracking can also result from exposure to high humidity [16,19]. This tube was also mounted in such a position that, although open to the atmosphere, rainwater could not enter it. All tubes were removed after 12 d and the fruit sampled for histological analysis after a further period of 8 d in the orchard.

(2) The time course of the duration of exposure to the atmosphere (Phase II) following removal of surface moisture was studied. The fruit surface was exposed to moisture at 31 DAFB (2019 season) for 6 or 12 d when the moisture treatment was terminated and the time course of exposure to the atmosphere began. Fruit were sampled for microcracking, CM strain and histology at 0, 1, 2, 3 or 4 d after termination of moisture exposure (Phase II) or at maturity (156 DAFB).

(3) The time course of the duration of moisture exposure (Phase I) was studied by exposing fruit surfaces from 21 DAFB (2018 season) or 31 DAFB (2019 season) onwards to moisture for 0, 2, 4, 6, 8, 12 or 16 d. Fruit were sampled either immediately after termination of the moisture treatment for microcracking, CM strain and histology or at maturity (156 DAFB) to quantify the frequency of fruit with russet and the percentage of russeted surface area.

(4) A developmental time course was established to identify any changes in periderm formation during fruit development. Moisture was applied to the surface of developing fruit, beginning at 31, 66 or 93 DAFB (2019 season) for 12 d (Phase I) and fruit were sampled 8 d after termination of the moisture treatment (Phase II). At this time, any periderm formed was clearly detectable by microscopy. Some fruit were left on the tree, sampled at maturity (156 DAFB) and used to quantify the frequency of fruit with russet and the percentage of russeted surface area.

4.4. Data Analyses and Presentation

Data are presented as means \pm SE. Where error bars are not visible, they were smaller than data symbols. Data for strain relaxation analysis and cuticle thickness were subjected to one-way analysis of variance (ANOVA) using SAS (Version 9.1.3; SAS Institute, Cary, NC, USA). Means were compared using Tukey's studentized test at $p \leq 0.05$.

Supplementary Materials: The following is available online at <http://www.mdpi.com/2223-7747/9/10/1293/s1>, Supplementary Table S1: Meteorological data.

Author Contributions: Conceptualization, M.K., T.D. and B.P.K.; funding acquisition, M.K. and T.D.; project administration, M.K. and T.D.; methodology, M.K., T.D. and B.P.K.; investigation, Y.-H.C., J.S. and B.P.K.; supervision, M.K., T.D. and B.P.K.; data curation, Y.-H.C., J.S. and B.P.K.; validation, Y.-H.C., J.S. and B.P.K.; visualization, Y.-H.C., J.S. and B.P.K.; formal analysis, Y.-H.C., J.S. and B.P.K.; Writing—Original draft, M.K., Y.-H.C. and B.P.K.; and Writing—Review and editing, M.K., Y.-H.C. and B.P.K. All authors have read and agreed to the published version of the manuscript.

Funding: This research was funded by a grant (KN 402) from the Deutsche Forschungsgemeinschaft (DFG). The publication of this article was funded by the Open Access fund of the Leibniz Universität Hannover.

Acknowledgments: We thank Traud Winkelmann and Raul Javier Morales Orellana for advice and support in sample preparation for histology. We also thank Simon Sitzenstock and Friederike Schröder for technical assistance, Alexander Lang for helpful comments on the earlier version of this manuscript and the Institute of Meteorology and Climatology, Leibniz University Hannover for making the weather records available to us.

Conflicts of Interest: There are no known competing interests that could influence the work reported in this paper.

References

1. Skene, D.S. The development of russet, rough russet and cracks on the fruit of the apple Cox's Orange Pippin during the course of the season. *J. Hortic. Sci.* **1982**, *57*, 165–174. [[CrossRef](#)]
2. Scharwies, J.D.; Grimm, E.; Knoche, M. Russeting and relative growth rate are positively related in 'Conference' and 'Condo' pear. *HortScience* **2014**, *49*, 746–749. [[CrossRef](#)]

3. Goffinet, M.C.; Pearson, R.C. Anatomy of russeting induced in Concord grape berries by the fungicide chlorothalonil. *Am. J. Enol. Vitic.* **1991**, *42*, 281–289.
4. Michailides, T.J. Russeting and russet scab of prune, an environmentally induced fruit disorder: Symptomatology, induction, and control. *Plant Dis.* **1991**, *75*, 1114–1123. [[CrossRef](#)]
5. Khanal, B.P.; Ikigu, G.M.; Knoche, M. Russeting partially restores apple skin permeability to water vapour. *Planta* **2019**, *249*, 849–860. [[CrossRef](#)]
6. Evert, R.F. *Esau's Plant Anatomy: Meristems, Cells, and Tissues of the Plant Body: Their Structure, Function, and Development*, 3rd ed.; John Wiley & Sons: Hoboken, NJ, USA, 2006.
7. Macnee, N.C.; Rebstock, R.; Hallett, I.C.; Schaffer, R.J.; Bulley, S.M. A review of current knowledge about the formation of native peridermal exocarp in fruit. *Funct. Plant Biol.* **2020**. [[CrossRef](#)] [[PubMed](#)]
8. Schreiber, L.; Franke, R.; Hartmann, K. Wax and suberin development of native and wound periderm of potato (*Solanum tuberosum* L.) and its relation to peridermal transpiration. *Planta* **2005**, *220*, 520–530. [[CrossRef](#)]
9. Simons, R.K.; Aubertin, M. Development of epidermal, hypodermal and cortical tissues in the Golden Delicious apple as influenced by induced mechanical injury. *Proc. Am. Soc. Hortic. Sci.* **1959**, *74*, 10–24.
10. Creasy, L.L.; Swartz, H.J. Agents influencing russet in 'Golden Delicious' apple fruit. *J. Am. Soc. Hortic. Sci.* **1981**, *106*, 203–206.
11. Sanchez, E.; Soto, J.M.; Uvalle, J.X.; Hernandez, A.P.; Ruiz, J.M.; Romero, L. Chemical treatments in "Golden Delicious spur" fruits in relation to russeting and nutritional status. *J. Plant Nutr.* **2001**, *24*, 191–202. [[CrossRef](#)]
12. Jones, K.M.; Bound, S.A.; Oakford, M.J.; Wilson, D. A strategy for reducing russet in Red Fuji apples while maintaining control of black spot (*Venturia inaequalis*). *Aust. J. Exp. Agric.* **1994**, *34*, 127–130. [[CrossRef](#)]
13. Gildemacher, P.; Heijne, B.; Silvestri, M.; Houbraken, J.; Hoekstra, E.; Theelen, B.; Boekhout, T. Interactions between yeasts, fungicides and apple fruit russeting. *FEMS Yeast Res.* **2006**, *6*, 1149–1156. [[CrossRef](#)]
14. Easterbrook, M.A.; Fuller, M.M. Russeting of apples caused by apple rust mite *Aculus schlechtendali* (Acarina: Eriophyidae). *Ann. Appl. Biol.* **1986**, *109*, 1–9. [[CrossRef](#)]
15. Lindow, S.E.; Desurmont, C.; Elkins, R.; McGourty, G.; Clark, E.; Brandl, M.T. Occurrence of indole-3-acetic acid-producing bacteria on pear trees and their association with fruit russet. *Phytopathology* **1998**, *88*, 1149–1157. [[CrossRef](#)] [[PubMed](#)]
16. Knoche, M.; Grimm, E. Surface moisture induces microcracks in the cuticle of 'Golden Delicious' apple. *HortScience* **2008**, *43*, 1929–1931. [[CrossRef](#)]
17. Knoche, M.; Khanal, B.P.; Stopar, M. Russeting and microcracking of 'Golden Delicious' apple fruit concomitantly decline due to gibberellin A4+7 application. *J. Am. Soc. Hortic. Sci.* **2011**, *136*, 159–164. [[CrossRef](#)]
18. Winkler, A.; Grimm, E.; Knoche, M.; Lindstaedt, J.; Köpcke, D. Late-season surface water induces skin spot in apple. *HortScience* **2014**, *49*, 1324–1327. [[CrossRef](#)]
19. Tukey, L.D. Observations on the russeting of apples growing in plastic bags. *Proc. Am. Soc. Hortic. Sci.* **1959**, *74*, 30–39.
20. Faust, M.; Shear, C.B. Russeting of apples, an interpretive review. *HortScience* **1972**, *7*, 233–235.
21. Faust, M.; Shear, C.B. Fine structure of the fruit surface of three apple cultivars. *J. Am. Soc. Hortic. Sci.* **1972**, *97*, 351–355.
22. Meyer, A. A Study of the skin structure of 'Golden Delicious' apples. *J. Am. Soc. Hortic. Sci.* **1944**, *45*, 105–110.
23. Khanal, B.P.; Knoche, M. Mechanical properties of cuticles and their primary determinants. *J. Exp. Bot.* **2017**, *68*, 5351–5367. [[CrossRef](#)] [[PubMed](#)]
24. Khanal, B.P.; Imoro, Y.; Chen, Y.H.; Straube, J.; Knoche, M. Surface moisture increases microcracking and water vapor permeance of apple fruit skin. *Plant Biol.* **2020**. [[CrossRef](#)] [[PubMed](#)]
25. Pratt, C. Periderm development and radiation stability of russet-fruited sports of apple. *Hortic. Res.* **1972**, *12*, 5–12.
26. Simons, R.K.; Chu, M.C. Periderm morphology of mature 'Golden Delicious' apple with special reference to russeting. *Sci. Hortic.* **1978**, *8*, 333–340. [[CrossRef](#)]
27. Wertheim, S.J. Fruit russeting in apple as affected by various gibberellins. *J. Hortic. Sci.* **1982**, *57*, 283–288. [[CrossRef](#)]

28. Creasy, L.L. The correlation of weather parameters with russet of Golden Delicious apples under orchard conditions. *J. Am. Soc. Hortic. Sci.* **1980**, *105*, 735–738.
29. Lai, X.; Khanal, B.P.; Knoche, M. Mismatch between cuticle deposition and area expansion in fruit skins allows potentially catastrophic buildup of elastic strain. *Planta* **2016**, *244*, 1145–1156. [[CrossRef](#)]
30. Khanal, B.P.; Knoche, M. Mechanical properties of apple skin are determined by epidermis and hypodermis. *J. Am. Soc. Hortic. Sci.* **2014**, *139*, 139–147. [[CrossRef](#)]
31. Knoche, M.; Peschel, S. Water on the surface aggravates microscopic cracking of the sweet cherry fruit cuticle. *J. Am. Soc. Hortic. Sci.* **2006**, *131*, 192–200. [[CrossRef](#)]
32. Becker, T.; Knoche, M. Deposition, strain, and microcracking of the cuticle in developing ‘Riesling’ grape berries. *Vitis* **2012**, *51*, 1–6. [[CrossRef](#)]
33. Athoo, T.O.; Winkler, A.; Knoche, M. Russeting in ‘Apple’ mango: Triggers and mechanisms. *Plants* **2020**, *9*, 898. [[CrossRef](#)] [[PubMed](#)]
34. Knoche, M.; Beyer, M.; Peschel, S.; Oparlakov, B.; Bukovac, M.J. Changes in strain and deposition of cuticle in developing sweet cherry fruit. *Physiol. Plant.* **2004**, *120*, 667–677. [[CrossRef](#)] [[PubMed](#)]
35. Peschel, S.; Knoche, M. Characterization of microcracks in the cuticle of developing sweet cherry fruit. *J. Am. Soc. Hortic. Sci.* **2005**, *130*, 487–495. [[CrossRef](#)]
36. Khanal, B.P.; Grimm, E.; Finger, S.; Blume, A.; Knoche, M. Intracuticular wax fixes and restricts strain in leaf and fruit cuticles. *New Phytol.* **2013**, *200*, 134–143. [[CrossRef](#)]
37. Khanal, B.P.; Knoche, M.; Bußler, S.; Schlüter, O. Evidence for a radial strain gradient in apple fruit cuticles. *Planta* **2014**, *240*, 891–897. [[CrossRef](#)]
38. Karnovsky, M.J. A formaldehyde-glutaraldehyde fixative of high osmolarity for use in electron microscopy. *J. Cell Biol.* **1965**, *27*, 1A–149A.
39. Brundrett, M.C.; Kendrick, B.; Peterson, C.A. Efficient lipid staining in plant material with Sudan Red 7B or Fluoral Yellow 088 in polyethylene glycol-glycerol. *Biotech. Histochem.* **1991**, *66*, 111–116. [[CrossRef](#)]
40. Orgell, W.H. The isolation of plant cuticle with pectic enzymes. *Plant Physiol.* **1955**, *30*, 78–80. [[CrossRef](#)]



© 2020 by the authors. Licensee MDPI, Basel, Switzerland. This article is an open access article distributed under the terms and conditions of the Creative Commons Attribution (CC BY) license (<http://creativecommons.org/licenses/by/4.0/>).

3.1. Supplementary data Chapter 3

Electronical File E1. Meteorological data (XLSX) (access through electronical appendix)

4. Russeting in apple is initiated after exposure to moisture ends. Molecular and biochemical evidence

Jannis Straube¹, Yun-Hao Chen², Bishnu P. Khanal², Alain Shumbusho², Viktoria Zeisler-Diehl³, Kiran Suresh³, Lukas Schreiber³, Moritz Knoche², Thomas Debener¹

¹Institute of Plant Genetics, Molecular Plant Breeding Section, Leibniz University Hannover, Herrenhäuser Straße 2, 30419 Hannover, Germany

²Institute of Horticultural Production Systems, Fruit Science Section, Leibniz University Hannover, Herrenhäuser Straße 2, 30419 Hannover, Germany

³Institute of Cellular and Molecular Botany (IZMB), Department of Ecophysiology, University of Bonn, Kirschallee 1, 53115 Bonn, Germany

Type of authorship: First author
Type of article: Research article
Contribution to the article: Designed and performed experiments to study histology and gene expression. Analyzed all data. Wrote the original draft of the manuscript and designed all figures and tables.

Contribution of other authors: Y.-H. Chen performed field work and prepared cuticles for GC-MS analysis. B.P. Khanal prepared bark samples for GC-MS analysis and contributed to writing, reviewing, and editing of the manuscript. A. Shumbusho conducted moisture treatment experiments during the 2016 season. V. Zeisler-Diehl and K. Suresh generated the GC-MS data. L. Schreiber contributed to writing, reviewing, and editing the manuscript. M. Knoche and T. Debener contributed to the design of the study and to writing, reviewing, and editing the manuscript.

Journal: Plants
Date of publication: 30.12.2020
Impact factor: 4.658 (2021)
DOI: 10.3390/plants10010065



Article

Russeting in Apple is Initiated after Exposure to Moisture Ends: Molecular and Biochemical Evidence

Jannis Straube ¹, Yun-Hao Chen ², Bishnu P. Khanal ², Alain Shumbusho ², Viktoria Zeisler-Diehl ³, Kiran Suresh ³, Lukas Schreiber ³, Moritz Knoche ² and Thomas Debener ^{1,*}

¹ Institute of Plant Genetics, Molecular Plant Breeding Section, Leibniz University Hannover, Herrenhäuser Straße 2, 30419 Hannover, Germany; straube@genetik.uni-hannover.de

² Institute of Horticultural Production Systems, Fruit Science Section, Leibniz University Hannover, Herrenhäuser Straße 2, 30419 Hannover, Germany; chen@obst.uni-hannover.de (Y.-H.C.); khanal@obst.uni-hannover.de (B.P.K.); shumbusho1@uniba.sk (A.S.); moritz.knoche@obst.uni-hannover.de (M.K.)

³ Institute of Cellular and Molecular Botany (IZMB), Department of Ecophysiology, University of Bonn, Kirschallee 1, 53115 Bonn, Germany; vzeisler@uni-bonn.de (V.Z.-D.); s6kisure@uni-bonn.de (K.S.); lukas.schreiber@uni-bonn.de (L.S.)

* Correspondence: debener@genetik.uni-hannover.de; Tel.: +49-511-762-2672

Abstract: Exposure of the fruit surface to moisture during early development is causal in russeting of apple (*Malus × domestica* Borkh.). Moisture exposure results in formation of microcracks and decreased cuticle thickness. Periderm differentiation begins in the hypodermis, but only after discontinuation of moisture exposure. Expressions of selected genes involved in cutin, wax and suberin synthesis were quantified, as were the wax, cutin and suberin compositions. Experiments were conducted in two phases. In Phase I (31 days after full bloom) the fruit surface was exposed to moisture for 6 or 12 d. Phase II was after moisture exposure had been discontinued. Unexposed areas on the same fruit served as unexposed controls. During Phase I, cutin and wax synthesis genes were down-regulated only in the moisture-exposed patches. During Phase II, suberin synthesis genes were up-regulated only in the moisture-exposed patches. The expressions of cutin and wax genes in the moisture-exposed patches increased slightly during Phase II, but the levels of expression were much lower than in the control patches. Amounts and compositions of cutin, wax and suberin were consistent with the gene expressions. Thus, moisture-induced russet is a two-step process: moisture exposure reduces cutin and wax synthesis, moisture removal triggers suberin synthesis.

Keywords: russet; cuticle; periderm; *Malus × domestica*; cutin; wax; suberin



Citation: Straube, J.; Chen, Y.-H.; Khanal, B.P.; Shumbusho, A.; Zeisler-Diehl, V.; Suresh, K.; Schreiber, L.; Knoche, M.; Debener, T. Russeting in Apple is Initiated after Exposure to Moisture Ends: Molecular and Biochemical Evidence. *Plants* **2021**, *10*, 65. <https://doi.org/10.3390/plants10010065>

Received: 9 December 2020

Accepted: 28 December 2020

Published: 30 December 2020

Publisher's Note: MDPI stays neutral with regard to jurisdictional claims in published maps and institutional affiliations.



Copyright: © 2020 by the authors. Licensee MDPI, Basel, Switzerland. This article is an open access article distributed under the terms and conditions of the Creative Commons Attribution (CC BY) license (<https://creativecommons.org/licenses/by/4.0/>).

1. Introduction

Russeting is a surface disorder of many fruitcrop species including of apple [1–5]. Russeting is characterized by the formation of rough, brownish patches on the fruit skin. The impaired appearance of the skin reduces the fruit's marketability and an associated increase in water vapor permeability compromises its postharvest performance [6]. In botanical terms, russet is the result of the formation of a periderm, the cell walls of the phellem being suberized. The periderm assumes the barrier functions of the epidermis and cuticle—the fractured epidermal cells soon drying and sloughing off. Despite of its economic importance, the sequence of processes that lead to russeting are not entirely clear.

Some progress has been made in genetic analyses. Using crosses of apple clones that differ in russet susceptibility Falginella [7] and Lashbrooke [8] identified several QTL (Quantitative Trait Locus) regions on chromosomes 2, 12 and 15 that affected russet susceptibility under field conditions [7,8]. Within these, SHN3 was located and identified as a candidate gene responsible for fruit skin development due to its differential expression in russeted and non-russeted clones [8]. Legay [9] compared gene expressions in russeted and non-russeted mature fruit of a range of apple cultivars. A number of differentially-regulated

genes were identified. Some of these were related to cutin, wax, suberin and lignin synthesis and others to the transport and transcriptional regulation of these moieties [9]. Unfortunately, all these studies focused on fruits at the mature stage. The only exception was Lashbrooke [8] who also investigated an early green stage. To our knowledge, there is no further information available on russeting during early fruit development of apple—when russeting susceptibility is at maximum [1,10–14]. Further, comparison of differential gene expressions in fruits from russeted and non-russeted genotypes may not be conclusive, since properties other than russet susceptibility may also differ.

Microscopic cracks ('microcracks') in the cuticle are the first visible symptom of russeting [10,15,16]. Microcracks form when the fruit skin is strained during periods of rapid surface expansion [17]. This period typically occurs during early fruit development [1,10–14,17]. Microcracking is exacerbated by surface moisture [18–20]. Recently, a system was developed that allows microcracks, and hence also russet, to be induced in the skins of developing apples by localized exposure to moisture [15]. The remaining unexposed skin of the same fruit may serve as the control. Briefly, a short length of tube is mounted on the fruit surface and filled with water. This procedure exposes a defined patch of the fruit surface to water, while the remaining fruit surface represents the unexposed control. A periderm forms in the skin area defined by the tube aperture due to the induction of microcracks by moisture. This experimental setup avoids a number of shortcomings associated with comparisons of fruits of different genotypes or fruits of the same genotype but collected from different sites, from different trees or even from different positions in the canopy of the same tree. It thus allows critical comparisons to be made by eliminating a range of potential sources of variability in russet formation, such as by the stage of fruit development, the microenvironment of the fruit in the canopy, etc. Using this system, the effect of moisture exposure on the histology of russet formation was investigated in greater detail [16]. Several findings were reported: (1) Microcracking of the cuticle occurred during moisture exposure, but there was no periderm formation during moisture exposure. (2) Cuticle deposition ceased during moisture exposure. (3) After removal of the moisture treatment a periderm formed within 4 d, regardless of the duration of moisture exposure. (4) The periderm formed in the hypodermis, several cell layers beneath a microcrack. (5) There was no difference in histology between natural and artificial moisture-induced russet. Unfortunately, the time resolution of such histological studies is limited. Moreover, changes at the transcriptional and biochemical levels will precede those detected at the histological level.

To develop a better understanding of the mechanism(s) of russet formation we (1) investigated the expressions of genes putatively involved in cutin, wax and suberin synthesis and (2) analyzed the compositions of the cuticle and the periderm during and after moisture exposure. To identify whether duration of moisture exposure was a factor in russeting, the fruit skin was exposed to continuous surface moisture for 6 or for 12 d periods. We focused on those genes that were found to be differentially expressed in russeted and non-russeted apple in previous studies [8,9,21].

2. Results

2.1. Changes in Gene Expression and Metabolism in Young Fruit During and after Moisture Exposure

During moisture exposure (Phase I) beginning at 31 days after full bloom (DAFB), genes involved in cutin (*ABCG11*, *GPAT6*) and wax (*KCS10*, *SHN3*, *WSD1* and *CER6*) synthases were significantly down-regulated compared to in the un-exposed (dry) control (Figures 1a–f and 2a–f). The down-regulation occurred fairly consistently for all genes and after both the 6 d and the 12d moisture exposure (Figures 1a–f and 2a–f). The longer exposure duration generally resulted in a greater down-regulation. The down-regulation was consistent for *ABCG11*, *GPAT6*, *KCS10* and *SHN3* in all three seasons of the experiment but down-regulation was less for *WSD1* and *CER6*, particularly in the 2018 season (Figures S1a–f and S2a–f).

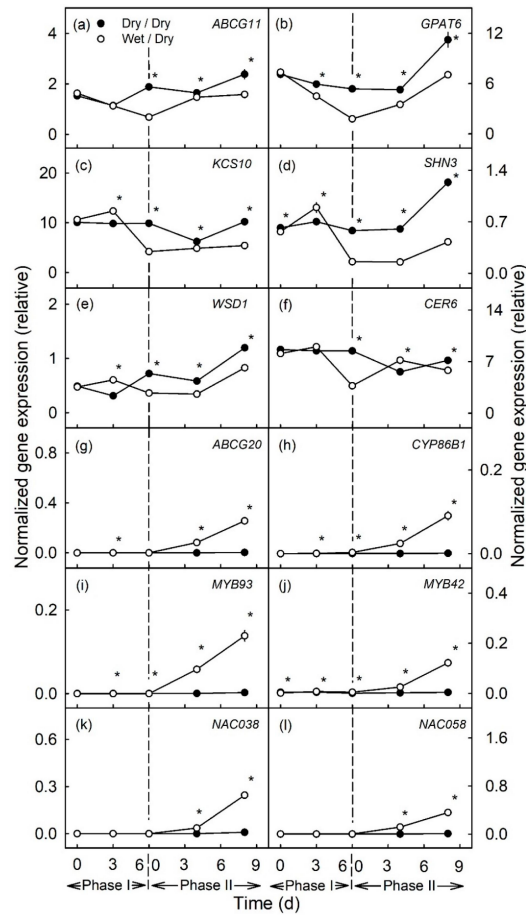


Figure 1. Time courses of expression of genes related to cutin and wax synthesis (a–f) and to suberin and lignin synthesis (g–l) of apple fruit skin during (Phase I) of exposure to moisture and after exposure was discontinued (Phase II). During Phase I, a patch of the fruit skin was exposed to moisture for 6 d beginning at 31 days after full bloom (DAFB) (wet). During the subsequent Phase II, moisture was removed, and the patch was exposed to the atmosphere (dry). Moisture-exposed patches of the fruit skin are referred to as wet/dry, unexposed control patches as dry/dry. The end of moisture exposure is indicated by the vertical dashed line. The expression values are means \pm SE of three independent biological replicates comprising ten fruit each. The ‘*’ indicates significant differences between dry/dry and wet/dry at $p \leq 0.05$ (Student’s *t*-test).

In contrast, there was no change in expression of genes related to suberin synthesis (*ABCG20*, *CYP86B1*, *MYB93*) during moisture exposure (Phase I) (Figures 1g–i and 2g–i). *MYB42*, a regulator of lignin synthesis, was slightly but significantly up-regulated during moisture exposure (Figures 1j and 2j). Meanwhile, *NAC038* and *NAC058*, that do not yet have assigned functions, were not differentially expressed during Phase I (Figures 1k–l and 2k–l).

After discontinuation of moisture exposure (Phase II), the expression of cutin- and wax-related genes in the moisture-exposed patches increased again slightly but the relative expressions were still significantly lower than the expressions of these genes in the control

patches of the same fruit. The relative expression of *CER6* in the 6 d moisture treatment, was generally similar in the moisture-exposed and control patches (Figures 1a–f and 2a–f).

In contrast, suberin- and lignin-related genes were consistently up-regulated, regardless of whether the moisture exposure during Phase I was for 6 or for 12 d (Figures 1g–l and 2g–l, Figures S1g–l and S2g–l). The up-regulation of expression increased from 4 to 8 d after discontinuation of moisture exposure. Only for *MYB42* was a transient peak in expression observed at 4 d after moisture exposure (Figure 2j).

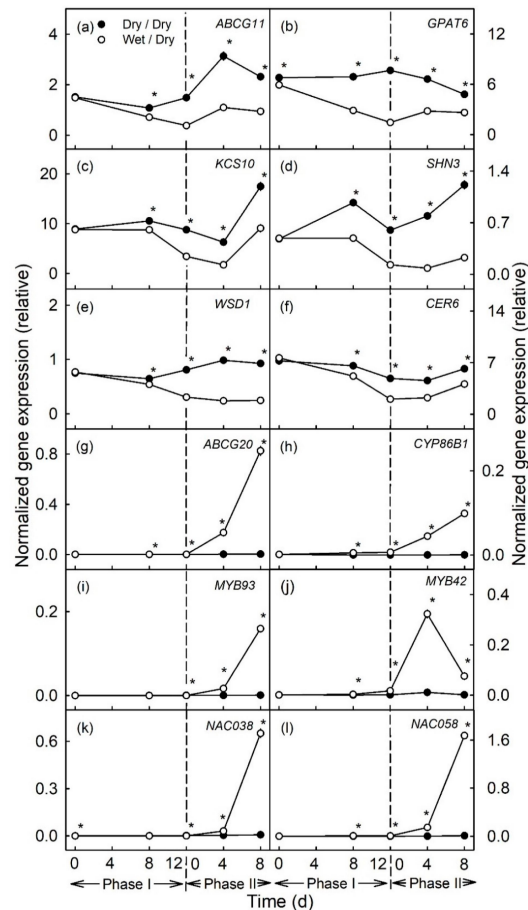


Figure 2. Time courses of expression of genes related to cutin and wax synthesis (a–f) and to suberin and lignin synthesis (g–l) of apple fruit skin during (Phase I) of exposure to moisture and after exposure to moisture was discontinued (Phase II). During Phase I, a patch of the fruit skin was exposed to moisture for 12 d beginning at 31 days after full bloom (DAFB) (wet). During the subsequent Phase II, moisture was removed, and the patch was exposed to the atmosphere (dry). Moisture-exposed patches of the fruit skin are referred to as wet/dry, unexposed control patches as dry/dry. The end of moisture exposure is indicated by the vertical dashed line. The expression values are means \pm SE of three independent biological replicates comprising ten fruit each. The “*” indicates significant differences between dry/dry and wet/dry at $p \leq 0.05$ (Student’s *t*-test).

2.2. Changes in Gene Expression and Metabolism Caused by Moisture Exposure (Phases I and II) during Later Stages of Fruit Development

In the later stages of fruit development moisture exposure [from 66–78 DAFB (Figure 3a–f) and from 93–105 DAFB (Figure 4a–f)] also caused the down-regulation of the genes related to cutin and wax synthesis, as compared to the unexposed controls. However, the magnitudes of the down-regulations of expression were markedly less than for moisture exposure during the early stages of fruit development (moisture exposure from 31–43 DAFB). There were no changes in expressions of genes related to suberin or lignin synthesis, either during Phase I or Phase II (Figures 3g–l and 4g–l).

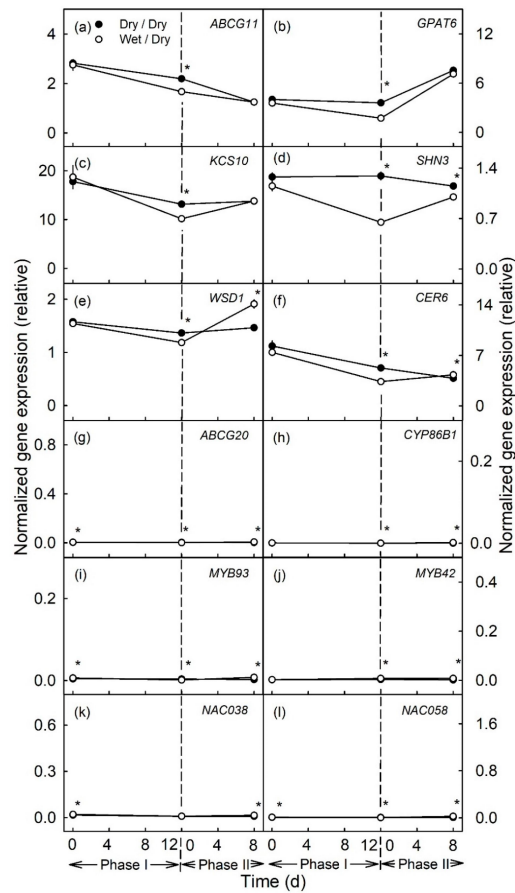


Figure 3. Time course of expression of genes related to cutin and wax synthesis (a–f) and to suberin and lignin synthesis (g–l) of apple fruit skin during moisture exposure (Phase I) and after exposure to moisture was discontinued (Phase II). During Phase I, a patch of the fruit skin was exposed to moisture for 12 d beginning at 66 days after full bloom (DAFB) (wet). During the subsequent Phase II, moisture was removed, and the patch was exposed to the atmosphere (dry). Moisture-exposed patches of the fruit skin are referred to as wet/dry, unexposed control patches as dry/dry. The end of moisture exposure is indicated by the vertical dashed line. The expression values are means \pm SE of three to five independent biological replicates comprising ten fruit each. The * indicates significant differences between dry/dry and wet/dry at $p \leq 0.05$ (Student's *t*-test).

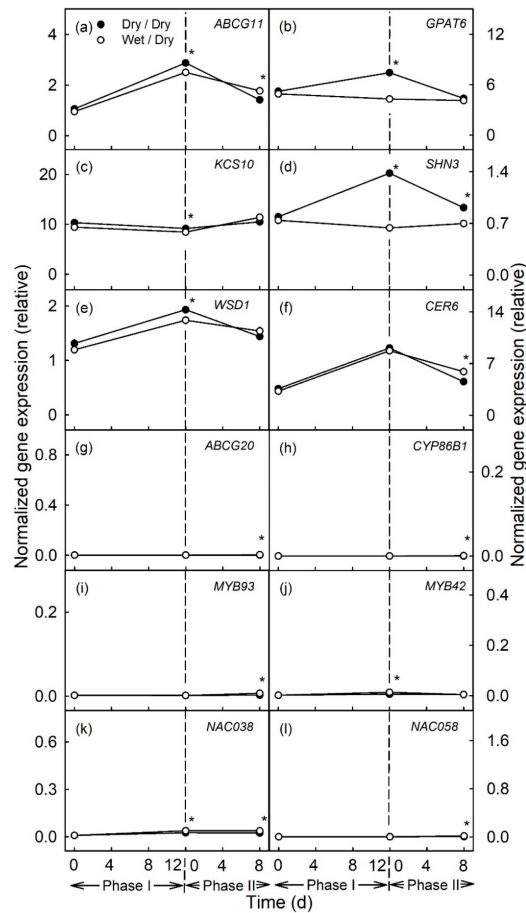


Figure 4. Time course of expression of genes related to cutin and wax synthesis (a–f) and to suberin and lignin synthesis (g–l) of apple fruit skin during exposure to moisture (Phase I) and after exposure to moisture was discontinued (Phase II). During Phase I, a patch of the fruit skin was exposed to moisture for 12 d beginning at 93 days after full bloom (DAFB) (wet). During the subsequent Phase II, moisture was removed, and the patch was exposed to the atmosphere (dry). Moisture exposed patches of fruit skin are referred to as wet/dry, unexposed control patches as dry/dry. The end of the moisture exposure is indicated by the vertical dashed line. The expression values are means \pm SE of three independent biological replicates comprising ten fruit each. The ‘*’ indicates significant differences between dry/dry and wet/dry at $p \leq 0.05$ (Student’s *t*-test).

2.3. Histological and Metabolic Changes during and after Moisture Exposure

The skin patches with and without moisture exposure differed in both appearance and composition. The surfaces of skin samples of the unexposed controls comprised a cuticle, occasionally interrupted by lenticels (Figure 5a,g). There was no macroscopically or microscopically detectable periderm, except for that associated with the lenticels (Figure 5c,i). However, for the moisture-exposed skin patches, there were large areas of periderm (Figure 5b,h). A periderm had begun to develop in the underlying hypodermis by 8 d after moisture exposure was discontinued (Figure 5d). By 113 d after discontinuation of moisture exposure, both the

periderm thickness and also the proportion of the area covered by periderm within the tube footprint had increased markedly (Figure 5h,j). At this stage, the periderm had reached the fruit surface and was visible macroscopically as irregular, brown patches.

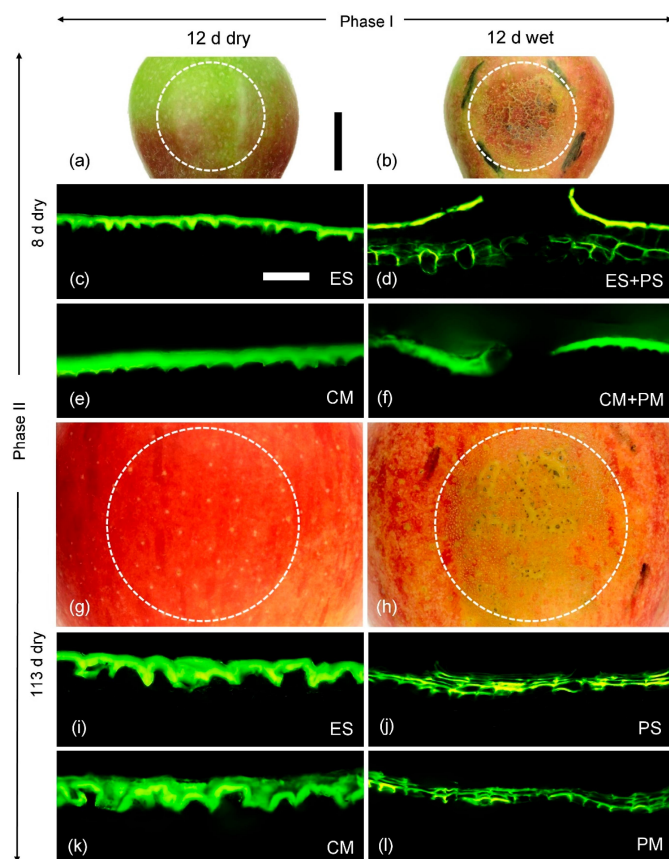


Figure 5. Macroscopic view of unexposed control patches (a,g) and moisture exposed (b,h) skin patches of apple fruit. Cross-sections of epidermal skin samples (ES) of control patches (c,i) and of the composite skins of moisture-exposed patches comprising epidermal plus peridermal sections (ES+PS) (d) or peridermal section only (PS) (j). Cross-sections of isolated cuticular membranes (CM) (e,k) and cuticular plus periderm membranes (CM+PM) (f) or periderm membranes only (PM) (l). The moisture treatment was applied as a two-phase experiment. During Phase I, a patch of the fruit skin was exposed to moisture for 12 d beginning at 31 days after full bloom (DAFB) (wet). During the subsequent Phase II moisture was removed, and the patch was exposed to the atmosphere (dry) (b,d,f,h,j,l). A portion of the unexposed surface on the same fruit served as control (a,c,e,g,i,k). Micrographs were taken 8 d (a–f) and 113 d (g–l) after moisture exposure was discontinued. Images in (c–f) and (i–l) were taken under incident fluorescent light (U-MWB) after staining with Fluorol Yellow 088. The scale bar in (a) equals 10 mm and is representative for all surface views (a,b,g,h). The scale bar in (c) equals 50 μ m and is representative for all cross-sections of the composite (c–f, i–l). The dotted circles in (b) and (h) mark the original footprint of the tube that was mounted on the fruit surface to enable moisture exposure, the dotted circles in (a) and (g) are unexposed control patches on the same fruit. For details of the moisture treatment, see Materials and Methods.

When skin patches were subjected to enzymatic isolation using cellulase and pectinase, the isolated polymers obtained 8 d after moisture exposure had been discontinued in the exposed, and also in the unexposed control patches, comprised only cutin and wax, but no periderm (Figure 5e,f). The periderm that had begun to develop in the hypodermis of moisture-exposed patches and that was also plainly visible in cross-sections under the light microscope (Figure 5d) was probably lost during the isolation process. Thus, it is not surprising that suberin was detectable only in trace amounts in the GC-MS analyses at 8 d after moisture exposure had been discontinued. In contrast, by 113 d after moisture exposure had been discontinued, the periderm in the moisture-exposed patches had extended to the surface and 'connected' to the overlying cuticle. This periderm also remained connected during isolation (Figure 5l). There was no detectable periderm in the polymer membrane isolated from the moisture-unexposed (control) patches (Figure 5k).

Moisture exposure also altered the cutin and wax compositions. The most abundant constituents of the cutin were the hydroxy fatty acids, i.e., 16-hydroxy-C₁₆ acid, 10,16-dihydroxy-C₁₆ acid and 9,10,18-trihydroxy-C₁₈ acid (Figure 6a). Compared with the unexposed controls, in the cuticles of the moisture-exposed patches these constituents were significantly reduced (Figure 6a,b). Moisture exposure also decreased the levels of trans-coumaric acid, α,ω -dicarboxylic-C₁₆ acid, 9,10-dihydroxy- α,ω -dicarboxylic-C₁₆ acid and 9,10-dihydroxy- α,ω -dicarboxylic-C₁₈ acid. Similarly, the content of carboxylic-C₁₆ acid was reduced after 12 d of moisture exposure. The reductions were even more pronounced as the duration of moisture exposure increased from 6 to 12 d. After discontinuation of moisture exposure (Phase II) the amounts of ω -hydroxy-C₂₀, -C₂₂ and -C₂₄ acids and of carboxylic-C₂₂ acid in the moisture-exposed patches all increased and were significantly higher than in the unexposed control patches. The amounts of α,ω -dicarboxylic acids, which decreased during Phase I, increased again during Phase II in the moisture-exposed patches (Figure 6c,d).

The ω -hydroxy-C₂₀, -C₂₂ and -C₂₄ acids are characteristic and unique suberin monomers as indexed by the composition of the pure periderm (i.e., no cuticle) of the bark of the apple tree trunk (Figure 7a). For all other constituents of cutin, and for the wax, there was significant overlap in composition between the cutin and wax of fruit cuticle and of the bark periderm (Figure 7a,b). Normalizing for the three unique characteristic constituents allowed estimation of suberin mass per unit area of the mixed cuticle/periderm composites of the moisture-exposed fruit skin patches.

The most abundant components of the wax were the triterpenes (oleanolic acid and ursolic acid), the sterols and C₂₈ aldehyde. All of these were significantly lower in the moisture-exposed patches compared with the unexposed patches (Figure 8). The mass per area remained constant in the moisture-exposed patches but continued to increase in the unexposed control patches (Figure 8a,b). This pattern was particularly evident for the amounts of ursolic acid and C₂₈ aldehyde that increased markedly up to maturity in the unexposed control patches—but not in the moisture-exposed patches (Figure 8).

The compositional changes of individual constituents described above resulted in significant changes in the masses per unit area of cutin, wax and suberin. The masses of cutin and wax per unit area were lower in moisture-exposed patches, compared to the unexposed controls (Figure 9a–d). The decreases in mass occurred primarily during Phase I. They remained at about the same levels during the subsequent Phase II until 8 d after moisture exposure had been discontinued. The changes were qualitatively identical for 6 and 12 d of moisture exposure but were larger quantitatively for the longer exposure time (Figure 9a–d). During Phase I, suberin was essentially undetectable, regardless of the duration of moisture exposure. However, low levels of suberin were detectable 8 d after moisture exposure had been discontinued, while levels were markedly higher at 113 d (Figure 9e,f). It is interesting to note that some suberin deposition—albeit at low levels—was also recorded in the unexposed control patches. This last is not surprising because lenticels occur naturally in the unexposed control patches of an apple fruit skin and represent small areas of periderm usually associated with degenerate stomata (Figure 5g) [22].

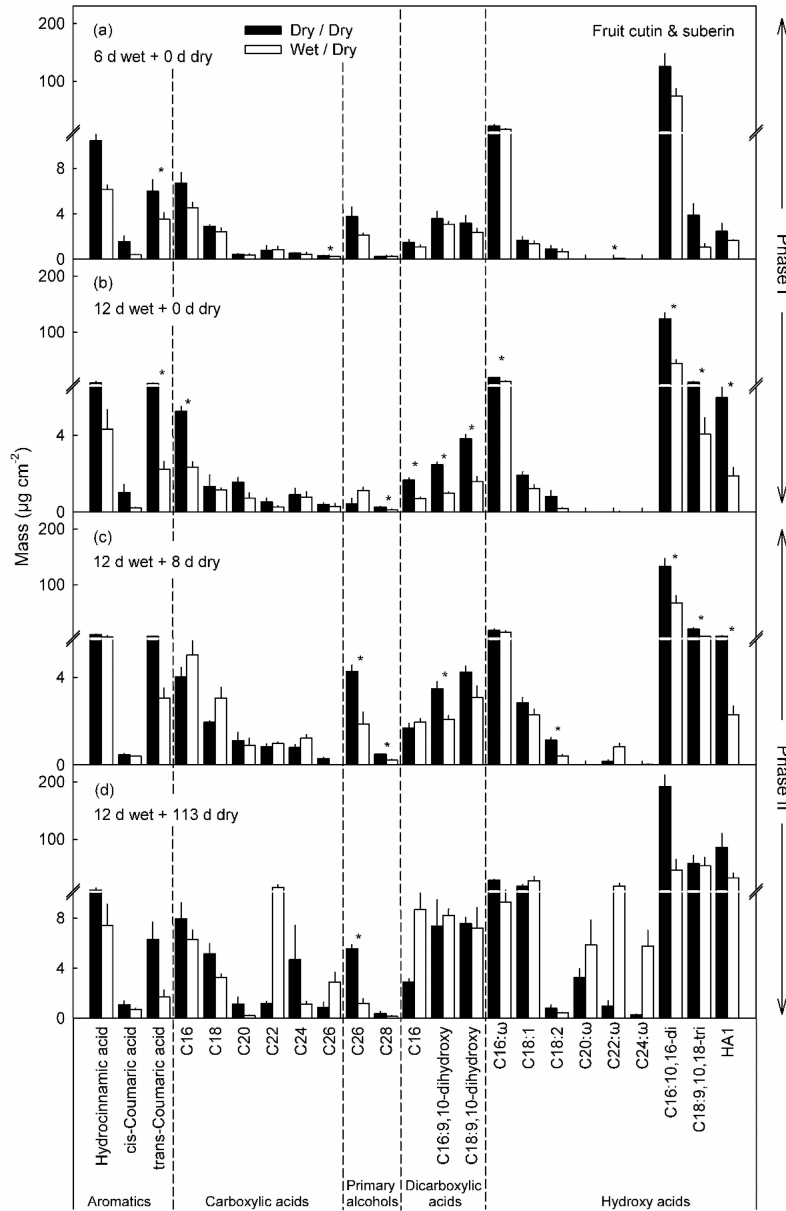


Figure 6. Cutin and suberin monomers in patches of apple fruit skin that were exposed to moisture for 6 d (a) and 12 d (b) (Phase I, wet). During the subsequent Phase II, the moisture exposure was discontinued (dry) and the cutin and suberin compositions of the patches analyzed after 8 d (c) and 113 d (d) after moisture exposure was discontinued. Unexposed patches of the fruit skin that remained dry throughout, served as controls (dry/dry). Data represent means \pm SE of two to three replicates comprising cuticles of five fruit each. Significance of differences between dry/dry and wet/dry at $p \leq 0.05$ are indicated by “*” (Student’s *t*-test).

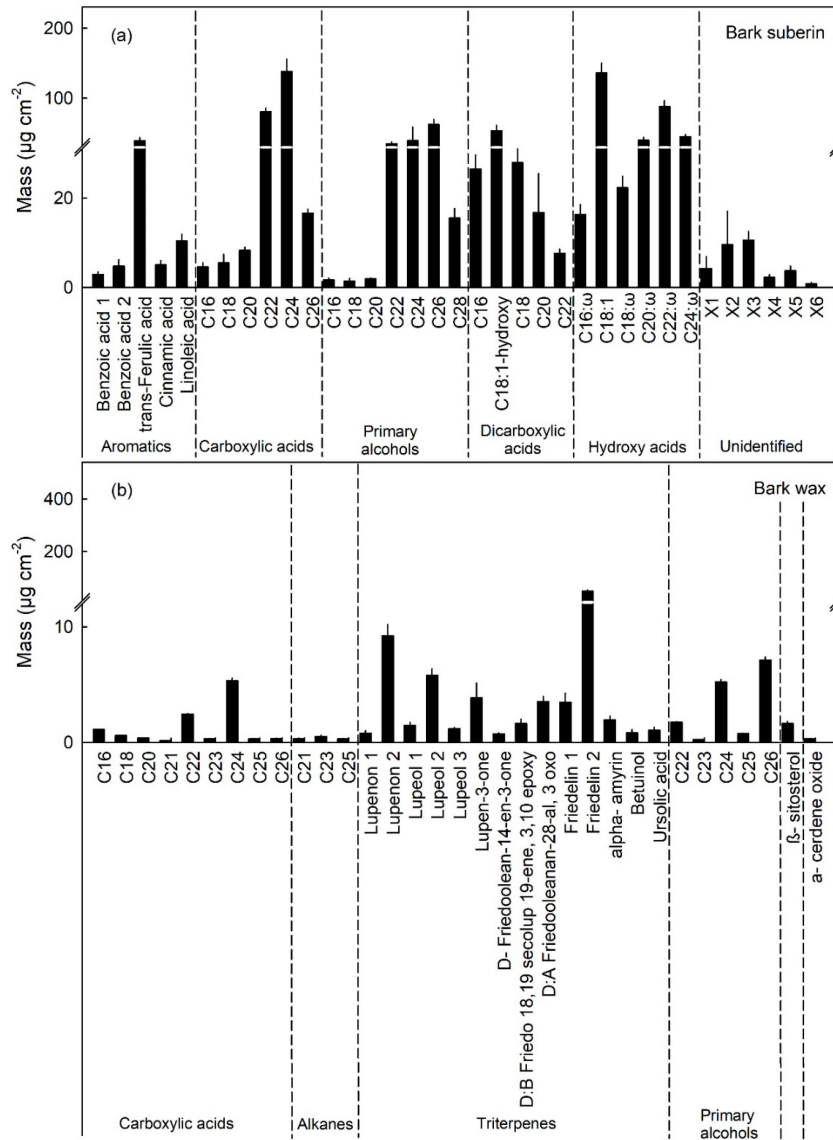


Figure 7. Composition of the periderm of the bark of the trunk (BP) of a 'Pinova' apple tree. (a) Constituents of the suberin and (b) constituents of the wax. The BP represents a pure periderm without any remnants of a cuticle.

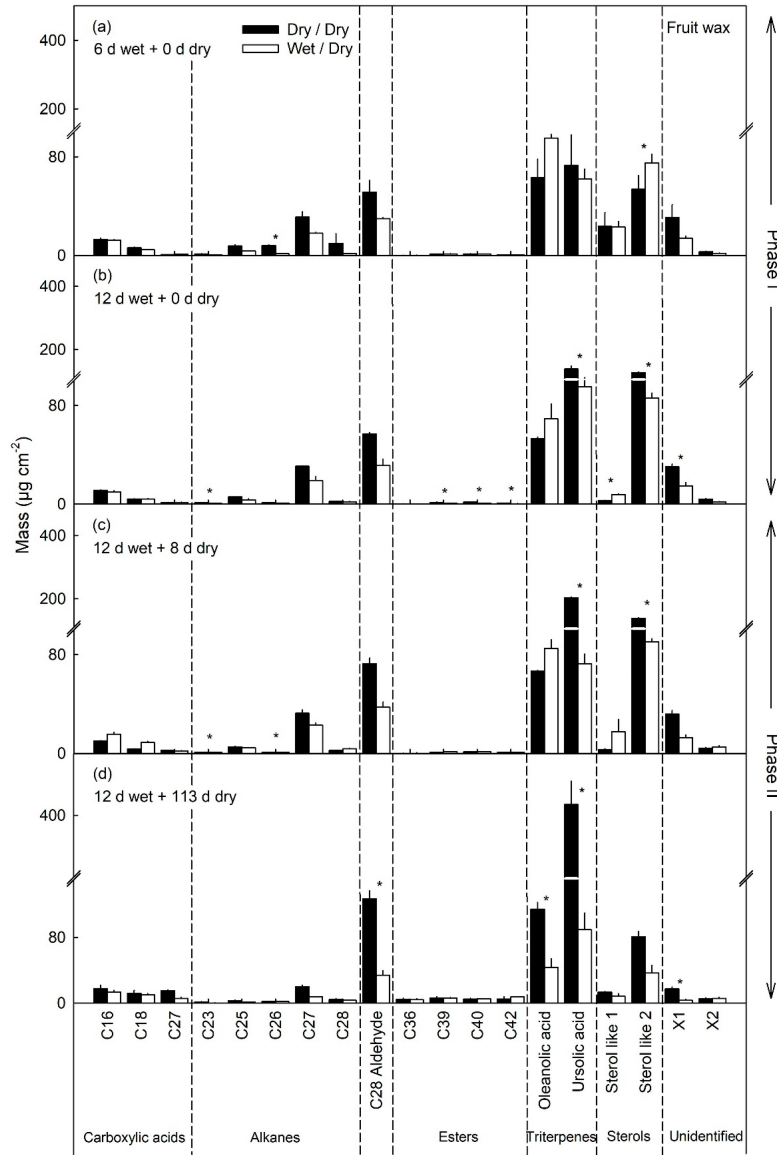


Figure 8. Wax constituents in patches of apple fruit skin that had been exposed to moisture for 6 d (a) and for 12 d (b) (Phase I, wet). During the subsequent Phase II, the moisture exposure was discontinued (dry) and the cutin and suberin compositions of the patches analyzed after 8 d (c) and 113 d (d). Unexposed patches of the fruit skin served as controls (dry/dry). Data represent means \pm SE of two or three replicates comprising cuticles of five fruit each. Significance of differences between dry/dry and wet/dry at $p \leq 0.05$ is indicated by '*' (Student's *t*-test).

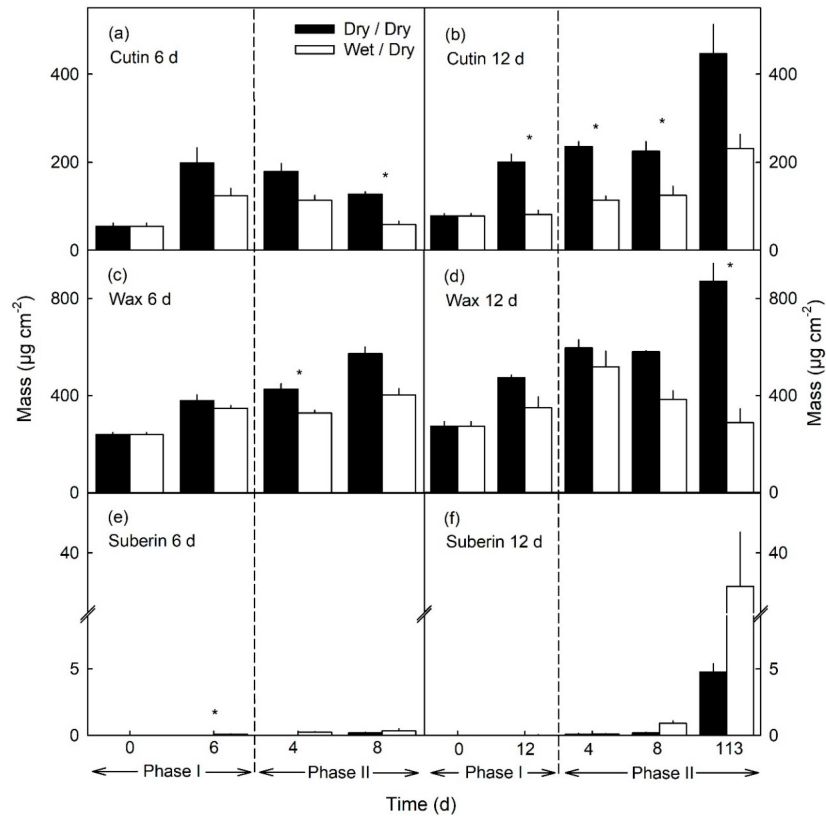


Figure 9. Total mass of cutin (a,b), wax (c,d) and suberin (e,f) in patches of the apple fruit skin during exposure to moisture (Phase I) and after exposure to moisture had been discontinued (Phase II). During Phase I, a patch of the skin was exposed to moisture for 6 d (a,c,e) or 12 d (b,d,f) beginning at 31 days after full bloom (DAFB) (wet). During the subsequent Phase II, the exposure to moisture was discontinued and the patch exposed to the atmosphere (dry). Moisture exposed patches of fruit skin are referred to as wet/dry, unexposed control patches as dry/dry. The end of the moisture exposure period is indicated by the vertical dashed line. The data represent the means \pm SE of two or three samples comprising five fruits each. Significance of differences between dry/dry and wet/dry at $p \leq 0.05$ is indicated by ^{*} (Student's *t*-test).

3. Discussion

Our results establish that:

- (1) Moisture exposure resulted in down-regulation of the genes involved in cutin and wax synthesis and deposition. The discontinuation of moisture exposure resulted in the up-regulation of genes involved in suberin synthesis.
- (2) The early fruit development stage was more responsive to moisture than later stages when effects of moisture exposure on cutin and wax deposition were much less and those on suberin deposition essentially absent.

3.1. Gene Expression

Expressions of the genes involved in all steps of cuticle formation, account for the decrease in cuticle deposition during exposure to surface moisture. These included genes involved in the synthesis of monomers and constituents (*GPAT6*, *KCS10*, *SHN3*, *WSD1*,

CER6) and their transport across the plasma membrane (*ABCG11*). The down-regulation occurred at the same time as microcracks formed [15,16], as cuticle thickness around microcracks decreased [16] and as the amounts of the amounts of the major constituents of cutin and wax decreased. These observations suggest a causal relation between moisture exposure, a reduction in the expressions of genes involved in cuticle synthesis, a decrease in cuticle mass and the subsequent formation of a periderm and the onset of suberin synthesis and deposition. Because moisture and its removal affected all levels of potential control (synthesis, transport and transcriptional regulation) it is most plausible that these associations are causal, rather than merely correlative.

3.1.1. Cutin, Wax and Suberin Synthesis

Moisture exposure during Phase I, down-regulated *GPAT6*. *GPAT6* and its orthologs have important functions in cuticle formation for example in the synthesis of 2-monoacylglycerols as shown for *Arabidopsis* [23]. A defect of an orthologous gene in tomato *SIGPAT6* led to reduced cutin content and decreased cuticle thickness compared to the wildtype [24]. Consistent with this is the observation by Legay [9] who reported decreased gene expression of *MdGPAT6* in russeted as compared to non-russeted apple cultivars. This is in line with our observation of decreased expression of *GPAT6* during moisture exposure.

Decreased expression during moisture exposure was also observed for *KCS10* in russeted fruit skins [9]. *KCS10* is involved in long-chain fatty acid synthesis in *Arabidopsis* [25]. Furthermore, Legay [9] also observed a down-regulation of genes involved in the synthesis of wax constituents such as *WSD1* and *CER6* in skins of russeted fruit. In *Arabidopsis*, *WSD1* is involved in the synthesis of wax esters. It also has diacylglycerol acyltransferase activity [26]. *CER6* is involved in the elongation of C_{24} very long chain fatty acids (VLCFAs). A loss of function in *Arabidopsis* led to an accumulation of the C_{24} wax component [27].

After moisture removal, genes related to the synthesis of suberin and, possibly, the formation of a periderm (*ABCG20*, *CYP86B1*, *MYB93*, *MYB42*, *NAC038* and *NAC058*) were subsequently up-regulated. This is consistent with an up-regulation of the expressions of *CYP86B1*, *MYB93*, *NAC038* and *NAC058* in skins of russeted apple fruit, but not in non-russeted mature fruit [9]. In *Arabidopsis*, *CYP86B1* is involved in the synthesis of ω -hydroxy- C_{22} and C_{24} acids and α,ω -dicarboxylic acids. A knockout of this gene led to an accumulation of C_{22} and C_{24} fatty acids [28]. For *NAC038* and *NAC058* an involvement in the synthesis of suberin monomers is not unlikely. Experiments on overexpression of *MdMyb93* in *N. benthamiana* not only led to an increased suberin formation but also to an upregulation of *NAC038* and *NAC058* orthologues of *Nicotiana* [21].

3.1.2. Transport of Cutin Monomers, Wax Constituents and Suberin Monomers

During moisture exposure (Phase I) genes involved in the transport of cutin monomers or wax constituents across the plasma membrane were down-regulated. These included *ABCG11* that encodes an ATP binding cassette transporter essential for the transport of cuticular lipids in *Arabidopsis* (*AtABCG11*; [29]). The related orthologous gene *MdABCG11* (MDP0000200335) of apple was localized in a major QTL controlling russeting of 'Renetta Grigia di Torriana' [7]. Also, *MdABCG11* was down-regulated in russeted as compared to non-russeted cultivars in a bulk transcriptomic study [9].

The ABCG transporters *ABCG2*, *ABCG6* and *ABCG20* are involved in the transport of suberin monomers in *Arabidopsis* [30]. The up-regulation of *ABCG20* after termination of moisture exposure (Phase II) during the period of periderm formation in apple fruit skin therefore implies a requirement for transport of suberin monomers across the plasma membrane as would be needed for suberin incrustation of the phellem cell walls. At 8 d after moisture removal, ω -hydroxy- C_{22} acid had increased there and even more so at 113 d. This monomer is associated with russeted fruit skin at maturity [31].

3.1.3. Transcriptional Regulation of Cutin, Wax, and Suberin Synthesis

Moisture exposure also affected the transcriptional regulation of cuticle development by *SHN3*. The SHN transcription factor genes are known as positive regulators of cuticle formation and of patterning of epidermal cells in *Arabidopsis* and tomato [32–34]. The silencing of *SISHN3* in tomato led to reduced amounts of cuticular lipids and alterations in cuticle morphology [34]. In apple fruit, markers linked to the *MdSHN3* gene co-segregate with decreased cuticle thickness, increased microcracking, decreased expression in russeted clones compared to non-russeted ones and increased potential for russet formation [8].

MYB93 is a key factor for the transcriptional regulation of suberin deposition in apple. It affects the synthesis and transport of suberin monomers, and their polymerization [21]. The transcription factor *MYB42* is involved in the synthesis of secondary cell wall, specifically in secondary cell wall thickening [35]. *MYB42* is also involved in the activation of genes for synthesis of lignin and phenylalanine, which serves as a precursor of many secondary metabolites in *Arabidopsis* [36]. We observed an up-regulation of the expression of *MYB42* during early formation of periderm whereas Legay [9] observed a down-regulation. The reason for this discrepancy is unknown. Increased expression of *MYB42* indicates concurrent lignin synthesis and secondary cell wall thickening during early phases of russeting. *NAC038* and *NAC058* also increased during Phase II of russet formation but their functions are not yet known.

3.2. Metabolites

The decreased expression of genes involved in cutin and wax synthesis resulted in decreased deposition in moisture-exposed skin patches. The 16-hydroxy- C_{16} acid, 10,16-dihydroxy- C_{16} acid and 9,10,18-trihydroxy- C_{18} acid are major constituents of cutin [37–39]. Furthermore, C_{16} acids are more abundant in the cutin of young and rapidly expanding organs and the amount of C_{18} acids increases as the organ develops and matures [38,39]. This was also observed in this study of apple fruit cutin. The mass of these three major constituents significantly decreases after 12 d moisture exposure. At maturity (113 d), the mass of the three major constituents was still lower in the moisture-exposed skin patches than in the control ones.

Within the wax fraction the C_{27} and C_{29} alkanes, the C_{26} and C_{28} primary alcohols, sterols and the triterpenes ursolic and oleanolic acid, are the dominant constituents in apple fruit wax [31,40–43]. These constituents are typical of the wax of *Rosaceae* species [44]. These constituents all decreased during moisture exposure indicating a decrease in the expressions of wax-related genes, paralleled by corresponding decreases in synthesis and deposition. Similarly, Legay [31] reported decreased masses of ursolic acid and oleanolic acid in russeted apple skins at maturity, compared to non-russeted skins.

Deposition of wax in microcracks is an effective repair mechanism that re-establishes the cuticle's barrier function [15,45,46]. Furthermore, wax deposition in the cuticle of an expanding fruit surface converts elastic strain into plastic strain, thereby fixing both strain and stress [47]. Our observations suggest that decreased expression of genes involved in cutin and wax synthesis during moisture exposure led to decreased deposition. This may have contributed to, or even caused, the increased microcracking of the cuticle.

The increase in suberin content is less clear from the analysis of composition. First, most constituents of suberin also serve as monomers in cutin synthesis. Notable exceptions are the long chain (C_{20} , C_{22} , C_{24}) ω -hydroxy acids that are unique for suberin [31,48]. Second, despite a marked and consistent up-regulation of genes involved in synthesis of monomers for suberin, there was no clear corresponding increase in suberin monomers 8 d after discontinuation of moisture exposure. At this stage, a periderm had begun to develop in the hypodermal cell layers, in this and also our earlier study, as inferred from cross-sections of skin patches [16]. However, when skin patches were incubated in pectinase and cellulase, the cell layers separating the periderm from the epidermis were digested and, hence, the developing islands of periderm were lost to the isolation medium. This observation explains, why the periderm was detectable in cross-sections of the skin 8 d

after discontinuation of moisture exposure but were not evident in the isolated cuticle polymer or as a major chemical constituent in the mass spectra of the moisture-exposed cuticles of fruit skins. By 113 d a complete periderm had developed, and this extended to the skin surface in the moisture-exposed fruit. This periderm remained attached to the cuticle during isolation at 113 d, but not at 8 d after moisture exposure was discontinued. Consequently, the characteristic constituents of suberin were clearly detectable. The slight increase in the un-exposed control patches does not conflict with the above conclusion. This suberin is accounted for by the presence of lenticels that form in the apple fruit skin during normal development.

Unfortunately, the overlap of many constituents between suberin and cutin made it impossible to calculate the amount of suberin deposited in moisture-exposed skin patches simply by summation. Further, moisture-treated skin patches are composite polymers comprising both cuticle and periderm to varying extents. For these a first estimate of the total amount of suberin present may be obtained by using pure suberin from the bark periderm of the trunk. In contrast to the moisture-treated fruit skin patches, the isolated periderm of the bark of the trunk is comprised of suberin only, there is no cuticle. Using the bark periderm of 'Pinova' apple trees as a reference, the masses of the suberin constituents relative to those of the three suberin-specific character constituents, i.e., the ω -hydroxy-C₂₀, -C₂₂ and -C₂₄ acids was calculated. This analysis revealed a marked increase in suberin deposition in line with that expected, based on the increases in gene expression.

3.3. Russet Susceptibility is Highest during Early Fruit Development

The histological, biochemical and molecular results demonstrate that moisture-induced russet is limited to the early stages of fruit development [16]. This is consistent with field observations where the first four weeks after full bloom are considered critical [1,10–14]. Moisture exposure occurring later in fruit development (for example between 66 and 78 DAFB or 93 and 105 DAFB) resulted in only slight decreases in expression of cutin- and wax-related genes and no increases in expression of suberin-related genes. This is consistent with the observed lack of periderm formation [16] and the lack of visual symptoms of russeting [15]. The higher susceptibility to russet during early fruit development results from the high relative area growth rates at this stage [49]. Unless matched by high rates of cutin and wax deposition [17], high relative area growth rates (high rates of strain) result in microcracking. Thus, growth strain, microcracking, macrocracking and russeting are interrelated [4,46,50–52].

3.4. Conclusion

The molecular and biochemical results presented here are consistent with the histological observations reported earlier [16]. Based on both studies, russeting must be viewed as a two-step process comprising the following sequence of events (Figure 10). A young fruit, that typically has a high growth rate and, hence, a strain rate of the skin [17], responds to surface moisture by decreasing cutin and wax synthesis and deposition due to the down-regulation of *ABCG11*, *GPAT6*, *KCS10*, *SHN3*, *WSD1* and *CER6*. As a consequence, the fixation of elastic strain by cutin and wax deposition is decreased and so, elastic strain builds up [47]. The increase in strain and (possibly) a change in the rheological properties of the cuticular membrane (CM) due to hydration [53] results in the formation of microcracks. These microcracks generally extend tangentially and so form a crack network on the fruit surface that continues to extend even after moisture exposure is discontinued. As a result, the cuticle's barrier function is impaired. A deposition of wax in developing microcracks may 'repair' the microcrack and so restore the cuticle's barrier function [45,54,55] and so avert the development of russeting. However, if this repair process lags too far behind, Phase II of the russeting cascade is initiated [46]. Following drying of the fruit surface, a yet unknown signal triggers the formation of a periderm. This signal must be transmitted from the microcrack (or the immediate vicinity thereof) deeper down to the hypodermal cell layers where a periderm begins to differentiate. Genes involved in suberin and lignin

synthesis including *ABCG20*, *CYP86B1*, *MYB93*, *MYB42*, *NAC038* and *NAC058* are all up-regulated. Suberin is deposited in the cell walls of the phellem. The process continues until the cuticle and epidermis and the outer hypodermis dry and are sloughed off and the phellem becomes exposed at the skin surface. The suberized phellem now appears as the typical rough, dull brown of a russeted fruit skin.

	Phase I - wet Minimum duration of 6 d	Phase II - dry Minimum duration of 4 d
Phenotypic changes	Decrease in cuticle thickness; Microcrack formation	Crack networking, widening and simultaneous sealing; Periderm formation in hypodermis
Transcriptional changes	Decrease in cutin and wax synthesis genes: <i>ABCG11</i> , <i>GPAT6</i> , <i>KCS10</i> , <i>SHN3</i> , <i>WSD1</i> , <i>CER6</i>	Increase in suberin and lignin synthesis genes: <i>ABCG20</i> , <i>CYP86B1</i> , <i>MYB93</i> , <i>MYB42</i> , <i>NAC038</i> , <i>NAC058</i>
Metabolic changes	Decrease in cutin and wax content	Decrease in cutin and wax content; Increase in suberin content

Figure 10. Schematic of the process of russeting at the phenotypic, transcriptional and metabolic level during exposure of apple fruit skin patches to moisture (Phase I) and following discontinuation of exposure (Phase II).

The triggers have not yet been identified that lead to the differential expression of both cutin- and wax-related genes during moisture exposure, nor those of the suberin-related genes after moisture exposure is discontinued. It is speculated that the expression of suberin-related genes is triggered by the impaired barrier properties of the cuticle. Potential candidates for this trigger are a high (O_2), a low (CO_2) or a more negative water potential in the tissues immediately subtending a microcrack. Interestingly, in potato, a low (O_2) inhibited suberization of the tuber following wounding [56]. Further experiments employing techniques such as transcriptomic analysis would be helpful in identifying the potential triggers for the down-regulation of expression of the genes associated with cutin and wax synthesis during moisture exposure, as well as for the up-regulation of suberin-synthesis genes after moisture exposure has been discontinued.

The model of periderm formation presented here will apply equally to other fruitcrop species that develop microcracks in the cuticle during the early phase of development and subsequently russeting (e.g., pear). However, fruitcrop species that bear fleshy fruit and that are susceptible to cracking, usually are not susceptible to russet. In these, a comparable mechanism for fixing the impaired barrier properties of the fruit skin at that stage of development is absent.

4. Materials and Methods

4.1. Plant Materials

'Pinova' apple trees (*Malus × domestica*, Borkh.) grafted on M9 rootstocks were cultivated in the experimental orchards of the horticultural research station of the Leibniz University Hanover at Ruthe (52°14' N, 9°49' E) according to current regulations for integrated fruit production. Developing fruit were sampled randomly over three growing seasons from a total of 125 trees. For comparison, bark sections were excised from the base of the trunks of 21-year-old 'Pinova' trees about 10 cm above the graft union.

4.2. Moisture Treatment

Flowering spurs were randomly selected, and the clusters thinned at full bloom to one flower per cluster—usually the king flower. The moisture treatments were started when fruits had reached 10–12 mm diameter (usually about 21–31 DAFB). Experiments were carried out in two consecutive Phases. During Phase I a skin patch was exposed to moisture. For the subsequent Phase II, exposure to moisture was discontinued. For the moisture treatment, a 2 mL polyethylene tube (8 mm diameter; Eppendorf, Hamburg, Germany) was cut to 17 mm length and a hole (1.4 mm diameter) drilled into the tip. The tube was fixed in the equatorial plane of the fruit using a non-phytotoxic silicone rubber (Dowsil™ SE 9186 Clear Sealant; Dow Toray, Japan) [15]. Following curing, the tube was filled through the hole in the tip with deionized water using a syringe. The hole in the tip was then sealed with silicone rubber. The silicone was inspected for leakage and resealed every second day. The opposite, un-treated side of the same fruit served as the control [15]. The duration of moisture exposure (Phase I) was either 6 or 12 d. Thereafter, the tube was carefully removed. Unless specified otherwise, formation of a periderm was monitored up to 113 d after termination of the moisture treatment (Phase II).

4.3. RNA Extraction

Apple fruit skin from moisture-exposed and unexposed (control) areas were excised using a razor blade and immediately frozen in liquid N₂. Fruit skins were stored at –80 °C till processing. The skin tissue was ground to a powder with pestle and mortar in liquid N₂. RNA extraction was done using the InviTrap Spin Plant RNA Mini Kit (STRATEC Molecular GmbH, Berlin, Germany) according to the manufacturer's protocol. To remove genomic DNA, total RNA was treated with DNase using the DNA-free™ Kit (Thermo Fisher Scientific, Waltham, MA, USA). RNA purity and quantity were determined by measuring the absorbance at 230, 260 and 280 nm using a Nanodrop 2000c spectrophotometer (Thermo Fisher Scientific, Waltham, MA, USA). RNA integrity was determined on a 1.5% agarose gel. cDNA synthesis was carried out with the LunaScript® RT SuperMix Kit (New England Biolabs, Ipswich, MA, USA) using 600 ng of RNA in a 40 µL reaction volume following the manufacturer's protocol. The number of biological replicates was from three to five. Each biological replicate comprised the skin from six to ten fruits.

4.4. Quantitative Real-Time PCR

Gene expression was determined by quantitative real-time PCR using the QuantStudio™ 6 Flex Real-Time PCR System (Applied Biosystems, Waltham, MA, USA). Genes observed in this study are listed in Table 1 and the corresponding specific primers in Table S1. Primer design was done using the Primer3 software (Primer3, <http://primer3.ut.ee/>). Gene expression values each represent three to five biological replicates and two to three technical replicates. To normalize gene expression, the reference genes *PROTEIN DISULFIDE ISOMERASE (PDI)* (MDP0000233444) and *MdeF-1alpha* (AJ223969.1) were used. Reactions were carried out using 1 µL undiluted cDNA in 8 µL volume of the Luna® Universal qPCR Master Mix (New England Biolabs, Ipswich, MA, USA) following manufacturer's guidelines. The final concentration was 200 nM for each specific primer. PCR cycle conditions were: one cycle of 95 °C for 60 s, 40 cycles of 95 °C for 15 s and 60 °C for 60 s. After amplification melting curve analysis (95 °C for 15 s, 60 °C for 60 s, 60 to 95 °C in 0.5 °C increments) was used. Primer efficiency was determined in a five-fold dilution series of a cDNA pool covering five dilution points, each using the QuantStudio™ Real-Time PCR Software v1.3 (Applied Biosystems, Waltham, MA, USA).

Relative gene expression was calculated according to Pfaffl [57]. Modifications were according to Chen [58].

Table 1. List of genes analyzed in the gene expression study.

Gene Name	Accession	AGI Locus Code	Description	Reference
Cuticle-related				
<i>ABCG11</i>	MDP0000200335	AT1G17840.1	ABCG11, white-brown complex homolog protein 11, cuticular lipid transport to the extracellular matrix	[29]
<i>CER6</i>	MDP0000392495	AT1G68530.1	3-Ketoacyl-CoA synthase 6, involved in the synthesis of VLCFAs	[27]
<i>FDH, KCS10</i>	MDP0000235280	AT2G26250.1	FIDDLEHEAD,3-Ketoacyl-CoA synthase 10, probably involved in synthesis of long-chain lipids	[25]
<i>GPAT6</i>	MDP0000479163	AT2G38110.1	Glycerol-3-phosphate acyl transferase 6, synthesis of cutin monomers	[24]
<i>SHN3</i>	MDP0000178263	AT5G25390	Positive transcriptional regulator of cuticle synthesis	[32]
<i>WSD1</i>	MDP0000701887	AT5G37300.1	Wax Ester Synthase/ Acyl-Coenzyme A:Diacylglycerol Acyltransferase, Wax ester synthesis and diacylglycerol acyltransfer	[26]
Periderm-related				
<i>ABCG20</i>	MDP0000265619	AT3G53510	ATP-binding cassette G20, involved in transport of aliphatic suberin polymer precursors	[30]
<i>CYP86B1</i>	MDP0000306273	AT5G23190.1	Cytochrome P450, family 86, subfamily B, polypeptide 1, synthesis of very long chain ω -hydroxyacid and α,ω -dicarboxylic acid in suberin polyester	[28]
<i>MYB42</i>	MDP0000787808	AT4G12350.1	MYB domain protein 42, involved in secondary cell wall biosynthesis and regulation of lignin synthesis	[35,36]
<i>MYB93</i>	MDP0000320772	AT1G34670.1	MYB domain protein 93, positive regulator of suberin synthesis	[21]
<i>NAC038</i>	MDP0000232008	AT2G24430.1	NAC domain containing protein 38	uncharacterized
<i>NAC058</i>	MDP0000130785	AT3G18400.1	NAC domain containing protein 58	uncharacterized

4.5. Isolation of Fruit Cuticular Membranes and Periderm Membranes and Bark Periderm Membrane

Cuticular membranes and periderm membranes (PM) of developing apple fruit and periderm membranes from the bark (BP) of the trunk were isolated enzymatically [59]. Moisture exposed and unexposed skin samples were excised using biopsy punches (8 mm diameter, Kai Europe, Solingen, Germany; or 10 or 12 mm diameter, Acuderm, Terrace, FL, USA). The sections of the trunk bark were excised using a scalpel. Skin discs or bark sections were incubated at room temperature in 50 mM citric acid buffer at pH 4.0 containing pectinase (90 mL L⁻¹; Panzym Super E flüssig, Novozymes A/S, Krogshoejvej, Bagsvaerd, Denmark), cellulase (5 mL L⁻¹; Cellubrix L; Novozymes A/S) and 30 mM NaN₃ [59]. The enzyme solution was periodically replaced until CMs and PMs separated from their adhering cellular debris. Isolated CMs, PMs and BPs were rinsed in deionized water, dried at 40 °C for 20 h and stored at room temperature.

4.6. Cross-Sections of Skin Segments and Isolated Cuticular Membranes/Periderm Membranes and Microscopy

Tissue blocks were cut from moisture exposed and unexposed control patches of the fruit skin, transferred into Karnovsky fixative [60] and stored at 4 °C. The blocks were rinsed in distilled water, transferred to 70% (v/v) aqueous ethanol (EtOH) for 16 h

and dehydrated in an increasing series of aqueous EtOH solutions (80%, 90% and 96% EtOH (*v/v*) for 30 min each). Subsequently, blocks were transferred to 100% isopropanol (twice for 40 min each) and then in a xylene substitute (AppiClear AppliChem, Münster, Germany; twice for 40 min each). The dehydrated blocks were infiltrated with a 1:1 (*v:v*) paraffin/xylene-substitute mixture (Carl Roth, Karlsruhe, Germany) for 40 min once, followed by two infiltrations with pure paraffin for 40 min each supported by a mild vacuum (absolute pressure 10.8 kPa). The embedded ES were stored at 4 °C. Sections of 10 µm thickness were cut using a rotatory microtome (Hydrax M 55, Zeiss, Oberkochen, Germany), collected on glass microscope slides and dried for 16 h at 37 °C. The paraffin was removed using xylene substitute (twice for 10 min each). Sections were rehydrated in a decreasing series of aqueous EtOH (96%, 80%, 70%, and 60%, all for 10 min each), followed by two final incubations in distilled water for of 5 min each. Cross-sections of isolated CM or PM were obtained by hand, using a razor blade.

Sections were stained for 1 h with 0.005% Fluorol Yellow 088 (Santa Cruz Biotechnology, TX, USA) [61] dissolved in a 1:1 mixture (*v:v*) of melted polyethylene glycol 4000 (SERVA Electrophoresis, Heidelberg, Germany) and 90% glycerol. Sections were inspected under incident fluorescent light (filter U-MWB, 450–480 nm excitation; ≥520 nm emission wavelength) using a fluorescence microscope (BX-60, Olympus, Hamburg, Germany). Three biological replicates each were observed for the ES, CM and PM.

4.7. Quantification of Wax Constituents by GC/FID and GC/MS

Isolated CM/PM discs and BP sections were cut into small pieces. An equal number of CM/PM pieces from five individual CM/PM discs (each represents a fruit) or of BP from samples of the trunk were pooled to make about 0.5 to 1 mg of material which represents a sample/replication. Samples were extracted in 5 mL chloroform overnight at room temperature on a horizontal rolling bench (CAT RM. 5–30 V, Staufen, Germany). The wax extract was immediately spiked with an adequate amount of internal standard (100 µL tetracosane of a chloroform solution of 10 mg tetracosane in 50 mL) later enabling the quantification of the single wax compounds. The chloroform volume was reduced under a gentle stream of N₂ at 60 °C in a heating block. The extracted CM, PM and BP pieces were dried on Teflon discs for further cutin/suberin analysis. Since some wax molecules contain polar hydroxyl- and carboxyl groups which negatively interfere with the GC column, all samples were derivatized by silylation yielding the corresponding trimethylsilyl ethers and -esters. For silylation 20 µL of BSTFA (N, O-bis(trimethylsilyl)-trifluoroacetamide, Machery-Nagel, Düren, Germany) and 20 µL of pyridine (Sigma Aldrich, Deisenhofen, Germany) were added to each sample. Derivatization took place for 45 min at 70 °C in a heating block. Of each sample 1 µL was injected on-column to a gas chromatograph coupled to a flame ionization detector (GC-FID; CG-Hewlett Packard 5890 series H, Hewlett-Packard, Palo Alto, CA, USA, 307 column-type: 30 m DB-1 i.d. 0.32 mm, film 0.2 µm; J&W Scientific, Folsom, CA, USA). For identification of wax constituents, the extracted wax was analyzed by GC-MS (Quadrupole mass selective detector HP 5971, Hewlett-Packard, Palo Alto, CA, USA) by injecting 1 µL on-column. The constituents were quantified using the internal standard. Identification of the molecules was carried out by comparing fragmentation patterns with literature data and with our own data library. Data are expressed as mass per unit fruit surface area or trunk surface area. The number of replications was two to three, where each replicate comprised a subsample of five pooled CM, PM discs from five different fruit. The number of replications for the BP was three, each representing a different tree.

4.8. Quantification of Apple Cutin and Suberin Monomers by GC/FID and GC/MS

The extracted and dried CM/PM and BP were transesterified in glass vials by incubation in 1 mL boron trifluoride-methanol solution (BF₃/MeOH) for 16 h at 70 °C. After cooling of the samples, 20 µg of internal standard (100 µL dotriacontane of a chloroform solution of 10 mg dotriacontane in 50 mL) was added to each sample. Saturated NaHCO₃

(2 mL) was added to stop the depolymerization reaction. Cutin/suberin monomers were extracted three times by adding 2 mL chloroform. The chloroform phase was collected, washed by adding 1 mL HPLC grade water and then dried using NaSO_4 . The water phase was discarded. The chloroform solution containing the cutin/suberin monomers was concentrated under a gentle stream of N_2 at 60 °C. Samples were derivatized as described above by adding 20 μL of BSTFA and 20 μL of pyridine. Monomers were quantified by injecting 1 μL of each sample on-column on a gas chromatograph coupled to a FID (GC-FID; CG-Hewlett Packard 5890 series H, Hewlett-Packard, Palo Alto, CA, USA, 307 column-type: 30 m DB-1 i.d. 0.32 mm, film 0.2 μm ; J&W Scientific, Folsom, CA, USA). The individual constituents were identified on a gas chromatograph coupled to a mass spectrometer (Quadrupole mass selective detector HP 5971, Hewlett-Packard, Palo Alto, CA, USA) relative to the internal standard in each sample. Monomers were identified by comparing the fragmentation patterns with known standards from the literature or from our own library. Data are expressed as mass per unit fruit surface area. The number of replications was two or three, where each replicate comprised pooled CM/PM from five individual CM/PM discs obtained from five different fruit. The number of replications for the BP was three, each representing a different tree.

4.9. Data Analyses

Because moisture exposure of a patch of fruit skin results in formation of a periderm only in parts of the moisture treated area, the polymer obtained following enzymatic isolation from such surfaces is a mixed polymer comprising cuticle (cutin and wax) and periderm (suberized phellem and wax) of varying amounts. Furthermore, cutin and suberin and their waxes share common monomers and constituents. This makes it impossible to quantify the amounts of cutin and suberin or the amounts of cuticular and periderm wax deposited per unit surface area of moisture-treated patches of fruit skin. However, for the dewaxed suberin fraction, the ω -hydroxy- C_{20} , -C_{22} and -C_{24} acids are major and unique constituents of suberin that together account for 17.6% of a pure suberin of bark periderm of apple tree. As a first approximation, we assumed the composition of the suberin of a composite cuticle with periderm of moisture-treated apple fruit skin and that of the bark of a trunk of the same apple cultivar to be identical. Hence, the total amount of suberin in the cuticle may be calculated relative to the amounts of the ω -hydroxy- C_{20} , -C_{22} and -C_{24} acids. In contrast to the cuticle, with periderm of the moisture-treated fruit surface, the bark periderm of a trunk is comprised of suberin only—a cuticle is absent. We therefore used the suberin of the bark periderm as a standard. The periderm from the bark of the trunk were extracted, depolymerized and analyzed by GC-MS. Using the three hydroxy acids, a normalized suberin composition of the moisture-treated fruit was then calculated. This procedure allowed quantification of the time course of cutin and suberin deposition of the mixed polymer of a moisture-treated fruit surface. Due to the lack of unique constituents, the same calculation could not be carried out for the wax of cuticles with periderm.

Data are presented as means \pm standard errors. When error bars are not shown, they were smaller than the data symbols. Paired sample Student's *t*-tests were run. Significant differences between dry/dry and wet/dry at $p \leq 0.05$ is indicated by '*'.

Supplementary Materials: The following are available online at <https://www.mdpi.com/2223-7747/10/1/65/s1>, Figure S1: Time course of expressions of genes related to cutin, wax (a–f) and suberin and lignin synthesis (g–l) of apple fruit skin during exposure to moisture (Phase I) and after exposure to moisture ceased (Phase II). Figure S2: Time course of expressions of genes related to cutin, wax (a–f) and suberin and lignin synthesis (g–l) of apple fruit skin during exposure to moisture (Phase I) and after exposure to moisture was discontinued (Phase II). Table S1 Primers for genes analyzed used in the present study [62], Table S2: Effect of moisture exposure on the composition of the cuticle/periderm polymer.

Author Contributions: Conceptualization, T.D., M.K. and B.P.K.; funding acquisition, T.D. and M.K.; project administration, T.D. and M.K.; methodology, M.K., T.D., L.S. and B.P.K.; investigation, J.S., Y.-H.C., A.S., V.Z.-D., K.S. and B.P.K.; supervision, T.D., M.K., L.S. and B.P.K.; data curation, J.S., Y.-H.C., B.P.K., V.Z.-D. and K.S.; validation, J.S., Y.-H.C., B.P.K., V.Z.-D. and K.S.; visualization, J.S., Y.-H.C. and B.P.K.; formal analysis, J.S., Y.-H.C., B.P.K., V.Z.-D. and K.S.; writing—original draft, J.S., T.D., M.K. and B.P.K.; and writing—review and editing, J.S., T.D., M.K., B.P.K. and L.S. All authors have read and agreed to the published version of the manuscript.

Funding: This research was supported by a grant (DE 511/9-1) from the Deutsche Forschungsgemeinschaft (DFG). The publication of this article was funded by the Open Access fund of the Leibniz Universität Hannover.

Institutional Review Board Statement: Ethical review and approval were waived for this study as not applicable.

Informed Consent Statement: Not applicable.

Data Availability Statement: Original data is available upon request from the corresponding author.

Acknowledgments: We thank Traud Winkelmann and Raul Javier Morales Orellana for advice and support in sample preparation for histology. We also thank Julia Schröter, Simon Sitzenstock and Friederike Schröder for technical assistance and Alexander Lang for helpful comments on an earlier version of this manuscript.

Conflicts of Interest: There are no known competing interests that could influence the work reported in this paper.

References

1. Skene, D.S. The development of russet, rough russet and cracks on the fruit of the apple Cox's Orange Pippin during the course of the season. *J. Hortic. Sci.* **1982**, *57*, 165–174. [[CrossRef](#)]
2. Goffinet, M.C.; Pearson, R.C. Anatomy of russeting induced in concord grape berries by the fungicide chlorothalonil. *Am. J. Enol. Vitic.* **1991**, *42*, 281–289.
3. Michailides, T.J. Russeting and russet scab of prune, an environmentally induced fruit disorder: Symptomatology, induction, and control. *Plant Dis.* **1991**, *75*, 1114–1123. [[CrossRef](#)]
4. Scharwies, J.D.; Grimm, E.; Knoche, M. Russeting and relative growth rate are positively related in 'Conference' and 'Condo' pear. *HortScience* **2014**, *49*, 746–749. [[CrossRef](#)]
5. Athoo, T.O.; Winkler, A.; Knoche, M. Russeting in 'Apple' mango: Triggers and mechanisms. *Plants* **2020**, *9*, 898. [[CrossRef](#)]
6. Khanal, B.P.; Ikigu, G.M.; Knoche, M. Russeting partially restores apple skin permeability to water vapour. *Planta* **2019**, *249*, 849–860. [[CrossRef](#)]
7. Falginella, L.; Cipriani, G.; Monte, C.; Gregori, R.; Testolin, R.; Velasco, R.; Troglio, M.; Tartarini, S. A major QTL controlling apple skin russeting maps on the linkage group 12 of 'Renetta Grigia di Torriana'. *BMC Plant Biol.* **2015**, *15*, 150. [[CrossRef](#)]
8. Lashbrooke, J.; Aharoni, A.; Costa, F. Genome investigation suggests *MdSHN3*, an APETALA2-domain transcription factor gene, to be a positive regulator of apple fruit cuticle formation and an inhibitor of russet development. *J. Exp. Bot.* **2015**, *66*, 6579–6589. [[CrossRef](#)]
9. Legay, S.; Guerriero, G.; Deleruelle, A.; Lateur, M.; Evers, D.; André, C.M.; Hausman, J.F. Apple russeting as seen through the RNA-seq lens: Strong alterations in the exocarp cell wall. *Plant Mol. Biol.* **2015**, *88*, 21–40. [[CrossRef](#)]
10. Faust, M.; Shear, C.B. Russeting of apples, an interpretive review. *HortScience* **1972**, *7*, 233–235.
11. Taylor, B.K. Reduction of apple skin russeting by gibberellin A 4+7. *J. Hortic. Sci.* **1975**, *50*, 169–172. [[CrossRef](#)]
12. Taylor, B.K. Effects of gibberellin sprays on fruit russet and tree performance of Golden Delicious apple. *J. Hortic. Sci.* **1978**, *53*, 167–169. [[CrossRef](#)]
13. Simons, R.K.; Chu, M.C. Periderm morphology of mature 'Golden Delicious' apple with special reference to russeting. *Sci. Hortic.* **1978**, *8*, 333–340. [[CrossRef](#)]
14. Wertheim, S.J. Fruit russeting in apple as affected by various gibberellins. *J. Hortic. Sci.* **1982**, *57*, 283–288. [[CrossRef](#)]
15. Khanal, B.P.; Imoro, Y.; Chen, Y.H.; Straube, J.; Knoche, M. Surface moisture increases microcracking and water vapor permeance of apple fruit skin. *Plant Biol.* **2020**. [[CrossRef](#)]
16. Chen, Y.-H.; Straube, J.; Khanal, B.P.; Knoche, M.; Debener, T. Russeting in apple is initiated after exposure to moisture ends-I. Histological evidence. *Plants* **2020**, *9*, 1293. [[CrossRef](#)]
17. Lai, X.; Khanal, B.P.; Knoche, M. Mismatch between cuticle deposition and area expansion in fruit skins allows potentially catastrophic buildup of elastic strain. *Planta* **2016**, *244*, 1145–1156. [[CrossRef](#)]
18. Knoche, M.; Grimm, E. Surface moisture induces microcracks in the cuticle of 'Golden Delicious' apple. *HortScience* **2008**, *43*, 1929–1931. [[CrossRef](#)]
19. Knoche, M.; Khanal, B.P.; Stopar, M. Russeting and microcracking of 'Golden Delicious' apple fruit concomitantly decline due to gibberellin A4+7 application. *J. Am. Soc. Hortic. Sci.* **2011**, *136*, 159–164. [[CrossRef](#)]

20. Winkler, A.; Grimm, E.; Knoche, M.; Lindstaedt, J.; Köpcke, D. Late-season surface water induces skin spot in apple. *HortScience* **2014**, *49*, 1324–1327. [[CrossRef](#)]
21. Legay, S.; Guerriero, G.; André, C.; Guignard, C.; Cocco, E.; Charton, S.; Boutry, M.; Rowland, O.; Hausman, J.F. MdMyb93 is a regulator of suberin deposition in russeted apple fruit skins. *New Phytol.* **2016**, *212*, 977–991. [[CrossRef](#)] [[PubMed](#)]
22. Khanal, B.P.; Si, Y.; Knoche, M. Lenticels and apple fruit transpiration. *Postharvest Biol. Technol.* **2020**, *167*, 111221. [[CrossRef](#)]
23. Yang, W.; Pollard, M.; Li-Beisson, Y.; Beisson, F.; Feig, M.; Ohlrogge, J. A distinct type of glycerol-3-phosphate acyltransferase with *sn*-2 preference and phosphatase activity producing 2-monoacylglycerol. *Proc. Natl. Acad. Sci. USA* **2010**, *107*, 12040–12045. [[CrossRef](#)] [[PubMed](#)]
24. Petit, J.; Bres, C.; Mauxion, J.P.; Tai, F.W.J.; Martin, L.B.; Fich, E.A.; Joubès, J.; Rose, J.K.; Domergue, F.; Rothan, C. The glycerol-3-phosphate acyltransferase GPAT6 from tomato plays a central role in fruit cutin biosynthesis. *Plant Physiol.* **2016**, *171*, 894–913. [[CrossRef](#)] [[PubMed](#)]
25. Pruitt, R.E.; Vielle-Calzada, J.P.; Ploense, S.E.; Grossniklaus, U.; Lolle, S.J. *FIDDLEHEAD*, a gene required to suppress epidermal cell interactions in *Arabidopsis*, encodes a putative lipid biosynthetic enzyme. *Proc. Natl. Acad. Sci. USA* **2000**, *97*, 1311–1316. [[CrossRef](#)]
26. Li, F.; Wu, X.; Lam, P.; Bird, D.; Zheng, H.; Samuels, L.; Jetter, R.; Kunst, L. Identification of the wax ester synthase/acyl-coenzyme A:diacylglycerol acyltransferase WSD1 required for stem wax ester biosynthesis in *Arabidopsis*. *Plant Physiol.* **2008**, *148*, 97–107. [[CrossRef](#)]
27. Millar, A.A.; Clemens, S.; Zachgo, S.; Michael Giblin, E.; Taylor, D.C.; Kunst, L. *CUT1*, an *Arabidopsis* gene required for cuticular wax biosynthesis and pollen fertility, encodes a very-long-chain fatty acid condensing enzyme. *Plant Cell* **1999**, *11*, 825–838. [[CrossRef](#)]
28. Compagnon, V.; Diehl, P.; Benveniste, I.; Meyer, D.; Schaller, H.; Schreiber, L.; Franke, R.; Pinot, F. CYP86B1 is required for very long chain ω -hydroxyacid and α , ω -dicarboxylic acid synthesis in root and seed suberin polyester. *Plant Physiol.* **2009**, *150*, 1831–1843. [[CrossRef](#)]
29. Bird, D.; Beisson, F.; Brigham, A.; Shin, J.; Greer, S.; Jetter, R.; Kunst, L.; Wu, X.; Yephremov, A.; Samuels, L. Characterization of *Arabidopsis* ABCG11/WBC11, an ATP binding cassette (ABC) transporter that is required for cuticular lipid secretion. *Plant J.* **2007**, *52*, 485–498. [[CrossRef](#)]
30. Yadav, V.; Molina, I.; Ranathunge, K.; Castillo, I.Q.; Rothstein, S.J.; Reed, J.W. ABCG transporters are required for suberin and pollen wall extracellular barriers in *Arabidopsis*. *Plant Cell* **2014**, *26*, 3569–3588. [[CrossRef](#)]
31. Legay, S.; Cocco, E.; André, C.M.; Guignard, C.; Hausman, J.-F.; Guerriero, G. Differential lipid composition and gene expression in the semi-russeted “Cox Orange Pippin” apple variety. *Front. Plant Sci.* **2017**, *8*, 1656. [[CrossRef](#)] [[PubMed](#)]
32. Aharoni, A.; Dixit, S.; Jetter, R.; Thoenes, E.; van Arkel, G.; Pereira, A. The SHINE clade of AP2 domain transcription factors activates wax biosynthesis, alters cuticle properties and confers drought tolerance when overexpressed in *Arabidopsis*. *Plant Cell* **2004**, *16*, 2463–2480. [[CrossRef](#)] [[PubMed](#)]
33. Shi, J.X.; Malitsky, S.; de Oliveira, S.; Branigan, C.; Franke, R.B.; Schreiber, L.; Aharoni, A. SHINE transcription factors act redundantly to pattern the archetypal surface of *Arabidopsis* flower organs. *PLoS Genet.* **2011**, *7*, e1001388. [[CrossRef](#)] [[PubMed](#)]
34. Shi, J.X.; Adato, A.; Alkan, N.; He, Y.; Lashbrooke, J.; Matas, A.J.; Meir, S.; Malitsky, S.; Isaacson, T.; Prusky, D.; et al. The tomato SISHINE3 transcription factor regulates fruit cuticle formation and epidermal patterning. *New Phytol.* **2013**, *197*, 468–480. [[CrossRef](#)]
35. Zhong, R.; Lee, C.; Zhou, J.; McCarthy, R.L.; Ye, Z.H. A battery of transcription factors involved in the regulation of secondary cell wall biosynthesis in *Arabidopsis*. *Plant Cell* **2008**, *20*, 2763–2782. [[CrossRef](#)]
36. Geng, P.; Zhang, S.; Liu, J.; Zhao, C.; Wu, J.; Cao, Y.; Fu, C.; Han, X.; He, H.; Zhao, Q. MYB20, MYB42, MYB43, and MYB85 regulate phenylalanine and lignin biosynthesis during secondary cell wall formation. *Plant Physiol.* **2020**, *182*, 1272–1283. [[CrossRef](#)]
37. Heredia, A. Biophysical and biochemical characteristics of cutin, a plant barrier biopolymer. *Biochim. Biophys. Acta Gen. Subj.* **2003**, *1620*, 1–7. [[CrossRef](#)]
38. Walton, T.J.; Kolattukudy, P.E. Determination of the structures of cutin monomers by a novel depolymerization procedure and combined gas chromatography and mass spectrometry. *Biochemistry* **1972**, *11*, 1885–1897. [[CrossRef](#)]
39. Kolattukudy, P.E. Biopolymer membranes of plants: Cutin and suberin. *Science* **1980**, *208*, 990–1000. [[CrossRef](#)]
40. Belding, R.D.; Blankenship, S.M.; Young, E.; Leidy, R.B. Composition and variability of epicuticular waxes in apple cultivars. *J. Am. Soc. Hortic. Sci.* **1998**, *123*, 348–356. [[CrossRef](#)]
41. Andre, C.M.; Greenwood, J.M.; Walker, E.G.; Rassam, M.; Sullivan, M.; Evers, D.; Perry, N.B.; Laing, W.A. Anti-inflammatory procyanidins and triterpenes in 109 apple varieties. *J. Agric. Food Chem.* **2012**, *60*, 10546–10554. [[CrossRef](#)] [[PubMed](#)]
42. Andre, C.M.; Larsen, L.; Burgess, E.J.; Jensen, D.J.; Cooney, J.M.; Evers, D.; Zhang, J.; Perry, N.B.; Laing, W.A. Unusual immunomodulatory triterpene-caffeates in the skins of russeted varieties of apples and pears. *J. Agric. Food Chem.* **2013**, *61*, 2773–2779. [[CrossRef](#)] [[PubMed](#)]
43. Andre, C.M.; Legay, S.; Deleruelle, A.; Nieuwenhuizen, N.; Punter, M.; Brendolise, C.; Cooney, J.M.; Lateur, M.; Hausman, J.-F.; Larondelle, Y.; et al. Multifunctional oxidosqualene cyclases and cytochrome P450 involved in the biosynthesis of apple fruit triterpenic acids. *New Phytol.* **2016**, *211*, 1279–1294. [[CrossRef](#)]
44. Peschel, S.; Franke, R.; Schreiber, L.; Knoche, M. Composition of the cuticle of developing sweet cherry fruit. *Phytochemistry* **2007**, *68*, 1017–1025. [[CrossRef](#)] [[PubMed](#)]

45. Curry, E.A. Growth-induced microcracking and repair mechanisms of fruit cuticles. In Proceedings of the SEM Annual Conference, Albuquerque, NM, USA, 1–4 June 2009.
46. Knoche, M.; Lang, A. Ongoing growth challenges fruit skin integrity. *CRC Crit. Rev. Plant Sci.* **2017**, *36*, 190–215. [[CrossRef](#)]
47. Khanal, B.P.; Grimm, E.; Finger, S.; Blume, A.; Knoche, M. Intracuticular wax fixes and restricts strain in leaf and fruit cuticles. *New Phytol.* **2013**, *200*, 134–143. [[CrossRef](#)] [[PubMed](#)]
48. Franke, R.; Briesen, I.; Wojciechowski, T.; Faust, A.; Yephremov, A.; Nawrath, C.; Schreiber, L. Apoplastic polyesters in *Arabidopsis* surface tissues—A typical suberin and a particular cutin. *Phytochemistry* **2005**, *66*, 2643–2658. [[CrossRef](#)]
49. Khanal, B.P.; Le, T.L.; Si, Y.; Knoche, M. Russet susceptibility in apple is associated with skin cells that are larger, more variable in size, and of reduced fracture strain. *Plants* **2020**, *9*, 1118. [[CrossRef](#)]
50. Sekse, L. Cuticular fracturing in fruits of sweet cherry (*Prunus avium* L.) resulting from changing soil water contents. *J. Hortic. Sci.* **1995**, *70*, 631–635. [[CrossRef](#)]
51. Sekse, L. Fruit cracking in sweet cherries (*Prunus avium* L.). Some physiological aspects—A mini review. *Sci. Hortic.* **1995**, *63*, 135–141. [[CrossRef](#)]
52. Sekse, L.; Bjerke, K.L.; Vangdal, E. Fruit cracking in sweet cherries—An integrated approach. *Acta Hortic.* **2005**, *667*, 471–474. [[CrossRef](#)]
53. Khanal, B.P.; Knoche, M. Mechanical properties of cuticles and their primary determinants. *J. Exp. Bot.* **2017**, *68*, 5351–5367. [[CrossRef](#)] [[PubMed](#)]
54. Roy, S.; Conway, W.S.; Watada, A.E.; Sams, C.E.; Erbe, E.F.; Wergin, W.P. Changes in the ultrastructure of the epicuticular wax and postharvest calcium uptake in apples. *HortScience* **1999**, *34*, 121–124. [[CrossRef](#)]
55. Curry, E.; Arey, B. Apple cuticle—The perfect interface. *Proc. SPIE* **2010**, *7729*, 77291P-1–77291P-11. [[CrossRef](#)]
56. Lipton, W.J. Some effects of low-oxygen atmospheres on potato tubers. *Amer. Potato J.* **1967**, *44*, 292–299. [[CrossRef](#)]
57. Pfaffl, M.W. A new mathematical model for relative quantification in real-time RT-PCR. *Nucleic Acids Res.* **2001**, *29*, E45. [[CrossRef](#)] [[PubMed](#)]
58. Chen, Y.H.; Khanal, B.P.; Linde, M.; Debener, T.; Alkio, M.; Knoche, M. Expression of putative aquaporin genes in sweet cherry is higher in flesh than skin and most are downregulated during development. *Sci. Hortic.* **2019**, *244*, 304–314. [[CrossRef](#)]
59. Orgell, W.H. The isolation of plant cuticle with pectic enzymes. *Plant Physiol.* **1955**, *30*, 78–80. [[CrossRef](#)]
60. Karnovsky, M.J. A formaldehyde-glutaraldehyde fixative of high osmolarity for use in electron microscopy. *J. Cell Biol.* **1965**, *27*, 1A–149A.
61. Brundrett, M.C.; Kendrick, B.; Peterson, C.A. Efficient lipid staining in plant material with Sudan Red 7B or Fluoral Yellow 088 in polyethylene glycol-glycerol. *Biotech. Histochem.* **1991**, *66*, 111–116. [[CrossRef](#)]
62. Storch, T.T.; Pegoraro, C.; Finatto, T.; Quecini, V.; Rombaldi, C.V.; Girardi, C.L. Identification of a novel reference gene for apple transcriptional profiling under postharvest conditions. *PLoS ONE* **2015**, *10*, e0120599. [[CrossRef](#)] [[PubMed](#)]

4.1. Supplementary data Chapter 4

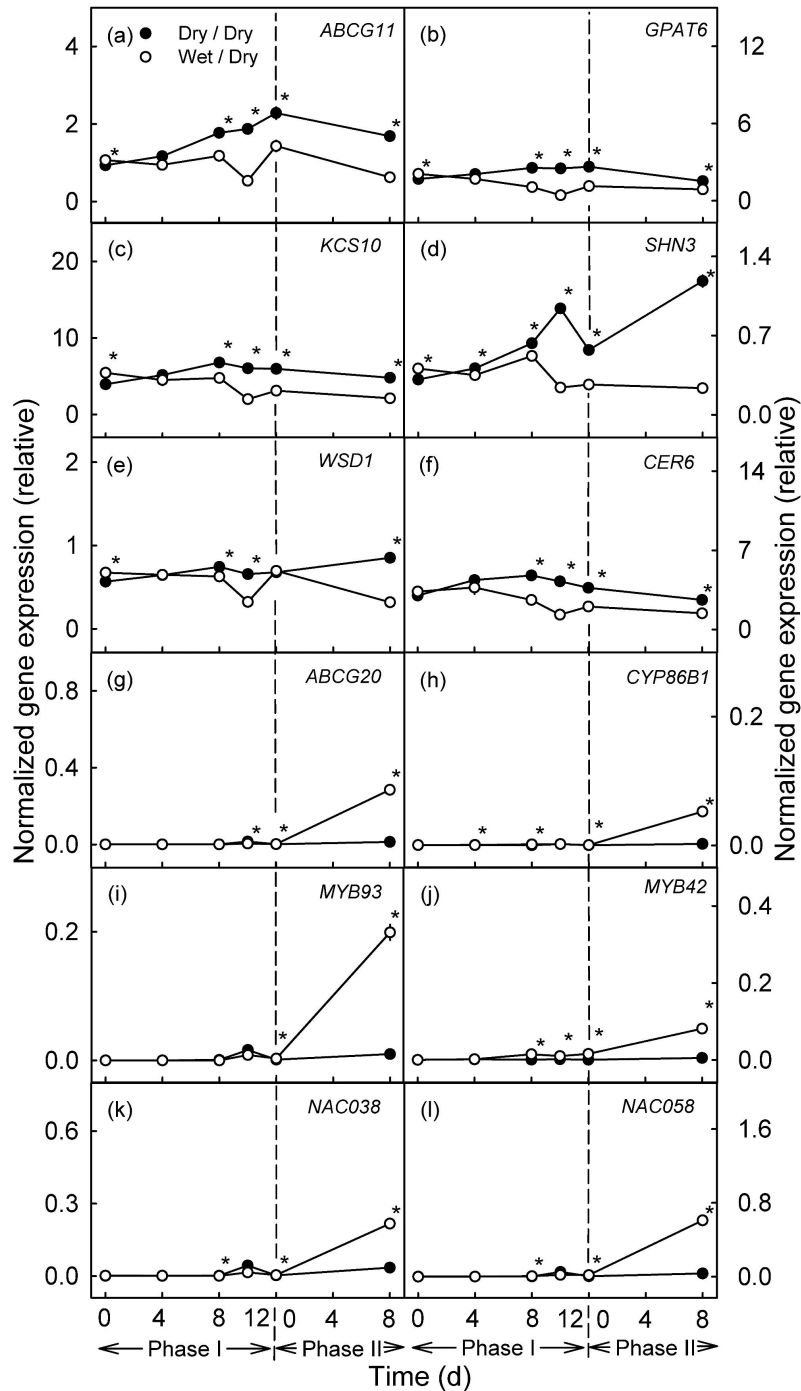


Figure S1. Time course of expressions of genes related to cutin, wax (a-f) and suberin and lignin synthesis (g-l) of apple fruit skin during exposure to moisture (Phase I) and after exposure to moisture ceased (Phase II). During Phase I, a patch of the fruit skin was exposed to moisture for 12 d beginning at 23 days after full bloom (DAFB) (wet). During the subsequent Phase II, moisture exposure was discontinued and the patch was exposed to the atmosphere (Dry). Moisture exposed patches of fruit skin are referred to as wet/dry, unexposed (control) patches as dry/dry. The end of the period of moisture exposure is indicated by the vertical dashed line. The expression values are means \pm SE of three independent biological replicates comprising six fruit each. The ‘*’ indicates significant difference between dry/dry and wet/dry at $p \leq 0.05$ (Student’s t-test).

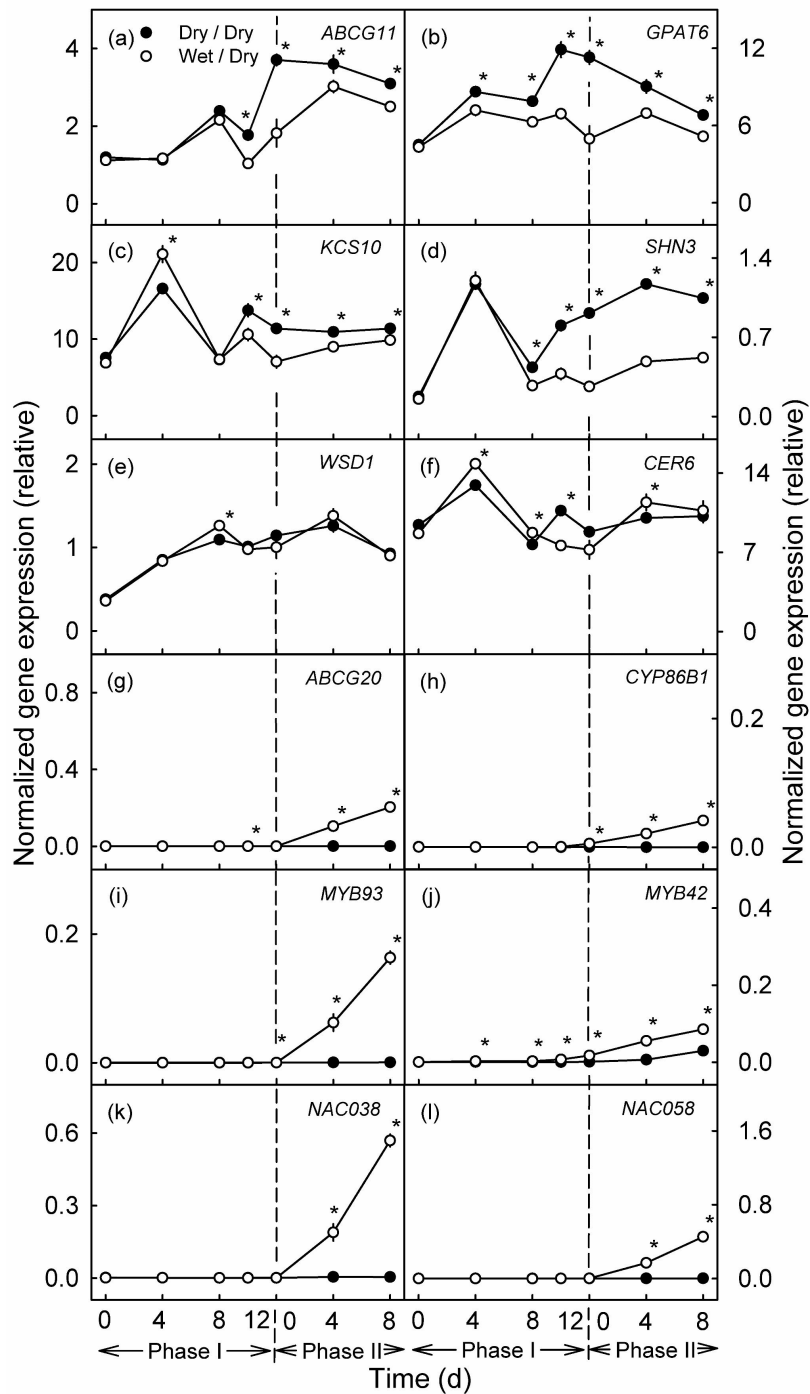


Figure S2. Time course of expressions of genes related to cutin, wax (a-f) and suberin and lignin synthesis (g-l) of Apple fruit skin during exposure to moisture (Phase I) and after exposure to moisture was discontinued (Phase II). During Phase I, a patch of the fruit skin was exposed to moisture for 12 d beginning at 21 days after full bloom (DAFB) (wet). During the subsequent Phase II, moisture exposure was discontinued and the patch exposed to the atmosphere (Dry). Moisture exposed patches of fruit skin are referred to as wet/dry, unexposed (control) patches as dry/dry. The end of the period of moisture exposure is indicated by the vertical dashed line. The expression values are means \pm SE of three independent biological replicates comprising six fruit each. The "*" indicates significant difference between dry/dry and wet/dry at $p \leq 0.05$ (Student's t-test).

Chapter 4 Russetting in apple is initiated after exposure to moisture ends.
Molecular and biochemical evidence

Supplementary Table S1. Primers for genes analyzed used in the present study.

Gene name	Accession	Primer sequence (5'-3')		PCR efficiency (%)	Reference
		Forward Primer	Reverse Primer		
<i>ABCG11</i>	MDP0000200335	TGGCGGGTTTCCTTCTTTCA	CACAAATGCAGTAACGCCGT	98.7	This study
<i>ABCG20</i>	MDP0000265619	ACTGGGCATGGACAACAACA	ATTTTCCCGACCCACTTGCT	102.9	This study
<i>CER6</i>	MDP0000392495	AGCAACAACCCTAAGAGCGT	GTTGGGCGGAATGTAGTGGA	85.0	This study
<i>CYP86B1</i>	MDP0000306273	CGCTTTGTGACCCCATCC	AATGACGTCTCCGCAAACCT	109.3	(Legay et al., 2015)
<i>eF-1alpha</i>	AJ223969.1	ACTGTTCTGTTGGACGTGTTG	TGGAGTTGGAAGCAACGTACCC	93.0	(Legay et al., 2015)
<i>GPAT6</i>	MDP0000479163	TCTTGAACCAGCTACCGTCG	AATCCCAAAGTCCCAGCCAA	91.0	This study
<i>KCS10</i>	MDP0000235280	TGCTGAGGTGGGAAGTTTGA	ACACCAAAGAACCCTAGCACA	91.6	This study
<i>MYB42</i>	MDP0000787808	CCTTGGCAATAGGTGGTCTGA	TGATGTGCGTGTTCAGTGA	94.2	This study
<i>MYB93</i>	MDP0000320772	TGGACAAACTATCTTAGGCCGG	GTTGCCGAGGATGGAATGGA	102.5	This study
<i>NAC038</i>	MDP0000232008	CGGCGGATCATCAAGTAGCA	AAACCCTCCTCCTCCTCAA	84.6	This study
<i>NAC058</i>	MDP0000130785	AGCCACAACAAGCAACAACA	TTTGGCAGCTCGATGTCTCC	90.7	This study
<i>PDI</i>	MDP0000233444	TGCTGTACACAGCCAACGAT	CATCTTTAGCGGCGTTATCC	100.6	(Storch et al., 2015)
<i>SHN3</i>	MDP0000178263	GGGACGTTTGAGACAGCAGA	TTTTGGTCGGTGGCAGGTTT	93.6	This study
<i>WSD1</i>	MDP0000701887	AGAAATGGTCAAACCCGACA	AGACGAAGTCAAGCGCATTT	91.1	(Legay et al., 2015)

Chapter 4 Russetting in apple is initiated after exposure to moisture ends.
Molecular and biochemical evidence

Supplementary Table S2. Effect of moisture exposure on the composition of the cuticle/periderm polymer. During exposure to moisture and following discontinuation of exposure a mixed polymer comprising cutin and suberin formed. Using the bark periderm of the trunk (BP) of ‘Pinova’ apple trees, the composition of pure suberin was determined. Assuming the suberin composition of periderms of terrestrial surfaces within the same species and cultivar to be identical, the content of ω -hydroxy-C₂₀, -C₂₂, and -C₂₄ acids in bark suberin was used to calculate a normalized suberin composition and mass per unit area for the mixed cuticle/periderm surface of the fruit. The experiment was run as a two-phase experiment. During Phase I, the fruit were exposed to moisture for 12 d beginning at 31 days after full bloom (DAFB) (‘wet’). Moisture exposure was discontinued at the onset of Phase II (‘dry’). The treated patches of fruit skin were sampled 113 d after moisture exposure ceased. Patches of fruit skin that remained dry during both phases served as control (dry/dry). For details of the analysis see Materials and Methods. The study was carried out using three replicates. ND = not detected.

	Fruit cutin and suberin ($\mu\text{g cm}^{-2}$)		Bark suberin ($\mu\text{g cm}^{-2}$)	Bark suberin (%)	Fruit cutin ($\mu\text{g cm}^{-2}$)		Fruit suberin ($\mu\text{g cm}^{-2}$)	
	Dry/Dry	Wet/dry			Dry/Dry	Wet/Dry	Dry/Dry	Wet/Dry
Aromatics								
Hydroxycinnamic acid	11.8 ± 3.3	7.4 ± 1.7	ND	ND	11.8 ± 3.3	7.4 ± 1.7	0.0 ± 0.0	0.0 ± 0.0
Cinnamic acid	ND	ND	5.0 ± 1.0	0.5	ND	ND	ND	ND
cis-Coumaric acid	1.1 ± 0.3	0.7 ± 0.1	ND	ND	1.1 ± 0.3	0.7 ± 0.1	0.0 ± 0.0	0.0 ± 0.0
trans-Coumaric acid	6.3 ± 1.4	1.7 ± 0.6	ND	ND	6.3 ± 1.4	1.7 ± 0.6	0.0 ± 0.0	0.0 ± 0.0
Benzoic acid 1	ND	ND	2.9 ± 0.6	0.3	ND	ND	ND	ND
Benzoic acid 1	ND	ND	4.8 ± 1.4	0.5	ND	ND	ND	ND
trans-Ferulic acid	ND	ND	39.3 ± 4.4	4.0	ND	ND	ND	ND
Linoleic acid	ND	ND	10.4 ± 1.5	1.1	ND	ND	ND	ND
Carboxylic acids								
C16	8.0 ± 1.2	6.3 ± 0.8	4.6 ± 0.9	0.5	8.0 ± 1.2	6.3 ± 0.8	0.0 ± 0.0	0.0 ± 0.0
C18	5.1 ± 0.8	3.2 ± 0.3	5.5 ± 1.9	0.6	5.1 ± 0.8	3.2 ± 0.3	0.0 ± 0.0	0.0 ± 0.0
C20	1.2 ± 0.5	0.2 ± 0.1	8.3 ± 0.7	0.8	1.2 ± 0.5	0.2 ± 0.1	0.0 ± 0.0	0.0 ± 0.0
C22	1.2 ± 0.2	16.4 ± 4.1	80.6 ± 5.3	8.2	1.2 ± 0.2	15.4 ± 3.7	0.0 ± 0.0	1.0 ± 0.4
C24	4.7 ± 2.7	1.1 ± 0.2	138.1 ± 17.5	14.0	4.6 ± 2.7	1.0 ± 0.2	0.1 ± 0.0	0.1 ± 0.0
C26	0.9 ± 0.4	2.9 ± 0.8	16.6 ± 0.9	1.7	0.9 ± 0.4	2.9 ± 0.8	0.0 ± 0.0	0.0 ± 0.0
Primary alcohols								
C16	ND	ND	1.7 ± 0.4	0.2	ND	ND	ND	ND
C18	ND	ND	1.4 ± 0.6	0.1	ND	ND	ND	ND
C20	ND	ND	1.9 ± 0.2	0.2	ND	ND	ND	ND
C22	ND	ND	34.8 ± 2.9	3.5	ND	ND	ND	ND
C24	ND	ND	39.4 ± 19.3	4.0	ND	ND	ND	ND
C26	5.5 ± 0.3	1.2 ± 0.4	62.5 ± 7.3	6.3	5.5 ± 0.4	1.1 ± 0.4	0.0 ± 0.0	0.0 ± 0.0
C28	0.4 ± 0.1	0.2 ± 0.0	15.5 ± 2.2	1.6	0.4 ± 0.1	0.2 ± 0.0	0.0 ± 0.0	0.0 ± 0.0

Chapter 4 Russeting in apple is initiated after exposure to moisture ends.
Molecular and biochemical evidence

Supplementary Table S2. Continued

	Fruit cutin and suberin ($\mu\text{g cm}^{-2}$)		Bark suberin ($\mu\text{g cm}^{-2}$)	Bark suberin (%)	Fruit cutin ($\mu\text{g cm}^{-2}$)		Fruit suberin ($\mu\text{g cm}^{-2}$)	
	Dry/Dry	Wet/dry			Dry/Dry	Wet/Dry	Dry/Dry	Wet/Dry
Dicarboxylic acids								
C16	2.9 ± 0.3	8.7 ± 1.5	26.5 ± 3.1	2.7	2.9 ± 0.3	8.5 ± 1.5	0.0 ± 0.0	0.2 ± 0.1
C16:9,10-dihydroxy	7.3 ± 2.1	8.2 ± 0.5	ND	ND	7.3 ± 2.1	8.2 ± 0.5	0.0 ± 0.0	0.0 ± 0.0
C18	ND	ND	27.9 ± 3.1	2.8	ND	ND	ND	ND
C18:1-hydroxy	ND	ND	53.6 ± 7.8	5.4	ND	ND	ND	ND
C18:9,10-dihydroxy	7.6 ± 0.5	7.2 ± 1.7	ND	ND	7.6 ± 0.5	7.2 ± 1.7	0.0 ± 0.0	0.0 ± 0.0
C20	ND	ND	16.8 ± 8.7	1.7	ND	ND	ND	ND
C22	ND	ND	7.6 ± 0.9	0.8	ND	ND	ND	ND
Hydroxy acids								
C16: ω	28.2 ± 2.3	9.3 ± 2.3	16.3 ± 2.2	1.7	28.2 ± 2.3	9.2 ± 2.3	0.0 ± 0.0	0.1 ± 0.0
C18: ω	ND	ND	22.3 ± 2.6	2.3	ND	ND	ND	ND
C18:1	17.9 ± 3.3	27.6 ± 7.6	136.0 ± 13.8	13.8	17.8 ± 3.3	25.0 ± 6.8	0.1 ± 0.0	2.7 ± 1.0
C18:2	0.8 ± 0.3	0.4 ± 0.0	ND	ND	0.8 ± 0.3	0.4 ± 0.0	0.0 ± 0.0	0.0 ± 0.0
C20: ω	3.3 ± 0.7	5.9 ± 2.0	39.9 ± 4.2	4.0	0.0 ± 0.0	0.0 ± 0.0	3.3 ± 0.7	5.9 ± 2.0
C22: ω	1.0 ± 0.4	18.7 ± 4.7	88.2 ± 8.3	9.0	0.0 ± 0.0	0.0 ± 0.0	1.0 ± 0.4	18.7 ± 4.7
C24: ω	0.3 ± 0.1	5.8 ± 1.3	45.1 ± 3.0	4.6	0.0 ± 0.0	0.0 ± 0.0	0.3 ± 0.1	5.8 ± 1.3
C16:10,16-di	192.1 ± 20.2	46.2 ± 18.9	ND	ND	192.1 ± 20.2	46.2 ± 18.9	0.0 ± 0.0	0.0 ± 0.0
C18:9,10,18-tri	58.1 ± 14.3	53.8 ± 14.7	ND	ND	58.1 ± 14.3	53.8 ± 14.7	0.0 ± 0.0	0.0 ± 0.0
HA1	85.8 ± 24.0	32.8 ± 8.3	ND	ND	85.8 ± 24.0	32.8 ± 8.3	0.0 ± 0.0	0.0 ± 0.0
Unidentified								
X1	ND	ND	4.2 ± 2.7	0.4	ND	ND	ND	ND
X2	ND	ND	9.6 ± 7.4	1.0	ND	ND	ND	ND
X3	ND	ND	10.6 ± 2.0	1.1	ND	ND	ND	ND
X4	ND	ND	2.2 ± 0.6	0.2	ND	ND	ND	ND
X5	ND	ND	3.8 ± 1.0	0.4	ND	ND	ND	ND
X6	ND	ND	0.9 ± 0.3	0.1	ND	ND	ND	ND
Total:	451.4 ± 65.2	265.7 ± 33.1	984.8 ± 86.8	100	446.6 ± 65.3	231.3 ± 32.2	4.8 ± 0.6	34.4 ± 9.0

5. Apple fruit periderms (russeting) induced by wounding or by moisture have the same histologies, chemistries and gene expressions

Yun-Hao Chen¹, Jannis Straube², Bishnu P. Khanal¹, Viktoria Zeisler-Diehl³, Kiran Suresh³, Lukas Schreiber³, Thomas Debener² and Moritz Knoche¹

¹Institute of Horticultural Production Systems, Fruit Science Section, Leibniz University Hannover, Herrenhäuser Straße 2, 30419 Hannover, Germany

²Institute of Plant Genetics, Molecular Plant Breeding Section, Leibniz University Hannover, Herrenhäuser Straße 2, 30419 Hannover, Germany

³Institute of Cellular and Molecular Botany (IZMB), Department of Ecophysiology, University of Bonn, Kirschallee 1, 53115 Bonn, Germany

Type of authorship:	Co-author
Type of article:	Research article
Contribution to the article:	Designed and performed experiments to study histology and gene expression. Analyzed data and prepared figures. Contributed to writing, reviewing, and editing the manuscript.
Contribution of other authors:	Y.-H. Chen performed the histology, gene expression, and GC-MS sample preparation experiments. He was also involved in writing, reviewing and editing of the manuscript. B. P. Khanal contributed to experimental design, data analysis, observation of microcracks as well as writing, reviewing, and editing the manuscript. V. Zeisler-Diehl and K. Suresh conducted GC-MS analysis. L. Schreiber contributed to the supervision as well as writing, reviewing, and editing of the manuscript. M. Knoche and T. Debener contributed to the design of the study and to writing, reviewing, and editing the manuscript.
Journal:	PloS One
Date of publication:	29.09.2022
Impact factor:	3.240 (2021)
DOI:	10.1371/journal.pone.0274733

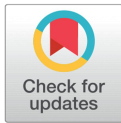
RESEARCH ARTICLE

Apple fruit periderms (russeting) induced by wounding or by moisture have the same histologies, chemistries and gene expressions

Yun-Hao Chen¹, Jannis Straube², Bishnu P. Khanal^{1*}, Viktoria Zeisler-Diehl³, Kiran Suresh³, Lukas Schreiber³, Thomas Debener², Moritz Knoche¹

1 Institute of Horticultural Production Systems, Fruit Science Section, Leibniz University Hannover, Hannover, Germany, **2** Institute of Plant Genetics, Molecular Plant Breeding Section, Leibniz University Hannover, Hannover, Germany, **3** Institute of Cellular and Molecular Botany (IZMB), Department of Ecophysiology, University of Bonn, Bonn, Germany

* khanal@obst.uni-hannover.de



OPEN ACCESS

Citation: Chen Y-H, Straube J, Khanal BP, Zeisler-Diehl V, Suresh K, Schreiber L, et al. (2022) Apple fruit periderms (russeting) induced by wounding or by moisture have the same histologies, chemistries and gene expressions. PLoS ONE 17(9): e0274733. <https://doi.org/10.1371/journal.pone.0274733>

Editor: Hernâni Gerós, Universidade do Minho, PORTUGAL

Received: April 15, 2022

Accepted: September 4, 2022

Published: September 29, 2022

Copyright: © 2022 Chen et al. This is an open access article distributed under the terms of the [Creative Commons Attribution License](https://creativecommons.org/licenses/by/4.0/), which permits unrestricted use, distribution, and reproduction in any medium, provided the original author and source are credited.

Data Availability Statement: All relevant data are within the paper and its [Supporting information files](#).

Funding: The funding of this study was provided by the following sources: German Science Foundation (DFG), grant nr. KN402/15-1 to MK and DE511/9-1 to TD. The publication of this article was funded by the Open Access fund of the Leibniz Universität Hannover. The funders had no role in

Abstract

Russeting is a cosmetic defect of some fruit skins. Russeting (botanically: induction of periderm formation) can result from various environmental factors including wounding and surface moisture. The objective was to compare periderms resulting from wounding with those from exposure to moisture in developing apple fruit. Wounding or moisture exposure both resulted in cuticular microcracking. Cross-sections revealed suberized hypodermal cell walls by 4 d, and the start of periderm formation by 8 d after wounding or moisture treatment. The expression of selected target genes was similar in wound and moisture induced periderms. Transcription factors involved in the regulation of suberin (*MYB93*) and lignin (*MYB42*) synthesis, genes involved in the synthesis (*CYP86B1*) and the transport (*ABCG20*) of suberin monomers and two uncharacterized transcription factors (*NAC038* and *NAC058*) were all upregulated in induced periderm samples. Genes involved in cutin (*GPAT6*, *SHN3*) and wax synthesis (*KCS10*, *WSD1*, *CER6*) and transport of cutin monomers and wax components (*ABCG11*) were all downregulated. Levels of typical suberin monomers (ω -hydroxy- C_{20} , $-C_{22}$ and $-C_{24}$ acids) and total suberin were high in the periderms, but low in the cuticle. Periderms were induced only when wounding occurred during early fruit development (32 and 66 days after full bloom (DAFB)) but not later (93 DAFB). Wound and moisture induced periderms are very similar morphologically, histologically, compositionally and molecularly.

Introduction

Russeting occurs on the skins of many fruit crop species, including of apples. In the smooth-skinned apple cultivars, russeting is perceived as a cosmetic impairment and so results in a quality downgrade in the packhouse, and so is the cause of significant economic loss for producers. In addition to cosmetic impairment, a russeted fruit skin is also more permeable to water vapor [1]. In this way, russeted fruit suffer increased rates of postharvest water loss in

study design, data collection and analysis, decision to publish, or preparation of the manuscript.

Competing interests: The authors have declared that no competing interests exist.

transit and storage and so a greater loss of packed weight and, hence, a yield loss at point of sale (apples are commonly priced on a per fresh weight basis). A further problem associated with increased postharvest water loss is an increased incidence of shrivel, so is a further cause of quality downgrade at point of sale.

In botanical terms, russeting represents the replacement of a relatively simple primary surface, an epidermis and hypodermis, by a more complex secondary surface, a periderm. This comprises a phellem, a phellogen and a phelloderm [2]. It is the suberized cell walls of the phellem that are responsible for the rough-textured, dull-brown appearance of a russeted fruit.

The etiology of russeting in fruit is complex and not entirely clear. Russeting can be triggered by mechanical damage caused by external biotic factors, such as feeding insects [3] or external abiotic factors such as abrasion—e.g., leaf rub [4] or the use of some agrochemicals [5]. More commonly, the causes of russeting are developmental, the first visible symptoms of the disorder being the appearance of cuticular microcracks [6–8]. Such microcracks result from various sources including from strain of the fruit surface caused by growth [9, 10] or exposure to surface moisture [11–15]. The latter includes exposure either to vapor-phase water (high humidity) or to liquid-phase water (fog, dew, rain) [16].

The formation of microcracks impairs the barrier properties of the cuticle. By a yet unknown mechanism, microcracks can then trigger the formation of a periderm in the hypodermis, just below the epidermis [17–20]. When fully formed, the periderm partially restores the barrier properties of the impaired primary surface [21]. From an evolutionary perspective, formation of a periderm is an effective repair mechanism [21].

A periderm is also formed in response to mechanical wounding of the fruit surface. Like microcracking, mechanical wounding impairs the barrier function of the cuticle. It is thus not unlikely, that the subsequent processes leading to periderm formation may therefore be the same. If this were the case, one would expect a periderm formed after wounding and after moisture induction of microcracking to have similar histologies, chemistries and gene expressions.

The objective of this study was to test the above hypothesis. We employed abrasion, using fine sandpaper, to induce periderm formation after wounding. This was compared to moisture induced periderms. Moisture often plays a role in the natural development of russeting. It can be induced experimentally by exposing the surfaces of a developing apple fruit to water [11, 12, 22].

Material and methods

Plant materials

‘Pinova’ apple (*Malus × domestica* Borkh.) grafted on M9 rootstocks were cultivated in an experimental orchard of the horticultural research station of Leibniz University Hannover at Ruthe (lat. 52°14’N, long. 9°49’E) according to current regulations for integrated fruit production. All fruit were selected to uniformity of size and color and freedom from defects, tagged and assigned to one of two treatments. A total of 125 trees in two adjacent rows were used for randomized sampling.

Treatments and experiments

Fruit were subjected to one of two treatments. To **induce a wound periderm**, the fruit skin was gently rubbed in the equatorial plane with sandpaper (grit size 1000; Bauhaus, Mannheim, Germany). The opposite surface of the same fruit served as the control.

To **induce a moisture periderm** we followed the procedure established earlier [12]. Briefly, a tube cut from the tip of a disposable Eppendorf reaction tube (8 mm inner diameter, cut to ~

17 mm in length) was mounted on the fruit surface using a non-phytotoxic, fast-curing silicone rubber (Dowsil™ SE 9186 Clear Sealant, Dow Toray, Tokyo, Japan). After curing, deionized water was injected into the tube through the hole in the tip. Thereafter, the hole was sealed with silicone rubber to prevent evaporative water loss. The tube was removed and resealed to the fruit surface every 2 d to avoid loosening as a result of surface expansion growth. Again, the opposite side of the fruit remained without treatment to serve as the control. Moisture exposure was terminated by carefully removing the tube and blotting the surface dry using a soft paper tissue. The attachment/detachment procedures themselves caused no visible damage to the fruit surface and, importantly, no russeting [12].

The following experiments were conducted:

A **time course study of periderm formation** following wounding or moisture treatments was conducted. Two batches of fruit were selected and tagged on the tree, 28 days after full bloom (DAFB). The first batch was wounded at 40 DAFB. The second batch was used for moisture induction, beginning at 28 DAFB. After 12 d of induction (at 40 DAFB), moisture treatment was terminated. For microcracking assessment, fruit were sampled at 0, 1, 2, 3, 4, 8 and 16 d after wounding or after termination of moisture treatment. For histology and analysis of gene expression, the sampling dates were 0, 2, 4, 8 and 16 after wounding or termination of moisture treatment.

The **compositions of periderms** induced by wounding, by moisture treatment, and that of a naturally russeted surface were investigated. In the subsequent season fruit reached a stage of development that was comparable to the time course study slightly earlier (at about 32 DAFB). Wounding was carried out at 32 DAFB and the fruit left on the tree until maturity (156 DAFB). The corresponding moisture treatment began at 31 DAFB and continued for 12 d. All fruit were harvested at maturity, photographed (Canon EOS 550D, lens: EF-S 18–55 mm, Canon Germany, Krefeld, Germany) and then either stored (sections of the fruit) in Karnovsky fixative or used for isolation of CMs and PMs, as described above.

The **developmental time course of periderm formation** following wounding was investigated by wounding fruit at 32 DAFB ('early'), 66 DAFB ('intermediate') or 93 DAFB ('late'). Samples for histology were taken 8 d after wounding and at maturity (156 DAFB).

Methods

Microscopy. Fruit surfaces were inspected for microcracks following exposure to wounding and to moisture [12]. For this, a fruit was dipped in 0.1% (w/v) aqueous acridine orange (Carl Roth, Karlsruhe, Germany) for 10 min, then rinsed with deionized water and blotted dry using a soft paper tissue. The treated and the control areas were then inspected using fluorescence microscopy (MZ10F; GFP-plus filter, 440–480 nm excitation wave length, ≥ 510 nm emission wave length; Leica Microsystems, Wetzlar, Germany). Three to four digital images were taken (DP71; Olympus Europa, Hamburg, Germany) on six to ten fruit, at each sampling date.

Periderm development was assessed by microscopy using thin anticlinal sections prepared from tissue blocks embedded in paraffin [11]. Briefly, excised tissue blocks (about 6×3×3 mm, two blocks per fruit per tree) comprising the fruit skin and some of the outer flesh were excised from the treated and control areas and fixed in Karnovsky fixative [23]. Blocks were then rinsed in deionized water, incubated in 70% (v/v) aqueous ethanol overnight (16 h) and then dehydrated in an ascending series of ethanol (70, 80, 90 and 96% v/v, for 30 min each). The ethanol was then displaced by isopropanol (100%, 40 min ×2) followed by a xylene substitute (AppliClear; AppliChem, Münster, Germany; 40 min ×2). For paraffin infiltration, blocks were transferred to a 1:1 (v/v) mixture of paraffin/xylene substitute (Carl Roth; 40 min ×1) at

60 °C followed by fresh paraffin wax (40 min ×2). All the incubation steps were carried out at reduced pressure (10.8 kPa). Finally, the blocks were cast in paraffin wax in a metal mold. Embedded blocks were then cooled and stored at 4 °C pending analysis.

Thin sections (10 μm) were cut using a rotatory microtome (Hyrax M 55; Carl Zeiss, Oberkochen, Germany). Sections were transferred to glass microscope slides, dried at 38 °C for 16 h and then rehydrated in xylene substitute (10 min, ×2) followed by a descending series of ethanol (96, 80, 70 and 60%; v/v; 10 min each) and finally in deionized water (5 min, ×2). Sections were stained in the dark using Fluorol Yellow (0.005%, w/v; Santa Cruz Biotechnology, Texas, USA) dissolved in glycerol (90%, v/v; Carl Roth) and melted (~90 °C) polyethylene glycol 4000 (PEG 4000; w/v; Carl Roth) in a ratio of 1:1 for 1 h [24]. Following washing in deionized water, the sections were viewed under transmitted white light or incident fluorescent light (filter U-MWB; 450–480 nm excitation; ≥520 nm emission wavelength; Olympus) using a fluorescence microscope (BX-60 equipped with a DP 73 digital camera; Olympus). We examined a minimum of 50 sections per block. Two blocks from the same fruit represented a single replication and there were a minimum of three replications.

RNA extraction. Using a razor blade, thin patches of skin were excised from wounded, or moisture-treated, or un-treated (control) surfaces [22]. Skin patches from six fruit taken from six trees (one apple per tree) were collected within 15 min of picking and combined to obtain one replicate. The patches were immediately frozen in liquid nitrogen and held at -80 °C. For RNA extraction, the patches were ground in liquid nitrogen using a pestle and mortar. The RNA was extracted using the InviTrap Spin Plant RNA Mini Kit (STRATEC Molecular GmbH, Berlin, Germany) according to the manufacturer's protocol. Genomic DNA was removed using the DNA-free™ Kit (Thermo Fisher Scientific, Waltham, Massachusetts, USA). The purity and quantity of the RNA was determined by measuring the absorbances at 230, 260 and 280 nm (Nanodrop 2000c; Thermo Fisher Scientific, Waltham, Massachusetts, USA). The RNA integrity was determined on a 1.5% agarose gel. Following dilution, the RNA samples (30 ng/μl) were converted into cDNA (LunaScript[®] RT SuperMix Kit; New England Biolabs, Ipswich, Massachusetts, USA). A standard PCR with a pair of actin primers (EB127077) [25] and the DCSPol DNA polymerase kit (DNA Cloning Service, Hamburg, Germany) was carried out. The amplification was checked on a 1.5% agarose gel. Samples were stored at -80 °C pending further use.

Quantitative real-time PCR. Twelve key genes associated with periderm formation, and suberin, cutin and wax metabolism were analyzed by qPCR (for details see in [S1 Table](#), Selected transcription factors and genes analyzed in the present study). These genes were selected because they all play key roles in moisture-induced periderm formation [22]. Specific primer pairs were designed on Primer3 (<http://primer3.ut.ee/>) (for details see in [S2 Table](#), Primers sequences of the genes analyzed in the present study). A total of 900 ng of RNA in a 60 μl reaction vial were reverse transcribed into cDNA (LunaScript[®] RT SuperMix Kit; New England Biolabs, Ipswich, Massachusetts, USA). Later, an 8 μl reaction volume containing 1 μl cDNA, primers (at 200 nM final concentration) and the Luna[®] Universal qPCR Master Mix (New England Biolabs) were used to carry out quantitative real-time PCRs (QuantStudio™ 6 Flex Real-Time PCR System; Applied Biosystems, Waltham, Massachusetts, USA). Conditions were: one cycle at 95 °C for 60 s, 40 cycles at 95 °C for 15 s and 40 cycles at 60 °C for 60 s. A melting curve analysis (95 °C for 15 s, 60 °C for 60 s, 60 to 95 °C in 0.5 °C increments) was carried out after the final amplification.

All expression values were obtained from the QuantStudio™ Real-Time PCR Software v1.3 (Applied Biosystems) and normalized using the two reference genes *Protein disulfide isomerase* (*PDI*) (MDP0000233444) and *MdeF-1 alpha* (AJ223969.1) [26, 27].

Isolation of cuticular membranes and periderm membranes. Cuticular membranes (CMs) and periderm membranes (PMs) were isolated enzymatically [28] from skin patches of wounded or moisture treated fruit. Skins of naturally russeted or non-russeted fruit served as controls. Excised skin segments (ES) were punched using a biopsy punch (12 mm diameter; Acuderm, Terrace, FL, USA). The ES were incubated in an isolation medium containing pectinase (9%, v/v; Panzym Super E flüssig; Novozymes A/S, Krogshøjvej, Bagsvaerd, Denmark), cellulase (0.5% v/v; Cellubrix L.; Novozymes A/S) and NaN_3 (30 mM) in 50 mM citric acid buffer adjusted to pH 4.0. The isolation medium was replaced periodically until CMs and PMs separated from the subtending tissues. The CMs and PMs were cleaned using a soft camel-hair brush, rinsed in deionized water, dried at 40 °C and kept above dry silica gel.

Quantification and identification of wax constituent by gas chromatography. Wax constituents of CM or PM were quantified and identified following the protocol of Baales et al. [29]. The CM and PM discs were cut into small fragments using a razor blade. Wax was extracted by incubating 0.5 to 1 mg of CMs and PMs in CHCl_3 (5 ml per replicate) at room temperature on a horizontal rolling bench (RM; Ingenieurbüro CAT, M. Zipperer, Staufen, Germany) overnight. Tetracosane (100 μl of 10 mg tetracosane in 50 ml CHCl_3) was added to the wax extract as an internal standard. The volume of the extract was reduced under a gentle stream of N_2 at 60 °C. The extracted dewaxed CM and PM were removed from the extract and dried on Teflon discs for analysis of cutin and suberin monomers.

To avoid interference of wax constituents containing polar hydroxyl- and carboxyl groups with the GC column, waxes were derivatized by silylation. This process yields trimethylsilyl ethers and -esters of the respective constituents. Samples were derivatized at 70 °C for 45 min following addition of 20 μl BSTFA (N, O-bis(trimethylsilyl)-trifluoroacetamid; Machery-Nagel, Düren, Germany) and 20 μl pyridine (Sigma Aldrich, Deisenhofen, Germany). Wax constituents were quantified using a gas chromatograph equipped with a flame ionization detector (GC-FID; CG-Hewlett Packard 5890 series H, Hewlett-Packard, Palo Alto, CA, USA; 307 column-type: 30 m DB-1 inner Diam. 0.32 mm, film thickness 0.2 μm ; J&W Scientific, Folsom, CA, USA). For quantification, the peak areas were normalized using the tetracosane internal standard and the areas of the PMs or CMs.

For identification, a GC coupled to a mass spectrometer was used (GC-MS; Quadrupole mass selective detector HP 5971; Hewlett-Packard, Palo Alto, CA, USA). Individual constituents were identified by comparing the fragmentation patterns with published data and with our own data library. The number of replicates was two to three.

Quantification and identification of suberin and cutin monomers by gas chromatography. Suberin and cutin monomers were quantified and identified following the protocol of Baales et al. [29]. The extracted CMs and PMs were transesterified by incubation in 1 ml BF_3/MeOH for 16 h at 70 °C. Thereafter, 20 μg of dotriacontane (100 μl of 10 mg dotriacontane in 50 ml CHCl_3) was added as an internal standard. Depolymerization was stopped and 2 ml of saturated NaHCO_3 was added.

The cutin and suberin monomers were extracted using CHCl_3 ($\times 3$, 2 ml each). The CHCl_3 phase was separated, washed with 1 ml HPLC grade water, dried with Na_2SO_4 and concentrated under a gentle stream of N_2 at 60 °C. Samples were derivatized as described above. The monomers and constituents were quantified by GC-FID and identified by GC-MS as described above. The data were normalized relative to the internal standard and to the fruit surface area. The fragmentation patterns were compared with published data and our in-house library. The number of replicates was two to three.

Data analysis

Total suberin, cutin and wax were calculated by summation of all individual constituents identified and quantified by gas chromatography. The PMs isolated from wounded, moisture treated or naturally russeted fruit often represent mixed polymers that comprise areas with patches covered by periderm adjacent to patches covered by cuticle and underlying epidermal and hypodermal cells. The area ratios may vary between replicates. Because suberin, cutin and wax share common monomers and constituents, it is impossible to attribute individual constituents obtained in the compositional analyses of these mixed polymers to either the cutin or the suberin fractions. However, in an earlier study we quantified the mass ratios for typical constituents of suberin from the trunk of 'Pinova' trees [22]. The constituents unique for suberin are the ω -hydroxy- C_{20} , $-C_{22}$ and $-C_{24}$ acids. These ω -hydroxy-acids account for 17.6% of the total suberin. Using these constituents and the composition of a 'pure' native periderm, the composition of mixed PMs could be calculated and assigned to the PM. As pointed out by Straube et al. [22], the calculation is based on the assumption that the suberin composition of a 'Pinova' fruit PM is identical to that of the trunk periderm of the same cultivar. Due to the lack of PM-specific wax constituents, this calculation was not possible for the wax fraction.

Data are presented as means \pm standard error (SE) of the means. Where error bars are not visible, they are smaller than data symbols. Data were subjected to analyses of analysis of variance, regression analysis or t-tests using the statistical software SAS[®] Studio (SAS 9.4; SAS Institute, Cary, NC, USA). Significance of *P*-values at the 0.05 level is indicated by *.

Results

Wounding by abrading the skin of developing apple fruit resulted in numerous microcracks in the cuticle. The microcracks and the surrounding dermal tissue were infiltrated by aqueous acridine orange. As growth progressed after wounding, the microcracks widened (Fig 1). Microcracks also formed after a 12-d moisture treatment (Fig 1). Like the microcracks resulting from wounding, those caused by surface moisture treatment also traversed the cuticle as indexed by infiltration with aqueous acridine orange. In contrast to microcracks resulting from abrasion, those caused by moisture treatment were not straight and parallel to one another but followed the pattern of the anticlinal cell walls of groups of epidermal cells. Furthermore, moisture-induced microcracks branched at tricellular junctions.

Cross-sections of wounded apple fruit skins revealed browning and death of epidermal and some hypodermal cells shortly after abrasion (Fig 2). By 4 d after wounding, cell walls in the hypodermal cell layers began to suberize (marked with arrows) as indexed by staining with Fluorol Yellow. By 8 d after wounding, and even more so by 16 d, stacks of cells with suberized cell walls had formed that are characteristic of a periderm.

In cross-sections of moisture treated fruit skins of the same developmental stage, microcracks were present in the cuticle. These microcracks widened and the cuticle curled upwards as fruit growth continued, indicating the presence of considerable growth strain. At 4 d after termination of moisture treatment, the cell walls of the hypodermal cells below the microcrack began to suberize. By 8 d and 16 d after termination of moisture treatment, periderm formation had begun (Fig 2).

The two transcription factors involved in the regulation of the synthesis processes of suberin (*MYB93*) and lignin (*MYB42*), a gene involved directly in the synthesis of suberin monomers (*CYP86B1*) and a gene involved in the transport of suberin monomers (*ABCG20*) were all upregulated. The other two transcription factors (*NAC038* and *NAC058*), that do not yet have assigned functions, were also upregulated. Relative normalized expressions of *MYB42*, *CYP86B1* and *NAC058* were highest at 4 d or at 8 d but then decreased slightly at 16 d

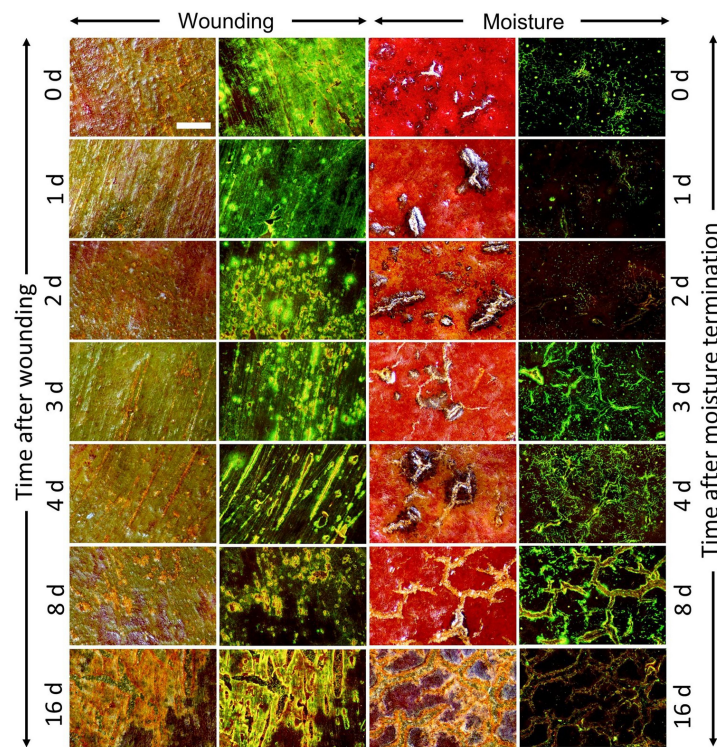


Fig 1. Time course of change in infiltration of 'Pinova' fruit skin patches following wounding by abrasion of the cuticle at 40 days after full bloom (DAFB) using fine sandpaper ('Wounding') or by exposure of the fruit skin to moisture for 12 d ('Moisture'). Moisture exposure began at 28 DAFB. At 40 DAFB, moisture exposure was terminated and the time-course of change in infiltrated fruit surface area was established. Micrographs from the same surface area were taken under incident white light or incident fluorescent light. The green/yellow fluorescence resulted from localized penetration of the tracer acridine orange through microcracks in the cuticle into the underlying tissues. Scale bar equals 400 μ m and is representative for all the images of the composite.

<https://doi.org/10.1371/journal.pone.0274733.g001>

(Fig 3C, 3E and 3K) whereas the expressions of *MYB93*, *ABCG20* and *NAC038* increased continuously to 16 d (Fig 3A, 3G and 3I). The log fold changes in expression are provided in the S1 Dataset.

Very similar expression profiles, but at somewhat lower levels, were obtained in the moisture treated patches (Fig 3B, 3D, 3F, 3H, 3J and 3L). The only exception was the upregulation of *MYB42* in moisture treated fruit at 4 d after termination of moisture treatment. This exceeded that in the wounded fruit (Fig 3D).

Genes involved in the synthesis of cutin (*SHN3*, *GPAT6*) and wax (*KCS10*, *WSD1*, *CER6*) and the transport of cutin monomers and wax components (*ABCG11*) were downregulated in both wounded and moisture treated skin patches (Fig 4). In general, the relative expressions

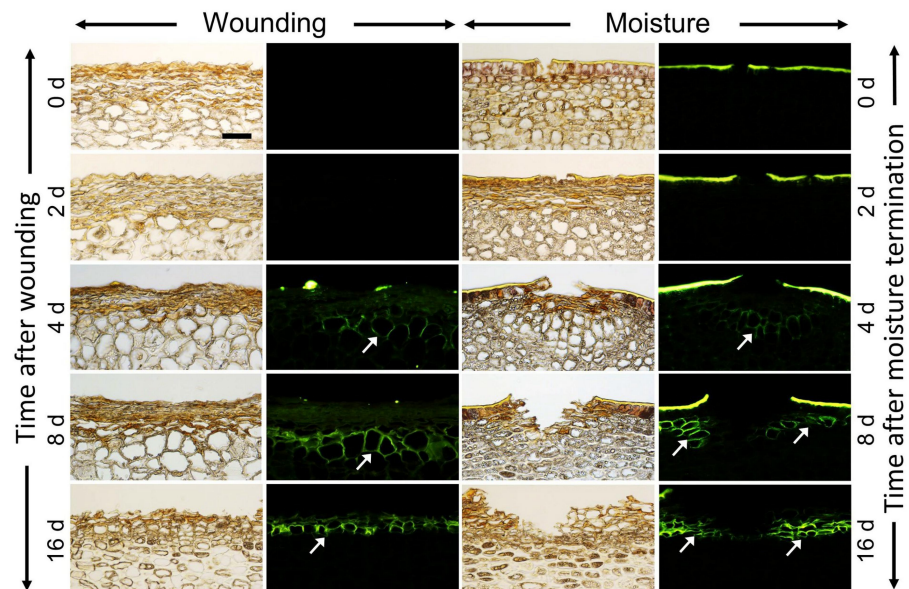


Fig 2. Time course of periderm development following wounding (left panel) and moisture exposure (right panel) of skin patches of 'Pinova' apple. Patches of skin were abraded 40 days after full bloom (DAFB) using fine sandpaper. Microcracks induced by surface moisture served as control ('Moisture'). Here, the fruit surface was exposed to surface moisture for 12 d from 28 to 40 DAFB. Pairs of micrographs were taken under transmitted white light or incident fluorescent light (filter module U-MWB) after staining with Fluorol Yellow. Fluorol Yellow stains the cuticle and suberized cell walls. Scale bar equals 50 μ m and is representative for all images of the composite.

<https://doi.org/10.1371/journal.pone.0274733.g002>

were qualitatively and quantitatively similar in the wounded and moisture treated skin patches.

Skin patches that were wounded or moisture treated for 12 d during early fruit development had formed a continuous periderm (marked with arrows) and developed a russeted surface by maturity. The periderms following wounding or moisture treatment were indistinguishable from the periderms of naturally russeted fruit of the same cultivar (Fig 5). At maturity, the skins of non-russeted patches had developed a thick cuticle (marked with arrows).

The monomer compositions of the periderms induced by wounding or by moisture treatment and that of the native periderm were very similar. The amounts of the typical suberin monomers ω -hydroxy- C_{20} , $-C_{22}$ and $-C_{24}$ acids were very similar in all three periderms (wound induced, moisture induced, and native), and were significantly lower in the cuticle. The contents of carboxylic- C_{22} acid were also very similar in the three types of periderms but were much lower in the cuticle (Fig 6). Minor differences between the three types of periderms were: (1) The 9,10-dihydroxydicarboxylic- C_{16} acid was similar in wound and moisture induced periderms but significantly lower in native periderm. (2) The 1-hydroxy- C_{18} acid was present in higher amounts in moisture induced periderm than in wound and native periderm. (3) The 2-hydroxy- C_{18} acid content was higher in wound periderm than in moisture induced or in native periderm. (4) The hydrocinnamic acid was higher in moisture induced periderm

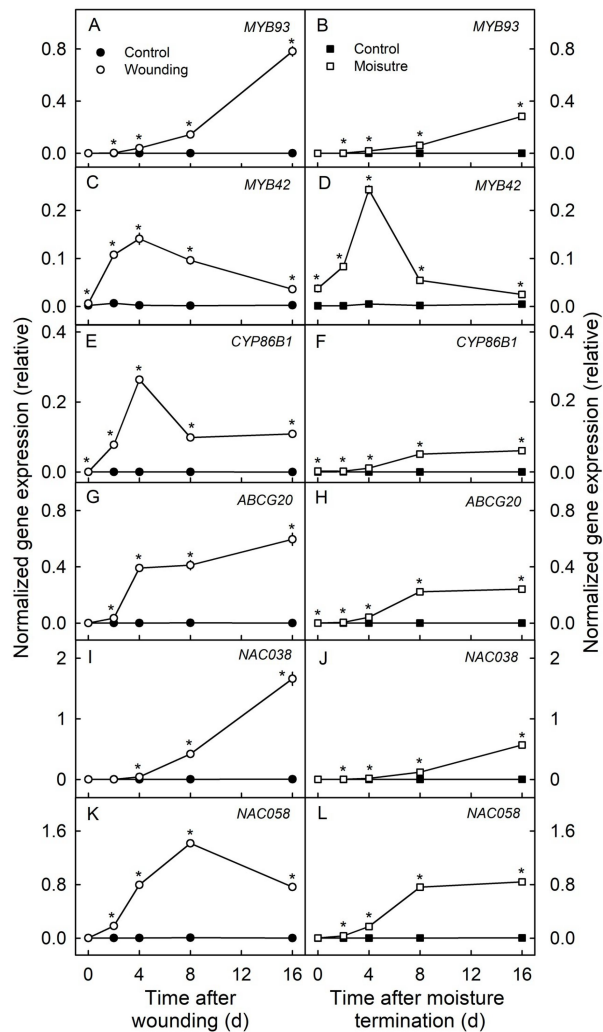


Fig 3. Time courses of change in the expressions of two transcription factors involved in the regulation of the synthesis of suberin (*MYB93*) and lignin (*MYB42*), a gene involved directly in the synthesis of suberin monomers (*CYP86B1*) and a gene involved in the transport of suberin monomers (*ABCG20*) and two uncharacterized transcription factors (*NAC038* and *NAC058*) in the skin of 'Pinova' apple fruit following wounding or following exposure of the fruit surface to moisture. Patches of fruit skin were wounded 40 days after full bloom (DAFB) by abrading the cuticle using fine sandpaper ('Wounding'). For comparison, microcracks were induced by exposure of skin patches to surface moisture ('Moisture'). Here, the fruit surface was exposed to surface moisture from 28 to 40 DAFB. Non-treated fruit served as the respective controls ('Control'). Expression values are means \pm SE of three biological replicates comprising six fruit each. The "*" indicates significant differences between the wounded patch and its control or between the moisture exposed patch and its control, $P \leq 0.05$ (Student's t-test).

<https://doi.org/10.1371/journal.pone.0274733.g003>

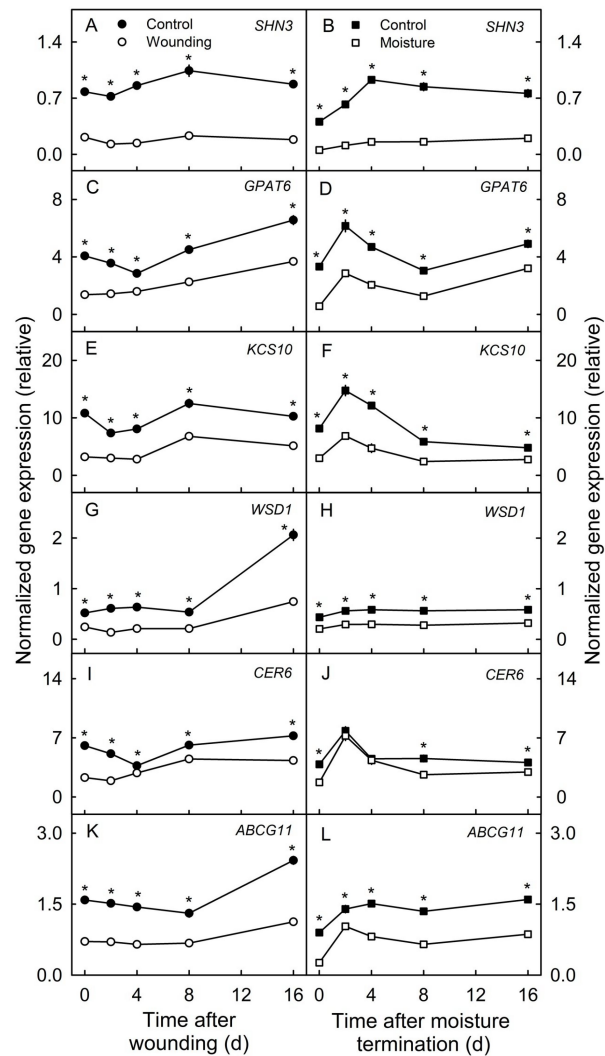


Fig 4. Time courses of change in the expression of genes involved in the synthesis of cutin monomers (*SHN3*, *GPAT6*) and wax constituents (*KCS10*, *WSD1*, *CER6*) and their transport (*ABCG11*) in the skin 'Pinova' apple fruit following wounding or following exposure of the fruit surface to moisture. Patches of fruit skin were wounded 40 days after full bloom (DAFB) by abrading the cuticle using fine sandpaper ('Wounding'). For comparison, microcracks were induced by exposure of skin patches to surface moisture ('Moisture'). Here, the fruit surface was exposed to surface moisture from 28 to 40 DAFB. Non-treated fruit served as control ('Control'). Expression values are means \pm SE of three biological replicates comprising six fruit each. The "*" indicates significant differences between the wounded patch and its control or between the moisture exposed patch and its control, $P \leq 0.05$ (Student's t-test).

<https://doi.org/10.1371/journal.pone.0274733.g004>

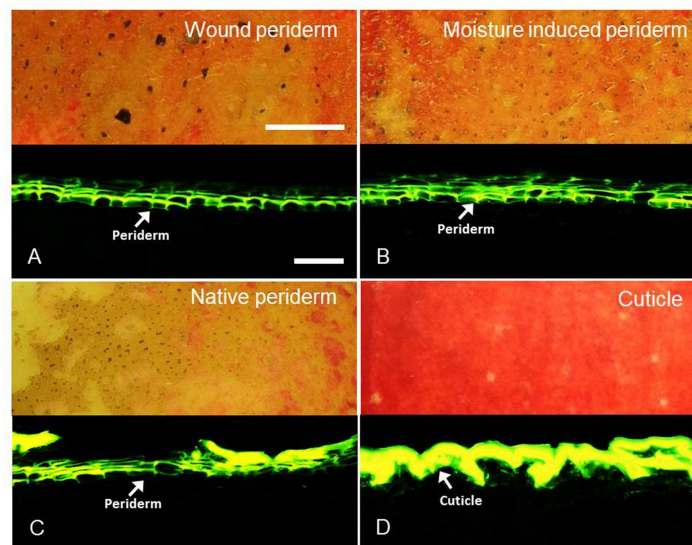


Fig 5. Cross-sections through patches of ‘Pinova’ apple fruit skin at the mature stage (156 days after full bloom (DAFB)) that had been wounded or exposed to surface moisture during early fruit development. Patches of fruit skin were wounded at 32 DAFB by abrading the cuticle using abrasive paper (‘Wound periderm’). For comparison, microcracks were induced by exposure of skin patches to surface moisture (‘Moisture-induced periderm’) from 31 to 43 DAFB. Non-treated naturally russeted surfaces (‘Native periderm’) and non-russeted surfaces served as control (‘Cuticle’). The cross-sections were stained with Fluorol Yellow. Scale bars in A 10 mm (upper) and 50 μ m (lower). Bars are representative for all bright field and all fluorescence images of the composite.

<https://doi.org/10.1371/journal.pone.0274733.g005>

than in the wound or native periderm. The abundances of this monomer were similar in the cuticle and moisture induced periderm (Fig 6).

Wax occurred in low amounts in the moisture induced and native periderm and was even lower in the wound periderm. The composition of wax was similar in the moisture induced and native periderm. Dominating wax components in moisture induced and native periderms and in the cuticle were C_{28} aldehydes, oleanolic and ursolic acids (Fig 7).

Total suberin was higher and total wax was lower, in the three periderms compared with in the cuticle. Accordingly, cutin occurred in higher amounts in the cuticle than in any of the three periderms (Fig 8).

Marked differences were found in periderm formation between different stages of fruit development. Wounding during early fruit development (32 DAFB) resulted in a typical periderm characterized by stacked and suberized phellem cells after 8 d of wounding, and which were still visible at maturity (156 DAFB; Fig 9). When wounding occurred at 66 DAFB a layer of cells with suberized cell walls had formed in the cortex within 8 d. At maturity, a typical periderm had developed (Fig 9). Interestingly, following wounding at a late stage of development (93 DAFB) only cells with suberized cell walls had formed in the cortex at maturity, but not a complete periderm (Fig 9).

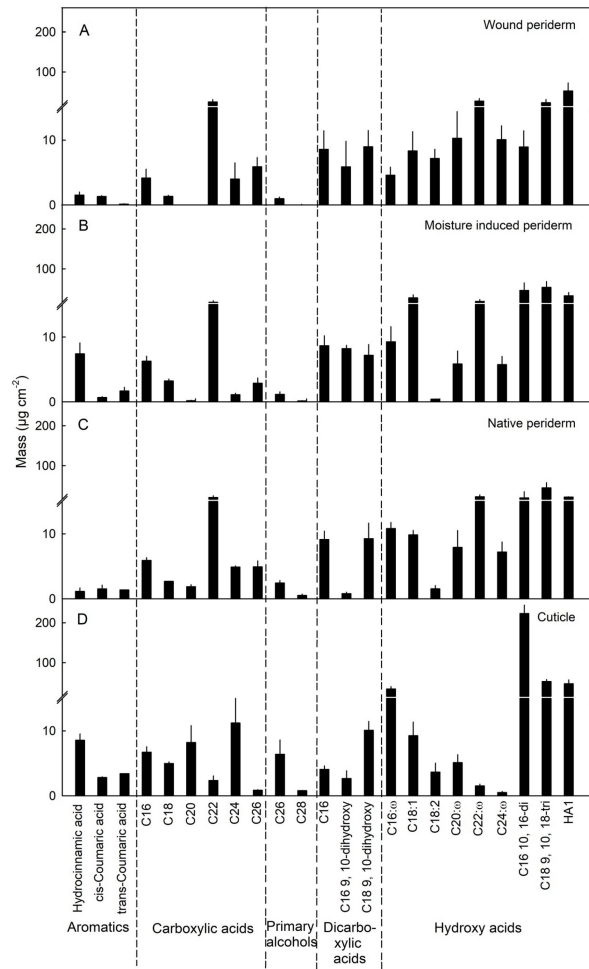


Fig 6. Composition of cutin and suberin of skins of mature apple fruit. Periderm formation in the fruit skin was induced during early development by abrading the cuticle using abrasive paper ('Wound periderm') (A) or by exposing the fruit skin to surface moisture for 12 d between 31 and 43 days after full bloom (DAFB; 'Moisture-induced periderm') (B). The treated patches of skin were excised at maturity 156 DAFB. Native periderm from naturally russeted fruit (C) and cuticles from non-treated non-russeted fruit served as controls (D). Data represent means \pm SE of two to three replicates comprising periderms and cuticles of five fruit each. The data shown in (B) were taken from Straube et al. [22].

<https://doi.org/10.1371/journal.pone.0274733.g006>

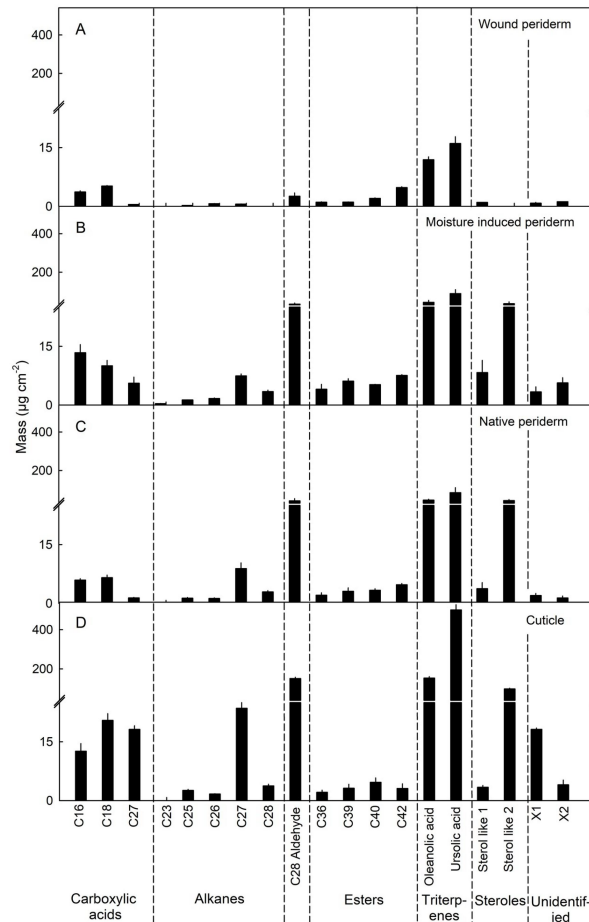


Fig 7. Wax constituents of the skins of mature apple fruit. Periderm formation in the fruit skin was induced during early development by abrading the cuticle using fine sandpaper ("Wound periderm") (A) or by exposing the fruit skin to surface moisture for 12 d between 31 and 43 days after full bloom (DAFB; "Moisture-induced periderm") (B). The treated patches of skin were excised at maturity 156 DAFB. Native periderm from naturally russeted fruit (C) and cuticles from non-treated non-russeted fruit served as controls (D). Data represent means \pm SE of two to three replicates comprising periderms and cuticles of five fruit each. The data shown in (B) were taken from Straube et al. [22].

<https://doi.org/10.1371/journal.pone.0274733.g007>

Discussion

Our results demonstrate that periderms induced by wounding and by surface moisture are similar and do not differ from periderms found on naturally russeted fruit surface. This conclusion is based on the following arguments.

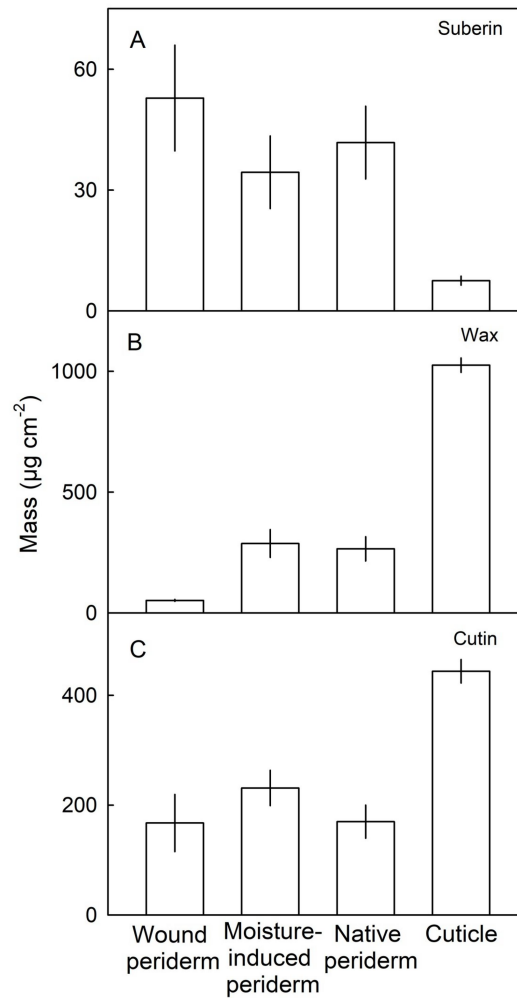


Fig 8. Total masses of suberin (A), wax (B) and cutin (C) in patches of skin of mature apple fruit. Periderm formation in the fruit skin was induced during early fruit development by abrading the cuticle using fine sandpaper ('Wound periderm') or by exposing the fruit skin to surface moisture for 12 d between 31 and 43 days after full bloom (DAFB; 'Moisture-induced periderm'; [22]). The treated patches of skin were excised at maturity 156 DAFB. Periderm from naturally russeted fruit (Native periderm) and cuticles from non-treated, non-russeted fruit (Cuticle) served as controls. Data represent means \pm SE of two to three replicates comprising periderms and cuticles of five fruit each.

<https://doi.org/10.1371/journal.pone.0274733.g008>

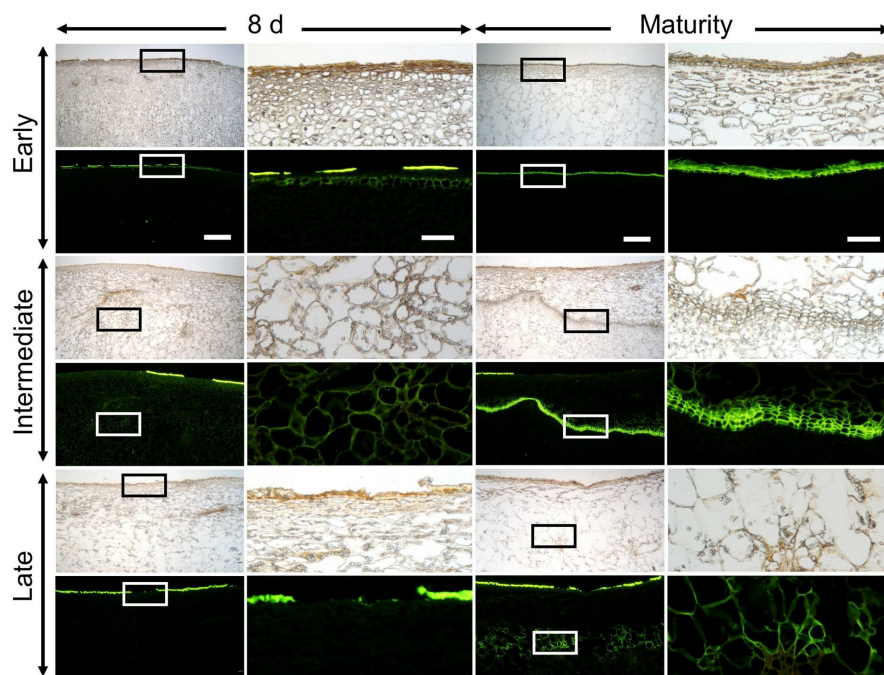


Fig 9. Developmental time course of periderm formation following wounding of 'Pinova' apple at 32 days after full bloom (DAFB) ('early'), 66 DAFB ('intermediate') and 93 DAFB ('late'). For wounding, the cuticle was abraded using fine sandpaper. Cross-sections were prepared 8 d after wounding (left panel) or at maturity (156 DAFB) (right panel). Pairs of micrographs were taken under transmitted white light or incident fluorescent light (filter module U-MWB) after staining with Fluorol Yellow. Fluorol Yellow stains the cuticle and suberized cell walls. Sections were viewed at 20 \times (scale bar 500 μ m, left column) or at 100 \times (scale bar 100 μ m, right column).

<https://doi.org/10.1371/journal.pone.0274733.g009>

First, there was no difference in morphology and histology between wound induced and moisture induced periderms and both were similar to those of a native periderm. The skin sections inspected revealed all typical characteristics of a periderm. These include stacks of phellem cells. These cells have suberized cell walls and therefore stain with Fluorol Yellow [30]. The 'stacked' arrangement indicates the cells in a stack originate from a single mother cell of the phellogen.

Second, gene expression was similar following wounding and following termination of moisture exposure. Genes related to the synthesis and transport of suberin monomers and transcription factors involved in periderm formation were all upregulated. Those involved in the synthesis and transport of cutin monomers and wax components were downregulated. In an earlier study, Straube et al. [22] observed an upregulated expression of *CYP86B1*, *MYB42*, *ABCG20*, *NAC038*, *NAC058* and *MYB93* in moisture exposed patches of apple skins after termination of the treatment. *CYP86B1* is a key gene involved in the synthesis of very long chain ω -hydroxy and α,ω -dicarboxylic acids, the monomers of suberin [22, 31]. The transcription factor *MYB42* is involved in regulation of lignin synthesis [32]. *ABCG20* is required for the

transport of suberin monomers [33]. *NAC038* and *NAC058* are transcription factors of the NAC family that are upregulated in russeted skins of apple [25, 34]. Expression of *MYB93*, another transcription factor, was also expressed in the russeted skin of apples [25, 34]. Its over-expression in *N. benthamiana* enhanced the expression of *NAC038* and *NAC058* [34]. Additionally a multispecies gene coexpression analysis highlighted a possible involvement of *NAC038* and *NAC058* in transcriptional regulation of suberin synthesis [35].

Third, there was little difference in composition between the wound induced, moisture induced or native periderms. While cutin and suberin share common monomers, the long chain ω -hydroxy acids (C_{20} , C_{22} , C_{24}) are unique for suberin [22, 36–38]. These dominated in all three periderms. Despite similarity in suberin composition, the wound periderm had a lower wax content compared to native and moisture induced periderms. The reason for this may be the following: the damage caused by abrading the cuticle was so harsh that most of the cuticle was removed and thus the developing periderm on the wounded surface contained no or very much less residual cuticle. In contrast, the native periderms contained significant amounts of dried cuticle residue on the surface [39, 40]. The moisture induced periderm is also expected to contain cuticle residues on the surface as the etiologies of periderm development and periderm morphology are similar to native periderm (Fig 5). The report of Schreiber et al. [41] for potato tubers, that the wound periderm contained 40 to 50% less wax than the native periderm, also supports our findings.

Fourth, the ontogenies of formation of wound induced periderm and moisture induced periderm were similar. Periderms formed in developing fruit but did not develop in mature fruit. This observation is also consistent with earlier observations [4, 11, 12, 22, 42–44]. Also, Winkler et al. [15] reported that overhead sprinklers induced russet in ‘Elstar’ apples during early fruit development, but not shortly before maturity or at maturity. Apparently, the ability to form a periderm is lost by the later stages of fruit development. A possible explanation to account for this may be a decrease in the rate of growth strain. Towards maturity, the relative area growth rate of the fruit surface decreases continuously. Growth strain represents the main driver of microcracking [9].

The similarity of the periderms induced by wounding or by moisture and native periderms suggests the processes triggering periderm formation are likely similar. In all three periderms, the barrier properties of the cuticle are impaired due to microcracking, the only difference being the reason for the microcracking. While microcracking of the cuticle occurs at the surface, periderm formation begins by a de-differentiation of the subtending hypodermal cells. This requires some sort of signal which connects the two events. Potential signals resulting from impaired barrier properties include: (1) a decreased CO_2 concentration, (2) an increased O_2 concentration and (3) a more negative water potential of the flesh due to a more rapid dehydration at the fruit surface [8, 11, 22].

Among those potential signals, the roles of O_2 and CO_2 have been studied in kiwifruit and potato tuber. In kiwifruit, wound periderm formation was reduced significantly when O_2 was eliminated from the storage atmosphere [45]. Similarly, in potato tuber, there was nearly no periderm on the tuber stored at low (0.5 to 1%) O_2 . In contrast, 2 to 4 layers of periderm cell had formed when tubers were stored at ambient (21%) O_2 concentrations [46]. Based on the observation in kiwifruit, the reduced suberization resulted from decreased activities of phenylalanine ammonia-lyase, peroxidase, catalase, and polyphenol oxidase [45]. Exposure to elevated CO_2 concentrations (10%) reduced periderm development in potato tuber [47]. To our knowledge, there are no reports of a potential role for a decreased water potential in the tissue surrounding a microcracked cuticle, in triggering periderm formation.

Conclusion

Periderms induced by wounding or moisture are similar from morphological, histological, compositional and molecular perspectives. Thus, the signal(s) linking the impaired barrier properties to the differentiation of a periderm in the hypodermis is likely to be the same after wounding and after moisture induced microcracking. These findings have important implications for experimental research. The data presented herein justify the use of wounding to study the relationship between the impaired barrier properties of the cuticle due to formation of microcracks and the beginning of periderm formation in the hypodermis, some cell layers below. The search for the linking signal may now begin.

Supporting information

S1 Table. Selected transcription factors and genes analyzed in the present study.
(DOCX)

S2 Table. Primer sequences of the genes analyzed in the present study.
(DOCX)

S1 Dataset. Excel file containing all data produced in figures throughout the manuscript.
(XLSX)

Acknowledgments

We thank Traud Winkelmann for advice and support in sample preparation for histology. We also thank Julia Schröter, Simon Sitzenstock and Friederike Schröder for technical assistance in the laboratory, Thomas Athoo and Andreas Winkler for assistance in the field and Alexander Lang for helpful comments on an earlier version of this manuscript.

Author Contributions

Conceptualization: Bishnu P. Khanal, Thomas Debener, Moritz Knoche.

Data curation: Yun-Hao Chen, Jannis Straube, Bishnu P. Khanal.

Formal analysis: Yun-Hao Chen, Jannis Straube, Bishnu P. Khanal.

Funding acquisition: Thomas Debener, Moritz Knoche.

Investigation: Yun-Hao Chen, Jannis Straube, Bishnu P. Khanal, Viktoria Zeisler-Diehl, Kiran Suresh.

Methodology: Bishnu P. Khanal, Thomas Debener, Moritz Knoche.

Project administration: Thomas Debener, Moritz Knoche.

Supervision: Bishnu P. Khanal, Lukas Schreiber, Thomas Debener, Moritz Knoche.

Validation: Yun-Hao Chen, Jannis Straube, Bishnu P. Khanal.

Visualization: Yun-Hao Chen, Jannis Straube, Bishnu P. Khanal.

Writing – original draft: Yun-Hao Chen, Bishnu P. Khanal, Moritz Knoche.

Writing – review & editing: Yun-Hao Chen, Bishnu P. Khanal, Lukas Schreiber, Thomas Debener, Moritz Knoche.

Chapter 5 Apple fruit periderms (russetting) induced by wounding or by moisture have the same histologies, chemistries and gene expressions

References

1. Khanal BP, Ikigu GM, Knoche M. Russetting partially restores apple skin permeability to water vapour. *Planta*. 2019; 249:849–860. <https://doi.org/10.1007/s00425-018-3044-1> PMID: 30448863
2. Evert RF. Periderm. In: Evert RF, editor. *Esau's Plant Anatomy: Meristems, Cells, and Tissues of the Plant Body—Their Structure, Function, and Development*. Hoboken: John Wiley & Sons Inc.; 2006, pp. 427–446.
3. Easterbrook MA, Fuller MM. Russetting of apples caused by apple rust mite *Aculus schlechtendali* (Acarina: Eriophyidae). *Ann Appl Biol*. 1986; 109:1–9. <https://doi.org/10.1111/j.1744-7348.1986.tb03178.x>
4. Simons RK, Aubertin M. Development of epidermal, hypodermal and cortical tissues in the Golden Delicious apple as influenced by induced mechanical injury. *Proc Amer Soc Hort Sci*. 1959; 74:1–9.
5. Goffinet MC, Pearson RC. Anatomy of russetting induced in Concord grape berries by the fungicide Chlorothalonil. *Amer J Enol Vitic*. 1991; 42:281–289.
6. Faust M, Shear CB. Russetting of apples, an interpretive review. *HortScience*. 1972; 7:233–235.
7. Faust M, Shear CB. Fine structure of the fruit surface of three apple cultivars. *J Amer Soc Hort Sci*. 1972; 97:351–355.
8. Winkler A, Athoo T, Knoche M. Russetting of fruits: Etiology and management. *Horticulturae*. 2022; 8:231. <https://doi.org/10.3390/horticulturae8030231>
9. Scharwies JD, Grimm E, Knoche M. Russetting and relative growth rate are positively related in 'Conference' and 'Condo' Pear. *HortScience*. 2014; 49:746–749. <https://doi.org/10.21273/HORTSCI.49.6.746>
10. Skene DS. The development of russet, rough russet and cracks on the fruit of the Apple Cox's Orange Pippin during the course of the season. *J Hort Sci*. 1982; 57:165–174. <https://doi.org/10.1080/00221589.1982.11515037>
11. Chen YH, Straube J, Khanal BP, Knoche M, Debener T. Russetting in apple is initiated after exposure to moisture ends-I. Histological evidence. *Plants*. 2020; 9:1293. <https://doi.org/10.3390/plants9101293> PMID: 33008020
12. Khanal BP, Imoro Y, Chen YH, Straube J, Knoche M. Surface moisture increases microcracking and water vapour permeance of apple fruit skin. *Plant Biol*. 2021; 23:74–82. <https://doi.org/10.1111/plb.13178> PMID: 32881348
13. Knoche M, Grimm E. Surface moisture induces microcracks in the cuticle of 'Golden Delicious' apple. *HortScience*. 2008; 43:1929–1931. <https://doi.org/10.21273/HORTSCI.43.6.1929>
14. Tukey LD. Observations on the russetting of apples growing in plastic bags. *Proc Amer Soc Hort Sci*. 1959; 74:30–39.
15. Winkler A, Grimm E, Knoche M, Lindstaedt J, Köpcke D. Late-season surface water induces skin spot in apple. *HortScience*. 2014; 49:1324–1327. <https://doi.org/10.21273/HORTSCI.49.10.1324>
16. Creasy LL. The correlation of weather parameters with russet of Golden Delicious apples under orchard conditions. *J Amer Soc Hort Sci*. 1980; 105:735–738.
17. MacDaniels LH, Heinicke AJ. To what extent is spray burn of apple fruit caused by freezing of the flowers. *Phytopathology*. 1930; 20:903–906.
18. Meyer A. A study of the skin structure of Golden Delicious apples. *Proc Amer Soc Hort Sci*. 1944; 45:105–110.
19. Pratt C. Periderm development and radiation stability of russet-fruited sports of apple. *Hort Res*. 1972; 12:5–12.
20. Simons RK. The origin of russetting in russet sports of the 'Golden Delicious' apple. *Hort Res*. 1965; 5:101–106.
21. Knoche M, Lang A. Ongoing growth challenges fruit skin integrity. *Crit Rev Plant Sci*. 2017; 36:190–215. <https://doi.org/10.1080/07352689.2017.1369333>
22. Straube J, Chen YH, Khanal BP, Shumbusho A, Zeisler-Diehl V, Suresh K, et al. Russetting in apple is initiated after exposure to moisture ends: Molecular and biochemical evidence. *Plants*. 2021; 10:65. <https://doi.org/10.3390/plants10010065>
23. Karnovsky MJ. A formaldehyde-glutaraldehyde fixative of high osmolarity for use in electron microscopy. *J Cell Biol*. 1965; 27:1A–149A.
24. Brundrett MC, Kendrick B, Peterson CA. Efficient lipid staining in plant material with Sudan Red 7B or Fluoral Yellow 088 in polyethylene glycol-glycerol. *Biotech Histochem*. 1991; 66:111–116. <https://doi.org/10.3109/10520299109110562>

Chapter 5 Apple fruit periderms (russeting) induced by wounding or by moisture have the same histologies, chemistries and gene expressions

25. Legay S, Guerriero G, Deleruelle A, Lateur M, Evers D, André CM, et al. Apple russeting as seen through the RNA-seq lens: Strong alterations in the exocarp cell wall. *Plant Mol Biol*. 2015; 88:21–40. <https://doi.org/10.1007/s11103-015-0303-4> PMID: 25786603
26. Pfaffl MW. A new mathematical model for relative quantification in real-time RT-PCR. *Nucleic Acids Res*. 2001; 29:e45. <https://doi.org/10.1093/nar/29.9.e45> PMID: 11328886
27. Chen YH, Khanal BP, Linde M, Debener T, Alkio M, Knoche M. Expression of putative aquaporin genes in sweet cherry is higher in flesh than skin and most are downregulated during development. *Sci Hort*. 2019; 244:304–314. <https://doi.org/10.1016/j.scienta.2018.09.065>
28. Orgell WH. The isolation of plant cuticle with pectic enzymes. *Plant Physiol*. 1955; 30:78–80. <https://doi.org/10.1104/pp.30.1.78> PMID: 16654733
29. Baales J, Zeisler-Diehl VV, Schreiber L. Analysis of Extracellular Cell Wall Lipids: Wax, Cutin, and Suberin in Leaves, Roots, Fruits, and Seeds. In: Bartels D, Dörmann P, editors. *Plant Lipids: Methods in Molecular Biology*. New York: Humana; 2021. pp. 275–293. https://doi.org/10.1007/978-1-0716-1362-7_15
30. Naseer S, Lee Y, Lapierre C, Franke R, Nawrath C, Geldner N. Casparian strip diffusion barrier in *Arabidopsis* is made of a lignin polymer without suberin. *Proc Natl Acad Sci USA*. 2012; 109:10101–10106. <https://doi.org/10.1073/pnas.1205726109> PMID: 22665765
31. Franke R, Schreiber L. Suberin—a biopolyester forming apoplastic plant interfaces. *Curr Opin Plant Biol*. 2007; 10:252–259. <https://doi.org/10.1016/j.pbi.2007.04.004> PMID: 17434790
32. Geng P, Zhang S, Liu J, Zhao C, Wu J, Cao Y, et al. *MYB20*, *MYB42*, *MYB43*, and *MYB85* regulate phenylalanine and lignin biosynthesis during secondary cell wall formation. *Plant Physiol*. 2020; 182:1272–1283. <https://doi.org/10.1104/pp.19.01070>
33. Yadav V, Molina I, Ranathunge K, Castillo IQ, Rothstein SJ, Reed JW. *ABCG* transporters are required for suberin and pollen wall extracellular barriers in *Arabidopsis*. *Plant Cell*. 2014; 26:3569–3588. <https://doi.org/10.1105/tpc.114.129049>
34. Legay S, Guerriero G, André C, Guignard C, Cocco E, Charton S, et al. *MdMyb93* is a regulator of suberin deposition in russeted apple fruit skins. *New Phytol*. 2016; 212:977–991. <https://doi.org/10.1111/nph.14170>
35. Lashbrooke JG, Cohen H, Levy-Samocho D, Tzfadia O, Panizel I, Zeisler V, et al. *MYB107* and *MYB9* homologs regulate suberin deposition in angiosperms. *The Plant cell*. 2016; 28:2097–2116. <https://doi.org/10.1105/tpc.16.00490> PMID: 27604696
36. Legay S, Cocco E, André CM, Guignard C, Hausman JF, Guerriero G. Differential lipid composition and gene expression in the semi-russeted 'Cox Orange Pippin' apple variety. *Front Plant Sci*. 2017; 8:1656. <https://doi.org/10.3389/fpls.2017.01656> PMID: 29018466
37. Beisson F, Li Y, Bonaventure G, Pollard M, Ohlrogge JB. The acyltransferase *GPAT5* is required for the synthesis of suberin in seed coat and root of *Arabidopsis*. *Plant Cell*. 2007; 19:351–368. <https://doi.org/10.1105/tpc.106.048033>
38. Franke R, Briesen I, Wojciechowski T, Faust A, Yephremov A, Nawrath C, et al. Apoplastic polyesters in *Arabidopsis* surface tissues—a typical suberin and a particular cutin. *Phytochemistry*. 2005; 66:2643–2658. <https://doi.org/10.1016/j.phytochem.2005.09.027>
39. Khanal BP, Grimm E, Knoche M. Russeting in apple and pear: A plastic periderm replaces a stiff cuticle. *AoB Plants*. 2013; 5:pls048. <https://doi.org/10.1093/aobpla/pls048> PMID: 23350024
40. Simons RK, Chu MC. Periderm morphology of mature 'Golden Delicious' apple with special reference to russeting. *Sci Hort*. 1978; 8:333–340. [https://doi.org/10.1016/0304-4238\(78\)90055-9](https://doi.org/10.1016/0304-4238(78)90055-9)
41. Schreiber L, Franke R, Hartmann K. Wax and suberin development of native and wound periderm of potato (*Solanum tuberosum* L.) and its relation to peridermal transpiration. *Planta*. 2005; 220:520–530. <https://doi.org/10.1007/s00425-004-1364-9>
42. de Vries HAMA. Development of the structure of the russeted apple skin. *Acta Bot. Neerl*. 1968; 17:405–415.
43. Knoche M, Khanal BP, Stopar M. Russeting and microcracking of 'Golden Delicious' apple fruit concomitantly decline due to gibberellin A_{4+7} application. *J Amer Soc Hort Sci*. 2011; 136:159–164. <https://doi.org/10.21273/JASHS.136.3.159>
44. Skene DS. Wound healing in apple fruits: The anatomical response of Cox's Orange Pippin at different stages of development. *J Hort Sci*. 1981; 56:145–153. <https://doi.org/10.1080/00221589.1981.11514980>
45. Wei X, Mao L, Han X, Lu W, Xie D, Ren X, et al. High oxygen facilitates wound induction of suberin polyphenolics in kiwifruit. *J Sci Food Agric*. 2018; 98:2223–2230. <https://doi.org/10.1002/jsfa.8709> PMID: 28963774

Chapter 5 Apple fruit periderms (russeting) induced by wounding or by moisture have the same histologies, chemistries and gene expressions

46. Lipton WJ. Some effects of low-oxygen atmospheres on potato tubers. *Amer Potato J.* 1967; 44:292–299. <https://doi.org/10.1007/BF02862531>.
47. Wigginton MJ. Effects of temperature, oxygen tension and relative humidity on the wound-healing process in the potato tuber. *Potato Res.* 1974; 17:200–214. <https://doi.org/10.1007/BF02360387>

5.1. Supplementary data Chapter 5

S1 Table. Selected transcription factors and genes analyzed in the present study.

Gene name	Accession	AGI locus code	Description	Reference
Suberin and lignin related				
<i>MYB93</i>	MDP0000320772	AT1G34670.1	MYB domain protein 93, positive regulator of suberin biosynthesis	(Legay et al., 2016)
<i>MYB42</i>	MDP0000787808	AT4G12350.1	MYB domain protein 42, involved in secondary cell wall biosynthesis and regulation of lignin synthesis	(Geng et al., 2020; Zhong et al., 2008)
<i>CYP86B1</i>	MDP0000306273	AT5G23190.1	Cytochrome P450, family 86, subfamily B, polypeptide 1, involved in the synthesis of very long chain ω -hydroxyacid and α,ω -dicarboxylic acid in suberin polyester	(Compagnon et al., 2009)
<i>ABCG20</i>	MDP0000265619	AT3G53510	ATP-binding cassette G20, involved in transport of aliphatic suberin polymer precursors	(Yadav et al., 2014)
<i>NAC038</i>	MDP0000232008	AT2G24430.1	NAC domain containing protein 38	uncharacterized
<i>NAC058</i>	MDP0000130785	AT3G18400.1	NAC domain containing protein 58	uncharacterized
Cutin and wax related				
<i>SHN3</i>	MDP0000178263	AT5G25390	Positive transcriptional regulator of cuticle synthesis	(Aharoni et al., 2004)
<i>GPAT6</i>	MDP0000479163	AT2G38110.1	Glycerol-3-phosphate acyl transferase 6, involved in synthesis of cutin monomers	(Petit et al., 2016)
<i>FDH, KCS10</i>	MDP0000235280	AT2G26250.1	FIDDLEHEAD, 3-Ketoacyl-CoA synthase 10, involved in the long-chain lipid synthesis	(Pruitt et al., 2000)
<i>CER6</i>	MDP0000392495	AT1G68530.1	3-Ketoacyl-CoA-synthase 6, involved in the biosynthesis of very long chain fatty acids (VLCFAs)	(Millar et al., 1999)
<i>WSD1</i>	MDP0000701887	AT5G37300.1	Wax ester synthase/Acyl-coenzyme A: Diacylglycerol acyltransferase, involved in the synthesis of wax esters and diacylglycerol acyltransfer activity	(Li et al., 2008)
<i>ABCG11</i>	MDP0000200335	AT1G17840.1	ABCG11, white-brown complex homolog protein 11, transport of cuticular lipids to the extracellular matrix	(Bird et al., 2007)

Table was adopted from Straube et al. (2020)

S2 Table. Primers sequences of the genes analyzed in the present study

Gene name	Accession	Primer sequence (5' to 3')		PCR efficiency (%)	Reference
		Forward Primer	Reverse Primer		
<i>ABCG11</i>	MDP0000200335	TGGCGGGTTTCCTTCTTTCA	CACAAATGCAGTAACGCCGT	98.7	(Straube et al., 2020)
<i>ABCG20</i>	MDP0000265619	ACTGGGCATGGACAACAACA	ATTTTCCCGACCCACTTGCT	102.9	(Straube et al., 2020)
<i>CER6</i>	MDP0000392495	AGCAACAACCCTAAGAGCGT	GTTGGGCGGAATGTAGTGGA	85.0	(Straube et al., 2020)
<i>CYP86B1</i>	MDP0000306273	CGCTTTGTGACCCCATCC	AATGACGTCTTCCGCAAACCT	109.3	(Legay et al., 2015)
<i>eF-1alpha</i>	AJ223969.1	ACTGTTCTGTTGGACGTGTTG	TGGAGTTGGAAGCAACGTACCC	93.0	(Legay et al., 2015)
<i>GPAT6</i>	MDP0000479163	TCTTGAACCAGCTACCGTCG	AATCCCAAAGTCCCAGCCAA	91.0	(Straube et al., 2020)
<i>KCS10</i>	MDP0000235280	TGCTGAGGTGGGAAGTTTGA	ACACCAAAGAACCCTAGCACA	91.6	(Straube et al., 2020)
<i>MYB42</i>	MDP0000787808	CCTTGGCAATAGGTGGTTCGA	TGATGTGCGTGTTCAGTGA	94.2	(Straube et al., 2020)
<i>MYB93</i>	MDP0000320772	TGGACAAACTATCTTAGGCCGG	GTTGCCGAGGATGGAATGGA	102.5	(Straube et al., 2020)
<i>NAC038</i>	MDP0000232008	CGGCGGATCATCAAGTAGCA	AAACCCTCCTCCTCCTCAA	84.6	(Straube et al., 2020)
<i>NAC058</i>	MDP0000130785	AGCCACAACAAGCAACAACA	TTTGGCAGCTCGATGTCTCC	90.7	(Straube et al., 2020)
<i>PDI</i>	MDP0000233444	TGCTGTACACAGCCAACGAT	CATCTTTAGCGGCGTTATCC	100.6	(Storch et al., 2015; Straube et al., 2020)
<i>SHN3</i>	MDP0000178263	GGGACGTTTGAGACAGCAGA	TTTTGGTCGGTGGCAGGTTT	93.6	(Straube et al., 2020)
<i>WSD1</i>	MDP0000701887	AGAAATGGTCAAACCCGACA	AGACGAAGTCAAGCGCATTT	91.1	(Legay et al., 2015)

Table was adopted from Straube et al. (2020)

Electronical File E2. Data produced in figures (XLSX) (access through electronical appendix)

6. Time course of changes in the transcriptome during russet induction in apple fruit

Jannis Straube^{1,2}, Shreya Suvarna¹, Yun-Hao Chen², Bishnu P. Khanal², Moritz Knoche² and Thomas Debener¹

¹Institute of Plant Genetics, Molecular Plant Breeding Section, Leibniz University Hannover, Herrenhäuser Straße 2, 30419 Hannover, Germany

²Institute of Horticultural Production Systems, Fruit Science Section, Leibniz University Hannover, Herrenhäuser Straße 2, 30419 Hannover, Germany

Type of authorship: First author
Type of article: Research article
Contribution to the article: Designed and performed the experiments, analyzed the data, and prepared the figures and tables. Wrote the original draft of the manuscript and designed all figures and tables. Contributed to reviewing and editing of the manuscript.

Contribution of other authors: S. Suvarna contributed to sample acquisition across different cultivars and histology. Y.-H. Chen performed some histological observations and growth curve analysis for the different cultivars. B.P. Khanal performed acridine orange observations for ‘Pinova’ during the 2019 growing season, and contributed to reviewing, and editing of the manuscript. M. Knoche and T. Debener contributed to the design of the study and to writing, reviewing, and editing the manuscript.

Journal: BMC Plant Biology
Date of publication: 30.09.2023
Impact factor: 5.26 (2022)
DOI: 10.1186/s12870-023-04483-6

RESEARCH

Open Access

Time course of changes in the transcriptome during russet induction in apple fruit



Jannis Straube^{1,2}, Shreya Suvarna¹, Yun-Hao Chen², Bishnu P. Khanal², Moritz Knoche² and Thomas Debener^{1*}

Abstract

Background Russetting is a major problem in many fruit crops. Russetting is caused by environmental factors such as wounding or moisture exposure of the fruit surface. Despite extensive research, the molecular sequence that triggers russet initiation remains unclear. Here, we present high-resolution transcriptomic data by controlled russet induction at very early stages of fruit development. During Phase I, a patch of the fruit surface is exposed to surface moisture. For Phase II, moisture exposure is terminated, and the formerly exposed surface remains dry. We targeted differentially expressed transcripts as soon as 24 h after russet induction.

Results During moisture exposure (Phase I) of 'Pinova' apple, transcripts associated with the cell cycle, cell wall, and cuticle synthesis (*SHN3*) decrease, while those related to abiotic stress increase. *NAC35* and *MYB17* were the earliest induced genes during Phase I. They are therefore linked to the initial processes of cuticle microcracking. After moisture removal (Phase II), the expression of genes related to meristematic activity increased (*WOX4* within 24 h, *MYB84* within 48 h). Genes related to lignin synthesis (*MYB52*) and suberin synthesis (*MYB93*, *WRKY56*) were upregulated within 3 d after moisture removal. *WOX4* and *AP2B3* are the earliest differentially expressed genes induced in Phase II. They are therefore linked to early events in periderm formation. The expression profiles were consistent between two different seasons and mirrored differences in russet susceptibility in a comparison of cultivars. Furthermore, expression profiles during Phase II of moisture induction were largely identical to those following wounding.

Conclusions The combination of a unique controlled russet induction technique with high-resolution transcriptomic data allowed for the very first time to analyse the formation of cuticular microcracks and periderm in apple fruit immediately after the onset of triggering factors. This data provides valuable insights into the spatial-temporal dynamics of russetting, including the synthesis of cuticles, dedifferentiation of cells, and impregnation of cell walls with suberin and lignin.

Keywords Russetting, *Malus x domestica*, Fruit skin, Periderm, Cuticle, Transcriptome, Suberin, Lignin, Wounding

*Correspondence:

Thomas Debener
debener@genetik.uni-hannover.de

¹Institute of Plant Genetics, Molecular Plant Breeding Section, Leibniz University Hannover, Herrenhäuser Straße 2, 30419 Hannover, Germany

²Institute of Horticultural Production Systems, Fruit Science Section, Leibniz University Hannover, Herrenhäuser Straße 2, 30419 Hannover, Germany



© The Author(s) 2023. **Open Access** This article is licensed under a Creative Commons Attribution 4.0 International License, which permits use, sharing, adaptation, distribution and reproduction in any medium or format, as long as you give appropriate credit to the original author(s) and the source, provide a link to the Creative Commons licence, and indicate if changes were made. The images or other third party material in this article are included in the article's Creative Commons licence, unless indicated otherwise in a credit line to the material. If material is not included in the article's Creative Commons licence and your intended use is not permitted by statutory regulation or exceeds the permitted use, you will need to obtain permission directly from the copyright holder. To view a copy of this licence, visit <http://creativecommons.org/licenses/by/4.0/>. The Creative Commons Public Domain Dedication waiver (<http://creativecommons.org/publicdomain/zero/1.0/>) applies to the data made available in this article, unless otherwise stated in a credit line to the data.

Background

Russetting is a skin disorder in many fruit crop species, including apple [1–5]. In russetting, the cuticle and the epidermis are replaced by periderm. In many apple cultivars, russetting compromises the visual appearance of the fruit, thereby reducing market value. Furthermore, postharvest performance is impaired by the increased permeance of the skin to water vapor, which may result in increased mass loss and shriveling [6–8].

Periderm formation begins in the hypodermis in the vicinity of microcracks in the cuticle [9–11]. Microcracks are minute microscopic cracks that are limited to the cuticle and not visible to the naked eye [12–14]. They are the first visible symptoms in russetting [12, 15] and result from a mismatch between cuticle deposition on the one hand and growth stress during periods of rapid surface expansion on the other hand [16, 17]. Russetting is influenced by both environmental and genetic factors. Environmental factors include the exposure of fruit surfaces to moisture or high humidity during periods of high strain or mechanical damage [13, 14, 18–21]. There are genetic differences in the susceptibility of cultivars to russetting. Generally, cultivars with high variability in the cell sizes of the epidermis and hypodermis are most susceptible [22].

Molecular studies indicate that the downregulation of cuticle synthesis is an important factor in russetting. QTLs (quantitative trait loci) for russetting on chromosomes 2, 12 and 15 were identified in populations segregating for russet susceptibility [23, 24]. Within these QTLs, the major cuticle regulator *MdSHN3* [24] as well as the cutin/wax transporter *MdABCG11* [23] were associated with russet susceptibility in apple under field conditions. Comparisons between a russet-resistant and a fully russeted sport of ‘Golden Delicious’ demonstrated downregulation of two oxidosqualene cyclases (*MdOSC1* and *MdOSC3*) during microcracking of the cuticle. A change in triterpene content from ursan-type to lupane-type triterpenes was observed in russeted skins, together with an increase in *MdOSC5*, which is activated by MdMYB66 and to a lesser extent by MdMYB52 [25]. Furthermore, a bulk transcriptomic study on russeted and nonrusseted fruits revealed a large number of cuticle-related genes to be downregulated in russeted apple fruit skins at maturity [26]. Additionally, suberin-associated genes were highly expressed, together with a dense network of possible transcriptional regulators of the later processes of russetting (e.g., maturation of the periderm, impregnation of cell walls with suberin) [26]. The transcription factor *MdMYB93* was later identified as a major regulator of suberin synthesis [27], and *MdMYB52* was identified as a regulator of lignin synthesis [28]. In addition, investigations at the multispecies level revealed MYB9 and MYB107 to be major regulators of suberin formation in

angiosperms [29]. The majority of transcription factors associated with the later processes of russetting belong to the R2R3-MYB family and, to a minor extent, to the AP2/EREBP, bHLH, C2H2, WRKY, and NAC-domain transcription factor families [25–27, 30–32]. Unfortunately, all of the above analyses were conducted on fruit at the mature stage, while russetting typically occurs during early development. In apple, russet susceptibility peaks during the first four weeks after full bloom [1, 12, 20, 33–36]. Unfortunately, only a few studies focused on this time period. We therefore used moisture treatment to induce russetting at defined developmental stages, including the period of highest russet susceptibility [19]. Khanal and coworkers [14] refined the system to specifically target early events in russet formation. This modification allowed a patch of fruit skin to be exposed to moisture (Phase I), while the remaining fruit surface stays dry and serves as a control. The moisture is then removed (Phase II), and the events occurring after moisture removal can be monitored [13, 21].

Here, we present a high-resolution transcriptomic study performed during the onset of russetting in apple. The objectives of this research were to analyze genes representative of Phase I and Phase II of moisture-induced russetting and to identify candidates with putative functions in russetting.

Results

We induced russetting on fruits of the cultivar ‘Pinova’ in the 2018 and 2019 growing seasons by exposing fruits 21 or 31 days after full bloom (DAFB) to moisture for 12 d (Phase I, ‘12 d wet+0 d dry’). During Phase I, the control fruit remained dry (‘12 d dry+0 d dry’). For the subsequent Phase II, moisture was removed, and samples were taken at 1 d (‘12 d wet+1 d dry’) to 8 d after moisture removal (‘12 d dry+8 d dry’). The number of read pairs obtained after quality filtering and trimming of raw reads ranged from 56.6 M to 70.5 M for independent replicates. Reads mapped uniquely to the HFTH1 genome with a frequency between 82.9 and 95.5% (Table S1).

Transcriptomic data obtained during the 2018 and 2019 seasons displayed low variability between replicates as indexed by principal component analysis (PCA) (Fig. 1A, B). Control samples clustered closely together for both seasons. In contrast, moisture-treated samples compared to untreated controls showed a pronounced diverging pattern, with distances between treatments increasing with time after moisture removal (Phase II). This corresponded to the observed progress of microcrack formation within Phase I and periderm development during the consecutive Phase II (Figure S1). Clusters observed in PCA for the 2018 season (Fig. 1A) were less compact than those in the 2019 season (Fig. 1B).

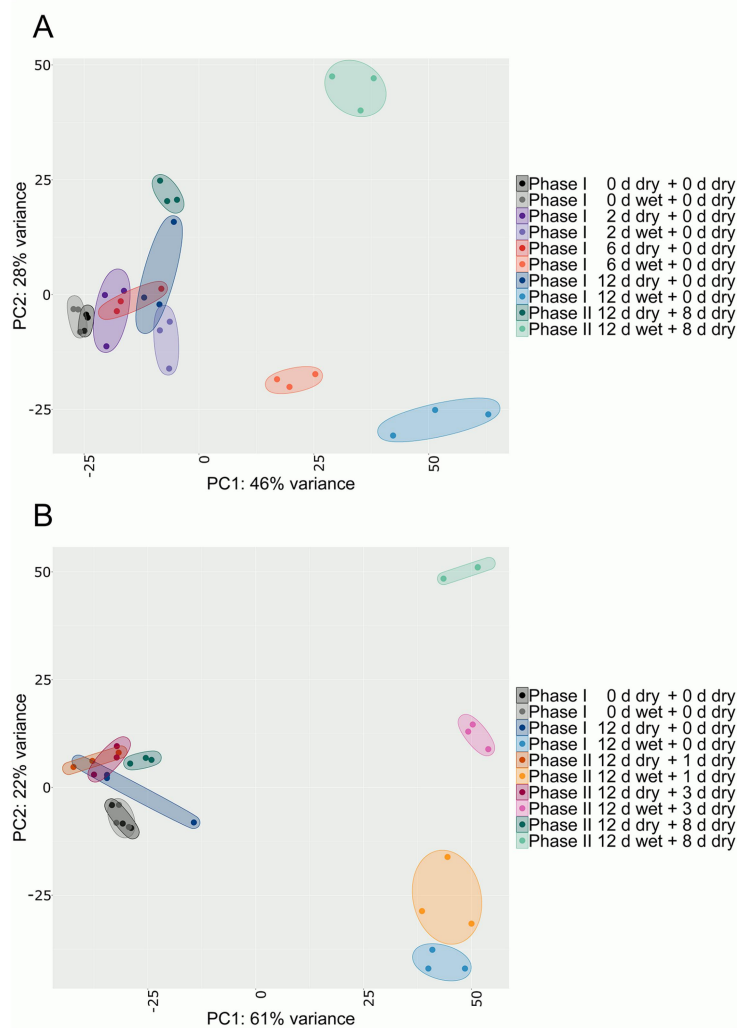


Fig. 1 Variability between biological replicates in the RNA-Seq datasets. Apple fruit skin patches of ‘Pinova’ apples were induced to russet by exposed to surface moisture for 12 d (Phase I). After termination of moisture exposure, the treated skin patch was exposed to ambient atmosphere (Phase II). Non-treated control surfaces remained dry during Phase I and Phase II. The distribution of the transcriptome during the 2018 (A) and 2019 (B) seasons was determined by principal component analysis (PCA) based on variance stabilization transformation in ‘DESeq2’. PCA revealed clear separation of clusters between moisture-exposed (‘x d wet+y d dry’) and control (‘x d dry+y d dry’) samples, whereas the biological replicates within each treatment were consistent (indicated by ellipses)

Transcripts differ between phases I and II of russet induction

Stringent filtering of the differentially expressed genes (DEGs) obtained from the various datasets revealed a total of 3533 DEGs. The number of DEGs was higher

in 2019 than in 2018 (Table S2). Four times more genes were downregulated and two times more genes were upregulated in 2019 than in 2018 between the corresponding time points at ‘12 d wet+0 d dry’ (Phase I) and ‘12 d wet+8 d dry’ (Phase II) (Table S2). Consistent with

this observation, there were more russeted fruits in the 2019 season than in the 2018 season (Figure S2A, B).

For both seasons, we found DEGs putatively involved in microcracking in Phase I as well as in periderm formation in Phase II.

In Phase I samples, in the 2018 season, 242 genes were downregulated compared to 22 in Phase II. Of the 242 genes, 54 genes were downregulated at '6 d wet+0 d dry' as well as '12 d wet+0 d dry' (Fig. 2A). In contrast, 700 genes were upregulated exclusively during Phase I and 310 during Phase II. Of the 700 genes specific to Phase I, 14 were already differentially expressed after 2 d of surface moisture ('2 d wet+0 d dry') (Fig. 2B).

In 2019, 421 genes were downregulated during Phase I and 335 during Phase II, whereas 32 genes were already downregulated at '12 d wet+1 d dry' in Phase II (Fig. 2C). The number of upregulated genes was 375 in Phase I and 959 in Phase II. Of the 959 genes, 103 were already upregulated at '12 d wet+1 d dry' during Phase II (Fig. 2D).

Three sampling dates were common in both seasons: '0 d wet+0 d dry' (Phase I), '12 d wet+0 d dry' (Phase I), and '12 d wet+8 d dry' (Phase II). The last two sampling times revealed a large number of season-specific DEGs. To avoid artifacts from confounding factors unrelated to russeting but differing between seasons, further analysis was restricted to DEGs consistent between seasons. These comprised 106 genes at '12 d wet+0 d dry' (Phase I) and one gene at '12 d wet+8 d dry' (Phase II) (Data S1). Eight genes were downregulated on both sampling dates (Fig. 2E). In both seasons, the number of upregulated genes was 414 at '12 d wet+0 d dry' (Phase I) and 238 at '12 d wet+8 d dry' (Phase II) (Fig. 2F; Data S1).

The DEGs downregulated in Phase I ('12 d wet+0 d dry') were characterized by gene ontology (GO) terms related to cellular processes (e.g., cell division, cell wall associated or cytoskeleton). Cuticle-related GO terms (e.g., lipid metabolic process, fatty acid metabolic process, fatty acid synthetic process, and cellular lipid metabolic process) were downregulated in 2019 and to a lesser extent (\log_2 -fold change (\log_2FC) ≤ -1) in 2018 (Fig. 3A, Data S2, S3, S4, S5). The DEGs upregulated in Phase I due to moisture exposure comprised stress-related genes (e.g., oxidative stress and osmotic stress) (Fig. 3B, Data S2, S3, S4).

The DEGs during early Phase II ('12 d wet+1 d dry') were similar to those at '12 d wet+0 d dry' (Phase I). The number of GO terms for downregulated DEGs decreased over time during Phase II. Beginning at '12 d wet+3 d dry', DEGs associated with suberin and lignin formation and cell wall metabolism were upregulated (Fig. 3C, Data S2, S3, S4). After '12 d wet+8 d dry' (Phase II), only one gene was consistently downregulated in both years (Fig. 2E). The upregulated genes at '12 d wet+8 d dry' (Phase II) included genes responsive to hormones,

including abscisic acid (ABA), and a range of transcription factors (Fig. 3C; Data S4). At '12 d wet+8 d dry' (Phase II), processes associated with the metabolism of phenylpropanoids, suberin, and secondary metabolites, as well as response to lipids and apoplasts, were activated (Fig. 3C).

Cluster analysis revealed four clusters of DEGs with highly correlated expression patterns, suggesting a close relation to the onset of russeting (Fig. 4).

The first cluster contained nine genes that were downregulated in Phase I as early as '2 d wet+0 d dry', which remained so until '12 d wet+8 d dry' in Phase II. *SHN3* [37–39] and *MYB94* [40, 41] were identified within this cluster, where orthologous genes had major regulatory functions in cuticle synthesis. The second cluster contained putative regulators for russeting, e.g., *MYB93*. This gene is a major regulator of suberin formation in apple [27]. This cluster was characterized by strong upregulation ($\log_2FC \geq 2$) several days after moisture removal ('12 d wet+3 d dry') in Phase II. The third cluster contained transcriptional regulators that were activated immediately or shortly after termination of the moisture treatment ('12 d wet+0 d dry' and '12 d wet+1 d dry') on the fruit skin patches. Within this cluster, *Wuschel-related homeobox 4 (WOX4)* and *MYB84* were observed, which are orthologous genes of major regulators during periderm initiation. Many genes in the fourth cluster were already slightly upregulated at the timepoint of moisture removal ('12 d wet+0 d dry'), especially in season 2019 (Fig. 4). This cluster contains *MYB36*, the orthologous gene of which in *Arabidopsis thaliana* regulates developmental transitions from proliferation to differentiation of cells in the root endodermis [42].

Validation of selected DEGs by qPCR

Earlier studies established that (1) microcracking of the cuticle occurs within 48 h of moisture exposure and (2) periderm initiation begins within 24 h of moisture removal [13, 14, 21, 43]. Therefore, putative regulators must be expressed early during Phase I and at the beginning of Phase II, i.e., at '12 d wet+1 d dry'. Based on these findings, a set of 12 DEGs was selected that represented candidate genes for early regulation during Phase I and Phase II (Fig. 5A) and/or are related to either cuticle (Phase I) or periderm formation (Phase II). These comprised transcription factors derived from clusters specific to Phase I (*MYB17*, *NAC35*) or Phase II (*AP2/B3-like transcription factor family protein (AP2B3)*, *WOX4*, *MYB84*, *MYB-like 102 (MYB102)*, *MYB52*, *WRKY56*, *MYB67*, *MYB93*), one *late embryogenesis abundant hydroxyproline-rich glycoprotein (LEA)* and one *SGNH hydrolase (SGNH)*. The genes were analyzed by quantitative real-time PCR (qPCR) to validate their expression patterns (Fig. 5B). The expression patterns of the selected

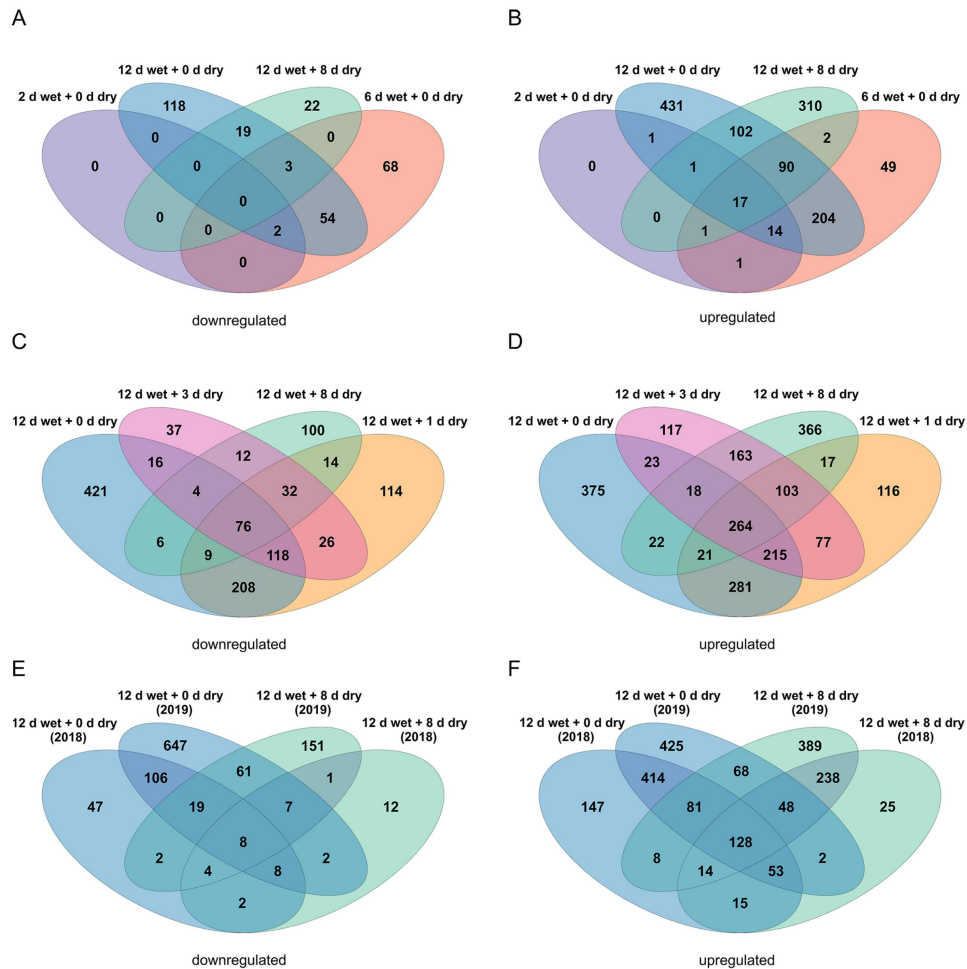


Fig. 2 Effect of the growing season on gene expression patterns in moisture-induced russetting in 'Pinova' apples. Venn diagrams of differentially expressed genes during the 2018 (**A, B**) and 2019 growing seasons (**C, D**). Comparison of common treatments and their respective controls between the two seasons (**E, F**). Only genes with a \log_2 -fold change (\log_2FC) ≥ 2 or ≤ -2 , a false discovery rate (FDR) ≤ 0.05 and a mean of at least five transcripts per million (TPM) for moisture-exposed ('x d wet+y d dry') or control ('x d dry+y d dry') samples are illustrated

genes were similar for RNA-Seq and qPCR. *MYB93* was used to trace the early processes of suberin synthesis [21, 27, 43] during Phase II and thus was representative of periderm formation as indexed by the occurrence of phellem cells.

NAC35 and *MYB17* were downregulated during early Phase I within both seasons at time points when micro-cracking occurred (Fig. 5A, B; Figure S1). The genes *AP2B3*, *WOX4* and *LEA* showed increased expression at

'12 d wet+1 d dry' (Fig. 5A, B). At '12 d wet+2 d dry', the expression of *MYB84*, *MYB102*, *MYB52* and *WRKY56* increased as indexed by qPCR. Upregulation of *MYB93* and *SGNH* started one day later at '12 d wet+3 d dry'. The increase continued until '12 d wet+8 d dry' (Fig. 5B). The expression pattern was consistent between the two seasons (Fig. 5A, B). The transcriptional regulator *MYB67* was only differentially expressed at '12 d wet+8 d dry',

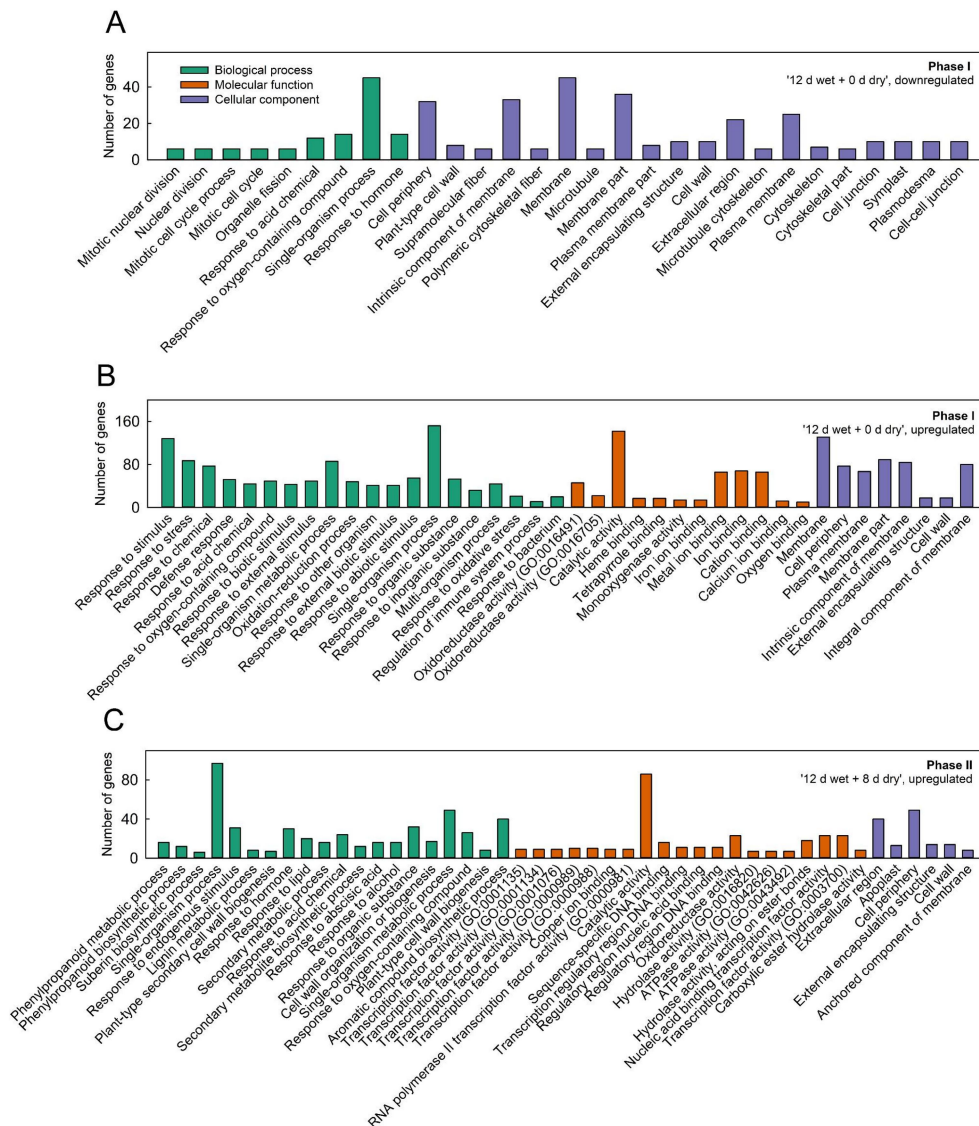


Fig. 3 GO term analysis following moisture-induced russeting of apple. Russeting on 'Pinova' apple fruits was induced by moisture in a two-phase experiment. During Phase I, a patch of fruit skin was exposed to surface moisture for 12 d (Phase I). After termination of moisture exposure (Phase II), the treated skin patch was exposed to the ambient atmosphere. The nontreated controls remained dry during Phase I and Phase II. Treatments and respective controls are listed in Table S3. Moisture exposure began at 21 or 31 days after full bloom (DAFB) during the 2018 and 2019 seasons. The GO term analysis indicated weakening of the cell structure during Phase I and hormone-regulated repair mechanisms of microcracks during Phase II. Common DEGs at '12 d wet + 0 d dry' (A, B) and '12 d wet + 8 d dry' (C) identified by the Venn diagrams (see Fig. 2) were subjected to singular enrichment analysis (SEA) to obtain GO terms associated specifically with Phase I or Phase II. The top 20 GO terms for biological process, molecular process and cellular component are shown, which were derived from the orthologous genes found in the TAIR10 database. Only GO terms with a minimum of five genes and an FDR ≤ 0.01 were selected

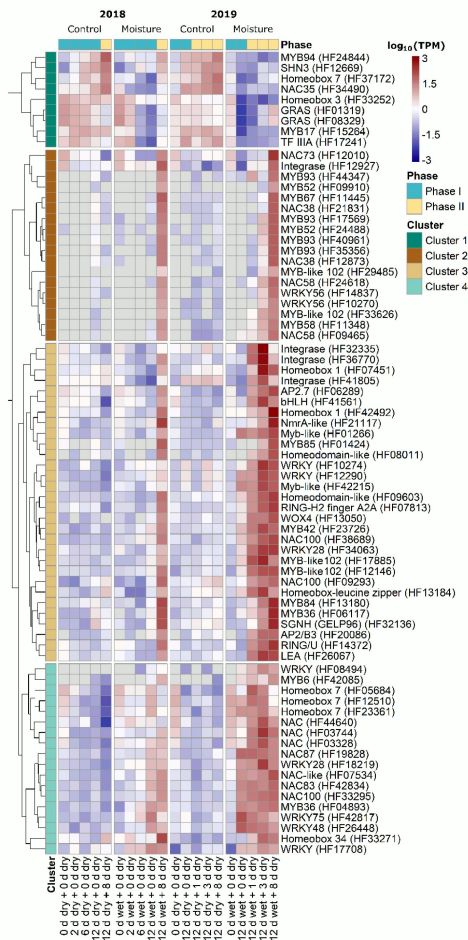


Fig. 4 Heatmap illustrating distinct expression patterns of transcriptional regulators during moisture-induced russeting. Russeting in 'Pinova' apples was induced in a two-phase experiment: During Phase I, a patch of fruit skin was exposed to surface moisture for 12 d (Phase I, '12 d wet'). After termination of moisture exposure (Phase II), the treated skin patch was exposed to the ambient atmosphere ('y d dry'). The nontreated control ('Control') remained dry during Phase I and Phase II ('x d dry+y d dry'). The heatmap revealed a dense network of transcriptional regulators that were differentially expressed during the early phase of russet formation. Cluster 1 contains Phase I-related genes, and Clusters 2 to 4 contain Phase II-related genes. Expression values are the mean \log_{10} (TPM) values of three independent biological replicates comprising six (season 2018) or ten (season 2019) fruits each. Genes with a $\log_2FC \geq 2$ or ≤ -2 , an FDR ≤ 0.05 and a mean of at least five TPM in 'Moisture' or 'Control' at any time during the two seasons are illustrated. Gene clusters were obtained via hierarchical clustering with the R package 'pheatmap'

when the first phellem cells had formed (Fig. 5, Figure S1).

Expression patterns of DEGs match russet susceptibility in cultivars differing in russet susceptibility

To confirm a role in russetting, the expression pattern of the selected DEGs was studied in four cultivars differing in russet susceptibility. Russet susceptibility decreased from 'Karmijn'>'Pinova'>'Idared'>'Gala', as indexed by the portion of russeted surface area within the moisture-exposed skin patch [44] (Figs. S3, S4). Downregulation of the Phase I-related gene *MYB17* correlated with the degree of russet susceptibility (Fig. 6). Only for *NAC35* was there no relationship to russet susceptibility (Fig. 6).

Generally, the expression patterns of Phase II-related genes (*LEA*, *WOX4*, *AP2B3*, *MYB52*, *MYB67*, *MYB84*, *MYB93*, *MYB102*, *WRKY56* and *SGNH*) corresponded to the extent of microcracking during Phase I (Figure S5) and matched the degree of russet susceptibility of the four cultivars during Phase II (Fig. 6, Figure S3).

Phase II genes display similar expression patterns in samples where russetting is induced by moisture or by mechanical wounding

Mechanical wounding of apple fruit skins induced russetting. Hence, the expression patterns of the DEGs were also analyzed following wounding [43].

The Phase I-specific transcription factors *MYB17* and *NAC35* were downregulated immediately after wounding (Fig. 7).

AP2B3, *WOX4*, *MYB84*, *MYB102*, *MYB52*, *WRKY56* and *LEA* were upregulated 2 d after wounding, and *SGNH*, *MYB67* and the suberin-specific gene *MYB93* were upregulated after 4 d (Fig. 7). The expression of *AP2B3*, *LEA* and *MYB102* peaked at 2 d and decreased to a constant level thereafter. The expression of *MYB67* was similar to that of *MYB93* and *SGNH*, although the increase was somewhat smaller. Similar DEGs were identified in the cultivar comparison following wounding. There was no relationship between the russet susceptibility of the cultivars and the DEGs (Figure S6). In contrast to moisture-induced russetting, which induced russetting only in a fraction of the exposed skin patch, russetting following wounding covered the entire area of the wounded patch in all four cultivars (Table S4).

Discussion

Our discussion focuses on (1) the suitability of moisture-induced microcracking for studying russetting in apples, (2) the changes in the transcriptome occurring during Phase I and (3) those occurring during Phase II of moisture-induced russetting.

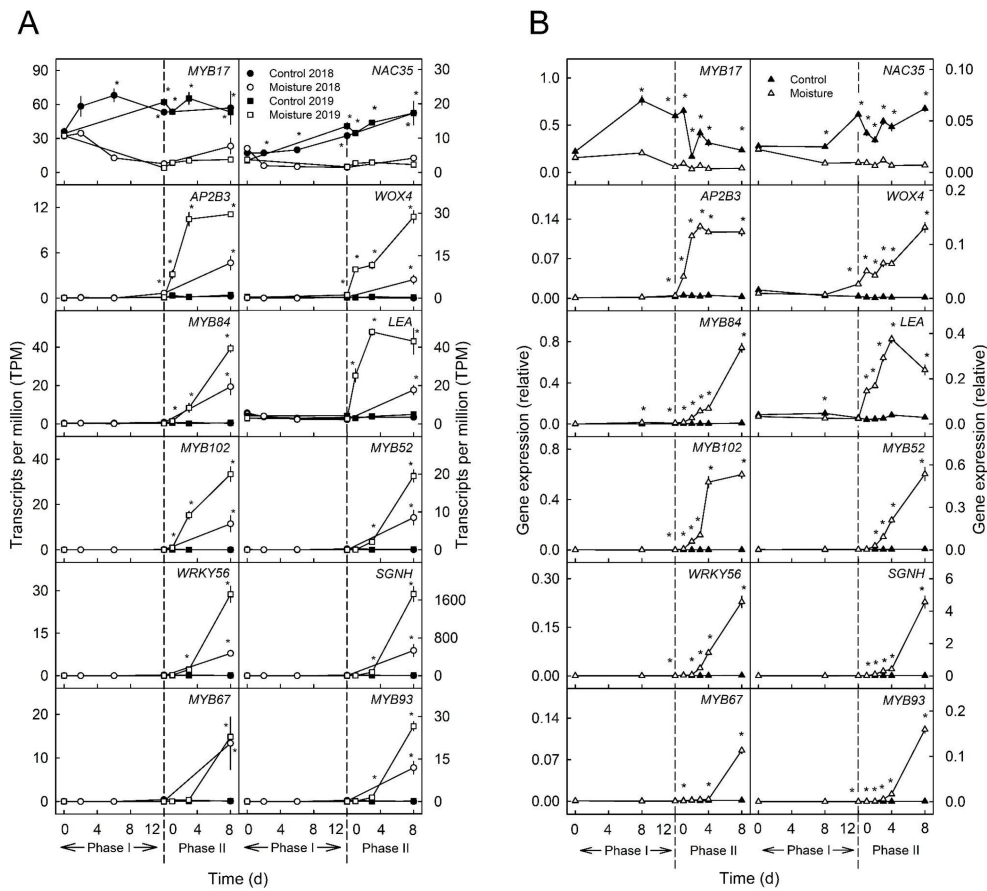


Fig. 5 Comparison of gene expression results obtained by RNA-Seq (A) and qPCR (B). The data obtained by the two methods reveal consistent gene expression. Russeting in ‘Pinova’ apples was induced in a two-phase experiment: During Phase I, a patch of fruit skin was exposed to surface moisture for 12 d (Phase I, ‘12 d wet’). After termination of moisture exposure (Phase II), the treated skin patch was exposed to the ambient atmosphere (‘y d dry’). The nontreated control (‘Control’) remained dry during Phase I and Phase II (‘x d dry + y d dry’). Moisture exposure began at 21 or 31 days after full bloom (DAFB) during the 2018 and 2019 seasons. The dashed line indicates the termination of moisture exposure. Genes with specific patterns for Phase I and Phase II were analyzed. Expression values obtained from RNA-Seq data (A) represent means \pm SEs of three independent biological replicates comprising six (season 2018) or ten (season 2019) fruits each. * indicates a significant difference between ‘Moisture’ and ‘Control’ at FDR \leq 0.05. Expression values derived from qPCR (B) represent means \pm SEs of three independent biological replicates comprising ten fruits each. ** indicates a significant difference between ‘Moisture’ and ‘Control’ at $p \leq 0.05$ (Student’s t test)

Moisture-induced russeting

Russeting in susceptible apple cultivars is triggered by a number of environmental factors [13, 14, 18–21, 36, 45–53]. Under field conditions, these factors are impossible to control, resulting in high variability of russeting within a tree, between trees, and between orchards, regions and seasons.

This makes systematic studies on russeting and the identification of triggers of russeting at a molecular level

difficult. Moisture-induced russeting is a promising system that offers several advantages. First, surface moisture is a common factor in the natural russeting of apples [15, 18, 36, 54]. Second, experimental induction of russeting using moisture may be performed at the developmental stage where fruit is most susceptible to russeting. This is the first 40 days after full bloom [1, 12, 20, 33–36]. However, most studies of transcriptomes of russeted apple fruit are based on natural russeting assessed at the

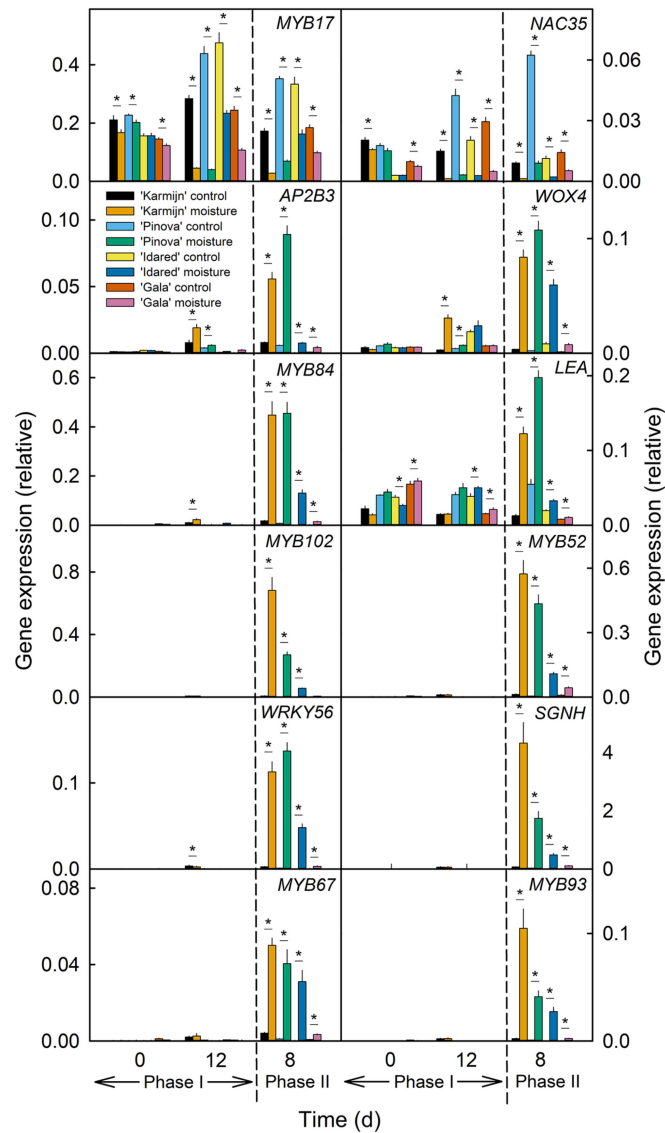


Fig. 6 Expression pattern of putative candidate genes during moisture-induced russeting of four apple cultivars. A two phase experiment was conducted to induce russeting in four apple cultivars ('Karmijn', 'Pinova', 'Idared', and 'Gala') that vary in their susceptibility to russet: During Phase I, a patch of fruit skin was exposed to surface moisture for 12 d (Phase I, 12 d wet). After termination of moisture exposure (Phase II), the treated skin patch was exposed to the ambient atmosphere (y d dry). The nontreated control ('Control') remained dry during Phase I and Phase II (x d dry + y d dry). The dashed line indicates the termination of moisture exposure. The expression of genes associated with Phase I (*MYB17*, *NAC35*) as well as Phase II (*AP2B3*, *WOX4*, *MYB84*, *LEA*, *MYB102*, *MYB52*, *WRKY56*, *SGNH*, *MYB67*, *MYB93*) was analyzed. Expression values represent the means \pm SEs of three independent biological replicates comprising six fruits each. "*" indicates a significant difference between 'Moisture' and 'Control' in each cultivar at $p \leq 0.05$ (Student's t test)

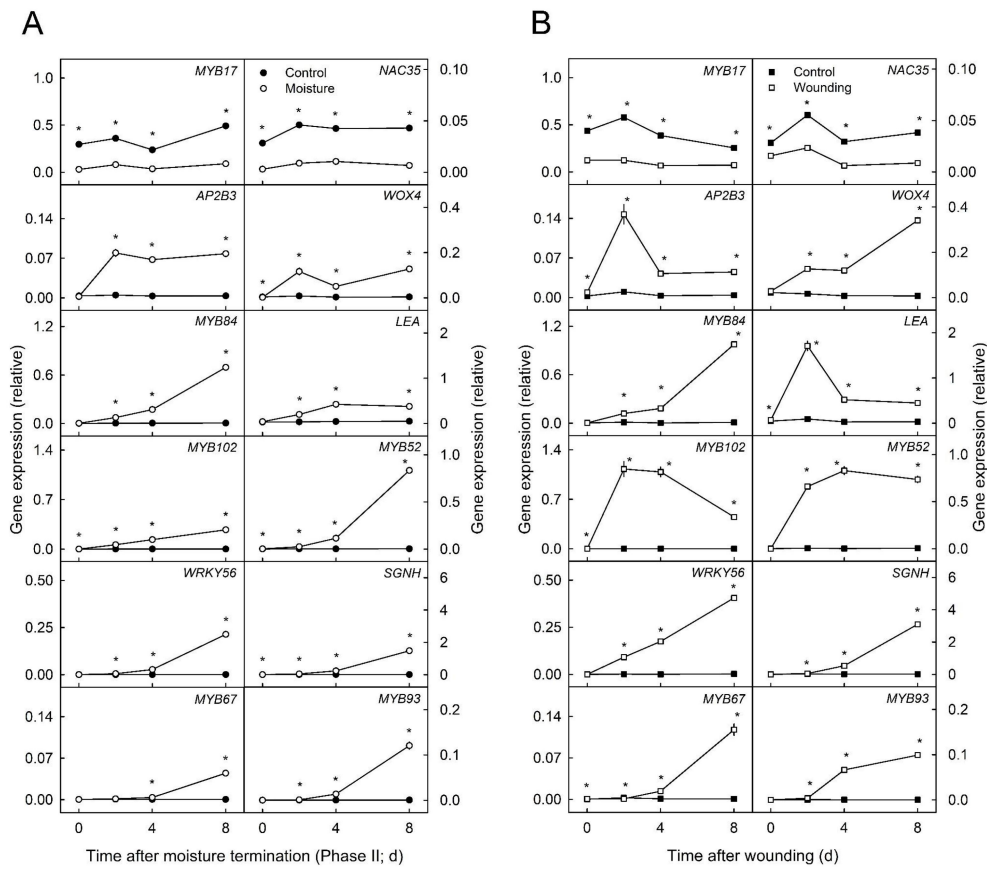


Fig. 7 Expression of putative candidate genes involved in russeting during moisture-induced (A) or wound-induced (B) russeting. Russeting in ‘Pinova’ apples was induced by surface moisture in a two-phase experiment: During Phase I, a patch of fruit skin was exposed to surface moisture for 12 d (Phase I, 12 d wet). After termination of moisture exposure (Phase II), the treated skin patch was exposed to the ambient atmosphere (y d dry). The nontreated control (‘Control’) remained dry during Phase I and Phase II (‘x d dry+y d dry’). Russeting was also induced by mechanical wounding using sandpaper (‘Wounding’). The nontreated fruit skin served as a control (‘Control’). The data revealed similar expression patterns between the two types of russet induction. Gene expression of candidate genes for the onset of periderm formation was determined at 0, 2, 4 and 8 d after moisture termination (A) or after wounding (B). Expression values represent the means \pm SEs of three independent biological replicates comprising six fruits each. ‘*’ indicates a significant difference between ‘Moisture’ and ‘Control’ or ‘Wounding’ and ‘Control’ at $p \leq 0.05$ (Student’s t test)

mature stage [24–26, 29–32]. Furthermore, the beginning of russet induction is precisely defined in moisture-induced russeting. In contrast, when assessing russeting at the mature stage, the time of the onset of russeting is unknown. This makes it impossible to establish causal relationships between potential trigger(s) of russeting. Third, our system of moisture-induced russeting allows us to compare the transcriptomes of the nonrusseted control and the russet-induced skin patch on an individual fruit basis. Thus, differential gene expression is

standardized for differences between cultivars, stages of fruit development and environmental factors to which the fruit is exposed in the tree canopy. This is not the case when susceptible and resistant cultivars are compared. In the latter case, differences between cultivars and the specific environment of the fruit cannot be separated from genetic differences in russet susceptibility. These arguments demonstrate that moisture-induced russeting offers a high degree of control. The system was successfully used previously [13, 14, 21, 43]. The data obtained

demonstrate that during Phase I within 48 h of moisture exposure, cuticle synthesis decreases, and microcracks are formed. The microcracks represent the first visible symptoms of russetting [10, 12, 15]. During the subsequent Phase II after moisture removal, microcracks are exposed to the ambient atmosphere, and the periderm begins to differentiate [13, 21, 43]. Stringent filtering of DEGs combined with high sequencing depth (59.8 to 75.1 million read pairs per biological replicate) allowed us to also identify lowly expressed genes such as transcription factors relevant to russetting. Furthermore, performing the experiment in different growing seasons allowed us to identify consistent changes between the two seasons. This comparison demonstrated a remarkable degree of overlap that was further confirmed by qPCR of selected genes in subsequent seasons. In addition, Phase II processes were consistently altered in the wounding treatments. Like exposure to surface moisture, the developmental stage of the wounding treatment is well defined, and the treatment is performed during the phase of maximum susceptibility to russetting. Based on these arguments, the induction of russetting by moisture exposure or wounding is a helpful tool in identifying triggers of russetting.

Genes differentially expressed in phase I

Phase I of russet induction was characterized by a large number of downregulated genes related to either cutin and wax synthesis (*SHN3* [37], *GPAT6* [55], *WSD1* [56], *ABCG11* [57], *LTP3* [30]), transcriptional regulation (*MYB17*, *NAC35*) or cell cycle and microtubule formation (*Tubulin/FTsZ family protein* (HF08104) and *ATP binding microtubule motor family protein* (HF30539)). These data are consistent between RNA-seq and qPCR. They also confirm the findings of earlier studies on cutin and wax deposition in relation to moisture-induced russetting [21, 43].

The downregulation of genes involved in cuticle formation is considered to be an early factor associated with microcracking during Phase I [23–26, 30]. We therefore compared the transcriptional dynamics of these genes to those of our new set of candidate genes in our RNA-Seq dataset (Figure S7). Cuticle-related genes decreased during Phase I after 6 d of moisture exposure ('6 d wet+0 d dry') in 2018 and after 12 d ('12 d wet+0 d dry') in both seasons (Figure S7). Several regulators in Cluster 1 (Fig. 4) were downregulated, including *homeobox 7*, *NAC35*, two *GRAS transcription factors*, *MYB17*, and *TF IIIA*. These were downregulated before the cuticle-related genes *SHN3*, *ABCG11*, *GPAT6*, *KCS10*, *WSD1* and *CER6* (Figure S7) were downregulated during Phase I.

The transcription factors *MYB17* and *NAC35* were the earliest genes downregulated after the beginning of the moisture treatments. The expression pattern of *MYB17*

correlated closely with that of *SHN3* [24, 38, 39]. However, the downregulation of *MYB17* occurred slightly earlier during Phase I as well as to a greater extent. *MYB17* is highly similar to *AtMYB16* and *AtMYB106*. The last two are involved in the regulation of epidermal cell growth and cuticle formation [58, 59]. A putative role of *MYB17* in cuticle formation is also consistent with the cultivar comparison of moisture-induced russetting (Fig. 6) and the experiment on wound-induced russetting (Figure S6). Here, the expression of *MYB17* was much lower in susceptible cultivars than in resistant cultivars. Wounding resulted in decreased expression of *MYB17*.

The second transcription factor, *NAC35*, was chosen because overexpression of *AtLOV1*, an ortholog of *NAC35* in *Arabidopsis thaliana*, changed epidermal cell organization and increased lignin content in cell walls when overexpressed in switchgrass [60]. The *MYB17* expression patterns of *NAC35* were consistent between the qPCR experiments and the RNA-Seq analysis.

The expression of *MYB17* and *NAC35* after moisture treatment was also confirmed in a fourth experiment in which russet induction by wounding and moisture was compared. In both treatments, *MYB17* and *NAC35* were downregulated. This downregulation is in line with that of other cuticle-specific genes, such as *SHN3*, *GPAT6*, *KCS10*, *WSD1*, *CER6* and *ABCG11*, described in earlier studies [43]. However, their differential regulation after mechanical wounding indicates that the downregulation is not related to microcracking typical of Phase I of russet induction but rather to the tissue damage that accompanies skin cracking.

Genes upregulated during Phase I were stress response genes such as *1-aminocyclopropane-1-carboxylic acid (acc) synthase 6* (HF20852), *peroxidase superfamily protein* (HF39739), and *heat shock protein 70* (HF0032) and genes related to oxidative stress, osmotic stress and salt stress. There were no upregulated genes that are involved in periderm formation.

Interestingly, the regulation of genes as indexed by the log₂FC in expression was larger in the 2019 than in the 2018 growing season. This was consistent with more severe russetting in 2019 than in 2018, probably as a result of seasonal differences in temperature and rainfall (Supplementary data, [13]) (Figure S2).

The mechanism of moisture-induced microcracking of the cuticle is probably related to failure of the hydrated cuticle when exposed to growth stress and strain. Cuticle hydration decreases the fracture force, which facilitates microcracking [61]. Additionally, the growth strain is particularly high during early fruit development, when the growth rate in surface area is high relative to the surface area present at that time (Figure S8). Importantly, the mechanical properties of the cuticle do not differ between russet-susceptible and nonsusceptible cultivars

[44]. In apple, the epidermis and hypodermal cell layers form the structural backbone of the fruit skin [62]. Russet-susceptible cultivars differ from nonsusceptible cultivars in that they have a higher variability of cell sizes in the epidermis and hypodermis [22]. Variable and larger cell sizes of the fruit skin cause stress concentration and failure when the skin is strained. During this process, the cuticle is dragged along and fails in response to the underlying cells [63]. Based on the above arguments, the change in mechanical properties of the cuticle and the decrease in cuticle deposition as a result of the down-regulation of genes involved in cuticle formation during a phase of high growth stress are causal in failure. Variable cell sizes predispose fruit skins to russetting.

Genes differentially regulated during phase II

Periderm formation occurs during Phase II. It requires the differentiation of a periderm in hypodermal cell layers underneath an epidermis with a microcracked cuticle. Periderm formation is a three-step process comprising (1) the formation of a meristem, the phellogen, that (2) then begins to divide to produce stacks of phellem cells. The final step in periderm formation (3) is the incrustation of the phellem cell walls with suberin and lignin. Earlier studies established that in moisture-induced russetting, this three-step process begins in Phase II only after removal of moisture when the treated skin patch is exposed to the ambient atmosphere [13, 21], irrespective of the duration of moisture exposure. Our findings are consistent with this conclusion.

Based on the above arguments, during the **early Phase II, differentially expressed genes should comprise genes characteristic of meristematic tissue**. This was indeed the case. Differentially expressed genes included various MYB, NAC, WRKY, and homeobox transcription factors, *WOX4*, *AP2/B3* and several LEAs, expansins, laccases and peroxidases (Figure S9, Data S6, S7). The expression of these genes increased immediately after moisture removal and exposure of the skin patch to the ambient atmosphere. Many of these genes are related to periderm formation (Figs. 4, [25, 30, 64–68]).

Recently published studies suggested that genes encoding proteins with acyltransferase or esterase/lipase activity, cell wall metabolism, pentacyclic triterpene synthesis, the phenylpropanoid pathway, suberin synthesis and transport of lipids are possible candidates in russetting [23, 25, 26, 30]. The cell wall-associated genes xyloglucan endotransglucosylases/hydrolases (XTH), expansins (EXP), peroxidases (PRX) and *laccase 7 (LAC7)* increased in moisture-exposed patches during the transition from Phase I to Phase II at '12 d wet+0 d dry'. Three acyltransferases associated with triterpene-hydroxycinnamates as well as several genes associated with esterases/lipases (GDSL), pentacyclic triterpene synthesis,

suberin synthesis, phenylpropanoid synthesis and lipid transport increased in gene expression at '12 d wet+3 d dry' or afterward (Figure S9). Transcriptional regulators found within Clusters 3 and 4 (Fig. 4) were upregulated earlier than most of the genes associated with phenylpropanoid or suberin synthesis (Figure S9), while genes found in Cluster 2 showed expression patterns similar to those of suberin-associated genes.

A total of four genes (*WOX4*, *AP2B3*, *LEA*, and *MYB84*) were validated by qPCR. The increase in expression was consistent between qPCR and RNA-Seq and occurred within 24 h (*WOX4*, *AP2B3*, *LEA*) and 48 h (*MYB84*) after exposure to the ambient atmosphere. Furthermore, the expression of all four genes was markedly higher in russet-susceptible cultivars than in nonsusceptible cultivars, implying a role in russetting.

The ortholog of *WOX4* in *Arabidopsis* [69–72] and poplar [73] is related to the formation of the vascular cambium. In moisture-induced russetting in apple, *WOX4* was among the earliest expressed genes in Phase II. In the 2019 and 2020 seasons (cultivar comparison), it was already expressed to some extent late in Phase I (Figs. 5 and 6). The upregulation, however, was restricted to cultivars of high susceptibility in Phase I (Fig. 6). In Phase II, *WOX4* was more regulated in susceptible than in resistant cultivars. Interestingly, *WOX4* was also expressed after mechanical wounding (Fig. 7, Figure S6). These arguments suggest that *WOX4* is a candidate gene for phellogen formation.

An ortholog of *AP2B3* in *Arabidopsis*, *AtNGAI*, regulates 9-cis-epoxycarotenoid dioxygenase 3 (*AtNCED3*), which is involved in ABA formation upon drought stress [74]. *AP2B3* was induced even earlier than *WOX4* (Fig. 5). The function of *AP2B3* is consistent with its expression during early Phase II. Moisture removal after Phase I increased water loss from the microcracked cuticle – the microcracks shunted the barrier properties of the cuticle [63]. The water loss, in turn, induced drought stress. In line with this, we found an ortholog of *NCED3* in apple (HF22773) that was differentially expressed in Phase II. *AP2B3* expression was also reported in russeted fruit at later developmental stages [25].

The early induction of LEA is consistent with the above arguments (Figs. 5 and 7). LEA proteins are known to be responsive to ABA and are enriched in response to abiotic stress, including drought [75]. The *LEA* gene in our study is an ortholog of *AtNHL26*, which is active within the phloem [76].

The DEG *MYB84* is an ortholog of *MYB1* of *Quercus suber*, where it is specific to phellem cells [66, 67]. Additionally, in *Arabidopsis* hypocotyls and roots, *MYB84/RAX3* are expressed in the periderm [65]. These arguments are consistent with a role of *MYB84* in the formation of the phellogen.

During the later Phase II of periderm formation, we expect differential expression of genes related to the incrustation of cell walls with suberin and lignin. This was confirmed in our experiment. The GO term analysis of the differentially expressed genes identified genes involved in suberin, phenylpropanoid and lignin metabolism and synthesis, genes involved in ABA metabolism and genes related to cell wall synthesis (Fig. 3). In addition, a number of transcription factors belonging to the MYB, WRKY and NAC families were found to be solely expressed during late Phase II (Fig. 4).

We selected six genes (*MYB93*, *MYB102*, *MYB52*, *WRKY56*, *SGNH*, and *MYB67*) with putative functions in suberin formation for further validation by qPCR. Again, the expression patterns obtained by qPCR and RNA-Seq were consistent. The increased expression of *MYB93* was consistent with that obtained in earlier studies [21, 43]. Its expression pattern perfectly mirrored the differential russet susceptibility in the cultivar comparison (Fig. 6). Additionally, the expression of *MYB93* after wounding further supported a role in russetting. In response to mechanical wounding, a periderm was induced after four days, which then began to divide to produce phellem [43]. The suberization of the cell wall is consistent with the expression of *MYB93*. *MYB93* has been reported to be involved in suberization of russet periderm [27]. *MYB93* was also reported to interact with other genes. When overexpressed in *N. benthamiana* leaves, *MYB93* induced the expression of *MYB52*, *MYB67*, *WRKY56* and *MYB84*, the last to a slightly lower extent.

Similar to *MYB93*, *MYB102* is another interesting candidate for periderm formation during late Phase II. The expression of its ortholog *AtMYB102* in *Arabidopsis* is directly induced by ABA. In *Arabidopsis thaliana*, ABA increased the suberization of roots [77]. Furthermore, *MYB102* responded to wounding [78], which is consistent with its role in the late phase of periderm formation.

Similarly, *AtGELP96*, an ortholog of *SGNH*, has key functions in the polymerization of suberin together with four other GELPs (*GELP22*, *GELP38*, *GELP49*, and *GELP51*) in *A. thaliana* roots [79]. This finding supports the putative functions of these genes in the accumulation of suberin in phellem cells after the phellogen has developed. Both the expression pattern and the annotations of *MYB52*, *MYB67*, *MYB102* and *WRKY56* indicated that these genes also contributed to the differentiation of the developing periderm during late Phase II rather than the development of the phellogen. *MYB52*, *MYB67*, *MYB102* and *WRKY56* were all induced at later stages of periderm formation. Their expression patterns were highly correlated with the extent of russetting in the cultivar comparison (Fig. 6).

Conclusion

The analysis of the transcriptome during periderm formation revealed a distinct pattern of gene expression. Based on the expression profiles and the supposed functions in heterologous plant systems, the following sequence of events results in periderm formation and, hence, russetting (Fig. 8). The downregulation of genes involved in cutin and wax synthesis and deposition and the simultaneous change in the mechanical properties of the cuticle due to hydration result in microcrack formation during moisture exposure. After moisture removal, the tissue underneath the microcracks comes into contact with the ambient atmosphere. A cascade of transcriptional regulatory events is now initiated. The increase in transpiration caused by the impaired barrier properties of the cuticle locally induces water stress as indexed by the expression of stress-related genes. At the same time, a yet unknown trigger induces the differentiation of the phellogen, as indexed by the expression of genes related to meristematic activity during early Phase II. The subsequent incrustation of the phellem with suberin and lignin (late Phase II) is consistent with the expression of genes involved in suberin and lignin synthesis and the regulation thereof. Notably, the differentially expressed genes identified in the transcriptomic analysis of the developmental time course during Phase II were also observed in the comparison of cultivars varying in russet susceptibility and the response to mechanical wounding.

This study provides transcriptomic resources for early events of artificially induced russetting in apple and further data on the comparison of mechanically induced versus moisture-induced russetting in terms of the expression of selected genes, which may help finally identify the molecular triggers of russet induction.

Materials and methods

Plant materials

Apple fruits (*Malus x domestica* Borkh.) of 'Karmijn', 'Pinova', 'Idared' and 'Gala', all grafted on M9 rootstocks, were cultivated in experimental orchards of the horticultural research station of the Leibniz University Hanover at Ruthe (52° 14' N, 9° 49' E). These cultivars differ in susceptibility to russetting in the order 'Karmijn' > 'Pinova' > 'Idared' > 'Gala' [44] (Figs. S3, S4).

A total of four experiments were conducted. First, the time course of change in the transcriptome was investigated in moisture-induced russetting in 'Pinova' using RNA-Seq and validated via qPCR. Samples were taken from a total of 125 trees. Second, gene expression in moisture-induced russetting was investigated in four cultivars differing in russet susceptibility using qPCR. The number of trees sampled was 30 per cultivar. Third, gene expression in wounding-induced russetting was investigated in four cultivars differing in russet susceptibility

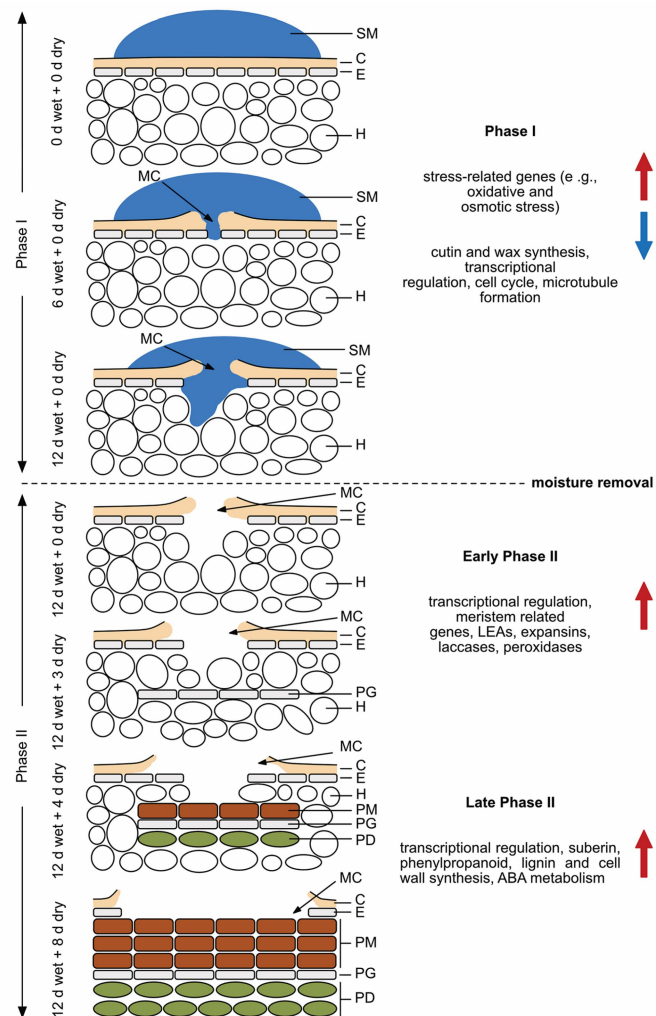


Fig. 8 Sketch of sequence of events in moisture-induced russeting of apple fruit skins. In Phase I, the skin patch is exposed to moisture for 12 d during early fruit development (21–31 days after full bloom (DAFB)). In Phase II, the moisture is removed and the fruit surface exposed to atmospheric conditions. In Phase I microcracks in the cuticle are detected as early as 2 d of moisture exposure. Over time, these microcracks expand tangentially and radially. They traverse the cuticle radially by day 6 of moisture exposure. As the fruit enters Phase II, meristem-related genes are activated indicating the formation of a phellogen in the hypodermis underneath a microcrack (0–3 d after moisture removal). During the late stage of Phase II (starting 3–4 d after moisture removal), the phellogen differentiates a phelloderm and produces suberized phellem cells. By 8 d after moisture exposure, a continuous periderm has developed. Gene groups that are up-regulated during each phase (Phase I, early Phase II, and late Phase II) are marked by a red arrow on the right side of the panel. Conversely, gene groups that are down-regulated during these phases are indicated by a blue arrow. SM= surface moisture, C= cuticle, E= epidermis, H= hypodermis, MC= microcrack, PG= phellogen, PM= phellem, PD= phelloderm.

using qPCR. The number of trees sampled was 20 per cultivar. Fourth, gene expression was compared between moisture- and wounding-induced russeting in 'Pinova' using qPCR. Here, the number of trees was 125. Experiments were performed in four different growing seasons (Table S3, Figure S10).

Russet induction

Russeting was induced either by moisture exposure or by mechanical wounding [13, 14, 21, 43]. For moisture exposure, two-phase experiments were conducted (Figure S11). Apple fruits 10–12 mm in diameter (21–32 DAFB) were selected (Table S3, [13, 14, 21, 43]). The tip of a 2.0 ml polyethylene tube (Eppendorf, Hamburg, Germany) was mounted in the equatorial plain of the apple fruit using nontoxic silicone rubber (Silicone RTV; Dow Toray, Japan). After curing (approximately 1 h), the tubes were filled with 1 ml deionized water for moisture exposure (Phase I) through a hole in the tip. The hole was then sealed, and the tube was checked for leakage on a daily basis. The opposite side of the fruit served as a control and remained dry [13, 14, 21]. The fruit skin was exposed to moisture ('Moisture') for 12 d ('12 d wet+0 dry'; ('Phase I+Phase II')) during Phase I. For termination of moisture exposure, the tube was removed, and the treated skin patch was exposed to the atmosphere (Phase II). At this point, the treatments were terminated. During the subsequent Phase II, changes in the treated fruit skin patches were observed for up to 136 d ('12 d wet+136 d dry') after termination of the moisture treatment (Phase II).

For wounding-induced periderms, the fruit skin was gently abraded in the equatorial plane using sandpaper (grit size 1000; Bauhaus, Mannheim, Germany) ('Wounding'). The opposite surface of the same fruit served as the control. Wounding was performed at 38–40 DAFB (Table S3). This time point corresponded to the time of moisture termination in the moisture-induced russeting experiment.

RNA extraction and quality assessment

Patches of treated, i.e., moisture-exposed or wounded, or nontreated, i.e., control, skins were excised using a razorblade, immediately frozen in liquid N₂ and held at -80 °C until further analysis. Each replicate comprised skin patches of a minimum of six fruits (approximately 60–80 mg). The tissue was ground in liquid N₂ to a fine powder using a mortar and pestle. Total RNA was extracted using the InviTrap Spin Plant RNA Mini Kit (STRATEC Molecular GmbH, Berlin, Germany) and lysis buffer RP according to the manufacturer's protocol. Total RNA was treated with DNase using the DNA-free™ Kit (Thermo Fisher Scientific, Waltham, Massachusetts, USA) to remove remaining DNA. The quantity and

purity of RNA were determined photometrically at 230, 260 and 280 nm on a Nanodrop 2000c spectrophotometer (Thermo Fisher Scientific, Waltham, Massachusetts, USA). The integrity and purity of the RNA were checked on a 1.5% agarose gel. Before RNA-Seq, the RNA integrity number (RIN) was determined using the Agilent RNA 6000 Nano Kit on a Bioanalyzer 2100 and the Plant RNA Nano parameters (Agilent Technologies, Santa Clara, CA, USA). The RIN ranged from 8.4 to 10.0 (Table S1).

RNA-Seq library preparation and sequencing

For each replicate, 1 µg of total RNA was sequenced (Novogene, Cambridge, UK). The library was prepared with the NEBNext® Ultra™ RNA Library Prep Kit (Ipswich, Massachusetts, USA) according to the manufacturer's instructions. For sequencing, 2×150 bp *paired-end* cDNA libraries were prepared. Sequencing was performed on an Illumina® NovaSeq™ 6000. A minimum of 59.8 million read pairs were generated for each sample (Table S1).

Mapping and counting of reads

Reads obtained from Illumina sequencing were trimmed and filtered with Trimmomatic (v0.39) [80] with the following parameters: TRAILING: 20 AVQUAL: 20 SLIDINGWINDOW: 5:20 MINLEN: 75. The quality of trimmed reads was checked by FastQC (v0.11.9) [81]. Afterward, reads were aligned to the *Malus x domestica* *HFTH1* v1.0 genome using STAR (v2.5.4b) followed by read count quantification with the "--quantMode Gene Counts" function [82, 83]. Annotations of transcripts were obtained by blastp against the *Arabidopsis thaliana* genome (TAIR10, www.arabidopsis.org, 31.01.2023) as described by Zhang and coworkers [83].

Differential gene expression and enrichment analysis

Differential gene expression analysis was conducted with DESeq2 (v1.32.0) [84]. Genes with a $\log_2FC \geq 2$, ≤ -2 ('Moisture' vs. 'Control') and a false discovery rate (FDR) ≤ 0.05 were considered to be differentially expressed and used for downstream analysis. Gene abundance was obtained through transcripts per million (TPM) calculation with StringTie (v2.1.3) [85]. Singular enrichment analysis (SEA) was performed with DEGs having a mean of at least five TPM for 'Moisture' or 'Control' samples. Orthologous genes from *Arabidopsis thaliana* were investigated using the webtool AgriGO (v2.0) and the parameters selected species: *Arabidopsis thaliana*; reference: TAIR genome locus (TAIR10_2017), user defined; statistical test method: hypergeometric; multiple adjustment method: Hochberg (FDR); significance level: 0.01; and minimum number of mapping entries:

5 [86]. Heatmaps of differentially expressed genes were generated with the R package ‘pheatmap’ (1.0.12) [87].

Quantitative real-time PCR

Quantitative real-time PCR (qPCR) was conducted on a QuantStudio™ 6 Flex Real-Time PCR System (Applied Biosystems, Waltham, MA, USA). Primer design, cDNA synthesis, primer efficiency testing and qPCR were performed as described earlier [21] (Table S5). Gene expression values were determined according to Pfaffl [88] with slight modifications described by Chen and coworkers [89]. Gene expression data were normalized using *PROTEIN DISULFIDE ISOMERASE* (PDI) (MDP0000233444) [90] and *MdeF-1alpha* (AJ223969.1) [26] as reference genes. Each data point comprised three independent replicates of two to three technical replicates each.

List of abbreviations

ABA	Abscisic acid
AP2B3	<i>AP2/B3-like transcription factor family protein</i>
AtNCED3	9-cis-epoxycarotenoid dioxygenase 3
C	Cuticle
DAFB	Days after full bloom
DEGs	Differentially expressed genes
E	Epidermis
EXP	Expansins
FDR	False discovery rate
GDSL	Esterases/lipases
GO	Gene ontology
H	Hypodermis
LAC7	Laccase 7
LEA	<i>Late embryogenesis abundant hydroxyproline-rich glycoprotein</i>
log ₂ FC	Log ₂ -fold change
MC	Microcrack
MYB102	<i>MYB-like 102</i>
PCA	Principal component analysis
PD	Phelloderm
PDI	<i>Protein disulfide isomerase</i>
PG	Phellogen
PM	Phellem
PRX	Peroxidases
qPCR	Quantitative real-time PCR
QTLs	Quantitative trait loci
SEA	Singular enrichment analysis
SGNH	<i>SGNH hydrolase</i>
SM	Surface moisture
TPM	Transcripts per million
>WOX4	<i>Wuschel-related homeobox 4</i>
XTH	Xyloglucan endotransglucosylases/hydrolases

Supplementary Information

The online version contains supplementary material available at <https://doi.org/10.1186/s12870-023-04483-6>.

Supplementary Material 1
Supplementary Material 2
Supplementary Material 3
Supplementary Material 4
Supplementary Material 5
Supplementary Material 6
Supplementary Material 7

Supplementary Material 8
Supplementary Material 9
Supplementary Material 10
Supplementary Material 11
Supplementary Material 12
Supplementary Material 13
Supplementary Material 14
Supplementary Material 15
Supplementary Material 16
Supplementary Material 17
Supplementary Material 18
Supplementary Material 19
Supplementary Material 20
Supplementary Material 21
Supplementary Material 22
Supplementary Material 23
Supplementary Material 24

Acknowledgements

We are very grateful for advice and support from Diana Carolina Lopez Aria in the analysis of the RNA-Seq data as well as for the technical support from Julia Schröter and Simon Sitzenstock. We also thank Henryk Straube for helpful comments on an earlier version of the manuscript.

Author contributions

Conceptualization, J.S., B.P.K., M.K. and T.D.; funding acquisition, M.K. and T.D.; project administration, M.K. and T.D.; methodology, J.S., B.P.K., M.K. and T.D.; investigation, J.S., S.S., Y.C. and B.P.K.; supervision, B.P.K., M.K. and T.D.; data curation, J.S.; validation, J.S.; visualization, J.S.; formal analysis, J.S.; writing—original draft, J.S. and T.D.; writing—review and editing, J.S., B.P.K., M.K. and T.D. All authors have read and agreed to the published version of the manuscript.

Funding

Open Access funding enabled and organized by Projekt DEAL. This research was funded by the following grants from the German Science Foundation (DFG): DE 511/9–1; DE 511/9–2 (T.D.) and KN402/15–1; KN402/15–2 (M.K.).

Data Availability

The datasets supporting the conclusions of this article are included within the article and its additional files. Raw Illumina sequencing data are available at the NCBI Sequence Read Archive (SRA) under the BioProject number PRJNA935373.

Declarations

Ethics approval and consent to participate

We declare that the experimental research and field study conducted on *Malus x domestica* Borkh. plants in this manuscript, comply with all relevant institutional, and international guidelines and legislation.

Consent for publication

Not applicable.

Competing interests

The authors declare no competing interests.

Links for review

SRA BioProject (publicly available upon publication): <https://dataview.ncbi.nlm.nih.gov/object/PRJNA935373?reviewer=efbmo3ejavqu9s1aeom137tpni>.

Data access for review:

<https://my.hidrive.com/share/wymikjrtwa>. Password: Russetting.

Received: 5 May 2023 / Accepted: 22 September 2023

Published online: 30 September 2023

References

1. Skene DS. The development of russet, rough russet and cracks on the fruit of the apple Cox's Orange Pippin during the course of the season. *J Horticult Sci*. 1982;57:165–74. <https://doi.org/10.1080/00221589.1982.11515037>.
2. Athoo TO, Winkler A, Knoche M. Russetting in 'Apple' mango: triggers and mechanisms. *Plants*. 2020;9(7):898. <https://doi.org/10.3390/plants9070898>.
3. Goffinet MC, Pearson RC. Anatomy of russetting induced in Concord grape berries by the fungicide chlorothalonil. *Am J Enol Vitic*. 1991;42:281–9.
4. Michailides TJ. Russetting and russet scab of prune, an environmentally induced fruit disorder: Symptomatology, induction, and control. *Plant Dis*. 1991;75:1114–23.
5. Scharniew JD, Grimm E, Knoche M. Russetting and relative growth rate are positively related in 'Conference' and 'Condo' pear. *HortScience*. 2014;49:746–9.
6. Lara I, Belge B, Goulou LF. The fruit cuticle as a modulator of postharvest quality. *Postharvest Biol Technol*. 2014;87:103–12. <https://doi.org/10.1016/j.postharvbio.2013.08.012>.
7. Lara I, Heredia A, Dominguez E. Shelf life potential and the fruit cuticle: the unexpected player. *Front Plant Sci*. 2019;10:770. <https://doi.org/10.3389/fpls.2019.00770>.
8. Khanal BP, Ikigu GM, Knoche M. Russetting partially restores apple skin permeability to water vapour. *Planta*. 2019;249:849–60. <https://doi.org/10.1007/s00425-018-3044-1>.
9. Bell HP. The origin of russetting in Golden Russet apple. *Can J Res*. 1937;15:560–6.
10. Meyer A. A study of the skin structure of Golden Delicious apples. *Proc Am Soc Horticult Sci*. 1944;45:105–10.
11. Pratt C. Periderm development and radiation stability of russet-fruited sports of apple. *Hortic Res*. 1972;12:5–12.
12. Faust M, Shear CB. Russetting of apples, an interpretive review. *HortScience*. 1972;7:233–5.
13. Chen Y-H, Straube J, Khanal BP, Knoche M, Debener T. Russetting in apple is initiated after exposure to moisture ends-I. histological evidence. *Plants*. 2020. <https://doi.org/10.3390/plants9101293>.
14. Khanal BP, Imoro Y, Chen YH, Straube J, Knoche M. Surface moisture increases microcracking and water vapour permeance of apple fruit skin. *Plant Biol*. 2020;23:74–82. <https://doi.org/10.1111/plb.13178>.
15. Faust M, Shear CB. Fine structure of the fruit surface of three apple cultivars. *J Amer Soc Hort Sci*. 1972;97:351–5. <https://doi.org/10.21273/JASHS.97.3.351>.
16. Khanal BP, Knoche M, Bußler S, Schlüter O. Evidence for a radial strain gradient in apple fruit cuticles. *Planta*. 2014;240:891–7. <https://doi.org/10.1007/s00425-014-2132-0>.
17. Lai X, Khanal BP, Knoche M. Mismatch between cuticle deposition and area expansion in fruit skins allows potentially catastrophic buildup of elastic strain. *Planta*. 2016;244:1145–56. <https://doi.org/10.1007/s00425-016-2572-9>.
18. Tukey LD. Observations on the russetting of apples growing in plastic bags. *Proc Am Soc Horticult Sci*. 1959;74:30–9.
19. Knoche M, Grimm E. Surface moisture induces microcracks in the cuticle of 'Golden Delicious' apple. *HortScience*. 2008;43:1929–31. <https://doi.org/10.21273/HORTSCI.43.6.1929>.
20. Winkler A, Grimm E, Knoche M, Lindstaedt J, Köpcke D. Late-season surface water induces skin spot in apple. *HortScience*. 2014;49:1324–7. <https://doi.org/10.21273/HORTSCI.49.10.1324>.
21. Straube J, Chen Y-H, Khanal BP, Shumbusho A, Zeisler-Diehl V, Suresh K, et al. Russetting in apple is initiated after exposure to moisture ends: Molecular and biochemical evidence. *Plants*. 2020. <https://doi.org/10.3390/plants10010065>.
22. Khanal BP, Le TL, Si Y, Knoche M. Russet susceptibility in apple is associated with skin cells that are larger, more variable in size, and of reduced fracture strain. *Plants*. 2020. <https://doi.org/10.3390/plants9091118>.
23. Falginella L, Cipriani G, Monte C, Gregori R, Testolin R, Velasco R, et al. A major QTL controlling apple skin russetting maps on the linkage group 12 of 'Renetta Grigia di Toriana'. *BMC Plant Biol*. 2015;15:150. <https://doi.org/10.1186/s12870-015-0507-4>.
24. Lashbrooke J, Aharoni A, Costa F. Genome investigation suggests *MdSHN3*, an APETALA2-domain transcription factor gene, to be a positive regulator of apple fruit cuticle formation and an inhibitor of russet development. *J Exp Bot*. 2015;66:6579–89. <https://doi.org/10.1093/jxb/erv366>.
25. Falginella L, Andre CM, Legay S, Lin-Wang K, Dare AP, Deng C, et al. Differential regulation of triterpene biosynthesis induced by an early failure in cuticle formation in apple. *Hortic Res*. 2021;8:75. <https://doi.org/10.1038/s41438-021-00511-4>.
26. Legay S, Guerriero G, Deleruelle A, Lateur M, Evers D, André CM, Hausman J-F. Apple russetting as seen through the RNA-seq lens: strong alterations in the exocarp cell wall. *Plant Mol Biol*. 2015;88:21–40. <https://doi.org/10.1007/s11103-015-0303-4>.
27. Legay S, Guerriero G, André C, Guignard C, Cocco E, Charton S, et al. MdMyb93 is a regulator of suberin deposition in russeted apple fruit skins. *New Phytol*. 2016;212:977–91. <https://doi.org/10.1111/nph.14170>.
28. Xu X, Guerriero G, Berni R, Sergeant K, Guignard C, Lenouvel A, et al. MdMYB52 regulates lignin biosynthesis upon the suberization process in apple. *Front Plant Sci*. 2022. <https://doi.org/10.3389/fpls.2022.1039014>.
29. Lashbrooke J, Cohen H, Levy-Samocho D, Tzfadia O, Panizel I, Zeisler V, et al. MYB107 and MYB9 homologs regulate suberin deposition in Angiosperms. *Plant Cell*. 2016;28:2097–116. <https://doi.org/10.1105/tpc.16.00490>.
30. André CM, Guerriero G, Lateur M, Charton S, Leclercq CC, Renaut J, et al. Identification of novel candidate genes involved in apple cuticle integrity and russetting-associated triterpene synthesis using metabolomic, proteomic, and transcriptomic data. *Plants*. 2022. <https://doi.org/10.3390/plants11030289>.
31. Yuan G, Bian S, Han X, He S, Liu K, Zhang C, Cong P. An integrated transcriptome and proteome analysis reveals new insights into russetting of bagging and non-bagging Golden Delicious apple. *Int J Mol Sci*. 2019. <https://doi.org/10.3390/ijms20184462>.
32. Wang Z, Liu S, Huo W, Chen M, Zhang Y, Jiang S. Transcriptome and metabolome analyses reveal phenotype formation differences between russet and non-russet apples. *Front Plant Sci*. 2022. <https://doi.org/10.3389/fpls.2022.1057226>.
33. Taylor BK. Reduction of apple skin russetting by gibberellin. *J Horticult Sci*. 1975;50:169–72. <https://doi.org/10.1080/00221589.1975.11514619>.
34. Taylor BK. Effects of gibberellin sprays on fruit russet and tree performance of Golden Delicious apple. *J Horticult Sci*. 1978;53:167–9. <https://doi.org/10.1080/00221589.1978.11514814>.
35. Wertheim SJ. Fruit russetting in apple as affected by various gibberellins. *J Horticult Sci*. 1982;57:283–8. <https://doi.org/10.1080/00221589.1982.11515054>.
36. Simons RK, Chu MC. Periderm morphology of mature 'Golden Delicious' apple with special reference to russetting. *Sci Hort*. 1978;8:333–40. [https://doi.org/10.1016/0304-4238\(78\)90055-9](https://doi.org/10.1016/0304-4238(78)90055-9).
37. Aharoni A, Dixit S, Jetter R, Thoenes E, van Arkel G, Pereira A. The SHINE clade of AP2 domain transcription factors activates wax biosynthesis, alters cuticle properties, and confers drought tolerance when overexpressed in *Arabidopsis*. *Plant Cell*. 2004;16:2463–80. <https://doi.org/10.1105/tpc.104.022897>.
38. Shi JX, Malitsky S, de Oliveira S, Branigan C, Franke RB, Schreiber L, Aharoni A. SHINE transcription factors act redundantly to pattern the archetypal surface of *Arabidopsis* flower organs. *PLoS Genet*. 2011;7:e1001388. <https://doi.org/10.1371/journal.pgen.1001388>.
39. Shi JX, Adato A, Alkan N, He Y, Lashbrooke J, Matas AJ, et al. The tomato SISHINE3 transcription factor regulates fruit cuticle formation and epidermal patterning. *New Phytol*. 2013;197:468–80. <https://doi.org/10.1111/nph.12032>.
40. Lee SB, Suh MC. Cuticular wax biosynthesis is up-regulated by the MYB94 transcription factor in *Arabidopsis*. *Plant Cell Physiol*. 2015;56:48–60. <https://doi.org/10.1093/pcp/pcu142>.
41. Lee SB, Kim HU, Suh MC. MYB94 and MYB96 additively activate cuticular wax biosynthesis in *Arabidopsis*. *Plant Cell Physiol*. 2016;57:2300–11. <https://doi.org/10.1093/pcp/pcw147>.
42. Liberman LM, Sparks EE, Moreno-Risueno MA, Petricka JJ, Benfey PN. MYB36 regulates the transition from proliferation to differentiation in the *Arabidopsis* root. *Proc Natl Acad Sci U S A*. 2015;112:12099–104. <https://doi.org/10.1073/pnas.1515576112>.
43. Chen Y-H, Straube J, Khanal BP, Zeisler-Diehl V, Suresh K, Schreiber L, et al. Apple fruit periderms (russetting) induced by wounding or by moisture have the same histologies, chemistries and gene expressions. *PLoS ONE*. 2022;17:e0274733. <https://doi.org/10.1371/journal.pone.0274733>.
44. Khanal BP, Shrestha R, Hückstädt L, Knoche M. Russetting in apple seems unrelated to the mechanical properties of the cuticle at maturity. *HortScience*. 2013;48:1135–8. <https://doi.org/10.21273/HORTSCI.48.9.1135>.

45. Daines R. Effect of early sprays on control of powdery mildew fruit russet on apples. *Plant Dis.* 1984;68:326. <https://doi.org/10.1094/PD-69-326>.
46. Heidenreich MCM, Corral-García MR, Momol EA, Burr TJ. Russet of apple fruit caused by *Aureobasidium pullulans* and *Rhodotorula glutinis*. *Plant Dis.* 1997;81:337–42. <https://doi.org/10.1094/PDIS.1997.81.4.337>.
47. Gildemacher P, Heijne B, Silvestri M, Houbraeken J, Hoekstra E, Theelen B, Boekhout T. Interactions between yeasts, fungicides and apple fruit russetting. *FEMS Yeast Res.* 2006;6:1149–56. <https://doi.org/10.1111/j.1567-1364.2006.00109.x>.
48. Gildemacher PR, Heijne B, Houbraeken J, Vromans T, Hoekstra ES, Boekhout T. Can phyllosphere yeasts explain the effect of scab fungicides on russetting of Elstar apples? *Eur. J Plant Pathol.* 2004;110:929–37. <https://doi.org/10.1007/s10658-004-8948-x>.
49. Li C, Yaegashi H, Kishigami R, Kawakubo A, Yamagishi N, Ito T, Yoshikawa N. Apple russet ring and apple green crinkle diseases: fulfillment of Koch's postulates by virome analysis, amplification of full-length cDNA of viral genomes, *in vitro* transcription of infectious viral RNAs, and reproduction of symptoms on fruits of apple trees inoculated with viral RNAs. *Front Microbiol.* 2020;11:1627. <https://doi.org/10.3389/fmicb.2020.01627>.
50. Wood GA. Russet ring and some associated viral disorders of apple (*Malus sylvestris* (L.) Mill.) in New Zealand. *New Z J Agric Res.* 1972;15:405–12. <https://doi.org/10.1080/00288233.1972.10421269>.
51. Welsh MF, May J. Virus etiology of foliar vein-flecking or ring pattern and fruit russetting or blotch on apple. *Can J Plant Sci.* 1967;47:703–8.
52. Easterbrook MA, Fuller MM. Russetting of apples caused by apple rust mite *Aculus schlechtendali* (Acarina: Eriophyidae). *Ann Appl Biol.* 1986;109:1–9. <https://doi.org/10.1111/j.1744-7348.1986.tb03178.x>.
53. Winkler A, Athoo T, Knoche M. Russetting of fruits: etiology and management. *Horticulturae.* 2022;8:231. <https://doi.org/10.3390/horticulturae8030231>.
54. Creasy LL. The correlation of weather parameters with russet of Golden Delicious apples under orchard conditions. *J Amer Soc Hort Sci.* 1980;5:735–8.
55. Petit J, Bres C, Mauxion JP, Tai F, Martin LB, Fich EA et al. The glycerol-3-phosphate acyltransferase GPAT6 from tomato plays a central role in fruit cutin biosynthesis. *Plant Physiol.* 2016;894–913.
56. Li Y, Beisson F, Koo AJK, Molina I, Pollard M, Ohlrogge J. Identification of acyltransferases required for cutin biosynthesis and production of cutin with suberin-like monomers. *Proc Natl Acad Sci U S A.* 2007;104:18339–44. <https://doi.org/10.1073/pnas.0706984104>.
57. Bird D, Beisson F, Brigham A, Shin J, Greer S, Jetter R, et al. Characterization of Arabidopsis ABCG11/WBC11, an ATP binding cassette (ABC) transporter that is required for cuticular lipid secretion. *Plant J.* 2007;48:5–98. <https://doi.org/10.1111/j.1365-3113.2007.03252.x>.
58. Jakoby MJ, Falkenhan D, Mader MT, Brininstool G, Wischnitzki E, Platz N, et al. Transcriptional profiling of mature Arabidopsis trichomes reveals that *NOECK* encodes the MIXTA-like transcriptional regulator MYB106. *Plant Physiol.* 2008;148:1583–602. <https://doi.org/10.1104/pp.108.126979>.
59. Oshima Y, Mitsuda N. The MIXTA-like transcription factor MYB16 is a major regulator of cuticle formation in vegetative organs. *Plant Signal Behav.* 2013;8:e26826. <https://doi.org/10.4161/psb.26826>.
60. Xu B, Sathitsuksanoh N, Tang Y, Udvardi MK, Zhang J-Y, Shen Z, et al. Overexpression of *AtLOV1* in Switchgrass alters plant architecture, lignin content, and flowering time. *PLoS ONE.* 2012;7:e47399. <https://doi.org/10.1371/journal.pone.0047399>.
61. Khanal BP, Knoche M. Mechanical properties of cuticles and their primary determinants. *J Exp Bot.* 2017;68:5351–67. <https://doi.org/10.1093/jxb/erx265>.
62. Khanal BP, Knoche M. Mechanical properties of apple skin are determined by epidermis and hypodermis. *J Amer Soc Hort Sci.* 2014;139:139–47. <https://doi.org/10.21273/JASHS.139.2.139>.
63. Knoche M, Khanal BP, Brüggewirth M, Thapa S. Patterns of microcracking in apple fruit skin reflect those of the cuticular ridges and of the epidermal cell walls. *Planta.* 2018;248:293–306. <https://doi.org/10.1007/s00425-018-2904-z>.
64. Xiao W, Molina D, Wunderling A, Ripper D, Vermeer JEM, Ragni L. Pluripotent pericycle cells trigger different growth outputs by integrating developmental cues into distinct regulatory modules. *Curr Biol.* 2020;30:4384–4398.e5. <https://doi.org/10.1016/j.cub.2020.08.053>.
65. Wunderling A, Ripper D, Barra-Jimenez A, Mahn S, Sajak K, Targem MB, Ragni L. A molecular framework to study periderm formation in Arabidopsis. *New Phytol.* 2018;219:216–29. <https://doi.org/10.1111/nph.15128>.
66. Almeida T, Pinto G, Correia B, Santos C, Gonçalves S. *QsMYB1* expression is modulated in response to heat and drought stresses and during plant recovery in *Quercus suber*. *Plant Physiol Biochem.* 2013;73:274–81. <https://doi.org/10.1016/j.plaphy.2013.10.007>.
67. Almeida T, Menéndez E, Capote T, Ribeiro T, Santos C, Gonçalves S. Molecular characterization of *Quercus suber MYB1*, a transcription factor up-regulated in cork tissues. *J Plant Physiol.* 2013;170:172–8. <https://doi.org/10.1016/j.jplph.2012.08.023>.
68. Leal AR, Barros PM, Parizot B, Sapeta H, Vangheluwe N, Andersen TG, et al. Translational profile of developing phellem cells in *Arabidopsis thaliana* roots. *Plant J.* 2022;110:899–915. <https://doi.org/10.1111/tpj.15691>.
69. Ji J, Strable J, Shimizu R, Koenig D, Sinha N, Scanlon MJ. *WOX4* promotes procambial development. *Plant Physiol.* 2010;152:1346–56. <https://doi.org/10.1104/pp.109.149641>.
70. Hirakawa Y, Kondo Y, Fukuda H. TDIF peptide signaling regulates vascular stem cell proliferation via the *WOX4* homeobox gene in Arabidopsis. *Plant Cell.* 2010;22:2618–29. <https://doi.org/10.1105/tpc.110.076083>.
71. Etchells JP, Provost CM, Mishra L, Turner SR. *WOX4* and *WOX14* act downstream of the PXY receptor kinase to regulate plant vascular proliferation independently of any role in vascular organization. *Development.* 2013;140:2224–34. <https://doi.org/10.1242/dev.091314>.
72. Zhang J, Eswaran G, Alonso-Serra J, Kucukoglu M, Xiang J, Yang W, et al. Transcriptional regulatory framework for vascular cambium development in Arabidopsis roots. *Nat Plants.* 2019;5:1033–42. <https://doi.org/10.1038/s41477-019-0522-9>.
73. Kucukoglu M, Nilsson J, Zheng B, Chaabouni S, Nilsson O. *WUSCHEL-RELATED HOMEOBOX4 (WOX4)*-like genes regulate cambial cell division activity and secondary growth in Populus trees. *New Phytol.* 2017;215:642–57. <https://doi.org/10.1111/nph.14631>.
74. Sato H, Takasaki H, Takahashi F, Suzuki T, Luchi S, Mitsuda N, et al. Arabidopsis thaliana *NGATHA1* transcription factor induces ABA biosynthesis by activating *NCED3* gene during dehydration stress. *Proc Natl Acad Sci U S A.* 2018;115:E1178–87. <https://doi.org/10.1073/pnas.1811491115>.
75. Battaglia M, Olvera-Carrillo Y, Garcarrubio A, Campos F, Covarrubias AA. The enigmatic LEA proteins and other hydrophilins. *Plant Physiol.* 2008;148:6–24. <https://doi.org/10.1104/pp.108.120725>.
76. Vilaine F, Kerchev P, Clément G, Batailler B, Cayla T, Bill L, et al. Increased expression of a phloem membrane protein encoded by *NHL26* alters phloem export and sugar partitioning in Arabidopsis. *Plant Cell.* 2013;25:1689–708. <https://doi.org/10.1105/tpc.113.111849>.
77. Barberon M, Vermeer JEM, de Bellis D, Wang P, Naseer S, Andersen TG, et al. Adaptation of root function by nutrient-induced plasticity of endodermal differentiation. *Cell.* 2016;164:447–59. <https://doi.org/10.1016/j.cell.2015.12.021>.
78. Denekamp M, Smeekens SC. Integration of wounding and osmotic stress signals determines the expression of the *AtMYB102* transcription factor gene. *Plant Physiol.* 2003;132:1415–23. <https://doi.org/10.1104/pp.102.019273>.
79. Ursache R, de Jesus Vieira Teixeira C, Déneraud Tendon V, Gully K, de Bellis D, Schmid-Siegert E, et al. GDSL-domain proteins have key roles in suberin polymerization and degradation. *Nat Plants.* 2021;7:353–64. <https://doi.org/10.1038/s41477-021-00862-9>.
80. Bolger AM, Lohse M, Usadel B. Trimmomatic: a flexible trimmer for Illumina sequence data. *Bioinformatics.* 2014;30:2114–20. <https://doi.org/10.1093/bioinformatics/btu170>.
81. Andrews S, FastQC: A Quality Control Tool for High Throughput Sequence Data; 2010.
82. Dobin A, Davis CA, Schlesinger F, Drenkow J, Zaleski C, Jha S, et al. STAR: ultrafast universal RNA-seq aligner. *Bioinformatics.* 2013;29:15–21. <https://doi.org/10.1093/bioinformatics/bts635>.
83. Zhang L, Hu J, Han X, Li J, Gao Y, Richards CM, et al. A high-quality apple genome assembly reveals the association of a retrotransposon and red fruit colour. *Nat Commun.* 2019;10:1494. <https://doi.org/10.1038/s41467-019-09518-x>.
84. Love MI, Huber W, Anders S. Moderated estimation of fold change and dispersion for RNA-seq data with DESeq2. *Genome Biol.* 2014;15:550. <https://doi.org/10.1186/s13059-014-0550-8>.
85. Perteau M, Perteau GM, Antonescu CM, Chang T-C, Mendell JT, Salzberg SL. StringTie enables improved reconstruction of a transcriptome from RNA-seq reads. *Nat Biotechnol.* 2015;33:290–5. <https://doi.org/10.1038/nbt.3122>.
86. Tian T, Liu Y, Yan H, You Q, Yi X, Du Z, et al. agrigo v2.0: a GO analysis toolkit for the agricultural community, 2017 update. *Nucleic Acids Res.* 2017;45:W122–9. <https://doi.org/10.1093/nar/gkx382>.
87. Kolde R. Pheatmap: pretty heatmap; 2019.
88. Pfaffl MW. A new mathematical model for relative quantification in real-time RT-PCR. *Nucleic Acids Res.* 2001;29:E45.

89. Chen Y-H, Khanal BP, Linde M, Debener T, Alkio M, Knoche M. Expression of putative aquaporin genes in sweet cherry is higher in flesh than skin and most are downregulated during development. *Sci Hortic*. 2019;244:304–14. <https://doi.org/10.1016/j.scienta.2018.09.065>.
90. Storch TT, Pegoraro C, Finatto T, Quecini V, Rombaldi CV, Girardi CL. Identification of a novel reference gene for apple transcriptional profiling under post-harvest conditions. *PLoS ONE*. 2015;10:e0120599. <https://doi.org/10.1371/journal.pone.0120599>.

Publisher's Note

Springer Nature remains neutral with regard to jurisdictional claims in published maps and institutional affiliations.

6.1 Supplementary data Chapter 6

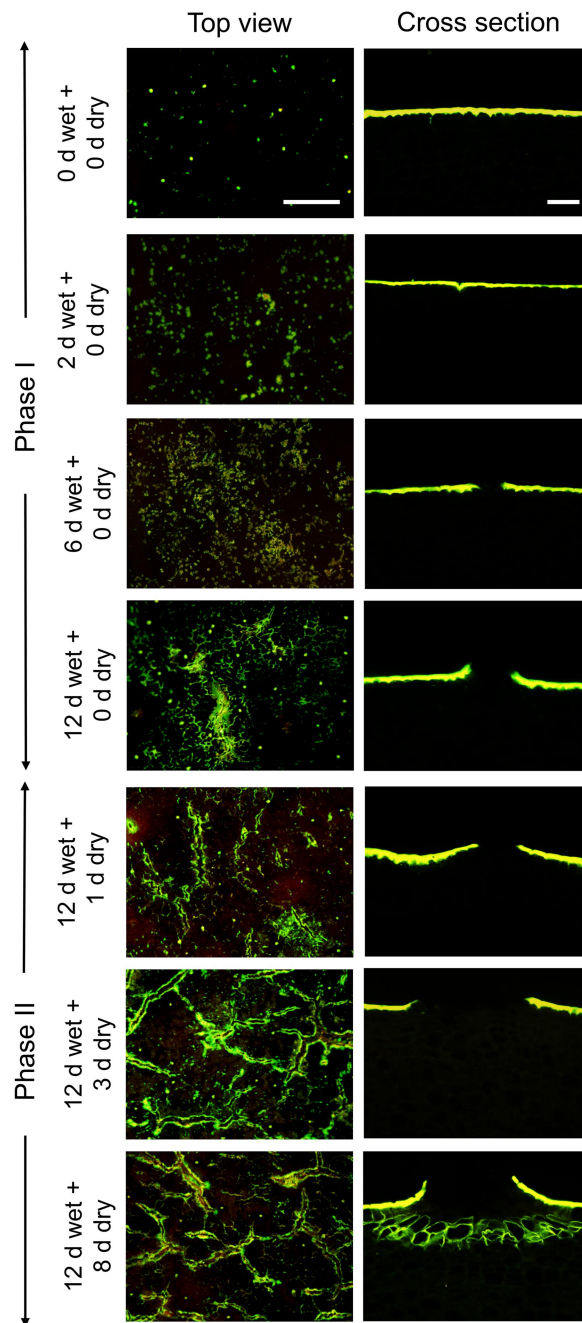


Figure S1 Time course of moisture-induced russeting of ‘Pinova’ apple as indexed by fluorescence microscopy. Russeting was induced in a two-phase experiment: During Phase I, a patch of fruit skin was exposed to surface moisture for 12 d (Phase I, ‘12 d wet’). After termination of moisture exposure (Phase II), the treated skin patch was exposed to the ambient atmosphere (‘y d dry’). The nontreated control (‘Control’) remained dry during Phase I and Phase II (‘x d dry + y d dry’). Moisture was applied at 31 days after full bloom (DAFB). Top view (left panel) and cross-sections of the fruit surface (right panel) during formation of

microcracks in the cuticle and initiation of a periderm. Microcracks were infiltrated with acridine orange (left panel), and the cross-sections were stained with Fluorol Yellow 088 (right panel). The scale bar in the top view of '0 d wet + 0 d dry' is 200 μ m long and representative of all top views ($n = 10$). The white scale bar in the '0 d wet + 0 d dry' cross-section is 50 μ m long and representative of all cross-sections ($n = 6$).

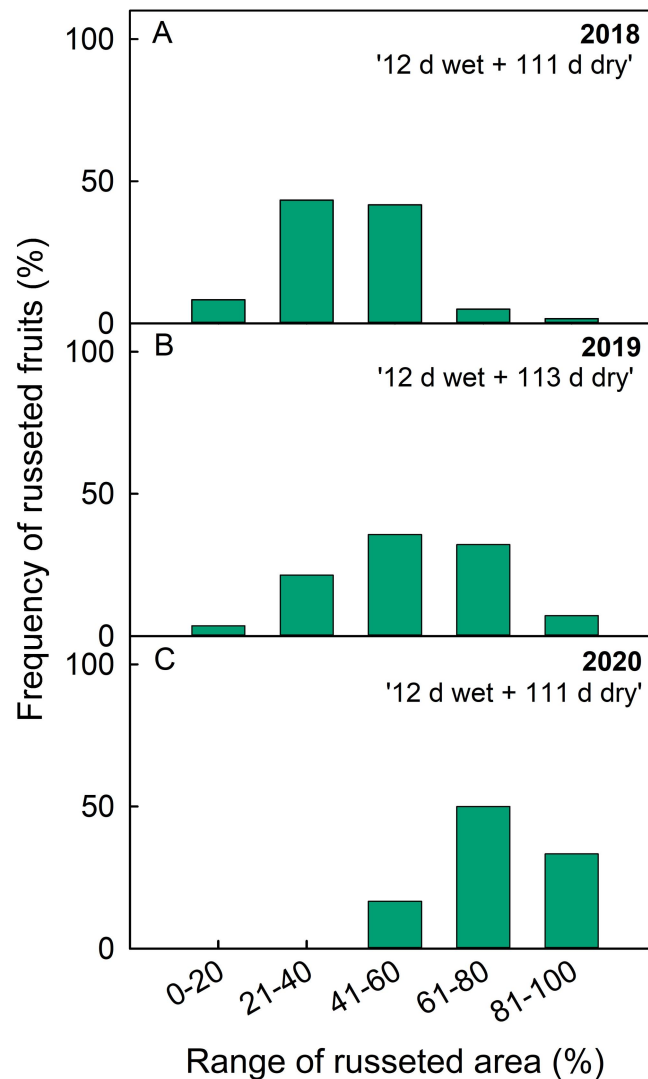


Figure S2 Frequency distribution of russeting of 'Pinova' apples in the 2018 ($n = 60$) (A), 2019 ($n = 28$) (B) and 2020 growing seasons ($n = 12$) (C). Russeting was induced by exposure to surface moisture for 12 d (Phase I) beginning at 21-31 DAFB. After termination of moisture exposure, the fruit skin patches remained dry (Phase II). The portion of the russeted surface area exposed to moisture was quantified at maturity.

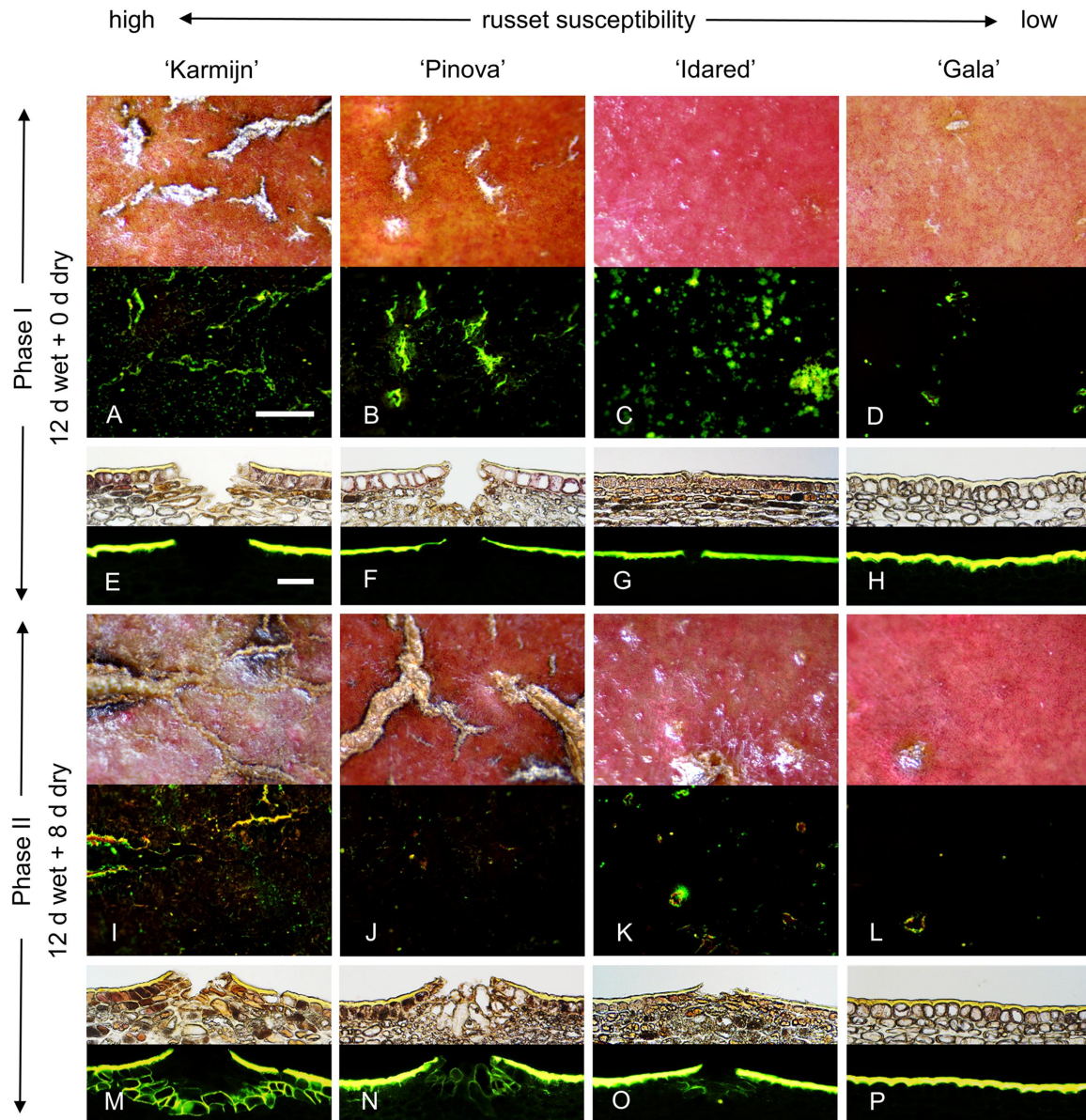


Figure S3 Comparison of microcrack and periderm formation in four apple cultivars differing in russet susceptibility. Russet susceptibility decreased from 'Karmijn' to 'Pinova' and from 'Idared' to 'Gala'. Russeting was induced in a two-phase experiment. During Phase I, skin patches of 'Karmijn' (A, E, I, M), 'Pinova' (B, F, J, N), 'Idared' (C, G, K, O) and 'Gala' (D, H, I, P) were exposed to moisture for 12 d ('x d wet'). After termination of moisture exposure (Phase II), the treated skin patch was exposed to the ambient atmosphere for up to 8 d ('y d dry'). The nontreated control ('Control') remained dry during Phase I and Phase II ('x d dry + y d dry').

Chapter 6 Time course of changes in the transcriptome during russet induction in apple fruit

Exposure to moisture started 28-32 days after full bloom (DAFB), equivalent to 10-12 mm diameter. Light micrographs and corresponding fluorescence micrographs of fruit surfaces after infiltration of microcracks with acridine orange (A-D, I-L). The scale bar in (A) is 200 μm long and is representative of the images in A, B, C, D, I, J, K and L ($n = 10$). Cross-sections through skin segments stained with Fluorol Yellow 088 were observed by transmitted white light (upper part) and incident fluorescent light (filter U-MWB) (E-H, M-P). The scale bar in (E) is 50 μm long and representative of the micrographs in E-H and M-P ($n = 6$).

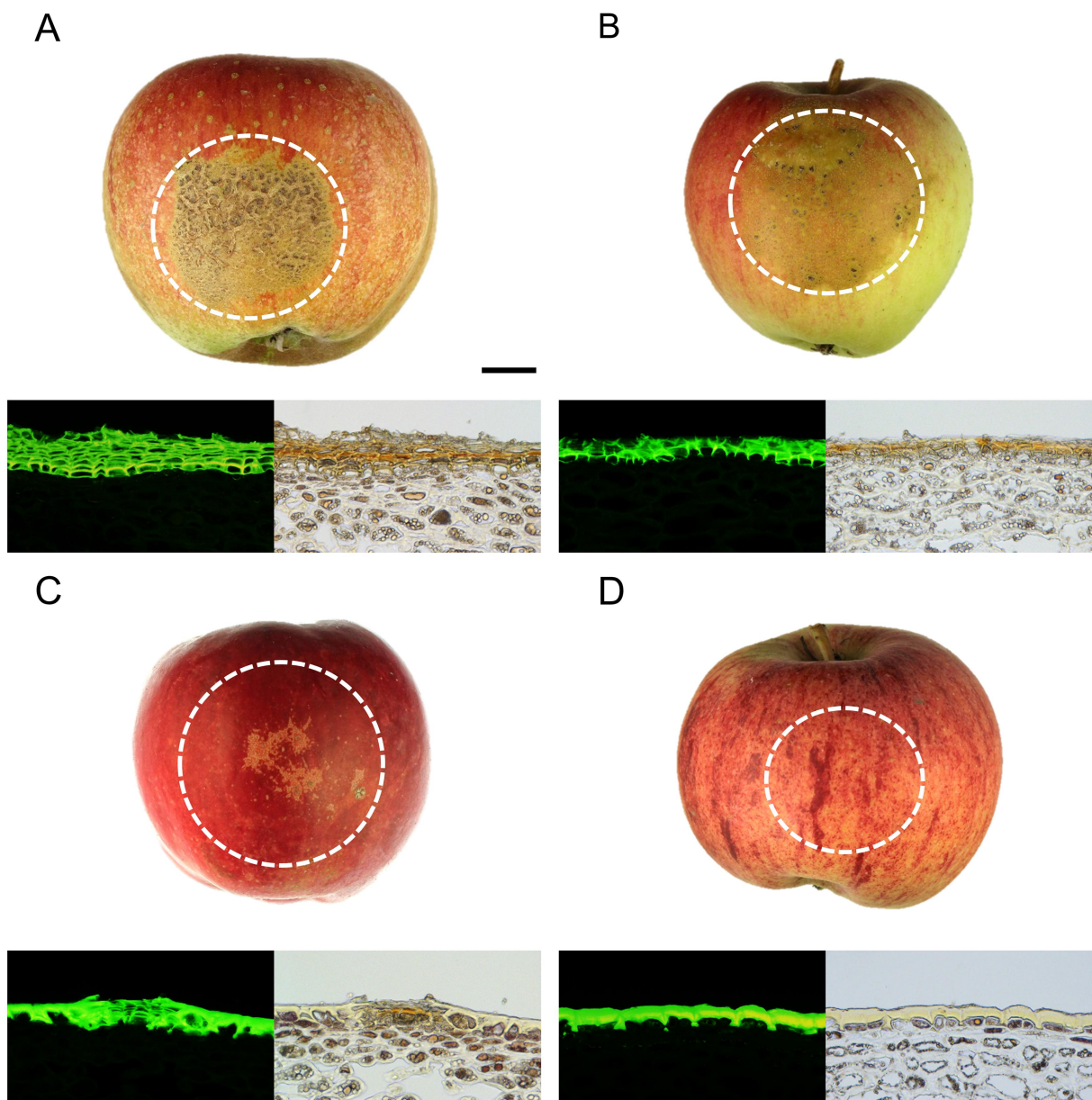


Figure S4 Macrographs and micrographs of moisture-exposed fruit surfaces of four apple cultivars differing in russet susceptibility. Russet susceptibility decreases in the order 'Karmijn' > 'Pinova' > 'Idared' > 'Gala'. Russeting was induced in a two-phase experiment. During Phase I, skin patches of 'Karmijn' (A), 'Pinova' (B), 'Idared' (C) and 'Gala' (D) apples were exposed to moisture for 12 d. After termination of moisture exposure (Phase II), the treated skin patch was exposed to the ambient atmosphere ('y d dry'). The nontreated control ('Control') remained dry during Phase I and Phase II ('x d dry + y d dry'). Moisture exposure began at 28-32 days after full bloom (DAFB). Russeting was evaluated at maturity. Macrographs were obtained by photography of the fruit; the micrographs were prepared by fluorescence microscopy of skin sections stained with Fluorol Yellow 088 and viewed under transmitted white light or incident fluorescent light (filter U-MWB) ($n = 3$). The black scale bar in (A) is 1 cm and representative of all photographs of whole fruit. The white scale bar in (A) is 50 μm and representative of all micrographs. The white dashed circle indicates the patch of fruit skin that was exposed to moisture.

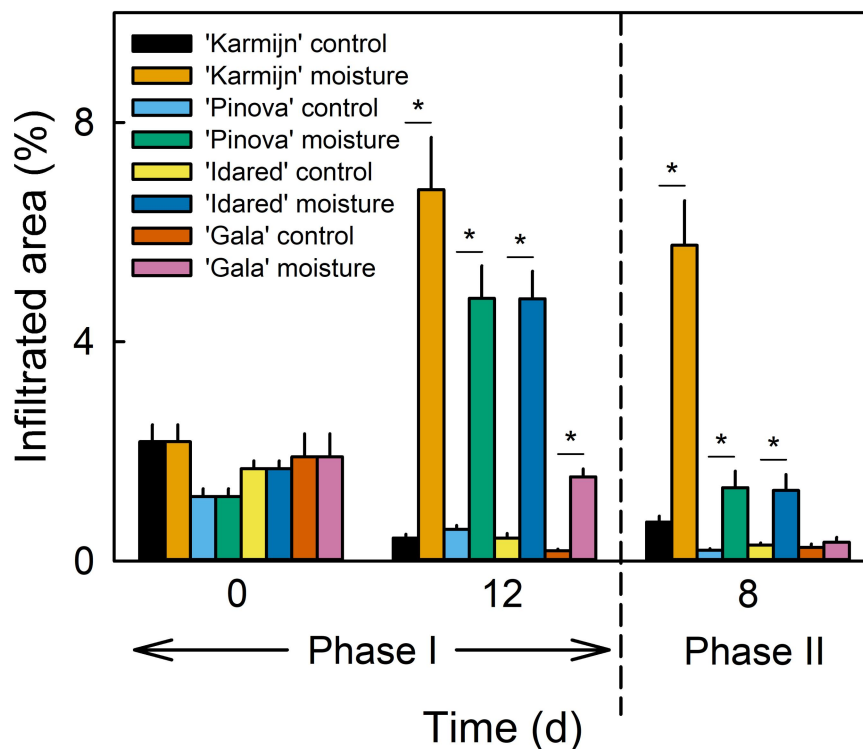


Figure S5 Microcrack formation in the cuticle of apples in four cultivars following exposure to moisture. Fruit skin patches of 'Karmijn', 'Pinova', 'Idared', and 'Gala' were exposed to surface moisture beginning at 28-32 days after full bloom (DAFB) for 12 d (Phase I). Afterwards, moisture was removed and the treated fruit skin patch remained dry (Phase II). The nonexposed surface of the same fruit served as a control. Microcracking was indexed by quantifying the area infiltrated with acridine orange. Data represent the means \pm SEs of ten fruits. '*' indicates a significant difference between 'Moisture' and 'Control' within each cultivar at $p \leq 0.05$ (Student's t test).

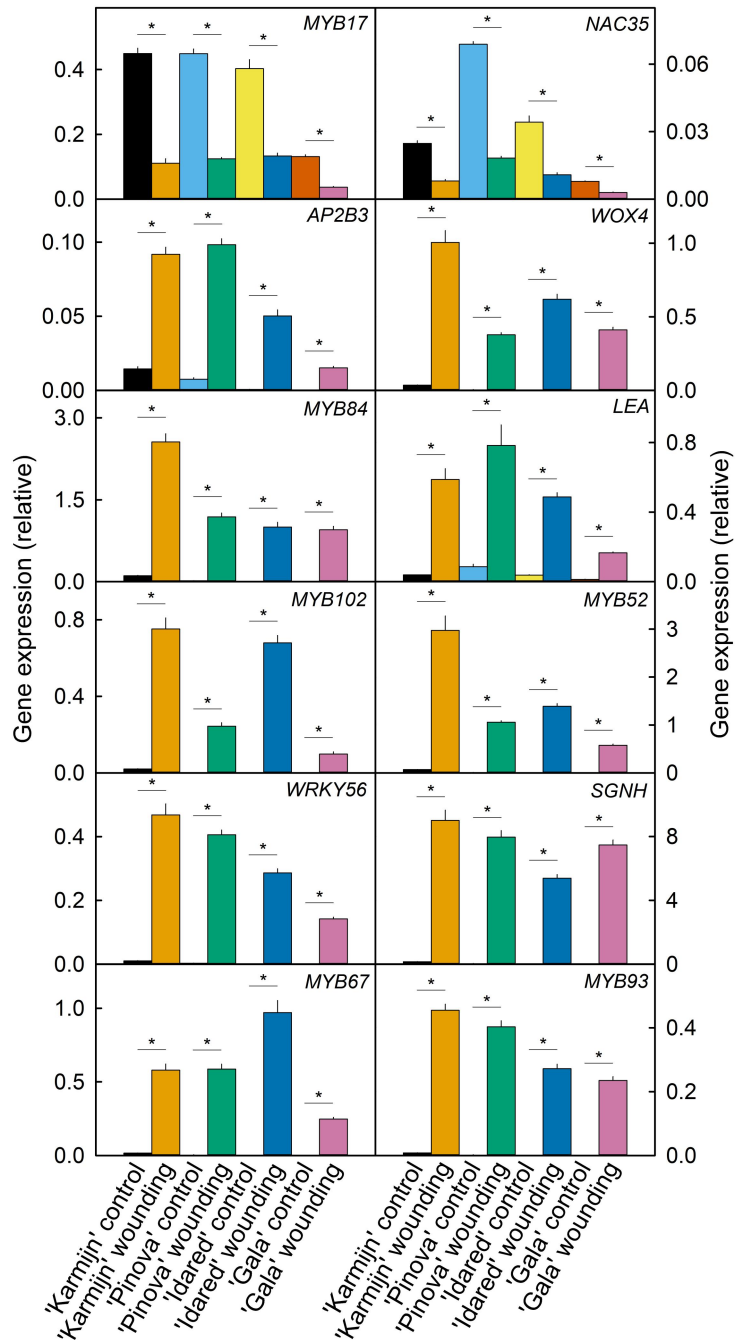


Figure S6 Expression of candidate genes after mechanical wounding of the skin of four apple cultivars. Russet susceptibility decreased in the order 'Karmijn'>'Pinova'>'Idared'>'Gala'. Fruit skins were wounded 38-40 days after full bloom (DAFB) using sandpaper ('Wounding'). The nontreated fruit skin served as the control ('Control'). Expression of genes associated with Phase I (*MYB17*, *NAC35*) or Phase II (*AP2B3*, *WOX4*, *MYB84*, *LEA*, *MYB102*, *MYB52*, *WRKY56*, *SGNH*, *MYB67*, *MYB93*) was analyzed. Expression values represent the means \pm SEs of three independent replicates

comprising six fruits each. “*” indicates a significant difference between ‘Wounding’ and ‘Control’ within each cultivar at $p \leq 0.05$ (Student’s t test).

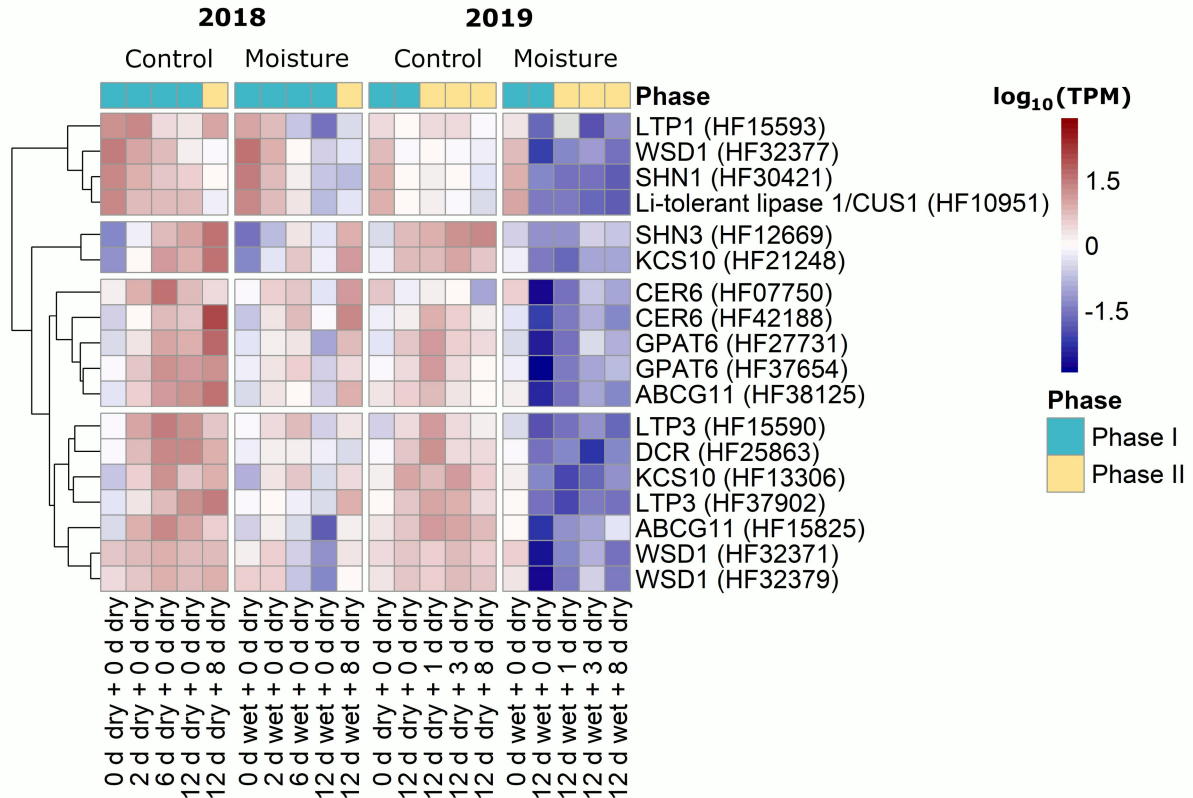


Figure S7 Heatmap of cutin and wax-related genes expression during moisture-induced russeting in ‘Pinova’ apple. Russeting was induced in a two-phase experiment. During Phase I, skin patches of ‘Pinova’ apples were exposed to moisture for 2, 6 or 12 d (‘x d wet’). After termination of moisture exposure (Phase II), the treated skin patch was exposed to the ambient atmosphere for 1, 3 or 8 d (‘y d dry’). The nontreated control (‘Control’) remained dry during Phase I and Phase II (‘x d dry + y d dry’). Cuticle-related genes (based on literature information) were downregulated during Phase I. Expression values are shown as the mean $\log_{10}(\text{TPM})$ (transcripts per million) values of three independent replicates comprising six (season 2018) or ten (season 2019) fruits each.

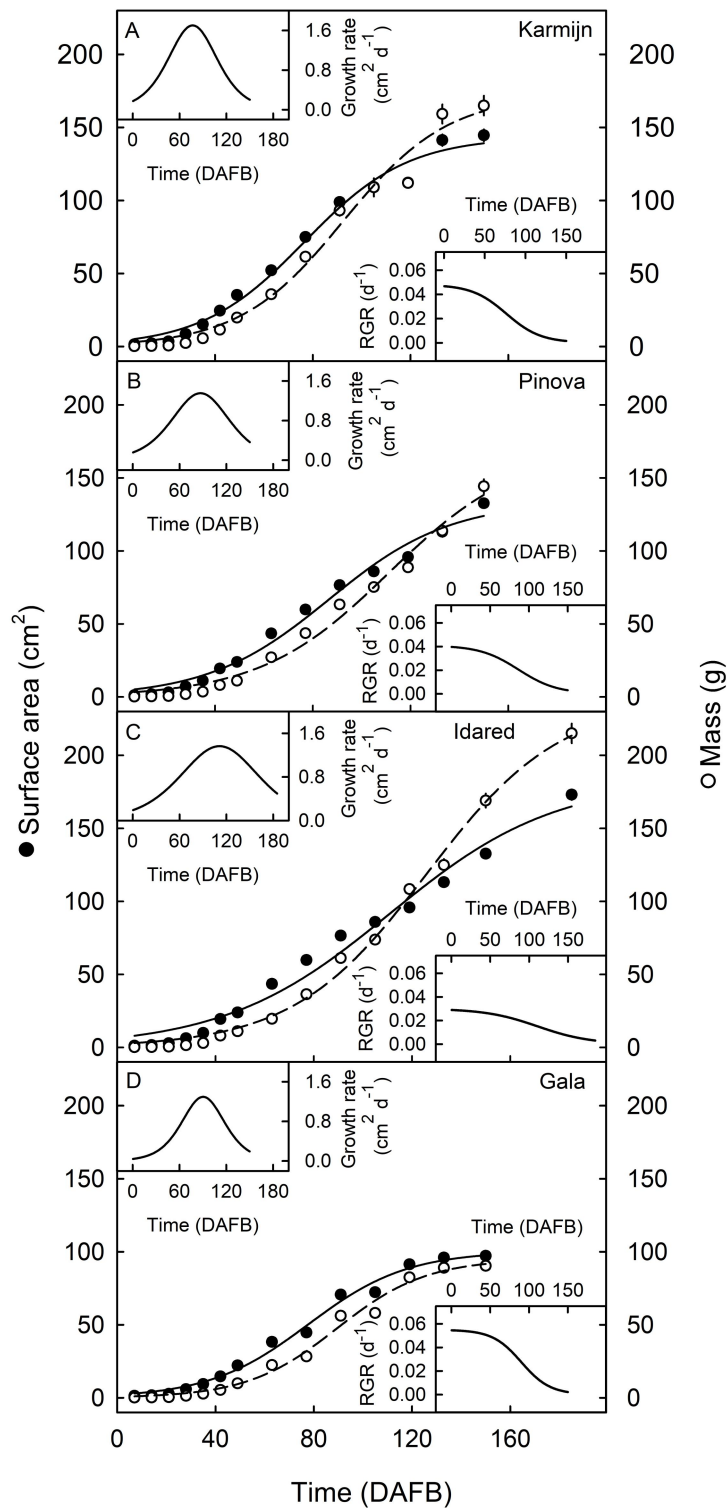


Figure S8 Time course of changes in mass and surface area of apples in four cultivars. Fruit growth parameters in 'Karmijn' (A), 'Pinova' (B), 'Idared' (C), and 'Gala' (D) were determined in the 2020 growing season. The two insets illustrate the surface area growth rate (upper left corner) and relative surface area growth rate (RGR; lower right corner) in

Chapter 6 Time course of changes in the transcriptome during russet induction in apple fruit

developing apple fruits. X-axis scale in days after full bloom (DAFB). Each value represents the mean \pm SE of 30 fruits.

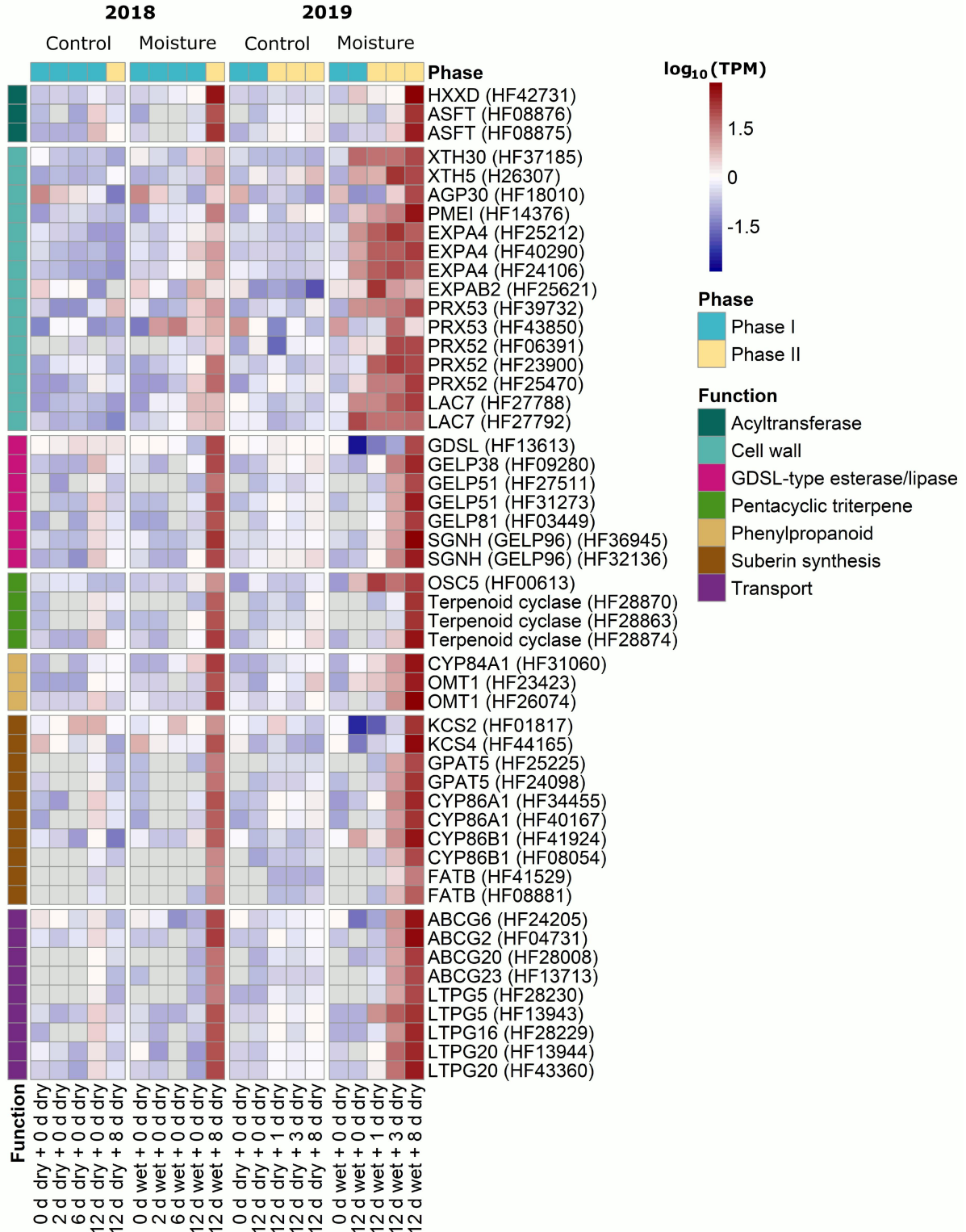


Figure S9 Heatmap of genes related to periderm formation during moisture-induced russeting in ‘Pinova’ apple. Russeting was induced in a two-phase experiment. During Phase I, skin patches of ‘Pinova’ apples were exposed to moisture for 2, 6 or 12 d (‘x d wet’). After termination of moisture exposure (Phase II), the treated skin patch was exposed to the ambient atmosphere for 1, 3 or 8 d (‘y d dry’). The nontreated control (‘Control’) remained dry during Phase I and Phase II (‘x d dry + y d dry’). Genes associated with russeting (based on literature information) were upregulated during Phase II. Expression values are shown as the mean \log_{10} (TPM) (transcripts per million) values of three independent replicates comprising six (season 2018) or ten (season 2019) fruits each.

Chapter 6 Time course of changes in the transcriptome during russet induction in apple fruit

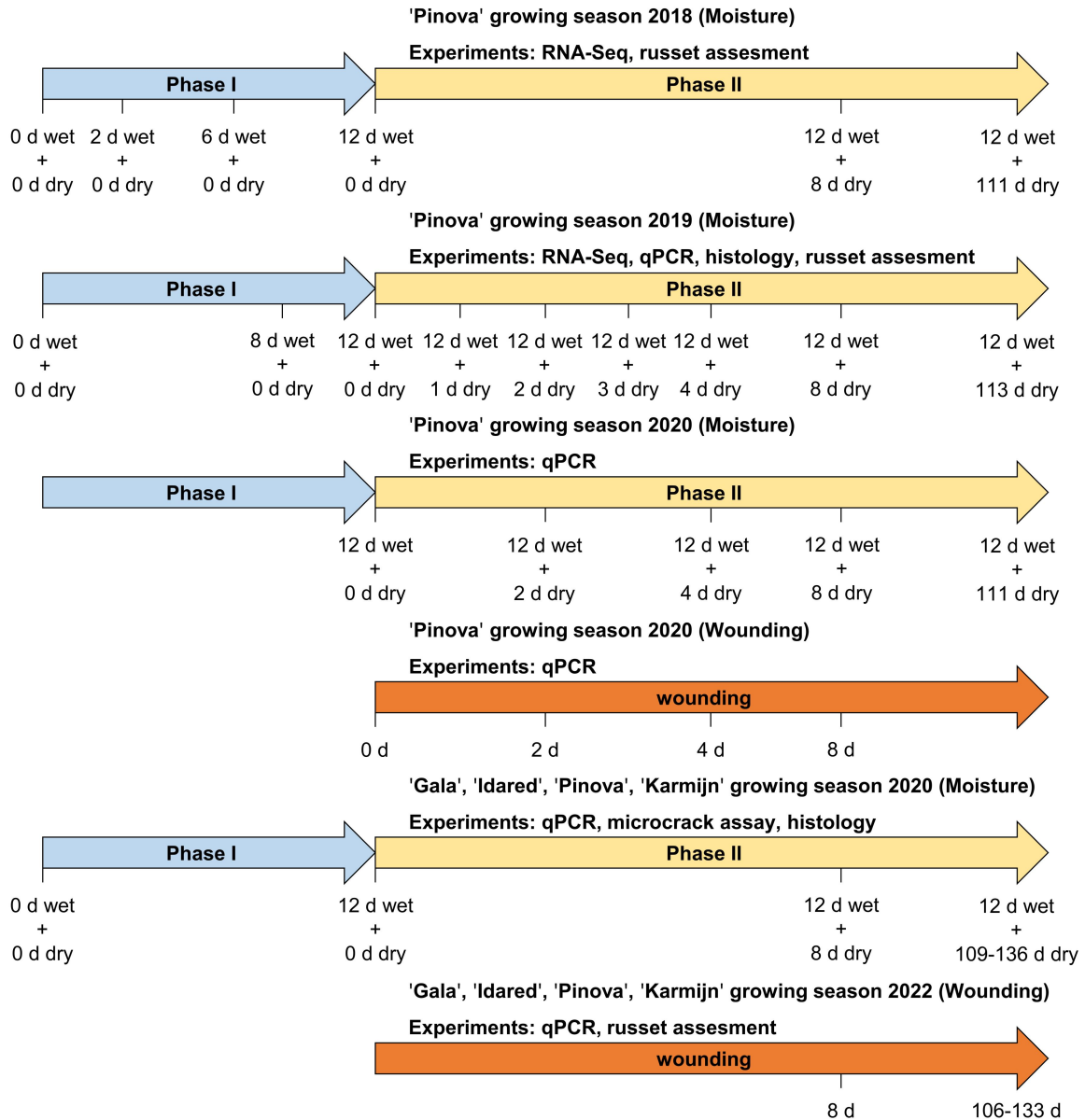


Figure S10 Sketch of experimental design. The moisture treatment (Moisture) experiment consisted of two phases: In Phase I (blue arrow) the fruit skin patches were exposed to moisture. In Phase II the moisture exposure was terminated and the skin patch exposed to atmospheric conditions. In the wounding experiments, the fruit skin patches were intentionally wounded by gently abrading them with sandpaper. The timing of the abrasion coincided with the end of moisture treatment in Phase I.

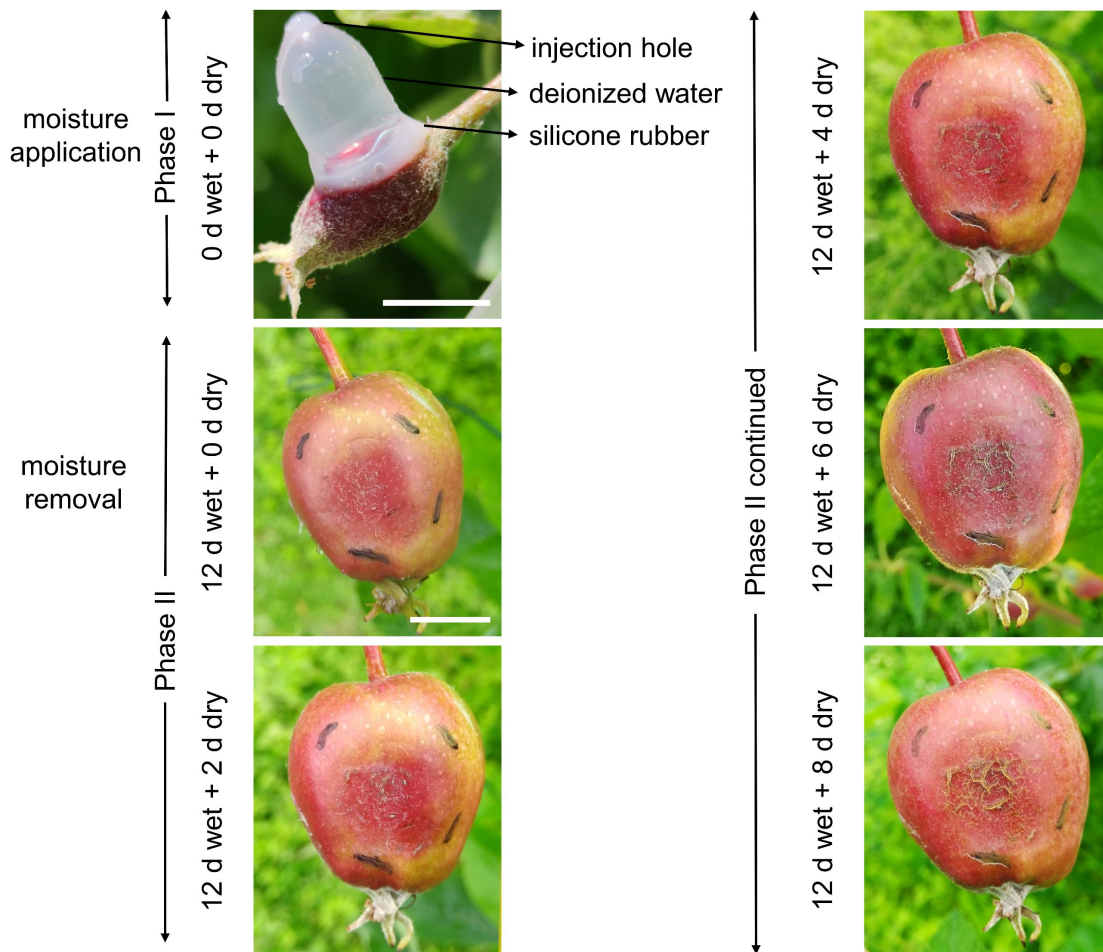


Figure S11 Russet induction by surface moisture. Russeting of 'Pinova' apple fruit skin was induced by applying moisture through a polyethylene tube mounted on the fruit surface using a non-phytotoxic silicone rubber during early stages of fruit development (21-31 days after full bloom (DAFB)). After curing, deionized water was injected through a hole at the top of the polyethylene tube using a syringe. The hole was sealed thereafter using silicone rubber. The fruit skin was exposed to surface moisture for a period of 12 d (Phase I). After this period, the tube was carefully removed, and the microcracked surface was exposed to atmospheric conditions (Phase II). The treated fruit skin patch was marked with a black, water-resistant marker. During Phase II, moisture-exposed fruit skins showed macroscopically visible cracks within 2 d after moisture removal (12 d wet + 2 d dry). A fully russeted skin patch formed after 12 d wet + 8 d dry. In the accompanying images, the white

Chapter 6 Time course of changes in the transcriptome during russet induction in apple fruit

scale bars for '0 d wet + 0 d dry' and '12 d wet + 0 d dry' are 1 cm long, the latter being representative of all other images.

Table S1. Summary of RNA integrity number (RIN), sequencing results, trimming and uniquely mapped reads of the HFTH1 genome.

Season	Time point	Biological replicate	RIN	Raw reads	Read pairs after trimming (Q ≥ 20)	Percentage of uniquely mapped reads (%)
2018	'0 d dry + 0 d dry'	1	8.8	121640060	57643670	94.25
	'0 d dry + 0 d dry'	2	9.4	128454744	61140644	95.18
	'0 d dry + 0 d dry'	3	9.1	123418270	57636005	94.24
	'0 d wet + 0 d dry'	1	9.8	150068214	70456595	93.88
	'0 d wet + 0 d dry'	2	9.4	150250946	70539939	94.72
	'0 d wet + 0 d dry'	3	9.2	141769224	66661960	94.51
	'2 d dry + 0 d dry'	1	9.9	123879264	58832415	94.45
	'2 d dry + 0 d dry'	2	9.6	128791720	61108589	94.22
	'2 d dry + 0 d dry'	3	9.8	124941598	58925324	93.99
	'2 d wet + 0 d dry'	1	9.6	130739500	62363018	94.60
	'2 d wet + 0 d dry'	2	9.7	121474696	57692471	94.34
	'2 d wet + 0 d dry'	3	8.4	123936980	58570379	93.34
	'6 d dry + 0 d dry'	1	9.3	122418652	58284983	94.95
	'6 d dry + 0 d dry'	2	9.8	120848968	57802019	93.86
	'6 d dry + 0 d dry'	3	9.9	124544584	59079988	95.11
	'6 d wet + 0 d dry'	1	9.8	123095348	58342147	90.33
	'6 d wet + 0 d dry'	2	9.6	126869850	60166854	82.89
	'6 d wet + 0 d dry'	3	9.8	127060892	60185343	90.32
	'12 d dry + 0 d dry'	1	8.8	119799220	56896654	93.84
	'12 d dry + 0 d dry'	2	9.3	128534002	60734209	93.79
	'12 d dry + 0 d dry'	3	8.8	123421432	58359708	93.56
	'12 d wet + 0 d dry'	1	9.9	123129710	58346280	92.98
	'12 d wet + 0 d dry'	2	10	122313942	58141580	93.17
	'12 d wet + 0 d dry'	3	9.7	123117832	58488243	93.14
	'12 d dry + 8 d dry'	1	9.3	121948016	57759425	94.77
	'12 d dry + 8 d dry'	2	10	121920638	57687317	95.40
	'12 d dry + 8 d dry'	3	10	124020262	58715966	95.52
	'12 d wet + 8 d dry'	1	8.8	122072708	57970170	94.28
	'12 d wet + 8 d dry'	2	9.9	124268364	58801142	94.45
	'12 d wet + 8 d dry'	3	9.9	146351032	69089407	94.46
2019	'0 d dry + 0 d dry'	1	9.7	133889700	63261870	94.88
	'0 d dry + 0 d dry'	2	9.6	119689572	56591648	94.14
	'0 d dry + 0 d dry'	3	10	125224450	59312334	93.81
	'0 d wet + 0 d dry'	1	9.9	137475904	64990547	94.55
	'0 d wet + 0 d dry'	2	9.7	124077252	57751485	93.64
	'0 d wet + 0 d dry'	3	9.8	122223580	57277739	93.63
	'12 d dry + 0 d dry'	1	9.5	121552076	57900489	94.52
	'12 d dry + 0 d dry'	2	9.8	130935978	61992895	94.02
	'12 d dry + 0 d dry'	3	9.7	129075842	61201544	94.55
	'12 d wet + 0 d dry'	1	9.7	123881026	58419444	93.29
	'12 d wet + 0 d dry'	2	10	122233530	57745233	94.04
	'12 d wet + 0 d dry'	3	9.9	126287244	59665259	93.90
	'12 d dry + 1 d dry'	1	9.7	128612160	60984921	94.67
	'12 d dry + 1 d dry'	2	9.8	123635836	59317591	93.80
	'12 d dry + 1 d dry'	3	9.6	123068870	57441459	93.88
	'12 d wet + 1 d dry'	1	10	122987230	57351930	94.11
	'12 d wet + 1 d dry'	2	10	121859564	57339366	93.74
	'12 d wet + 1 d dry'	3	10	119907316	56615752	93.94
	'12 d dry + 3 d dry'	1	9.5	123202362	58500246	94.47
	'12 d dry + 3 d dry'	2	9.8	122097110	57908035	94.03
	'12 d dry + 3 d dry'	3	9.6	122280412	57978514	94.02
	'12 d wet + 3 d dry'	1	10	121481146	57128431	94.79
	'12 d wet + 3 d dry'	2	9.8	133529112	63057053	94.68
	'12 d wet + 3 d dry'	3	10	123702882	58426916	94.46
	'12 d dry + 8 d dry'	1	9.8	132175454	62733354	94.62
	'12 d dry + 8 d dry'	2	9.9	123778558	58738285	94.37
	'12 d dry + 8 d dry'	3	9.8	121345836	56774298	94.04
	'12 d wet + 8 d dry'	1	10	123826376	58422565	95.22
	'12 d wet + 8 d dry'	2	10	124522250	58469468	94.45
	'12 d wet + 8 d dry'	3	10	123605066	58066909	94.74

Chapter 6 Time course of changes in the transcriptome
during russet induction in apple fruit

Table S2. Summary of differentially expressed genes detected in the RNA-seq analysis. Genes with a \log_2 -fold change (\log_2FC) ≥ 2 or ≤ -2 , a false discovery rate (FDR) ≤ 0.05 and a mean of at least five TPM (transcripts per million) in control ('x d dry + y d dry') or moisture-exposed ('x d wet + y d dry') samples were assumed to be differentially expressed.

Season	Time point	Number up-regulated genes ($\log_2FC \geq 2$, FDR ≤ 0.05)	Number down-regulated genes ($\log_2FC \leq -2$, FDR ≤ 0.05)
2018	'0 d wet + 0 d dry' vs '0 d dry + 0 d dry'	0	0
	'2 d wet + 0 d dry' vs '2 d dry+ 0 d dry'	35	2
	'6 d wet + 0 d dry' vs '6 d dry+ 0 d dry'	378	127
	'12 d wet + 0 d dry' vs '12 d dry+ 0 d dry'	860	196
	'12 d wet + 8 d dry' vs '12 d dry + 8 d dry'	523	44
2019	'0 d wet + 0 d dry' vs '0 d dry+ 0 d dry'	0	0
	'12 d wet + 0 d dry' vs '12 d dry+ 0 d dry'	1219	858
	'12 d wet + 1 d dry' vs '12 d dry + 1 d dry'	1094	597
	'12 d wet + 3 d dry' vs '12 d dry + 3 d dry'	980	321
	'12 d wet + 8 d dry' vs '12 d dry + 8 d dry'	974	253

Chapter 6 Time course of changes in the transcriptome
during russet induction in apple fruit

Table S3. Sampling time points in the 2018, 2019, 2020 and 2022 growing seasons for experiments on gene expression and histology of apple fruit skins.

Season	Time point	Treatment	Cultivar	DAFB	Date
2018	'0 d wet + 0 d dry' vs '0 d dry + 0 d dry'	Moisture	'Pinova'	21	2018-05-13
	'2 d + 0 d dry' wet' vs '2 d dry+ 0 d dry'	Moisture	'Pinova'	23	2018-05-15
	'6 d wet + 0 d dry' vs '6 d dry+ 0 d dry'	Moisture	'Pinova'	27	2018-05-19
	'12 d wet + 0 d dry' vs '12 d dry+ 0 d dry'	Moisture	'Pinova'	33	2018-05-25
	'12 d wet + 8 d dry' vs '12 d dry + 8 d dry'	Moisture	'Pinova'	41	2018-06-01
	'12 d wet + 111 d dry' vs. '12 d dry + 111 d dry'	Moisture	'Pinova'	152	2018-09-20
2019	'0 d wet + 0 d dry' vs '0 d dry + 0 d dry'	Moisture	'Pinova'	31	2019-05-23
	'8 d wet + 0 d dry' vs '8 d dry + 0 d dry'	Moisture	'Pinova'	39	2019-05-31
	'12 d wet + 0 d dry' vs '12 d dry+ 0 d dry'	Moisture	'Pinova'	43	2019-06-04
	'12 d wet + 1 d dry' vs. '12 d dry + 1 d dry'	Moisture	'Pinova'	44	2019-06-05
	'12 d wet + 2 d dry' vs. '12 d dry + 2 d dry'	Moisture	'Pinova'	45	2019-06-06
	'12 d wet + 3 d dry' vs. '12 d dry + 3 d dry'	Moisture	'Pinova'	46	2019-06-07
	'12 d wet + 4 d dry' vs. '12 d dry + 4 d dry'	Moisture	'Pinova'	47	2019-06-08
	'12 d wet + 8 d dry' vs '12 d dry + 8 d dry'	Moisture	'Pinova'	51	2019-06-12
	'12 d wet + 113 d dry' vs. '12 d dry + 113 d dry'	Moisture	'Pinova'	156	2019-09-25
2020	'12 d wet + 0 d dry' vs '12 d dry+ 0 d dry'	Moisture	'Pinova'	40	2020-06-02
	'12 d wet + 2 d dry' vs. '12 d dry + 2 d dry'	Moisture	'Pinova'	42	2020-06-04
	'12 d wet + 4 d dry' vs. '12 d dry + 4 d dry'	Moisture	'Pinova'	44	2020-06-06
	'12 d wet + 8 d dry' vs '12 d dry + 8 d dry'	Moisture	'Pinova'	48	2020-06-10
	'12 d wet + 111 d dry' vs. '12 d dry + 111 d dry'	Moisture	'Pinova'	151	2020-09-21
	'0 d wounding' vs. '0 d control'	Wounding	'Pinova'	40	2020-06-02
	'2 d wounding' vs. '2 d control'	Wounding	'Pinova'	42	2020-06-04
	'4 d wounding' vs. '4 d control'	Wounding	'Pinova'	44	2020-06-06
	'8 d wounding' vs. '8 d control'	Wounding	'Pinova'	48	2020-06-10
	'0 d wet + 0 d dry' vs '0 d dry + 0 d dry'	Moisture	'Karmijn'	28	2020-05-23
	'12 d wet+ 0 d dry' vs '12 d dry+ 0 d dry'	Moisture	'Karmijn'	40	2020-06-04
	'12 d wet + 8 d dry' vs '12 d dry + 8 d dry'	Moisture	'Karmijn'	48	2020-06-12
	'12 d wet + 109 d dry' vs. '12 d dry + 109 d dry'	Moisture	'Karmijn'	149	2020-09-21
	'0 d wet + 0 d dry' vs '0 d dry + 0 d dry'	Moisture	'Pinova'	30	2020-05-23
	'12 d wet + 0 d dry' vs '12 d dry+ 0 d dry'	Moisture	'Pinova'	42	2020-06-04
	'12 d wet + 8 d dry' vs '12 d dry + 8 d dry'	Moisture	'Pinova'	50	2020-06-12
	'12 d wet + 109 d dry' vs. '12 d dry + 109 d dry'	Moisture	'Pinova'	151	2020-09-21
	'0 d wet + 0 d dry' vs '0 d dry + 0 d dry'	Moisture	'Idared'	32	2020-05-23
	'12 d wet + 0 d dry' vs '12 d dry+ 0 d dry'	Moisture	'Idared'	44	2020-06-04
	'12 d wet + 8 d dry' vs '12 d dry + 8 d dry'	Moisture	'Idared'	52	2020-06-12
'12 d wet + 136 d dry' vs. '12 d dry + 136 d dry'	Moisture	'Idared'	180	2020-10-26	
'0 d wet + 0 d dry' vs '0 d dry + 0 d dry'	Moisture	'Gala'	29	2020-05-23	
'12 d wet + 0 d dry' vs '12 d dry+ 0 d dry'	Moisture	'Gala'	41	2020-06-04	
'12 d wet + 8 d dry' vs '12 d dry + 8 d dry'	Moisture	'Gala'	49	2020-06-12	
'12 d wet + 109 d dry' vs. '12 d dry + 109 d dry'	Moisture	'Gala'	150	2020-09-21	
2022	'8 d wounding' vs. '8 d control'	Wounding	'Karmijn'	38	2022-06-09
	'119 d wounding' vs. '119 d control'	Wounding	'Karmijn'	159	2022-10-06
	'8 d wounding' vs. '8 d control'	Wounding	'Pinova'	39	2022-06-09
	'106 d wounding' vs. '106 d control'	Wounding	'Pinova'	145	2022-09-23
	'8 d wounding' vs. '8 d control'	Wounding	'Idared'	40	2022-06-09
	'133 d wounding' vs. '133 d control'	Wounding	'Idared'	173	2022-10-20
	'8 d wounding' vs. '8 d control'	Wounding	'Gala'	40	2022-06-09
	'106 d wounding' vs. '106 d control'	Wounding	'Gala'	146	2022-09-23

Table S4. Russeting after mechanical wounding during early fruit development (38-40 days after full bloom (DAFB)) of ‘Karmijn’, ‘Pinova’, ‘Idared’ and ‘Gala’ apples in the 2022 season. Russeting was quantified at commercial maturity.

Cultivar	Developmental stage (DAFB)	Number of fruits	Frequency of russeted fruits (%)	Russeted area (% of treated area)
				Wounded
‘Karmijn’	159	35	100	100
‘Pinova’	145	49	100	100
‘Idared’	173	46	100	100
‘Gala’	146	49	100	100

Table S5. List of primers used in this study.

Gene name	Accession	Primer sequence (5'-3')		PCR efficiency (%)	Reference
		Forward Primer	Reverse Primer		
Phase I related					
<i>MYB17</i>	HF15264	CCACAAACACACGAGCCTCT	GCCTAGCACTCTCCCATTGT	94.2	This study
<i>NAC035</i>	HF34490	CGGAGTTGAAGACCACCCAT	GGTCGTCGATTGAGCCACTA	102.5	This study
Phase II related					
<i>AP2B3</i>	HF20086	CCACACGGATCGACTCTTCAT	CACCACCACTGCTACTCTCAA	85.7	This study
<i>MYB52</i>	HF24488	CCCAAGAATCAACAGGAACCC T	GCCTTGCAATAACAGCCCATC	82.9	This study
<i>MYB67</i>	HF11445	ACATCTGGGCTTCTGGTACTG	TTCCATCTGATCCAAGAGCGT	89.4	This study
<i>MYB84</i>	HF13180	AGTTCTTCTGCTCCTGTGGC	ATTACCGCCTTGCCCTTGAA	90.5	This study
<i>MYB93</i>	MDP0000320772	TGGACAAACTATCTTAGGCCG G	GTTGCCGAGGATGGAATGGA	102.5	[1]
<i>MYB102</i>	HF33626	ACAAATGGTCAGGTATTGCAGC	CCCATTTCGGAGGAGCCTTTT	93.6	This study
<i>WOX4</i>	HF13050	TGGTTCCAGAATCACAAGGCA	CCAGAGGAGTCGGTGTCTT	92.3	This study
<i>WRKY56</i>	HF14837	ATTAGTGGCTCTGCTGGGAAT	CGAGTCTGGAACGCAAACCT	90.8	This study
<i>SGNH</i>	HF32136	CCCAGGGGCAAACTCTCAT	TGCAACACGGAAGTTTCGAA	97.2	This study
<i>LEA</i>	HF26067	TGCCACCACAATTCTCTCCA	TGAGTTGGACGGACGAGTTG	97.9	This study
Reference genes					
<i>eF-1alpha</i>	AJ223969.1	ACTGTTCCCTGTTGGACGTGTTG	TGGAGTTGGAAGCAACGTACCC	93.0	[2]
<i>PDI</i>	MDP0000233444	TGCTGTACACAGCCAACGAT	CATCTTTAGCGGCGTTATCC	100.6	[3]

References

1. Straube J, Chen Y-H, Khanal BP, Shumbusho A, Zeisler-Diehl V, Suresh K, et al. Russeting in apple is initiated after exposure to moisture ends: Molecular and biochemical evidence. *Plants* 2020. doi:10.3390/plants10010065.
2. Legay S, Guerriero G, Deleruelle A, Lateur M, Evers D, André CM, Hausman J-F. Apple russeting as seen through the RNA-seq lens: strong alterations in the exocarp cell wall. *Plant Mol Biol*. 2015;88:21–40. doi:10.1007/s11103-015-0303-4.
3. Storch TT, Pegoraro C, Finatto T, Quecini V, Rombaldi CV, Girardi CL. Identification of a novel reference gene for apple transcriptional profiling under postharvest conditions. *PLoS One*. 2015;10:e0120599. doi:10.1371/journal.pone.0120599.

Electronical File E3. Data S1 List of DEGs at corresponding timepoints in 2018 and 2019.
(Spreadsheet in .xlsx file) (access through electronical appendix)

Electronical File E4. Data S2 Results GO terms season 2018 (Spreadsheet in .xlsx file)
(access through electronical appendix)

Electronical File E5. Data S3 Results GO terms season 2019 (Spreadsheet in .xlsx file)
(access through electronical appendix)

Electronical File E6. Data S4 GOterms at corresponding time points the seasons 2018 and
2019 (Spreadsheet in .xlsx file) (access through electronical appendix)

Electronical File E7. Data S5 Results GO terms season 2018 12 d wet + 0 d dry $\log_2FC \leq -1$
(Spreadsheet in .xlsx file) (access through electronical appendix)

Electronical File E8. Data S6 List of DEGs during season 2018 (Spreadsheet in .xlsx file)
(access through electronical appendix)

Electronical File E9. Data S7 List of DEGs during season 2019 (Spreadsheet in .xlsx file)
(access through electronical appendix)

7. Functional analysis of candidate genes potentially involved in apple fruit russeting

Jannis Straube^{1,2}, Julia Goldberg¹, Moritz Knoche² and Thomas Debener¹

¹Institute of Plant Genetics, Molecular Plant Breeding Section, Leibniz University Hannover,
Herrenhäuser Straße 2, 30419 Hannover, Germany

²Institute of Horticultural Production Systems, Fruit Science Section, Leibniz University Hannover,
Herrenhäuser Straße 2, 30419 Hannover, Germany

Type of authorship:	First author
Type of article:	Research article
Contribution to the article:	Designed and performed the experiments, analyzed the data and prepared the figures and tables. Wrote the first draft of the manuscript and designed all of the figures and tables. Contributed to reviewing and editing of the manuscript.
Contribution of other authors:	J. Goldberg performed <i>A. thaliana</i> transformations, conducted infiltration experiments, and carried out qPCR analyses. M. Knoche and T. Debener contributed to the conception of the study and writing, reviewing, and editing of the manuscript.
Journal	not submitted

Functional analysis of candidate genes potentially involved in apple fruit russeting

Jannis Straube^{1,2}, Julia Goldberg¹, Moritz Knoche² and Thomas Debener^{1*}

¹Institute of Plant Genetics, Molecular Plant Breeding Section, Leibniz University Hannover, Herrenhäuser Straße 2, 30419 Hannover, Germany, straube@genetik.uni-hannover.de (J.S.)³, julia.goldberg@stud.uni-hannover.de (J.G.), debener@genetik.uni-hannover.de (T.D.)

²Institute of Horticultural Production Systems, Fruit Science Section, Leibniz University Hannover, Herrenhäuser Straße 2, 30419 Hannover, Germany, moritz.knoche@obst.uni-hannover.de (M.K.)

³Present address: jannis.straube@obst.uni-hannover.de (J.S.)

* Correspondence: debener@genetik.uni-hannover.de (T.D.) Tel.: +49-511-762-2672

Key words

russeting; *Malus x domestica*; *Nicotiana benthamiana*, *Arabidopsis thaliana*, periderm; suberin; transcriptional regulation

Introduction

Russeting is a disorder affecting the skin of commercially important fruit species such as apple (*Malus x domestica*, Borkh.) (Skene, 1982). It is characterized by the formation of a corky periderm in the hypodermis under cuticular microcracks, which replaces the cuticle (Bell, 1937; Meyer, 1944; Pratt, 1972). Russeting can be induced by abiotic factors such as high humidity and prolonged periods of surface moisture during early fruit development (Tukey, 1959; Knoche and Grimm, 2008; Winkler et al., 2014; Chen et al., 2020; Khanal et al., 2020a; Straube et al., 2020) as well as by biotic factors such as mechanical wounding (Chen et al., 2022).

Previous research has identified several quantitative trait loci (QTLs) that are associated with russeting on linkage groups 2, 6, 7, 9, 12, 13, and 15 as well as chromosomes 2 and 15 (Falginella et al., 2015; Lashbrooke et al., 2015; Powell et al., 2023). Within these QTLs, genes related to cuticle formation, such as *SHN3* and *ABCG11*, have been identified (Falginella et al., 2015; Lashbrooke et al., 2015). Lashbrooke et al. (2015) have observed downregulation of *SHN3* in the fruit skin of russeted progeny.

Transcriptomic profiling of mature russeted fruit skins has identified downregulation of cuticle genes and upregulation of lignin and phenylpropanoid genes (Legay et al., 2015; Falginella et al., 2021; André et al., 2022; Wang, Z. et al., 2022). Further research has identified several candidate genes that are involved in the later stages of russeting, such as *MdMYB52* (MD05G1011100 (Daccord et al., 2017); HF31835 (Zhang, L. et al., 2019)) as a major lignin regulator (Xu, X. et al., 2022), *MdMYB68* (MD08G1076200; HF21464) (Xu et al., 2023) and *MdMYB93* (MD15G1323500; HF40961) (Legay et al., 2016) as a major regulator of suberization. Despite the characterization of several candidate genes involved in later stages of russeting, the molecular sequence of russet initiation is still unclear.

The morphological and molecular sequence of russet formation after a predefined trigger was studied in greater detail by our research group using a defined russet induction method based on prolonged periods of surface moisture and mechanical abrasion (Khanal et al., 2020a; Chen et al., 2020; Straube et al., 2020; Chen et al., 2022). The research revealed a biphasic behavior during the moisture-induced russeting of apple fruit skins (Chen et al., 2020; Straube et al., 2020). In Phase I, the fruit skin was exposed to moisture and a decrease in cuticle was observed, along with the formation of microcracks. In Phase II, the moisture was removed and periderm formation was observed as early as 4 days after exposure to atmospheric conditions. The sequence of periderm formation during Phase II of moisture-induced russeting was found to be similar to that of wound-induced periderm in

apple fruit skins (Chen et al., 2022). Our recent study (Straube et al., not published) identified the transcriptomic events during the initiation of russeting and highlighted new candidate genes, two for Phase I and nine for Phase II, including several transcriptional regulators.

The aim of this study is to investigate the functional roles of some of these candidate genes that may be involved in the formation of russeted fruit skins. Specifically, we will focus on *MYB17* (MD01G1054800; HF15264) as a Phase I related gene, and *WOX4* (MD15G1079000; HF13050), *MYB52* (MD14G1242300; HF24488), *MYB67* (MD05G1239200; HF11445), and *WRKY56* (MD07G1131000; HF14837) as Phase II related genes. Here, we present our preliminary findings on the functional characterization of these candidate genes, and their potential involvement in the formation of russeted fruit skins.

Results

Infiltration experiments in *N. benthamiana*

To screen for russet-associated genes, we established an overexpression assay in *Nicotiana benthamiana*, based on previously published work by Legay et al. (2016). Initially, infiltration experiments were conducted with *WRKY56* (*35S::WRKY56*), *MYB52* (*35S::MYB52*), and *MYB93* (*35S::MYB93*), as well as an empty vector control (*ProAtUbi::GFP*), without simultaneous silencing suppressor *p19* (*35S::p19*). However, six days after overexpression, no significant expression of downstream genes expected to be upregulated upon activation of suberin-related genes was observed (Fig. 1). Downstream targets of *MYB93* were activated only upon co-infiltration with the silencing suppressor *p19* (Fig. 2A,B).

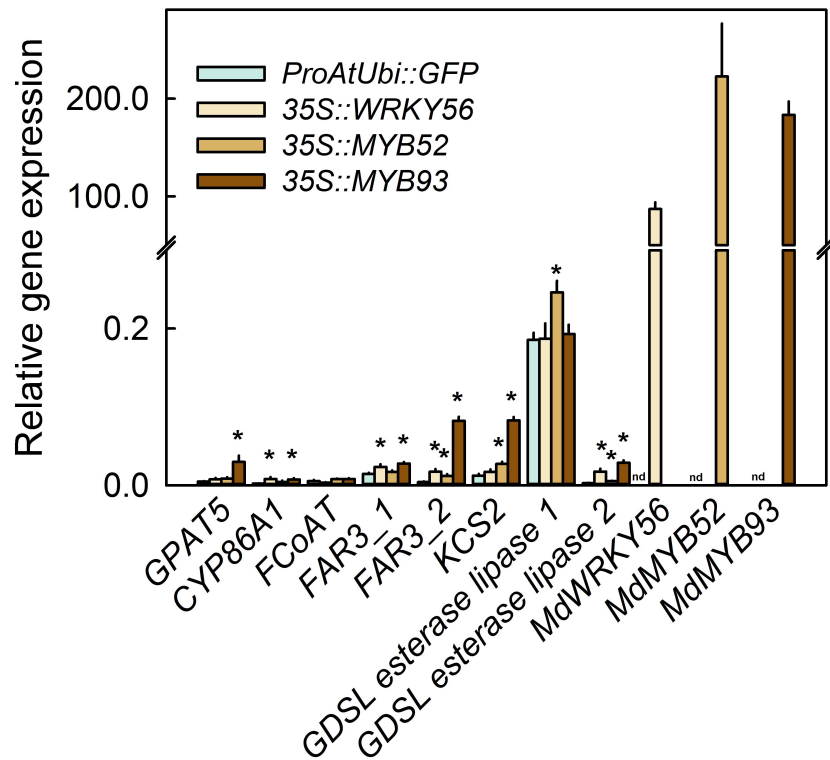


Figure 1. Gene expression profile of suberin-related genes in detached *N. benthamiana* leaves. Leaves from three-week-old *N. benthamiana* plants were detached and infiltrated with GV3101 ($OD_{600}=0.5$) containing the empty vector (*ProAtUbi::GFP*) or different transcriptional regulators (*35S::WRKY56*, *35S::MYB52*, *35S::MYB93*) associated with russetting in *Malus x domestica*. Expression profiles of suberin-related genes were observed six days after infiltration. Each value represents the mean \pm SE of three independent biological replicates comprising two infiltrated leaves each. The ‘*’ indicates a significant difference at $p \leq 0.05$ (Student’s *t*-test) between the *ProAtUbi::GFP* and the gene of interest. nd, not detected.

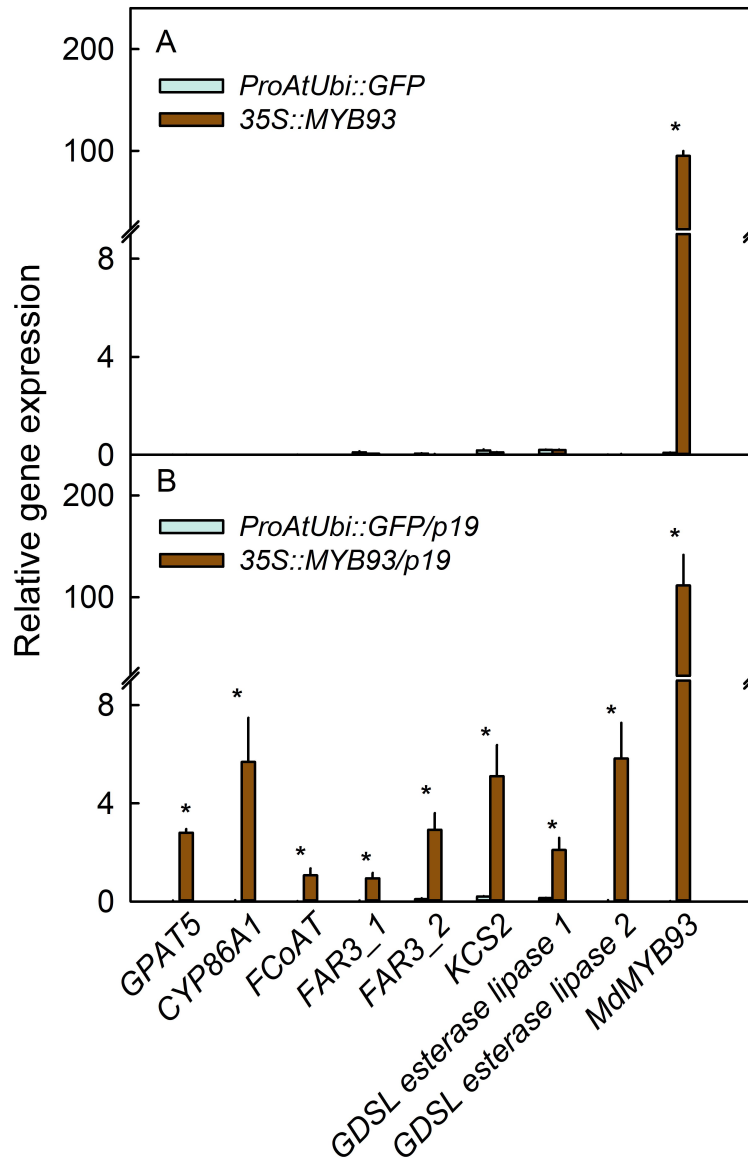


Figure 2. Comparative gene expression profile of suberin-related genes in *N. benthamiana* leaves, with and without *p19*. (A) Leaves from three-week-old *N. benthamiana* plants were infiltrated with GV3101 ($OD_{600}=0.8$) containing either the empty vector (*ProAtUbi::GFP*) or the transcriptional regulator *MYB93* (*35S::MYB93*), known to be involved in russetting in *Malus x domestica*. Gene expression profiles of suberin-related genes were analyzed six days post-infiltration. (B) Leaves from three week-old *N. benthamiana* plants were infiltrated with GV3101 ($OD_{600}=0.8$) containing either the empty vector (*ProAtUbi::GFP/p19*) or the transcriptional regulator *MYB93* (*35S::MYB93/p19*) in combination with C58C1 carrying the silencing suppressor *p19* ($OD_{600}=1$). The gene expression profile of suberin-related genes was then examined six days after infiltration. Each data point represents the mean \pm SE of two to three independent biological replicates, with each replicate comprising three infiltrated leaves. The ‘*’ indicates a significant difference at $p \leq 0.05$ (Student’s *t*-test) between the *ProAtUbi::GFP* and the gene of interest.

From our RNA-seq dataset (Straube et al., not published), we selected the four most promising candidates for the initiation of russeting and overexpressed them in *N. benthamiana* leaves. 35S::*MYB93* was used as a positive control for the functionality of our assay. The empty vector control infiltrations (*ProAtUbi*::*GFP*) did not show any observable macroscopic changes (Fig. 2A). Similarly, infiltrated spots that overexpressing *WOX4*, *MYB67*, and *WRKY56* showed no macroscopic visible alterations, resembling the empty vector control (Fig. 2A-D). In contrast, infiltrated spots overexpressing *MYB93* displayed pronounced suberization (Fig. 2E), while those overexpressing *MYB52* exhibited some chlorotic/necrotic spots on the youngest emerging infiltrated leaves (Fig. 2F).

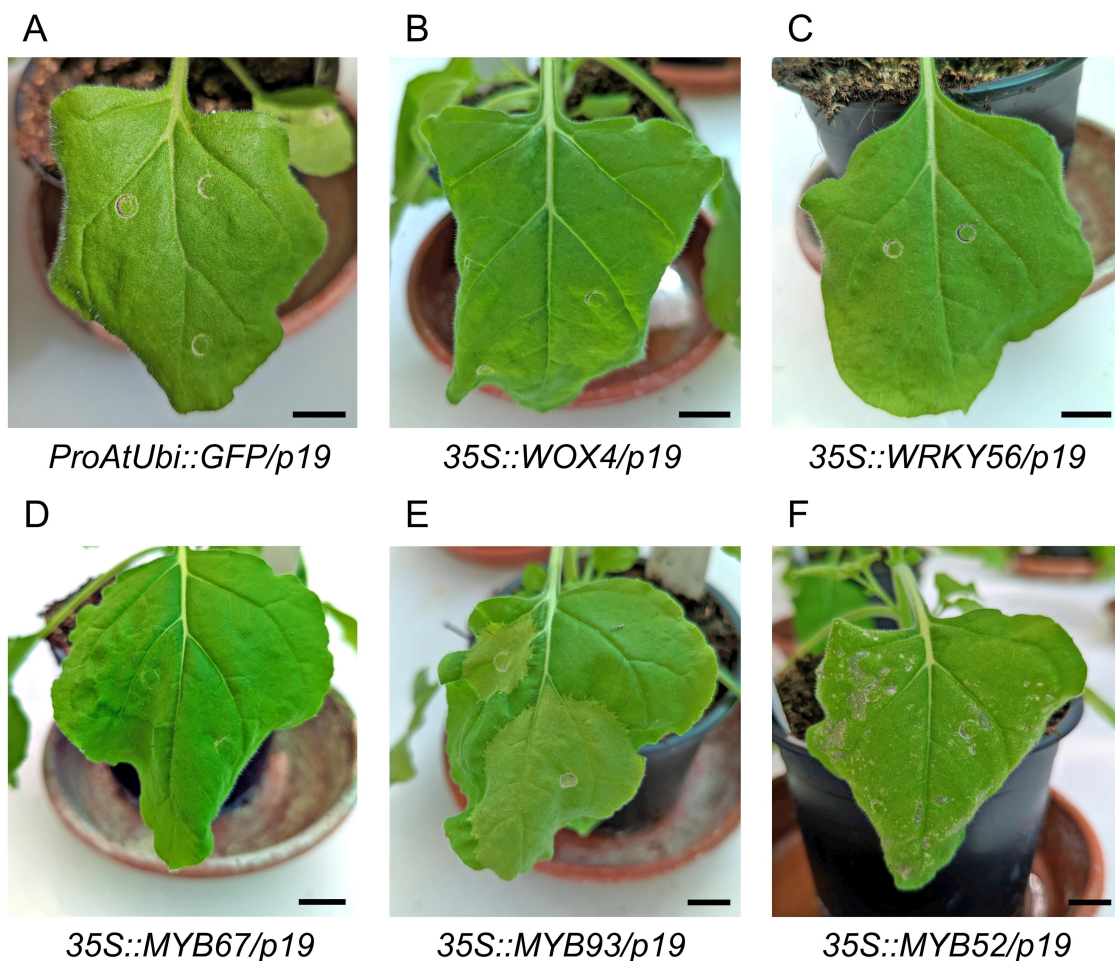


Figure 3. Macroscopic changes observed after heterologous overexpression of *MYB52*, *MYB67*, *MYB93*, *WOX4*, and *WRKY56* in *N. benthamiana*. Three-week-old *N. benthamiana* leaves were infiltrated with GV3101 ($OD_{600}=0.8$) carrying either (A) the empty vector (*ProAtUbi*::*GFP/p19*) or the following transcriptional regulators: (B) *WOX4* (*35S*::*WOX4/p19*), (C) *WRKY56* (*35S*::*WRKY56/p19*), (D) *MYB67* (*35S*::*MYB67/p19*), (E) *MYB93* (*35S*::*MYB93/p19*), and (F) *MYB52* (*35S*::*MYB52/p19*) along with C58C1 containing *p19* ($OD_{600}=1.0$) ($n = 3$). Macroscopic changes were observed six days after infiltration. Black scale bars represent a length of 1 cm.

To test whether periderm associated processes are activated, we performed expression analysis of suberin-associated genes in *N. benthamiana* leaves overexpressing the candidate genes together with the silencing suppressor *p19* (Fig. 4). We observed minimal upregulation of suberin genes, with the exception of the well-established suberin master regulator *MYB93*. However, there was a slight increase in the expression of *KCS2* when *WRKY56* and *WOX4* were overexpressed, along with *FCoAT*, *FAR3_1*, and *FAR3_2* through the involvement of *MYB52*.

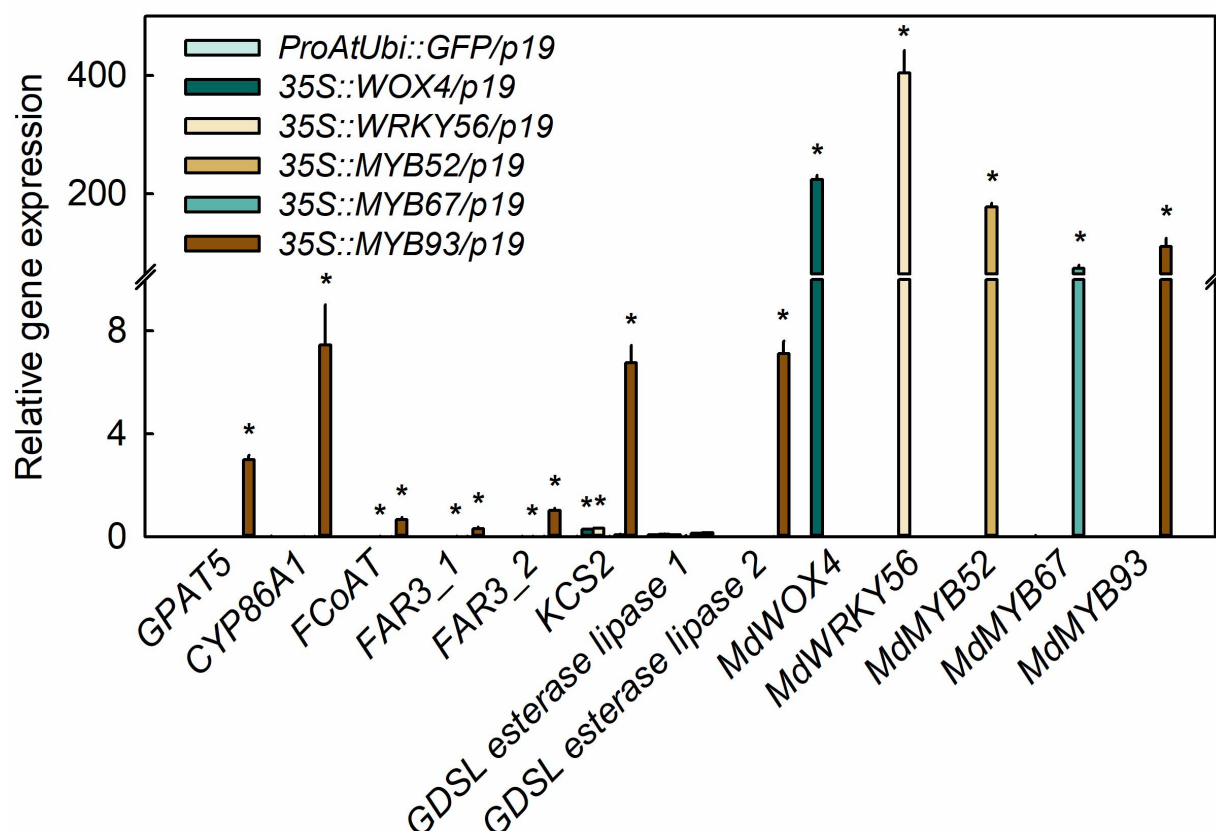


Figure 4. Gene expression profile of suberin-related genes in *N. benthamiana* leaves overexpressing *MYB52*, *MYB67*, *MYB93*, *WOX4*, and *WRKY56* with *p19*. *N. benthamiana* leaves were infiltrated with GV3101 ($OD_{600}=0.8$) carrying either the empty vector (*ProAtUbi::GFP/p19*) or the following transcriptional regulators: *WOX4* (*35S::WOX4/p19*), *WRKY56* (*35S::WRKY56/p19*), *MYB67* (*35S::MYB67/p19*), *MYB93* (*35S::MYB93/p19*), and *MYB52* (*35S::MYB52/p19*) along with C58C1 containing *p19* ($OD_{600}=1.0$) ($n = 3$). Gene expression profiles of suberin-related genes were evaluated six days after infiltration. Each value represents the mean \pm SE of three independent biological replicates, with each replicate consisting of three infiltrated leaves. Statistical significance ($p \leq 0.05$, Student's *t*-test) is indicated by asterisks, highlighting the significant difference between the *ProAtUbi::GFP* control and the gene of interest.

Phenotypic observations of *MYB52* overexpression were repeated. Infiltration experiments were performed using different OD₆₀₀ values for the GV3101 strain carrying *35S::MYB52* or the empty vector *ProAtUbi::GFP* together with *p19*. In this experiment, despite a reduction in necrotic reactions (5/27 leaves with necrotic spots, even at the lowest OD₆₀₀), we noticed a distinct glossy surface on the dorsal side of all infiltrated areas (Figure 5A). This characteristic was not observed on control infiltrated leaves. Furthermore, the leaves infiltrated with *MYB52* showed strong curling.

In a subsequent experiment, we repeated the infiltrations using an OD₆₀₀ of 0.8 in four-week-old *N. benthamiana* plants (Fig. 5B). In this case, we observed no formation of necrotic spots and no leaf curling in both the *MYB52* infiltrated leaves and the control leaves. However, similar to the previous experiment, we noticed the presence of a shiny surface on the dorsal side of the *35S::MYB52* areas infiltrated, which was absent in the control leaves.

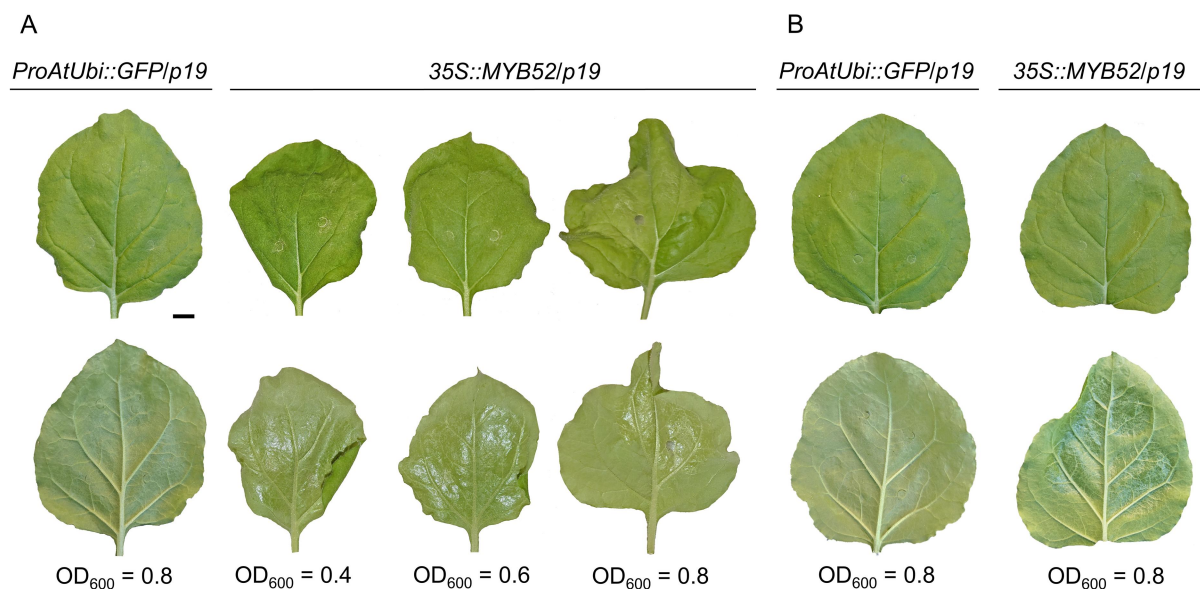


Figure 5. Overexpression of *MYB52* in *N. benthamiana* leaves results in a conspicuous shiny appearance on the dorsal side. (A) Three-week-old *N. benthamiana* leaves, still attached to the plant, were subjected to infiltration with GV3101 at different concentrations (OD₆₀₀=0.4, OD₆₀₀=0.6, OD 0.8) carrying either the empty vector (*ProAtUbi::GFP/p19*) or the transcriptional regulator *MYB52* (*35S::MdMYB52/p19*) and C58C1 carrying *p19* (OD₆₀₀=1) ($n = 3$). (B) Four-week-old attached leaves of *N. benthamiana* were infiltrated with GV3101 (OD₆₀₀=0.8) carrying the empty vector (*ProAtUbi::GFP/p19*) or the transcriptional regulator *MdMYB52* (*35S::MdMYB52/p19*), together with C58C1 carrying *p19* (OD₆₀₀=1) ($n = 3$). Macroscopic images of the ventral and dorsal side of representative infiltrated leaves were taken six days after infiltration. Macroscopic images of the ventral and dorsal side of representative infiltrated leaves were taken six days after infiltration. The black scale bar in Figure A represents a length of 1 cm.

Studies in *Arabidopsis thaliana*

We generated several transgenic lines overexpressing the candidate genes associated with russeting. Furthermore, additional complementation lines have also been generated. Currently, the majority of these lines are still in a heterozygous state and need to be propagated to the T2 generation to allow the identification of homozygous plants (Table 1).

Table 1. List of transformed *A. thaliana* lines and their status. OE = overexpression; CO = complementation.

Name	Background	Vector	Gene ID	Accession	Generation	Purpose
35S::MYB17_OE	Col-0	C757	MYB17	HF15264	T1	OE
35S::MYB52_OE	Col-0	C757	MYB52	HF24488	T1	OE
35S::MYB93_OE	Col-0	C757	MYB93	HF40961	T1	OE
35S::WRKY56_OE	Col-0	C757	WRKY56	HF14837	T1	OE
35S::WOX4_OE	Col-0	C757	WOX4	HF13050	T1	OE
35S::MYB67_OE	Col-0	C757	MYB67	HF11445	T2	OE
<i>ProAtUbi::GFP</i>	Col-0	C757	-	-	T2	OE
35S::MYB17_CO	SALK_020792	C757	MYB17	HF15264	T0	CO
<i>MYB17mu_empty_CO</i>	SALK_020792	C757	-	-	T0	CO
35S::MYB52_CO	SALK_118938	C757	MYB52	HF24488	T0	CO
<i>MYB52mu_empty_CO</i>	SALK_118938	C757	-	-	T0	CO
35S::WRKY56_CO	SALK_130727	C757	WRKY56	HF14837	T0	CO
<i>WRKY56mu_empty_CO</i>	SALK_130727	C757	-	-	T0	CO
35S::WOX4_CO1	GK-462 G 01.02	C757	WOX4	HF13050	T0	CO
<i>WOX4mu_empty_CO1</i>	GK-462 G 01.02	C757	-	-	T0	CO
35S::WOX4_CO2	GK-462 G 01.03	C757	WOX4	HF13050	T0	CO
<i>WOX4mu_empty_CO2</i>	GK-462 G 01.03	C757	-	-	T0	CO
35S::WOX4_CO3	GK-462 G 01.07	C757	WOX4	HF13050	T0	CO
<i>WOX4mu_empty_CO3</i>	GK-462 G 01.07	C757	-	-	T0	CO
35S::WOX4_CO4	GK-462 G 01.08	C757	WOX4	HF13050	T0	CO
<i>WOX4mu_empty_CO4</i>	GK-462 G 01.08	C757	-	-	T0	CO
35S::WOX4_CO5	GK-462 G 01.10	C757	WOX4	HF13050	T0	CO
<i>WOX4mu_empty_CO5</i>	GK-462 G 01.10	C757	-	-	T0	CO
35S::MYB67_CO1	GK-765A08.01	C757	MYB67	HF11445	T2	CO
<i>MYB67mu_empty_CO1</i>	GK-765A08.01	C757	-	-	T2	CO
35S::MYB67_CO2	GK-765A08.02	C757	MYB67	HF11445	T2	CO
<i>MYB67mu_empty_CO2</i>	GK-765A08.02	C757	-	-	T2	CO
35S::MYB67_CO3	GK-765A08.03	C757	MYB67	HF11445	T2	CO
<i>MYB67mu_empty_CO3</i>	GK-765A08.03	C757	-	-	T2	CO

Interestingly, during the screening of *Arabidopsis* mutants we observed differences in suberization levels in the hypocotyl region of *MYB67* mutants, compared to *Arabidopsis* Col-0 by histological analysis (Figure 6A,B). This finding was further confirmed in two other *MYB67* mutant lines (GK-765A08.02, GK-765A08.03) through microscopic examination (data not shown). Complementation lines for the three *MYB67* mutant lines are currently being generated (Table 1).

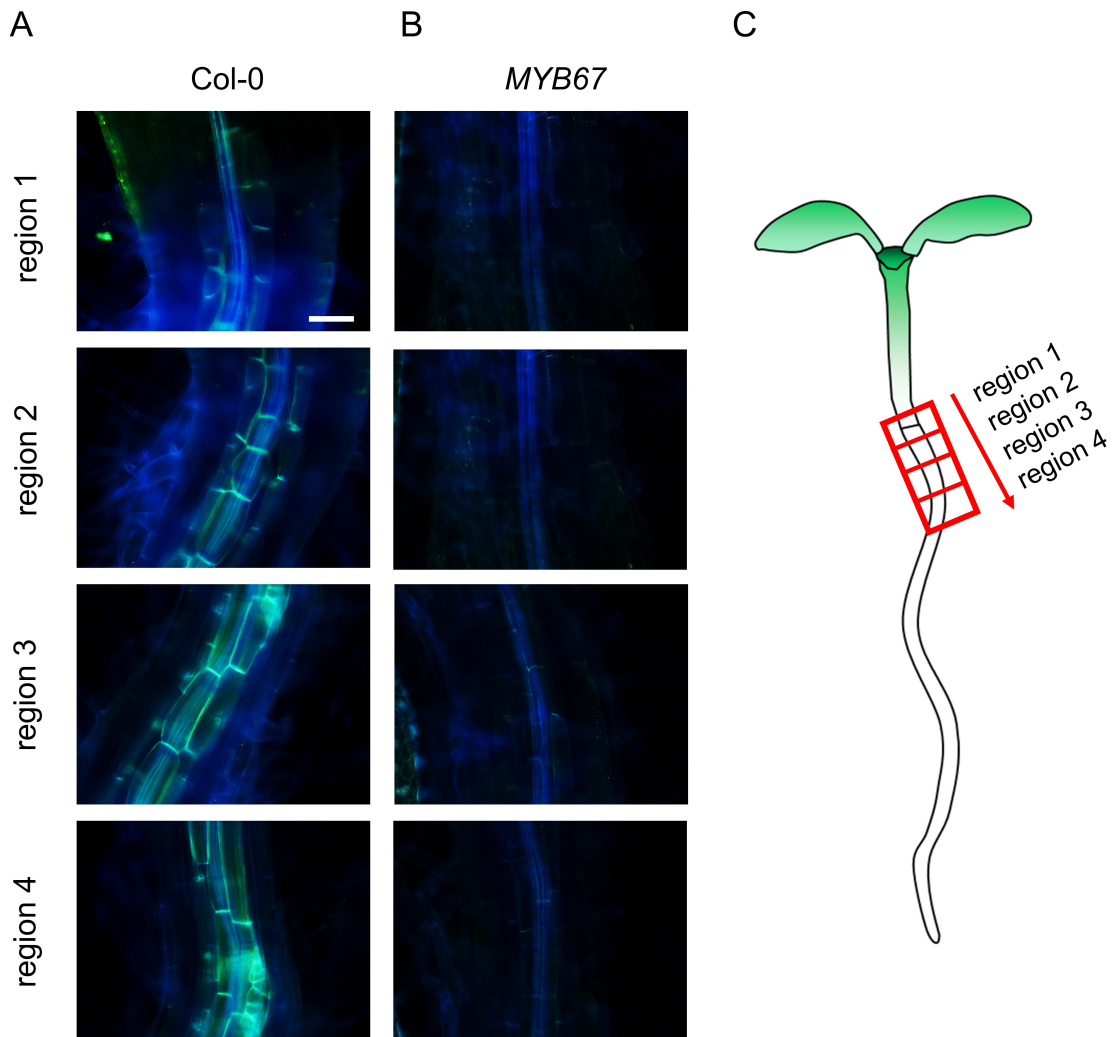


Figure 6. Microscopic observation of visible suberin deficiency in *MYB67* mutants. A. *thaliana* Col-0 and a *MYB67* mutant (GK-765A08.01) were grown on ½ MS medium for two days in the dark, followed by five days under continuous light. To evaluate suberization at the hypocotyl/root interface, seedlings were stained with Fluorol Yellow 088 and examined under incident fluorescent light through a U-MWU filter. (A) Microscopic observation of suberin formation in *Arabidopsis* Col-0 seven days after soawing ($n = 10$). (B) Microscopic observation of suberin formation at the hypocotyl/root border in the *MYB67* mutant (GK-765A08.01) ($n = 10$). (C) The illustration depicts the orientation of the regions selected for microscopic observations (regions 1-4). The scale bar in (A) is 1 cm and applies to all microscopic images.

Discussion

The discussion primarily revolves around two main aspects: (1) the preliminary results obtained in this work, and (2) the future implications that can help establish the involvement of the studied factors in russeting formation.

The preliminary results presented in this research provide important insights into the mechanisms potentially associated with russeting. Previous studies have demonstrated the upregulation of *MdMYB52* (HF31835; MD05G1011100) in mature russeted fruit skins (Legay et al., 2015; Legay et al., 2017; Falginella et al., 2021) and its binding to the promoter sequence of *MdOSC5*, a gene involved in the synthesis of lupane-type triterpenes (Falginella et al., 2021). In addition, *MdMYB52* has been characterized for its role in lignin synthesis (Xu, X. et al., 2022). Interestingly, we identified a distinct variant of the *MYB52* gene (HF24488; MD14G1242300) located on a different chromosome (chromosome 14) than the previously reported gene.

Overexpression of *MYB52* in our study resulted in distinct phenotypic features, including partial cell death in the infiltrated areas of young *N. benthamiana* leaves and a consistent glossy appearance on the dorsal side. In *Arabidopsis*, the *MYB52* ortholog is known to negatively regulate pectin demethylesterification in seed coat mucilage (Shi et al., 2018; Ding et al., 2021). Therefore, it is plausible that overexpression of *MYB52* in *N. benthamiana* could lead to the negative regulation of primary cell wall enzymes, potentially contributing to the development of necrotic spots. The shiny appearance observed on the lower surface of the leaves could be attributed to the elevation of the cuticle as a result of the disintegration of the underlying cell walls. It is also worth considering that the shiny surface on the dorsal side of the infiltrated areas could possibly be due to the deposition of waxes. These waxes may contribute to the reflective properties and enhance the shiny appearance observed on the leaf surface. A thorough microscopic examination, as well as expression analysis of cell wall and wax-associated genes, would provide a deeper understanding of the potential role of *MYB52*.

Several studies, including Legay et al. (2015), Falginella et al. (2021), André et al. (2022), Wang, Z. et al. (2022), and Straube et al. (not published), have consistently demonstrated the upregulation of *MYB67* during the later stages of russeting in apple fruit skins. Moreover, Lashbrooke et al. (2016) conducted a co-expression network analysis and demonstrated that *MYB67* and *WRKY56* serve as suberin-associated transcriptional regulators. Wang, Z. et al. (2022) further reported the upregulation of *WRKY56* in mature russeted fruit skins,

suggesting its potential involvement in russeting development. However, neither *MYB67* nor *WRKY56* significantly activated suberin genes, when overexpressed in *N. benthamiana*. Notably, loss-of-function mutants of *MYB67* in *A. thaliana* were suberin deficient. It would be interesting to conduct further studies in which these mutants are complemented with apple *MYB67* to determine whether the phenotype of wild-type Col-0 plants can be restored.

The available data on *WOX4* and *MYB17* are currently limited and require additional research to gain a comprehensive understanding. Although overexpression of *WOX4* in *N. benthamiana* does not result in macroscopically visible changes, it is worth noting that the orthologous gene from *A. thaliana* plays a crucial role as a regulator of cell division processes in the vascular cambium. Therefore, using the protocol established by Wunderling et al. (2018), it would be valuable to investigate the effects of apple *WOX4* overexpression in *A. thaliana* on the vascular cambium. Such observations may provide valuable insights into the potential involvement of *WOX4* in the development of russeting. *MYB17* shares homology with two other genes, *AtMYB16* (*MIXTA*) and *AtMYB106* (*NOECK*), which are known to be involved in petal epidermal patterning and trichome branching repression (Baumann et al., 2007; Jakoby et al., 2008). Moreover, *MYB16* has been investigated for its role in cuticle regulation in Arabidopsis (Oshima and Mitsuda, 2013). Thus, *MYB17* emerges as a compelling candidate for Phase I investigation. By studying *A. thaliana* plants overexpressing *MYB17* and examining loss-of-function mutants with a particular focus on cuticle and epidermal cell properties, it is possible to gain valuable insight into the processes observed during russet formation in Phase I, including microcracking and thinning of the cuticle layer.

Conclusion

The initial functional evaluation of candidate genes associated with russet initiation in apple fruit has identified *MYB52* as a promising candidate worthy of further investigation. Although apple *MYB67* has not yet shown significant effects, the suberin deficiency observed in *A. thaliana* loss-of-function mutants has attracted considerable interest. Detailed studies of these genes in stable transformed *A. thaliana* plants would be an important step in understanding their role in russet formation on apple.

Materials and methods

Plant material and transformation

Apple (*Malus x domestica*, Borkh.) fruits used in the study were obtained from 'Pinova' trees grafted on 'M9' rootstocks grown in experimental orchards at the Horticultural Research Station of Leibniz University in Ruthe (52° 14' N, 9° 49' E). *Nicotiana benthamiana* and *Arabidopsis thaliana* (L.) Heynh. plants were grown in a greenhouse on the campus of Leibniz University in Herrenhausen (52° 23' N, 9° 42' E) for transformation and propagation purposes.

A. thaliana T-DNA insertion lines carrying loss-of-function mutations in orthologous genes were obtained from the Nottingham Arabidopsis Stock Centre (Scholl et al., 2000).

Stable transformation of *A. thaliana* plants was performed using the floral dip method as described by Zhang et al. (2006). Details of the established *A. thaliana* lines are given in Table 1.

To study the root morphology, 7-day-old *A. thaliana* seedlings were used. The seeds were first immersed in 70% ethanol for 10 min and washed three times with autoclaved deionized water. Seed sterilization was performed under a sterile bench. The surface-sterilized seeds were then transferred to three slant agar plates containing ½ MS medium (0.5x MS salts and vitamins, 1% sucrose, 0.8% plant agar; pH = 5.7) and germinated in the dark at room temperature for 2 d, followed by seedling growth under 24 h light for 5 d at 22 °C according to Barberon et al. (2016).

RNA isolation

Russeted fruit skin patches from apples were excised with a razor blade, immediately frozen in liquid nitrogen, and stored at -80 °C. Each replicate contained skin patches from six fruits, totaling approximately 60-80 mg of tissue. Tissue was ground to a fine powder using a mortar and pestle and chilled in liquid nitrogen. Total RNA was extracted using the InviTrap Spin Plant RNA Mini Kit (STRATEC Molecular GmbH, Berlin, Germany) and Lysis Buffer RP according to the manufacturer's instructions. To remove residual DNA, the extracted RNA was treated with the DNA-free™ Kit (Thermo Fisher Scientific, Waltham, Massachusetts, USA).

Extraction of RNA from *N. benthamiana* leaves was performed 6 d after infiltration using the Zymo Quick-RNA Miniprep Kit (Zymo Research, Irvine, California, USA) according to the

manufacturer's instructions. For each plant, six leaf discs of 2 cm diameter taken from three infiltrated leaves were pooled.

The Nanodrop 2000c spectrophotometer (Thermo Fisher Scientific, Waltham, Massachusetts, USA) was used to assess the quantity and purity of RNA by measuring the absorbance at 230 nm, 260 nm, and 280 nm. The integrity and purity of the RNA was also confirmed by running the samples on a 1.5% agarose gel.

Cloning of target genes

The coding sequences (CDS) of candidate genes associated with russeting in apple fruit skins were obtained from the HFTH1 genome available in GDR (Genome Database for *Rosaceae*, Jung et al., 2019). To amplify the target genes from 'Pinova' cDNA samples derived from russeted tissue, we used proofreading Phusion® High-Fidelity DNA polymerase (New England Biolabs, Ipswich, Massachusetts, USA) and gene-specific primers (listed in Table S1) under optimized PCR conditions: one cycle of 98 °C for 120 s, 35 cycles of 98 °C for 30 s, 60 °C for 30 s, 72 °C for 120 s, and one cycle of 72 °C for 300 s. The resulting PCR fragments were separated on a 0.8% agarose gel, and specific bands were extracted using the Macherey-Nagel™ NucleoSpin™ Gel and PCR Clean-up Kit (Macherey-Nagel, Düren, Germany). The gene fragments were then directionally cloned into plasmid C757pGFPU10-35s-ocs-LH (C757) (DNA cloning service, Hamburg, Germany), which had been linearized with *Bam*HI (New England Biolabs, Ipswich, Massachusetts, USA) and *Hind*III (New England Biolabs, Ipswich, MA, USA) using the In-Fusion® HD Cloning Kit (Clontech, Takara Bio USA Inc., San Jose, California, USA). The vector contains a *green fluorescent protein (GFP)* gene under the control of the *Arabidopsis ubiquitin promoter (ProAtUbi::GFP)* and a *35S* promoter upstream of the multiple cloning site (*35S::GOI* (gene of interest)), which drives the expression of the GOI. The resulting plasmids were extracted using the NucleoSpin™ Plasmid (NoLid) Kit (Macherey-Nagel, Düren, Germany) and sent to Microsynth SeqLab GmbH (Göttingen, Germany) for Sanger sequencing. The plasmids were then used for transformation of *Rhizobium radiobacter* GV3101 by electroporation.

Heterologous overexpression in *N. benthamiana*

Rhizobium radiobacter-mediated overexpression was used to study possible function of candidate genes in periderm related processes. Single bacterial colonies of the two *Rhizobium radiobacter* strains GV3101 (*ProAtUbi::GFP*, *35S::MYB17*, *35S::MYB52*, *35S::MYB67*, *35S::MYB93*, *35S::WOX4*, *35S::WRKY56*) and C58C1 (*35S::p19*) were

transferred into YEP liquid medium (yeast extract (10 g l⁻¹), tryptone (10 g l⁻¹), NaCl (5 g l⁻¹); pH = 7.5) containing streptomycin (100 mg l⁻¹), spectinomycin (100 mg l⁻¹) and rifampicin (50 mg l⁻¹) or kanamycin (50 mg l⁻¹) and rifampicin (100 mg l⁻¹). Bacterial cultures were grown under continuous agitation at 120 rpm and 28 °C for 24 h. Fresh YEP liquid medium was inoculated with 1% of the final volume of the grown bacterial culture. Bacterial cultures were grown under continuous agitation at 120 rpm and 28 °C for 24 h.

To establish the infiltration assay, initial experiments were conducted as follows. First, leaves of three-week-old *N. benthamiana* were detached and infiltrated with GV3101 carrying *ProAtUbi::GFP*, *35S::MYB52*, *35S::MYB93* or *35S::WRKY56* (OD₆₀₀ = 0.5), which were resuspended in infiltration buffer (10 mM MES, 10 mM MgCl₂ x 6H₂O, pH = 5.6). The infiltrated leaves were then incubated in a plastic box with a wet paper towel. Second, leaves of three-week-old *N. benthamiana*, still attached to the plants, were infiltrated with GV3101 carrying the empty vector (*ProAtUbi::GFP*) or *MYB93* (*35S::MYB93*) (OD₆₀₀ = 0.8), with or without C58C1 carrying the pBin61 vector with *p19* (*35S::p19*) (OD₆₀₀ = 1.0) as a silencing suppressor of the tomato bushy stunt virus.

For the initial characterization of the candidate genes, the following experiments were performed. First, attached leaves of three-week-old *N. benthamiana* were infiltrated with GV3101 carrying the empty vector (*ProAtUbi::GFP*) or the transcriptional regulators *WOX4* (*35S::WOX4/p19*), *WRKY56* (*35S::WRKY56*), *MYB52* (*35S::MYB52*), *MYB67* (*35S::MYB67*), *MYB93* (*35S::MYB93*) (OD₆₀₀ = 0.8), and C58C1 carrying *p19* (OD₆₀₀ = 1). Second, leaves of three-week-old *N. benthamiana* were infiltrated with GV3101 carrying the empty vector (*ProAtUbi::GFP*) or the transcriptional regulator *MYB52* (*35S::MYB52*) at different bacterial densities (OD₆₀₀ = 0.4, OD₆₀₀ = 0.6, OD₆₀₀ = 0.8), together with C58C1 carrying *p19* (OD₆₀₀ = 1). Finally, four-week-old *N. benthamiana* leaves were infiltrated with GV3101 carrying the empty vector (*ProAtUbi::GFP*) or the transcriptional regulator *MYB52* (*35S::MYB52*) (OD₆₀₀ = 0.8) along with C58C1 carrying *p19* (OD₆₀₀ = 1).

All bacteria were suspended in the identical infiltration buffer used in the first infiltration experiment. Three to four plants were used for each infiltration experiment, with three leaves infiltrated for each construct. After infiltration, all treated leaves were incubated for six days.

Quantitative real-time PCR

Quantitative real-time PCR (qPCR) was performed using a QuantStudio™ 6 Flex Real-Time PCR System (Applied Biosystems, Waltham, MA, USA) according to the protocol described by Straube et al. (2020). Gene-specific primers are listed in Table S2. Gene expression levels were determined using the method described by Pfaffl (2001) with minor modifications

as described by Chen, Y.-H. et al. (2019). To normalize the gene expression data, we used *uridylylate kinase (UK)* and *sand family protein (SAND)* as reference genes (Liu et al., 2012) (Table S2). Each data point is based on three independent replicates, each with two to three technical replicates.

Histological observations

Observations on root morphology and suberin accumulation in *A. thaliana* roots were made as follows. 7-d-old seedlings grown on slant agar plates (see plant material and transformation section) were picked up with forceps, and the remaining media was removed before transferring the seedlings into Petri dishes. The seedlings were then covered with Fluorol Yellow 088 (Santa Cruz Biotechnology, Texas, USA) staining solution (0.005% Fluorol Yellow 088 in lactic acid) and stained at 70 °C for 30 min. After staining, the seedlings were counterstained with aniline blue staining solution (0.5% in deionized water) at room temperature for 30 min. The seedlings were gently rinsed with deionized water and transferred to microscope slides. Histological observations were carried out using a fluorescence microscope (BX60; Olympus, Hamburg, Germany) under incident fluorescence light with an excitation wavelength of 330-385 nm and an emission wavelength of 420 nm (U-MWU; Olympus, Hamburg, Germany). Calibrated images were captured using a digital camera (DP73; Olympus, Hamburg, Germany).

Acknowledgments

We express our gratitude to Sylvain Legay for generously providing the plasmid containing the *MdMYB93* sequence used in this project. We are very grateful to Marco Herde and Markus Niehaus for their contribution in providing the C58C1 carrying the *p19* silencing suppressor. We would also like to thank Julia Schröter for her valuable technical advice and support throughout the project.

Author Contributions

Conceptualization, J.S., and T.D.; funding acquisition, M.K. and T.D.; project administration, M.K. and T.D.; methodology, J.S. and T.D.; investigation, J.S., and J.G.; supervision, M.K. and T.D.; data curation, J.S.; validation, J.S.; visualization, J.S.; formal analysis, J.S.; writing—original draft, J.S.; writing—review and editing, J.S., M.K. and T.D.

Funding

This research was supported by following grants from the German Research Foundation (DFG): DE 511/9-1, DE 511/9-2.

Conflicts of Interest

There are no known competing interests that could influence the work reported in this paper.

7.1 Supplementary data Chapter 7

Electronical File E10. Sequence and alignment of *WRKY56* (HF14837) used in this study. (access through electronical appendix)

Electronical File E11. Sequence and alignment of *WOX4* (HF13050) used in this study. (access through electronical appendix)

Electronical File E12. Sequence and alignment of *MYB17* (HF15264) used in this study. (access through electronical appendix)

Electronical File E13. Sequence and alignment of *MYB52* (HF24488) used in this study. Comparison between the *MYB52* identified by Xu, X. et al. (2022) and the *MYB52* presented in this study. (access through electronical appendix)

Electronical File E14. Sequence and alignment of *MYB67* (HF11445) used in this study. (access through electronical appendix)

Electronical File E15. Sequence and alignment of *MYB93* (MDP0000320772) used in this study. (access through electronical appendix)

Table S1. List of primers used in this study for In-Fusion® cloning of gene fragments into the C757pGFPU10-35s-ocs-LH vector. Start codon is highlighted in red and stop codon is highlighted in blue.

Gene name	Accession	Primer sequence (5'-3')		Product size (bp)	Reference
		Forward Primer	Reverse Primer		
Phase I related					
<i>MYB17</i>	HF15264	GACTACTAGTTGGATC ATG GGG AGGACTCCATGTTGTG	CGACACGCGTAAGCT TC AGAGG GGCAAATGAAAGAATTG	1133	This study
Phase II related					
<i>MYB52</i>	HF24488	GACTACTAGTTGGATC ATG TGCA CTAGAGGCCATT	CGACACGCGTAAGCT TTA TGAA GAAGTCCCATTATTAACA	890	This study
<i>MYB67</i>	HF11445	GACTACTAGTTGGATC ATG GGC CACCGCTGCTGC	CGACACGCGTAAGCT CTA AATAT CTCCATGCAAATTACAC	1060	This study
<i>MYB93</i>	MDP0000320772	GACTACTAGTTGGATC ATG GGAA GATCTCCTTGTTGTG	CGACACGCGTAAGCT TTA AAGCA ATCTCATTGAAAAAAGGG	1115	This study
<i>WOX4</i>	HF13050	GACTACTAGTTGGATC ATG GGAA TGAGCAGCATGA	CGACACGCGTAAGCT TC ATCTT CTTCCTTCTGGATGT	776	This study
<i>WRKY56</i>	HF14837	GACTACTAGTTGGATC ATG GAG GATCATCATCAACAGCA	CGACACGCGTAAGCT TTA AAAC CTAGAGAGGAACTGCA	745	This study

Table S2. List of primers used for qPCR in this study.

Gene name	Accession	Primer sequence (5'-3')		PCR efficiency (%)	Reference
		Forward Primer	Reverse Primer		
<i>GPAT5</i>	Nbv5tr6232718	TCATGCAACAACAGCTAGGG	ACGTGGCTTCTACTGGCAAC	N.D.	(Legay et al., 2016)
<i>CYP86A1</i>	Nbv5tr6408715	GGAGCGTCATGAACAATCG	AGGGACCGAAGGGTACAGAC	N.D.	(Legay et al., 2016)
<i>FCoAT</i>	Nbv5tr6212895	TTCATGGCAAATGAGAGCTG	TGTGGCTTTGCCAGAGAAG	N.D.	(Legay et al., 2016)
<i>FAR3_1</i>	Nbv5tr6203423	CTGACGATCCGACCTGGTAT	CGACCCTAAAGCCGTTATTG	N.D.	(Legay et al., 2016)
<i>FAR3_2</i>	Nbv5tr6203422	TACCTTCAACCCAACCAGGA	TTATGGATGGCCAAACACCT	N.D.	(Legay et al., 2016)
<i>KCS2</i>	Nbv5tr6245119	CCAATTTTCATCCATCCAAGG	ATTGCATTTGGCTCAGGATT	N.D.	(Legay et al., 2016)
<i>GDSL esterase/lipase 1</i>	Nbv5tr6216569	TTTGCACATGTTCTGGAGA	TTGTCACTCACCCAGCTGAT	N.D.	(Legay et al., 2016)
<i>GDSL esterase/lipase 2</i>	Nbv5tr6222730	CAACGGATGATGTTGGACAG	AGTCGCCCATGTTCTGAATC	N.D.	(Legay et al., 2016)
<i>MYB52</i>	HF24488	CCCAAGAATCAACAGGAACCCT	GCCTTGCAATAACAGCCCATC	82.9	Straube et al., not published
<i>MYB67</i>	HF11445	ACATCTGGGCTTCTGGTACTG	TTCCATCTGATCCAAGAGCGT	89.4	Straube et al., not published
<i>MYB93</i>	MDP0000320772	TGGACAAACTATCTTAGGCCGG	GTTGCCGAGGATGGAATGGA	102.5	Straube et al. 2020
<i>WOX4</i>	HF13050	TGGTTCCAGAATCACAAGGCA	CCAGAGGAGTCGGTGTCTT	92.3	Straube et al., not published
<i>WRKY56</i>	HF14837	ATTAGTGGCTCTGCTGGGAAT	CGAGTCTGGAACGCAAACCT	90.8	Straube et al., not published
Reference genes					
<i>UK</i>	EH363935	CTAGGAGTATATTGGAAGAGCG	AAAGATACATCGCCTTGCTGAA	N.D.	(Liu et al., 2012)
<i>SAND</i>	Niben.v0.3.Ctg2518 8435	ACCACCAACACCTATGAATGCT	CAGTCTCGCCTCATCTGGGTCA	N.D.	(Liu et al., 2012)

8. General discussion

Overall, the purpose of this dissertation was to gain new insights into the early initiation and formation processes of russeting in apple fruit skins. During the course of this research, several important findings were uncovered:

(1) We developed a split fruit technique to investigate the russet formation and gained insight into the underlying mechanisms. Microcracks on apple fruit skins increase rapidly after exposure to moisture during early fruit development and decrease when moisture is removed. Microcrack formation is dependent on the developmental stage of the fruit. (Chapter 2)

(2) The formation of russeting in apple based on moisture exposure revealed a biphasic pattern (Phase I / Phase II) at the morphological level. Moisture-induced microcracking is associated with a decrease in the rate of cuticle deposition. (Chapter 3)

(3) Long-term exposure of apple fruit skins to moisture (Phase I) leads to downregulation of the processes involved in cutin/wax synthesis and deposition, while an increase in suberin synthesis begins after cessation of moisture exposure (Phase II). These effects were most pronounced during early fruit development, although some effects on cutin/wax synthesis and deposition were observed at later developmental stages. Interestingly, no effects on suberin synthesis and deposition were observed during these later stages. (Chapter 4)

(4) The formation of periderm on apple fruit skins, induced by either wounding or moisture, has similar morphological and molecular characteristics and sequences. From an experimental point of view, the use of wounding in apple fruit can be justified as a suitable model to study the processes related to periderm (russet) formation after the impairment of the cuticle (e.g. microcracks). (Chapter 5)

(5) Transcriptomic analysis revealed that genes associated with cell wall, cell division, cuticle formation, and abiotic stress, are dominantly affected by moisture exposure during Phase I. The sequence of transcriptomic changes during Phase II highlights the initiation process of meristematic tissue (phellogen) within the first few days after moisture removal, followed by the establishment of phellem cells and the subsequent impregnation of cell walls with suberin. Interestingly, we also identified a potential role for ABA in the development of russeting in apple, as well as new candidate genes that may contribute to this process. (Chapter 6)

(6) *MYB52* shows promising potential as a regulatory candidate that controls crucial cell wall or wax-related processes during the onset of russeting in Phase II. Moreover, *MYB67* is emerging an intriguing candidate with potential roles in the suberization process. (Chapter 7)

The results of this study provide new insights into the molecular mechanisms underlying russet formation in apple fruit. Our data reveal a previously unknown interplay between multiple signaling pathways and transcription factors that regulate the synthesis of cuticular lipids, suberin, and lignin. These findings provide a significant contribution to the scientific understanding of this complex physiological process and have the potential to inform the development of targeted strategies to reduce russeting in apple fruit. Such strategies could have far-reaching implications for the apple industry, including improved fruit quality as well as improved pre- and postharvest performance, resulting in reduced economic losses. This chapter discusses future perspectives for the study of apple russeting based on our findings.

8.1. Russet induction: Exploring opportunities for future study and advancement

Previous studies have explored the natural occurrence of russeting in fruits and provided valuable data on the development of periderm barrier properties such as suberin and lignin synthesis (Lashbrooke et al., 2015; Legay et al., 2015; Falginella et al., 2015; Legay et al., 2017; Yuan et al., 2019; Falginella et al., 2021; André et al., 2022; Wang, Z. et al., 2022) . However, the study of natural russeting lacks a well-defined starting point and does not provide information on the initial triggers for cuticular microcracking and subsequent periderm formation. By using russeting induction techniques involving moisture treatment and mechanical wounding, we have gained new insights into the underlying mechanisms at very early stages after the onset of the respective trigger. The biphasic behavior observed during russet induction based on moisture exposure, along with the ability to replicate Phase II by mechanical wounding, offers exciting prospects for further studies of the specific changes that occur during microcrack and periderm formation, especially at early time points.

8.1.1. Uncovering the mechanisms behind russet induction: Insights from Phase I studies and future perspectives

During Phase I of moisture induction, the appearance of cuticular microcracks is the defining characteristic of russeting, but the molecular and genetic factors responsible for this phenomenon remain unknown. Previous studies have identified several physiological factors that are crucial for microcrack formation. Primarily, reduced cuticle deposition combined with rapid surface expansion during early fruit development results in increased elastic strain, and leads to cuticular microcracking (Knoche et al., 2004; Peschel and Knoche, 2005; Lai et al., 2016) . In addition, the hydration status of the cuticle can alter its mechanical properties (Knoche and Peschel, 2006; Khanal and Knoche, 2017).

The mechanical properties of the fruit skin are determined by the underlying epidermal and hypodermal cell layers (Khanal and Knoche, 2014), with the size and arrangement of these cells influencing susceptibility to russeting (Khanal et al., 2020b). As fruits grow, tension forces increase in the tangential direction of the skin. This tension causes a reorientation of the epidermal cells, resulting in a shift from anticlinal to periclinal cell walls (Knoche and Lang, 2017). This change likely disrupts down cell-cell adhesion, increasing strain in the cuticle above the anticlinal cell walls and leading to microcrack formation in these regions (Knoche et al., 2018). One possible factor involved in the arrangement of the epidermal cell structure is *SHN3* (Aharoni et al., 2004; Shi et al., 2011; Shi et al., 2013), which was one of the first genes to be downregulated in our experiments and has been implicated in apple russeting in recent studies (Lashbrooke et al., 2015).

In our induction experiments, microcrack formation was observed solely in the region of the anticlinal cell walls, consistent with previous studies (Knoche et al., 2018). Cuticle thickness was largely reduced above the anticlinal epidermal cell walls compared to the periclinal walls, and strain in the cuticle increased over time upon exposure to moisture. This increase in strain is likely due to decreased cutin and wax synthesis, which was confirmed at the expression and metabolic levels. Wax embedded in the cutin polymer matrix is the primary mechanism for strain fixation (Khanal et al., 2013a). Microcracks appeared in the outer part of the cuticle within 2 d of moisture exposure and gradually traversed the entire cuticle after 6 d. This pattern is likely due to a radial gradient of strain observed in apple fruit cuticles, where the outer cuticle is more strained than the inner parts (Khanal et al., 2014).

The high-resolution transcriptomic data presented in Chapter 6 shed new light on the molecular processes underlying microcrack formation. In particular, the data show a decrease in the expression of genes involved in cell wall synthesis, cell division, and cuticle synthesis, which are likely to be key factors in microcrack formation. When cell division is restricted, there are fewer cells per unit surface area, which may result in a weaker cellular structure for the cuticle (Khanal and Knoche, 2017). This could lead to increased loosening of cell-cell adhesion during periods of tensional stress, which has been suggested as a driving factor for microcrack formation (Knoche and Lang, 2017; Knoche et al., 2018).

Of particular interest for future research investigating the genetic basis of susceptibility to cuticular microcracking in apples are the earliest downregulated genes during Phase I, *MYB17* and *NAC35*. Furthermore, given the importance of *SHN3* in the regulatory network, it would be valuable to perform a detailed characterization of all genes that are co-expressed with *SHN3*. A promising method to investigate these co-expression patterns could be a weighted correlation network analysis (WGCNA) (Langfelder and Horvath, 2008). By

applying WGCNA to our transcriptomic data, it would be possible to identify distinct modules of co-expressed genes and gain insight into potential regulatory mechanisms involving *SHN3*.

Our work has highlighted several open questions regarding microcracking. The induction method presented here may provide a means to address some of these questions, and the following issues should be addressed next:

- What is the underlying mechanism that leads to decreased cuticle biosynthesis upon exposure to moisture?
- Which genetic factors primarily determine the arrangement of epidermal and hypodermal cellular structures?
- How are the repair mechanisms regulated that address the formation of microcracks that not traverse the cuticle, such as the deposition of waxes that was reported by Curry (2009)?
- How does external application of phytohormones such as gibberellin A_{4+7} prevent microcracking of the cuticle?
- What is the regulation of cell division processes in apple fruit skin and how do they contribute to microcrack formation?

Addressing these questions will improve our understanding of the mechanisms underlying microcracking in apple fruit skins and ultimately lead to the development of new strategies to prevent or mitigate this problem.

8.1.2. Unraveling the mechanism of russet induction in Phase II: Insights into the underlying processes

During Phase II of moisture induction, the main characteristic is the formation of a periderm in the hypodermis in close proximity to microcracks. The formation of periderm beneath microcracks in the hypodermis was previously reported by Bell (1937), Meyer (1944b), and Pratt (1972). However, the spatio-temporal sequence during the onset of russetting in apple fruit skin has not been addressed. In order to distinguish between the processes involved in the formation of meristematic cells (phellogen), the dedifferentiation into multiple cell layers (phellem), and the impregnation of cell walls with suberin and lignin, it is crucial to develop a time course for the formation of a periderm. In addition, none of the previous literature has focused on the potential triggers of these processes. By inducing russetting through moisture and wounding, we were able to determine the sequence of periderm initiation and identify potential triggers.

Our studies have shown that a minimum of 6 d exposure to Phase I conditions is required to initiate russeting in Phase II. This exposure time is critical for the development of microcracks that traverse the cuticle, indicating that the underlying epidermal cells must be exposed to initiate russet formation. Regardless of the duration of Phase I exposure (which ranged from 6 to 16 d), a minimum of 4 d was required to observe the first suberized phellem cells following wound exposure to atmospheric conditions. Similar observations were made in potato, where phellogen formation was observed 3 d after wounding and multiple phellem stacks were formed at 19 d after wounding (Serra et al., 2022). Similarly, in *Arabidopsis* hypocotyl, phellogen formation was observed 13 d after sowing, with the first phellem cells appearing 18 d after sowing (Wunderling et al., 2018).

Our findings suggest that exposure of the wound to atmospheric conditions, rather than the wound itself, is the trigger for periderm initiation. Possible triggers at this point include changes in gas levels (O_2 , CO_2), a negative water potential, and changes in tissue pH. Early studies of wound periderm formation in potato also identified oxygen as a necessary factor for suberization (Priestly and Woffenden, 1923; Herklots, 1924; Lipton, 1967), as well as a potential driving force for phellogen initiation in *Eucalyptus camaldulensis* (Liphschitz and Waisel, 1970). In addition, pH was found to be a determining factor for the initiation of meristematic tissue and the degree of suberization in potato wound periderm (Herklots, 1924). Our transcriptomic data showed an upregulation of stress-related genes, suggesting an increase in oxidative stress, which may further indicate the involvement of oxygen.

In a study conducted by Vulavala et al. (2019), the use of laser capture dissection and RNA-Seq analysis enabled the generation of a comprehensive transcriptomic dataset specifically focused on potato phellogen. Building on their findings, our own experiments have observed phellogen formation in response to moisture removal, and our induction system provides a valuable tool for exploring its precise functionality. By integrating the russet induction method with the precise dissection of cell types such as phellogen and phellem, in combination with cell type-specific RNA-seq analysis, we would now be able to gain a comprehensive understanding of the molecular events underlying apple russeting. Remarkably, these events can be followed within minutes after exposing the wound to the atmosphere.

Our transcriptomic analysis identified several potential factors that are likely involved in the initiation of russeting at the molecular level. In particular, *WOX4* and *MYB84* emerged as the most promising candidates for the early stages of periderm formation. Research on orthologous genes suggests that these factors may play a role in phellogen initiation or cell division (Wunderling et al., 2018; Zhang, L. et al., 2019; Xiao et al., 2020). Understanding the regulation of cell division processes that lead to phellem cell formation is crucial. To achieve

this, it is essential to select appropriate time points during the first three days after exposure of a wound to atmospheric conditions.

A strong activation of ABA genes (*LEA*, *AP2B3*) has been observed after removal of moisture. ABA is a phytohormone produced during abiotic stress, and its importance for the suberization process has been demonstrated in *Arabidopsis* and kiwifruit (Barberon et al., 2016; Wei et al., 2020; Xu, H. et al., 2022). Further investigations using our induction system to examine the role of ABA in apple russetting is a necessary step to gain a better understanding of the triggering process. Possible tools for this would be the application of ABA inhibitors such as ABA Antagonist1 (AA1) (Ye et al., 2017) or fluoridone (Cox et al., 2004).

Our induction systems also provide a means to narrow down the spatio-temporal deposition of lignin (*MYB42*, *MYB52*) and suberin (*MYB93*, *SGNH*), providing additional information on the synthesis, polymerization process, and the attachment of the suberin polymer to the primary cell wall. A co-expression analysis using the WGCNA developed by Langfelder and Horvath (2008) on the genes analyzed in our study could be useful to identify additional candidate genes. To elucidate the specific roles of the candidate genes in these processes, we started to investigate their function using heterologous expression systems like *N. benthamiana*, stable transformed *Arabidopsis*, and *Arabidopsis* complementation lines for loss-of-function mutants of the orthologs. Although transformation and regeneration of apple fruit is time-consuming due to the long juvenile phase (between four to eight years) (Visser, 1964), hairy roots can serve as a useful model to study the function of candidate genes in apple (Wu et al., 2012; Stanišić et al., 2019).

8.2. Advancing functional characterization models for russetting in apple

Functional characterization of fruit-related traits, such as russetting, remains a challenging task due to several bottlenecks. To overcome these obstacles, future research should prioritize the development of new techniques and methods. Heterologous expression systems, such as transient infiltration in *N. benthamiana* or the use of genetically modified *A. thaliana* plants, as demonstrated in our preliminary studies, can provide insight into some aspects of fruit function. However, to gain a comprehensive understanding of fruit traits, it is essential to develop specific approaches that are optimized to study these processes directly in apples. Therefore, it is critical to utilize innovative strategies that can reveal the underlying molecular mechanisms of fruit traits in apples.

Scientists have employed several techniques to overcome the challenges associated with studying apple fruit traits. These methods include stable transformation of apple trees using

CRISPR-Cas9-mediated gene editing to introduce mutations (Nishitani et al., 2016) as well as *Agrobacterium*-mediated gene transfer (Vanblaere et al., 2011; Kost et al., 2015). One prominent example is the Arctic apple, where several polyphenol oxidase (PPO) genes were silenced to obtain non-browning fruit (Carter, 2012; Stowe and Dhingra, 2021). In addition, studies have investigated transient expression systems within the apple (Zhang et al., 2022; Wang et al., 2023), pear (Wang, Y. et al., 2022) or sand pear (Shi et al., 2021) peel to further improve our understanding of fruit traits such as russeting. In addition, researchers have explored the use of CRISPR-Cas9 to generate transformed callus and virus-induced gene silencing (VIGS) in apple fruit, as a means to study fruit-related traits (Jiang, S. et al., 2019; Zhou et al., 2022). Using these methods to investigate the molecular sequence of russet initiation may be a viable approach.

Another potential approach to accelerate the study of russet initiation is the use of the transgenic apple line T1190, which has a shorter juvenile phase resulting due to the overexpression of the silver birch *BpMADS4* gene (Flachowsky et al., 2007; Flachowsky et al., 2009; Flachowsky et al., 2011). This can be achieved by generating loss-of-function mutations using CRISPR-Cas9 (Osakabe et al., 2018) or stable transformation of apple plants for candidate genes associated with russeting in the T1190 line. Subsequently, studying the russeting ability of these fruits using our russet induction systems based on moisture exposure or wounding would provide a useful tool for future functional characterization. However, initial attempts to induce russeting in the T1190 line using moisture exposure did not result in severe russeting (data not shown). This may be due to the fact that the T1190 line is an offspring of 'Pinova' and 'Idared' (Luo et al., 2019), the latter being a low russeting cultivar (Khanal et al., 2013b). Alternatively, the incorporation of the early-flowering gene *BpMADS4* into a russet-susceptible cultivar could be a valuable strategy to create an apple line specifically designed for future studies aimed at understanding the functional aspects of russeting.

The integration of these approaches with heterologous expression systems in *N. benthamiana* and *A. thaliana* offers an exciting way to investigate potential candidate genes identified through our transcriptomic dataset during the initiation of russeting.

8.3. Conclusion

This dissertation presents fundamental insights into the initiation of russeting in apple fruit, including a comprehensive examination of its morphological, transcriptomic, and metabolic features. It highlights a biphasic behavior in moisture-induced russeting, providing important information for future research in this field. Although the underlying cause of russeting remains unknown, our data point to oxygen as the initial trigger. Based on our team's ongoing experiments, it appears that oxygen plays a critical role in the suberization process of the wound periderm. The comprehensive transcriptomic data presented is a remarkable resource for the identification of novel candidate genes, making it valuable for future molecular breeding programs. Overall, this dissertation sheds new light on the mechanisms underlying russeting in apple fruit and lays the groundwork for further research in this area.

References

- Aarts, M.G.M., Keijzer, C.J., Stiekema, W.J., Pereira, A., 1995. Molecular characterization of the *CER1* gene of *Arabidopsis* involved in epicuticular wax biosynthesis and pollen fertility. *The Plant Cell* 7 (12), 2115–2127, doi: 10.1105/tpc.7.12.2115.
- Agrawal, V.P., Kolattukudy, P.E., 1977. Biochemistry of suberization. *Plant Physiology* 59 (4), 667–672, doi: 10.1104/pp.59.4.667.
- Aharoni, A., Dixit, S., Jetter, R., Thoenes, E., van Arkel, G., Pereira, A., 2004. The SHINE clade of AP2 domain transcription factors activates wax biosynthesis, alters cuticle properties, and confers drought tolerance when overexpressed in *Arabidopsis*. *The Plant Cell* 16 (9), 2463–2480, doi: 10.1105/tpc.104.022897.
- Alejandro, S., Lee, Y., Tohge, T., Sudre, D., Osorio, S., Park, J., Bovet, L., Lee, Y., Geldner, N., Fernie, A.R., Martinoia, E., 2012. AtABCG29 is a monolignol transporter involved in lignin biosynthesis. *Current Biology* 22 (13), 1207–1212, doi: 10.1016/j.cub.2012.04.064.
- Almeida, T., Menéndez, E., Capote, T., Ribeiro, T., Santos, C., Gonçalves, S., 2013a. Molecular characterization of *Quercus suber MYB1*, a transcription factor up-regulated in cork tissues. *Journal of Plant Physiology* 170 (2), 172–178, doi: 10.1016/j.jplph.2012.08.023.
- Almeida, T., Pinto, G., Correia, B., Santos, C., Gonçalves, S., 2013b. *QsMYB1* expression is modulated in response to heat and drought stresses and during plant recovery in *Quercus suber*. *Plant Physiology and Biochemistry* 73, 274–281, doi: 10.1016/j.plaphy.2013.10.007.
- Anders, S., Pyl, P.T., Huber, W., 2015. HTSeq—a Python framework to work with high-throughput sequencing data. *Bioinformatics* 31 (2), 166–169, doi: 10.1093/bioinformatics/btu638.
- Andersen, T.G., Molina, D., Kilian, J., Franke, R.B., Ragni, L., Geldner, N., 2021. Tissue-autonomous phenylpropanoid production is essential for establishment of root barriers. *Current Biology* 31 (5), 965–977.e5, doi: 10.1016/j.cub.2020.11.070.
- André, C.M., Greenwood, J.M., Walker, E.G., Rassam, M., Sullivan, M., Evers, D., Perry, N.B., Laing, W.A., 2012. Anti-inflammatory procyanidins and triterpenes in 109 apple varieties. *Journal of Agricultural and Food Chemistry* 60 (42), 10546–10554, doi: 10.1021/jf302809k.
- André, C.M., Guerriero, G., Lateur, M., Charton, S., Leclercq, C.C., Renaut, J., Hausman, J.-F., Legay, S., 2022. Identification of novel candidate genes involved in apple cuticle integrity and russeting-associated triterpene synthesis using metabolomic, proteomic, and transcriptomic data. *Plants* 11 (3), doi: 10.3390/plants11030289.
- Andrews, S., 2010. FastQC: A Quality Control Tool for High Throughput Sequence Data.

- Athoo, T.O., Winkler, A., Knoche, M., 2020. Russeting in 'Apple' Mango: Triggers and mechanisms. *Plants* 9 (7), doi: 10.3390/plants9070898.
- Ayaz, A., Saqib, S., Huang, H., Zaman, W., Lü, S., Zhao, H., 2021. Genome-wide comparative analysis of long-chain acyl-CoA synthetases (LACSs) gene family: A focus on identification, evolution and expression profiling related to lipid synthesis. *Plant Physiology and Biochemistry* 161, 1–11, doi: 10.1016/j.plaphy.2021.01.042.
- Barberon, M., Vermeer, J.E.M., Bellis, D. de, Wang, P., Naseer, S., Andersen, T.G., Humbel, B.M., Nawrath, C., Takano, J., Salt, D.E., Geldner, N., 2016. Adaptation of root function by nutrient-induced plasticity of endodermal differentiation. *Cell* 164 (3), 447–459, doi: 10.1016/j.cell.2015.12.021.
- Bargel, H., Koch, K., Cerman, Z., Neinhuis, C., 2006. Structure-function relationships of the plant cuticle and cuticular waxes - a smart material? *Functional Plant Biology* 33 (10), 893–910, doi: 10.1071/FP06139.
- Barthlott, W., Neinhuis, C., 1997. Purity of the sacred lotus, or escape from contamination in biological surfaces. *Planta* 202 (1), 1–8, doi: 10.1007/s004250050096.
- Battaglia, M., Olvera-Carrillo, Y., Garcíarrubio, A., Campos, F., Covarrubias, A.A., 2008. The enigmatic LEA proteins and other hydrophilins. *Plant physiology* 148 (1), 6–24, doi: 10.1104/pp.108.120725.
- Baumann, K., Perez-Rodriguez, M., Bradley, D., Venail, J., Bailey, P., Jin, H., Koes, Ronald, Roberts, Keith, Martin, C., 2007. Control of cell and petal morphogenesis by R2R3 MYB transcription factors. *Development* 134, 1691–1701, doi: 10.1242/dev.02836.
- Beisson, F., Li, Y., Bonaventure, G., Pollard, M., Ohlrogge, J.B., 2007. The acyltransferase GPAT5 is required for the synthesis of suberin in seed coat and root of Arabidopsis. *The Plant Cell* 19 (1), 351–368, doi: 10.1105/tpc.106.048033.
- Belding, R.D., Blankenship, S.M., Young, E., Leidy, R.B., 1998. Composition and variability of epicuticular waxes in apple cultivars. *Journal of the American Society for Horticultural Science* 123 (3), 348–356.
- Bell, H.P., 1937. The origin of russeting in Golden Russet apple. *Canadian Journal of Research*. 15, 560–566.
- Bellis, D. de, Kalmbach, L., Marhavy, P., Daraspe, J., Geldner, N., Barberon, M., 2022. Extracellular vesiculo-tubular structures associated with suberin deposition in plant cell walls. *Nature Communications* 13 (1), 1489, doi: 10.1038/s41467-022-29110-0.
- Berhin, A., Bellis, D. de, Franke, R.B., Buono, R.A., Nowack, M.K., Nawrath, C., 2019. The root cap cuticle: A cell wall structure for seedling establishment and lateral root formation. *Cell* 176 (6), 1367-1378.e8, doi: 10.1016/j.cell.2019.01.005.
- Bernards, M.A., 2002. Demystifying suberin. *Canadian Journal of Botany* 80 (3), 227–240, doi: 10.1139/b02-017.

- Bernards, M.A., Fleming, W.D., Llewellyn, D.B., Priefer, R., Yang, X., Sabatino, A., Plourde, G.L., 1999. Biochemical characterization of the suberization-associated anionic peroxidase of potato. *Plant Physiology* 121 (1), 135–145, doi: 10.1104/pp.121.1.135.
- Bessire, M., Borel, S., Fabre, G., Carrac,a, L., Efremova, N., Yephremov, A., Cao, Y., Jetter, R., Jacquat, A.-C., Métraux, J.-P., Nawrath, C., 2011. A member of the PLEIOTROPIC DRUG RESISTANCE family of ATP binding cassette transporters is required for the formation of a functional cuticle in *Arabidopsis*. *The Plant Cell* 23 (5), 1958–1970, doi: 10.1105/tpc.111.083121.
- Bird, D., Beisson, F., Brigham, A., Shin, J., Greer, S., Jetter, Reinhard, Kunst, L., Wu, X., Yephremov, A., Samuels, L., 2007. Characterization of *Arabidopsis* ABCG11/WBC11, an ATP binding cassette (ABC) transporter that is required for cuticular lipid secretion. *The Plant Journal* 52, 485–498, doi: 10.1111/j.1365-313X.2007.03252.x.
- Boher, P., Serra, O., Soler, M., Molinas, M., Figueras, M., 2013. The potato suberin feruloyl transferase FHT which accumulates in the phellogen is induced by wounding and regulated by abscisic and salicylic acids. *Journal of Experimental Botany* 64 (11), 3225–3236, doi: 10.1093/jxb/ert163.
- Bolger, A.M., Lohse, M., Usadel, B., 2014. Trimmomatic: a flexible trimmer for Illumina sequence data. *Bioinformatics* 30 (15), 2114–2120, doi: 10.1093/bioinformatics/btu170.
- Bomal, C., Bedon, F., Caron, S., Mansfield, S.D., Lévasseur, C., Cooke, J.E.K., Blais, S., Tremblay, L., Morency, M.-J., Pavy, N., Grima-Pettenati, J., Séguin, A., Mackay, J., 2008. Involvement of *Pinus taeda* MYB1 and MYB8 in phenylpropanoid metabolism and secondary cell wall biogenesis: a comparative in planta analysis. *Journal of Experimental Botany* 59 (14), 3925–3939, doi: 10.1093/jxb/ern234.
- Borevitz, J.O., Xia, Y., Blount, J., Dixon, R.A., Lamb, C., 2000. Activation tagging identifies a conserved MYB regulator of phenylpropanoid biosynthesis. *The Plant Cell* 12 (12), 2383–2394, doi: 10.1105/tpc.12.12.2383.
- Brackmann, K., Qi, J., Gebert, M., Jouannet, V., Schlamp, T., Grünwald, K., Wallner, E.-S., Novikova, D.D., Levitsky, V.G., Agustí, J., Sanchez, P., Lohmann, J.U., Greb, T., 2018. Spatial specificity of auxin responses coordinates wood formation. *Nature Communications* 9 (1), 875, doi: 10.1038/s41467-018-03256-2.
- Brundrett, M.C., Kendrick, B., Peterson, C.A., 1991. Efficient lipid staining in plant material with Sudan Red 7B or Fluoral Yellow 088 in polyethylene glycol glycerol. *Biotechnic & Histochemistry* 66 (3), 111–116. doi: 10.3109/10520299109110562.
- Buschhaus, C., Jetter, R., 2011. Composition differences between epicuticular and intracuticular wax substructures: how do plants seal their epidermal surfaces? *Journal of Experimental Botany* 62 (3), 841–853, doi: 10.1093/jxb/erq366.

- Byers, M.A., 1977. A scarfkin like disorder of apples. *HortScience* 12 (3), 226–227, doi:10.21273/HORTSCI.12.3.226
- Cajuste, J.F., González-Candelas, L., Veyrat, A., García-Breijo, F.J., Reig-Armiñana, J., Lafuente, M.T., 2010. Epicuticular wax content and morphology as related to ethylene and storage performance of 'Navelate' orange fruit. *Postharvest Biology and Technology* 55 (1), 29–35, doi: 10.1016/j.postharvbio.2009.07.005.
- Capote, T., Barbosa, P., Usié, A., Ramos, A.M., Inácio, V., Ordás, R., Gonçalves, S., Morais-Cecílio, L., 2018. ChIP-Seq reveals that QsMYB1 directly targets genes involved in lignin and suberin biosynthesis pathways in cork oak (*Quercus suber*). *BMC Plant Biology* 18 (1), 198, doi: 10.1186/s12870-018-1403-5.
- Carter, N., 2012. Petition for determination of nonregulated status: Arctic™ apple (*Malus x domestica*) events GD743 and GS784. APHIS. Interpretative rule on Okanagan Speciality Fruits (Docket No. APHIS-2012-0025).
- Castola, V., Bighelli, A., Rezzi, S., Melloni, G., Gladiali, S., Desjobert, J.-M., Casanova, J., 2002. Composition and chemical variability of the triterpene fraction of dichloromethane extracts of cork (*Quercus suber* L.). *Industrial Crops and Products* 15 (1), 15–22, doi: 10.1016/S0926-6690(01)00091-7.
- Chen, X., Li, S., Zhang, D., Han, M., Jin, X., Zhao, C., Wang, S., Xing, L., Ma, J., Ji, J., An, N., 2019. Sequencing of a wild apple (*Malus baccata*) genome unravels the differences between cultivated and wild apple species regarding disease resistance and cold tolerance. *G3:Genes|Genomes|Genetics* 9 (7), 2051–2060, doi: 10.1534/g3.119.400245.
- Chen, Y.-H., Khanal, B.P., Linde, M., Debener, T., Alkio, M., Knoche, M., 2019. Expression of putative aquaporin genes in sweet cherry is higher in flesh than skin and most are downregulated during development. *Scientia Horticulturae* 244, 304–314, doi: 10.1016/j.scienta.2018.09.065.
- Chen, Y.-H., Straube, J., Khanal, B.P., Knoche, M., Debener, T., 2020. Russeting in apple is initiated after exposure to moisture ends-I. Histological evidence. *Plants* 9 (10), doi: 10.3390/plants9101293.
- Chen, Y.-H., Straube, J., Khanal, B.P., Zeisler-Diehl, V., Suresh, K., Schreiber, L., Debener, T., Knoche, M., 2022. Apple fruit periderms (russeting) induced by wounding or by moisture have the same histologies, chemistries and gene expressions. *PLOS ONE* 17 (9), e0274733, doi: 10.1371/journal.pone.0274733.
- Cohen, H., Fedyuk, V., Wang, C., Wu, S., Aharoni, A., 2020. SUBERMAN regulates developmental suberization of the Arabidopsis root endodermis. *The Plant Journal* 102 (3), 431–447, doi: 10.1111/tpj.14711.

- Cominelli, E., Sala, T., Calvi, D., Gusmaroli, G., Tonelli, C., 2008. Over-expression of the *Arabidopsis AtMYB41* gene alters cell expansion and leaf surface permeability. *The Plant Journal* 53, 53–64, doi: 10.1111/j.1365-313X.2007.03310.x.
- Compagnon, V., Diehl, P., Benveniste, I., Meyer, D., Schaller, H., Schreiber, L., Franke, R., Pinot, F., 2009. CYP86B1 is required for very long chain omega-hydroxyacid and alpha, omega -dicarboxylic acid synthesis in root and seed suberin polyester. *Plant Physiology* 150 (4), 1831–1843, doi: 10.1104/pp.109.141408.
- Cox, M.C., Benschop, Joris, J., Vreeburg, R.A., Wagemaker, C.A., Moritz, T., Peeters, A.J., Voeselek, L.A., 2004. The roles of ethylene, auxin, abscisic acid, and gibberellin in the hyponastic growth of submerged *Rumex palustris* petioles. *Plant Physiology* 136 (2), 2948–2960, doi: 10.1104/pp.104.049197.
- Creasy, L.L., 1980. The correlation of weather parameters with russet of Golden Delicious apples under orchard conditions. *Journal of the American Society for Horticultural Science* 5 (105), 735–738, doi: 10.21273/JASHS.105.5.735
- Creasy, L.L., Swartz, H.J., 1981. Agents influencing russet on 'Golden Delicious' apple fruits. *Journal of the American Society for Horticultural Science* 106 (2), 203–206, doi: 10.21273/JASHS.106.2.203
- Curry, E., 2012. Increase in epidermal planar cell density accompanies decreased russeting of 'Golden Delicious' apples treated with gibberellin A₄₊₇. *HortScience* 47 (2), 232–237, doi: 10.21273/HORTSCI.47.2.232.
- Curry, E.A., 2009. Growth-induced microcracking and repair mechanisms of fruit cuticles. *Proceedings of the SEM Annual Conference*. Albuquerque, New Mexico, USA, June 1–4. Society for Experimental Mechanics Inc.
- Daccord, N., Celton, J.-M., Linsmith, G., Becker, C., Choisne, N., Schijlen, E., van de Geest, H., Bianco, L., Micheletti, D., Velasco, R., Di Pierro, E.A., Gouzy, J., Rees, D.J.G., Guérif, P., Muranty, H., Durel, C.-E., Laurens, F., Lespinasse, Y., Gaillard, S., Aubourg, S., Quesneville, H., Weigel, D., van de Weg, E., Troggio, M., Bucher, E., 2017. High-quality *de novo* assembly of the apple genome and methylome dynamics of early fruit development. *Nature Genetics* 49 (7), 1099–1106, doi: 10.1038/ng.3886.
- Dai, X., Zhai, R., Lin, J., Wang, Z., Meng, D., Li, M., Mao, Y., Gao, B., Ma, H., Zhang, B., Sun, Y., Li, S., Zhou, C., Lin, Y.-C.J., Wang, J.P., Chiang, V.L., Li, W., 2023. Cell-type-specific PtrWOX4a and PtrVCS2 form a regulatory nexus with a histone modification system for stem cambium development in *Populus trichocarpa*. *Nature Plants* 9 (1), 96–111, doi: 10.1038/s41477-022-01315-7.
- Daines, R., Weber, D.J., Bunderson, E.D., Roper, T., 1984. Effect of early sprays on control of powdery mildew fruit russet on apples. *Plant Disease* 68 (4), 326, doi: 10.1094/PD-69-326.

- Debono, A., Yeats, T.H., Rose, J.K.C., Bird, D., Jetter, R., Kunst, L., Samuels, L., 2009. *Arabidopsis* LTPG is a glycosylphosphatidylinositol-anchored lipid transfer protein required for export of lipids to the plant surface. *The Plant Cell* 21 (4), 1230–1238, doi: 10.1105/tpc.108.064451.
- Deeken, R., Saupe, S., Klinkenberg, J., Riedel, M., Leide, J., Hedrich, R., Mueller, T.D., 2016. The nonspecific lipid transfer protein AtLtp1-4 is involved in suberin formation of *Arabidopsis thaliana* crown galls. *Plant Physiology* 172 (3), 1911–1927, doi: 10.1104/pp.16.01486.
- Deluc, L., Barrieu, F., Marchive, C., Lauvergeat, V., Decendit, A., Richard, T., Carde, J.-P., Mérillon, J.-M., Hamdi, S., 2006. Characterization of a grapevine R2R3-MYB transcription factor that regulates the phenylpropanoid pathway. *Plant Physiology* 140 (2), 499–511, doi: 10.1104/pp.105.067231.
- Denekamp, M., Smeekens, S.C., 2003. Integration of wounding and osmotic stress signals determines the expression of the AtMYB102 transcription factor gene. *Plant Physiology* 132 (3), 1415–1423, doi: 10.1104/pp.102.019273.
- Deshmukh, A.P., Simpson, A.J., Hadad, C.M., Hatcher, P.G., 2005. Insights into the structure of cutin and cutan from *Agave americana* leaf cuticle using HRMAS NMR spectroscopy. *Organic Geochemistry* 36 (7), 1072–1085, doi: 10.1016/j.orggeochem.2005.02.005.
- Ding, A., Tang, X., Yang, D., Wang, M., Ren, A., Xu, Z., Hu, R., Zhou, G., O'Neill, M., Kong, Y., 2021. ERF4 and MYB52 transcription factors play antagonistic roles in homogalacturonan de-methylesterification in *Arabidopsis* seed coat mucilage. *The Plant Cell* 33 (2), 381–403, doi: 10.1093/plcell/koaa031.
- Do, C.-T., Pollet, B., Thévenin, J., Sibout, R., Denoue, D., Barrière, Y., Lapierre, C., Jouanin, L., 2007. Both caffeoyl Coenzyme A 3-O-methyltransferase 1 and caffeic acid O-methyltransferase 1 are involved in redundant functions for lignin, flavonoids and sinapoyl malate biosynthesis in *Arabidopsis*. *Planta* 226 (5), 1117–1129, doi: 10.1007/s00425-007-0558-3.
- Dobin, A., Davis, C.A., Schlesinger, F., Drenkow, J., Zaleski, C., Jha, S., Batut, P., Chaisson, M., Gingeras, T.R., 2013. STAR: ultrafast universal RNA-seq aligner. *Bioinformatics* 29 (1), 15–21, doi: 10.1093/bioinformatics/bts635.
- Domergue, F., Vishwanath, S.J., Joubès, J., Ono, J., Lee, J.A., Bourdon, M., Alhattab, R., Lowe, C., Pascal, S., Lessire, R., Rowland, O., 2010. Three *Arabidopsis* fatty acyl-coenzyme A reductases, FAR1, FAR4, and FAR5, generate primary fatty alcohols associated with suberin deposition. *Plant Physiology* 153 (4), 1539–1554, doi: 10.1104/pp.110.158238.

- Domínguez, E., Cuartero, J., Heredia, A., 2011a. An overview on plant cuticle biomechanics. *Plant Science* 181 (2), 77–84, doi: 10.1016/j.plantsci.2011.04.016.
- Domínguez, E., Heredia-Guerrero, J.A., Heredia, A., 2011b. The biophysical design of plant cuticles: an overview. *The New Phytologist* 189 (4), 938–949, doi: 10.1111/j.1469-8137.2010.03553.x.
- Dong, X., Rao, J., Huber, D.J., Chang, X., Xin, F., 2012. Wax composition of ‘Red Fuji’ apple fruit during development and during storage after 1-methylcyclopropene treatment. *Horticulture Environment and Biotechnology* 53 (4), 288–297, doi: 10.1007/s13580-012-0036-0.
- Dou, J., Kim, H., Li, Y., Padmakshan, D., Yue, F., Ralph, J., Vuorinen, T., 2018. Structural characterization of lignins from willow bark and wood. *Journal of Agricultural and Food Chemistry* 66 (28), 7294–7300, doi: 10.1021/acs.jafc.8b02014.
- Duso, C., Castagnoli, M., Simoni, S., Angeli, G., 2010. The impact of eriophyoids on crops: recent issues on *Aculus schlechtendali*, *Calepitrimerus vitis* and *Aculops lycopersici*. *Experimental and Applied Acarology* 51 (1-3), 151–168, doi: 10.1007/s10493-009-9300-0.
- Easterbrook, M.A., Fuller, M.M., 1986. Russetting of apples caused by apple rust mite *Aculus schlechtendali* (Acarina: Eriophyidae). *Annals of Applied Biology* 109 (1), 1–9, doi: 10.1111/j.1744-7348.1986.tb03178.x.
- Elejalde-Palmett, C., Martinez San Segundo, I., Garroum, I., Charrier, L., Bellis, D. de, Mucciolo, A., Guerault, A., Liu, J., Zeisler-Diehl, V., Aharoni, A., Schreiber, L., Bakan, B., Clausen, M.H., Geisler, M., Nawrath, C., 2021. ABCG transporters export cutin precursors for the formation of the plant cuticle. *Current biology* 31 (10), 2111-2123.e9, doi: 10.1016/j.cub.2021.02.056.
- El-Sharkawy, I., Liang, D., Xu, K., 2015. Transcriptome analysis of an apple (*Malus × domestica*) yellow fruit somatic mutation identifies a gene network module highly associated with anthocyanin and epigenetic regulation. *Journal of Experimental Botany* 66 (22), 7359–7376, doi: 10.1093/jxb/erv433.
- Espelie, K.E., Dean, B.B., Kolattukudy, P.E., 1979. Composition of lipid-derived polymers from different anatomical regions of several plant species. *Plant Physiology* 64, 1089–1093, doi: 10.1104/pp.64.6.1089.
- Espelie, K.E., Franceschi, V.R., Kolattukudy, P.E., 1986. Immunocytochemical localization and time course of appearance of an anionic peroxidase associated with suberization in woundhealing potato tuber tissue. *Plant Physiology* 81, 487–492, doi: 10.1104/pp.81.2.487
- Etchells, J.P., Provost, C.M., Mishra, L., Turner, S.R., 2013. WOX4 and WOX14 act downstream of the PXY receptor kinase to regulate plant vascular proliferation

- independently of any role in vascular organisation. *Development* 140 (10), 2224–2234, doi: 10.1242/dev.091314.
- Etchells, J.P., Provost, C.M., Turner, S.R., 2012. Plant vascular cell division is maintained by an interaction between PXY and ethylene signalling. *PLoS genetics* 8 (11), e1002997, doi: 10.1371/journal.pgen.1002997.
- Evert, R.F., 2006. *Esau's plant anatomy: Meristems, cells, and tissues of the plant body—Their structure, function, and development* (3rd ed.). John Wiley & Sons, Inc. Hoboken, New Jersey.
- Fagerstedt, K.V., Saranpää, P., Tapanila, T., Immanen, J., Serra, J.A.A., Nieminen, K., 2015. Determining the composition of lignins in different tissues of silver birch. *Plants* 4 (2), 183–195, doi: 10.3390/plants4020183.
- Falginella, L., Andre, C.M., Legay, S., Lin-Wang, K., Dare, A.P., Deng, C., Rebstock, R., Plunkett, B.J., Guo, L., Cipriani, G., Espley, R.V., 2021. Differential regulation of triterpene biosynthesis induced by an early failure in cuticle formation in apple. *Horticulture Research* 8 (1), 75, doi: 10.1038/s41438-021-00511-4.
- Falginella, L., Cipriani, G., Monte, C., Gregori, R., Testolin, R., Velasco, R., Troglio, M., Tartarini, S., 2015. A major QTL controlling apple skin russeting maps on the linkage group 12 of 'Renetta Grigia di Torriana'. *BMC Plant Biology* 15, 150, doi: 10.1186/s12870-015-0507-4.
- FAO (FAOSTAT), 2021. Food and Agriculture Organization of the United Nations. <https://www.fao.org/faostat>. Date of access: 04 March 2023
- Faust, M., Shear, C.B., 1972a. Fine structure of the fruit surface of three apple cultivars. *Journal of the American Society for Horticultural Science* 97 (3), 351–355.
- Faust, M., Shear, C.B., 1972b. Russeting of apples, an interpretive review. 7 (3), 233–235.
- Fernández, V., Guzmán-Delgado, P., Graça, J., Santos, S., Gil, L., 2016. Cuticle structure in relation to chemical composition: Re-assessing the prevailing model. *Frontiers in Plant Science* 7, 427, doi: 10.3389/fpls.2016.00427.
- Fich, E.A., Segerson, N.A., Rose, J.K.C., 2016. The plant polyester cutin: Biosynthesis, structure, and biological roles. *Annual Review of Plant Biology* 67, 207–233, doi: 10.1146/annurev-arplant-043015-111929.
- Figueiredo, R., Portilla Llerena, J.P., Kiyota, E., Ferreira, S.S., Cardeli, B.R., Souza, S.C.R. de, Dos Santos Brito, M., Sodek, L., Cesarino, I., Mazzafera, P., 2020. The sugarcane ShMYB78 transcription factor activates suberin biosynthesis in *Nicotiana benthamiana*. *Plant Molecular Biology* 104 (4-5), 411–427, doi: 10.1007/s11103-020-01048-1.
- Flachowsky, H., Hanke, M.-V., Peil, A., Strauss, S.H., Fladung, M., 2009. A review on transgenic approaches to accelerate breeding of woody plants. *Plant Breeding* 128 (3), 217–226, doi: 10.1111/j.1439-0523.2008.01591.x.

- Flachowsky, H., Le Roux, P.-M., Peil, A., Patocchi, A., Richter, K., Hanke, M.-V., 2011. Application of a high-speed breeding technology to apple (*Malus × domestica*) based on transgenic early flowering plants and marker-assisted selection. *The New Phytologist* 192 (2), 364–377, doi: 10.1111/j.1469-8137.2011.03813.x.
- Flachowsky, H., Peil, A., Sopanen, T., Elo, A., Hanke, V., 2007. Overexpression of *BpMADS4* from silver birch (*Betula pendula* Roth.) induces early-flowering in apple (*Malus × domestica* Borkh.). *Plant Breeding* 126, 137–145, doi: <https://doi.org/10.1111/j.1439-0523.2007.01344.x>.
- Fornalé, S., Sonbol, F.-M., Maes, T., Capellades, M., Puigdomènech, P., Rigau, J., Caparrós-Ruiz, D., 2006. Down-regulation of the maize and *Arabidopsis thaliana caffeic acid O-methyl-transferase* genes by two new maize R2R3-MYB transcription factors. *Plant Molecular Biology* 62 (6), 809–823, doi: 10.1007/s11103-006-9058-2.
- Franke, R., Briesen, I., Wojciechowski, T., Faust, A., Yephremov, A., Nawrath, C., Schreiber, L., 2005. Apoplastic polyesters in *Arabidopsis* surface tissues--a typical suberin and a particular cutin. *Phytochemistry* 66 (22), 2643–2658, doi: 10.1016/j.phytochem.2005.09.027.
- Franke, R., Höfer, R., Briesen, I., Emsermann, M., Efremova, N., Yephremov, A., Schreiber, L., 2009. The *DAISY* gene from *Arabidopsis* encodes a fatty acid elongase condensing enzyme involved in the biosynthesis of aliphatic suberin in roots and the chalazamicropyle region of seeds. *The Plant Journal* 57 (1), 80–95, doi: 10.1111/j.1365-313X.2008.03674.x.
- Franke, R., Schreiber, L., 2007. Suberin--a biopolyester forming apoplastic plant interfaces. *Current Opinion in Plant Biology* 10 (3), 252–259, doi: 10.1016/j.pbi.2007.04.004.
- Gális, I., Simek, P., Narisawa, T., Sasaki, M., Horiguchi, T., Fukuda, H., Matsuoka, K., 2006. A novel R2R3 MYB transcription factor NtMYBJS1 is a methyl jasmonate-dependent regulator of phenylpropanoid-conjugate biosynthesis in tobacco. *The Plant Journal* 46 (4), 573–592, doi: 10.1111/j.1365-313X.2006.02719.x.
- Gao, L., Gonda, I., Sun, H., Ma, Q., Bao, K., Tieman, D.M., Burzynski-Chang, E.A., Fish, T.L., Stromberg, K.A., Sacks, G.L., Thannhauser, T.W., Foolad, M.R., Diez, M.J., Blanca, J., Canizares, J., Xu, Y., van der Knaap, E., Huang, S., Klee, H.J., Giovannoni, J.J., Fei, Z., 2019. The tomato pan-genome uncovers new genes and a rare allele regulating fruit flavor. *Nature Genetics* 51 (6), 1044–1051, doi: 10.1038/s41588-019-0410-2.
- Geng, P., Zhang, S., Liu, J., Zhao, C., Wu, J., Cao, Y., Fu, C., Han, X., He, H., Zhao, Q., 2020. MYB20, MYB42, MYB42 and MYB85 regulate phenylalanine and lignin biosynthesis during secondary cell wall formation. *Plant Physiology* 182 (3), 1272–1283, doi: 10.1104/pp.19.01070

- Gildemacher, P., Heijne, B., Silvestri, M., Houbraken, J., Hoekstra, E., Theelen, B., Boekhout, T., 2006. Interactions between yeasts, fungicides and apple fruit russetting. *FEMS yeast research* 6 (8), 1149–1156, doi: 10.1111/j.1567-1364.2006.00109.x.
- Gildemacher, P.R., Heijne, B., Houbraken, J., Vromans, T., Hoekstra, E.S., Boekhout, T., 2004. Can phyllosphere yeasts explain the effect of scab fungicides on russetting of Elstar apples? *European Journal of Plant Pathology* 110 (9), 929–937, doi: 10.1007/s10658-004-8948-x.
- Girard, A.-L., Mounet, F., Lemaire-Chamley, M., Gaillard, C., Elmorjani, K., Vivancos, J., Runavot, J.-L., Quemener, B., Petit, J., Germain, V., Rothan, C., Marion, D., Bakan, B., 2012. Tomato GDSL1 is required for cutin deposition in the fruit cuticle. *The Plant Cell* 24 (7), 3119–3134, doi: 10.1105/tpc.112.101055.
- Goffinet, M.C., Pearson, R.C., 1991. Anatomy of russetting induced in Concord grape berries by the fungicide chlorothalonil. *American Journal of Enology and Viticulture* 42 (4), 281–289.
- Goicoechea, M., Lacombe, E., Legay, S., Mihaljevic, S., Rech, P., Jauneau, A., Lapierre, C., Pollet, B., Verhaegen, D., Chaubet-Gigot, N., Grima-Pettenati, J., 2005. EgMYB2, a new transcriptional activator from Eucalyptus xylem, regulates secondary cell wall formation and lignin biosynthesis. *The Plant Journal* 43 (4), 553–567, doi: 10.1111/j.1365-313X.2005.02480.x.
- Gou, J.-Y., Yu, X.-H., Liu, C.-J., 2009. A hydroxycinnamoyltransferase responsible for synthesizing suberin aromatics in Arabidopsis. *Proceedings of the National Academy of Sciences* 106 (44), 18855–18860, doi: 10.1073/pnas.0905555106.
- Gou, M., Hou, G., Yang, H., Zhang, X., Cai, Y., Kai, G., Liu, C.-J., 2017. The MYB107 transcription factor positively regulates suberin biosynthesis. *Plant Physiology* 173 (2), 1045–1058, doi: 10.1104/pp.16.01614.
- Graça, J., 2010. Hydroxycinnamates in suberin formation. *Phytochemistry Reviews* 9 (1), 85–91, doi: 10.1007/s11101-009-9138-4.
- Graça, J., Pereira, H., 2000. Methanolysis of bark suberins: analysis of glycerol and acid monomers. *Phytochemical Analysis* 11 (1), 45–51, doi: 10.1002/(SICI)1099-1565(200001/02)11:1<45:AID-PCA481>3.0.CO;2-8.
- Graça, J., Pereira, H., 2004. The periderm development in *Quercus suber*. *IAWA Journal* 25 (3), 325–335, doi: 10.1163/22941932-90000369.
- Graça, J., Santos, S., 2007. Suberin: a biopolyester of plants' skin. *Macromolecular Bioscience* 7 (2), 128–135, doi: 10.1002/mabi.200600218.
- Grimm, E., Khanal, B.P., Winkler, A., Knoche, M., Köpcke, D., 2012. Structural and physiological changes associated with the skin spot disorder in apple. *Postharvest Biology and Technology* 64 (1), 111–118, doi: 10.1016/j.postharvbio.2011.10.004.

- Gui, J., Luo, L., Zhong, Y., Sun, J., Umezawa, T., Li, L., 2019. Phosphorylation of LTF1, an MYB transcription factor in *Populus*, acts as a sensory switch regulating lignin biosynthesis in wood cells. *Molecular Plant* 12 (10), 1325–1337, doi: 10.1016/j.molp.2019.05.008.
- Gutierrez, B.L., Zhong, G.-Y., Brown, S.K., 2018. Increased phloridzin content associated with russetting in apple (*Malus domestica* (Suckow) Borkh.) fruit. *Genetic Resources and Crop Evolution* 65 (8), 2135–2149, doi: 10.1007/s10722-018-0679-5.
- Hannoufa, A., McNevin, J., Lemieux, B., 1993. Epicuticular waxes of *eceriferum* mutants of *Arabidopsis thaliana*. *Phytochemistry* 33 (4), 851–855, doi: 10.1016/0031-9422(93)85289-4.
- Havir, E.A., Hanson, K.R., 1970. [72a] l-phenylalanine ammonia-lyase (potato tubers). *Methods in Enzymology* 17, 575–581, doi: 10.1016/0076-6879(71)17243-6
- Heidenreich, M.C.M., Corral-Garcia, M.R., Momol, E.A., Burr, T.J., 1997. Russet of apple fruit caused by *Aureobasidium pullulans* and *Rhodotorula glutinis*. *Plant Disease* 81 (4), 337–342, doi: 10.1094/PDIS.1997.81.4.337.
- Heredia, A., 2003. Biophysical and biochemical characteristics of cutin, a plant barrier biopolymer. *Biochimica et Biophysica Acta* 1620 (1-3), 1–7, doi: 10.1016/s0304-4165(02)00510-x.
- Herklots, G.A.C., 1924. The effects of an artificially controlled hydron concentration upon wound healing in the potato. *The New Phytologist* 23 (5), 240–255.
- Heumann, H.G., 1990. A simple method for improved visualization of the lamellated structure of cutinized and suberized plant cell walls by electron microscopy. *Stain Technology* 65 (4), 183–187, doi: 10.3109/10520299009108068.
- Hirakawa, Y., Kondo, Y., Fukuda, H., 2010. TDIF peptide signaling regulates vascular stem cell proliferation via the *WOX4* homeobox gene in *Arabidopsis*. *The Plant Cell* 22 (8), 2618–2629, doi: 10.1105/tpc.110.076083.
- Höfer, R., Briesen, I., Beck, M., Pinot, F., Schreiber, L., Franke, R., 2008. The *Arabidopsis* cytochrome P450 *CYP86A1* encodes a fatty acid ω -hydroxylase involved in suberin monomer biosynthesis. *Journal of Experimental Botany* 59 (9), 2347–2360, doi: 10.1093/jxb/ern101.
- Hoffmann, L., Maury, S., Martz, F., Geoffroy, P., Legrand, M., 2003. Purification, cloning, and properties of an acyltransferase controlling shikimate and quinate ester intermediates in phenylpropanoid metabolism. *The Journal of Biological Chemistry* 278 (1), 95–103, doi: 10.1074/jbc.M209362200.
- Holloway, P.J., 1973. Cutins of *Malus pumila* fruits and leaves. *Phytochemistry* 12, 2913–2920.

- Hong, L., Brown, J., Segerson, N.A., Rose, J.K.C., Roeder, A.H.K., 2017. CUTIN SYNTHASE 2 maintains progressively developing cuticular ridges in *Arabidopsis* sepals. *Molecular Plant* 10 (4), 560–574, doi: 10.1016/j.molp.2017.01.002.
- Hosmani, P.S., Kamiya, T., Danku, J., Naseer, S., Geldner, N., Guerinot, M.L., Salt, D.E., 2013. Dirigent domain-containing protein is part of the machinery required for formation of the lignin-based Casparian strip in the root. *Proceedings of the National Academy of Sciences* 110 (35), 14498–14503, doi: 10.1073/pnas.1308412110.
- Humphreys, J.M., Hemm, M.R., Chapple, C., 1999. New routes for lignin biosynthesis defined by biochemical characterization of recombinant ferulate 5-hydroxylase, a multifunctional cytochrome P450-dependent monooxygenase. *Proceedings of the National Academy of Sciences* 96 (18), 10045–10050, doi: 10.1073/pnas.96.18.10045.
- Hunt, G.M., Baker, E.A., 1980. Phenolic constituents of tomato fruit cuticles. *Phytochemistry* 19 (7), 1415–1419, doi: [https://doi.org/10.1016/0031-9422\(80\)80185-3](https://doi.org/10.1016/0031-9422(80)80185-3).
- Ingram, G., Nawrath, C., 2017. The roles of the cuticle in plant development: organ adhesions and beyond. *Journal of Experimental Botany* 68 (19), 5307–5321, doi: 10.1093/jxb/erx313.
- Jakobson, L., Lindgren, L.O., Verdier, G., Laanemets, K., Brosché, M., Beisson, F., Kollist, H., 2016. BODYGUARD is required for the biosynthesis of cutin in *Arabidopsis*. *The New Phytologist* 211 (2), 614–626, doi: 10.1111/nph.13924.
- Jakoby, M.J., Falkenhan, D., Mader, M.T., Brininstool, G., Wischnitzki, E., Platz, N., Hudson, A., Hülskamp, M., Larkin, J., Schnittger, A., 2008. Transcriptional profiling of mature *Arabidopsis* trichomes reveals that *NOECK* encodes the MIXTA-like transcriptional regulator MYB106. *Plant Physiology* 148 (3), 1583–1602, doi: 10.1104/pp.108.126979.
- Jeffree, C.E., 2006. The fine structure of the plant cuticle. *Annual Plant Reviews* 23, 11–115.
- Jetter, R., Kunst, L., Samuels, A.L., 2006. Composition of plant cuticular waxes. In: Riederer M., Müller C., eds. *Biology of the plant cuticle*. Oxford: Blackwell, 145–181.
- Ji, J., Strable, J., Shimizu, R., Koenig, D., Sinha, N., Scanlon, M.J., 2010. *WOX4* promotes procambial development. *Plant Physiology* 152 (3), 1346–1356, doi: 10.1104/pp.109.149641.
- Jiang, S., Chen, M., He, N., Chen, X., Wang, N., Sun, Q., Zhang, T., Xu, H., Fang, H., Wang, Y., Zhang, Z., Wu, S., Chen, X., 2019. *MdGSTF6*, activated by MdMYB1, plays an essential role in anthocyanin accumulation in apple. *Horticulture Research* 6, 40, doi: 10.1038/s41438-019-0118-6.
- Jiang, S., Luo, J., Wang, X., An, H., Zhang, J., Li, S., 2022. QTL mapping and transcriptome analysis to identify genes associated with green/russet peel in *Pyrus pyrifolia*. *Scientia Horticulturae* 293, 110714, doi: 10.1016/j.scienta.2021.110714.

- Jiang, S.-H., Sun, Q.-G., Chen, M., Wang, N., Xu, H.-F., Fang, H.-C., Wang, Y.-C., Zhang, Z.-Y., Chen, X.-S., 2019. Methylome and transcriptome analyses of apple fruit somatic mutations reveal the difference of red phenotype. *BMC Genomics* 20 (1), 117, doi: 10.1186/s12864-019-5499-2.
- Jin, H., Cominelli, E., Bailey, P., Parr, A., Mehrtens, F., Jones, J., Tonelli, C., Weisshaar, B., Martin, C., 2000. Transcriptional repression by AtMYB4 controls production of UV-protecting sunscreens in *Arabidopsis*. *The EMBO Journal* 19 (22), 6150–6161, doi: 10.1093/emboj/19.22.6150.
- Ju, Z., Bramlage, W.J., 2001. Developmental changes of cuticular constituents and their association with ethylene during fruit ripening in ‘Delicious’ apples. *Postharvest Biology and Technology* 21 (3), 257–263, doi: 10.1016/S0925-5214(00)00156-3.
- Jung, S., Lee, T., Cheng, C.-H., Buble, K., Zheng, P., Yu, J., Humann, J., Ficklin, S.P., Gasic, K., Scott, K., Frank, M., Ru, S., Hough, H., Evans, K., Peace, C., Olmstead, M., DeVetter, L.W., McFerson, J., Coe, M., Wegrzyn, J.L., Staton, M.E., Abbott, A.G., Main, D., 2019. 15 years of GDR: New data and functionality in the Genome Database for *Rosaceae*. *Nucleic Acids Research* 47 (D1), D1137-D1145, doi: 10.1093/nar/gky1000.
- Kallio, H., Nieminen, R., Tuomasjukka, S., Hakala, M., 2006. Cutin composition of five finnish berries. *Journal of Agricultural and Food Chemistry* 54 (2), 457–462, doi: 10.1021/jf0522659.
- Karnovsky, M., 1965. A formaldehyde-glutaraldehyde fixative of high osmolarity for use in electron microscopy. *The Journal of Cell Biology* 27 (2), 1A–149A.
- Karpinska, B., Karlsson, M., Srivasta, M., Stenberg, A., Schrader, J., Sterky, F., Bhalerao, R., Wingsle, G., 2004. MYB transcription factors are differentially expressed and regulated during secondary vascular tissue development in hybrid aspen. *Plant Molecular Biology* 56, 255–270, doi: 10.1007/s11103-004-3354-5.
- Kaur, H., Jha, P., Ochatt, S.J., Kumar, V., 2023. Single-cell transcriptomics is revolutionizing the improvement of plant biotechnology research: recent advances and future opportunities. *Critical Reviews in Biotechnology* 12, 1–16, doi: 10.1080/07388551.2023.2165900.
- Kawaoka, A., Kaothien, P., Yoshida, K., Endo, S., Yamada, K., Ebinuma, H., 2000. Functional analysis of tobacco LIM protein Ntlm1 involved in lignin biosynthesis. *The Plant Journal* 22 (4), 289–301, doi: 10.1046/j.1365-313x.2000.00737.x.
- Khan, A., Carey, S.B., Serrano, A., Zhang, H., Hargarten, H., Hale, H., Harkess, A., Honaas, L., 2022. A phased, chromosome-scale genome of ‘Honeycrisp’ apple (*Malus domestica*). doi: 10.46471/gigabyte.69

- Khanal, B.P., Grimm, E., Finger, S., Blume, A., Knoche, M., 2013a. Intracuticular wax fixes and restricts strain in leaf and fruit cuticles. *The New Phytologist* 200 (1), 134–143, doi: 10.1111/nph.12355.
- Khanal, B.P., Ikigu, G.M., Knoche, M., 2019. Russeting partially restores apple skin permeability to water vapour. *Planta* 249 (3), 849–860, doi: 10.1007/s00425-018-3044-1.
- Khanal, B.P., Imoro, Y., Chen, Y.H., Straube, J., Knoche, M., 2020a. Surface moisture increases microcracking and water vapour permeance of apple fruit skin. *Plant Biology* 23 (1), 74–82, doi: 10.1111/plb.13178.
- Khanal, B.P., Knoche, M., 2014. Mechanical properties of apple skin are determined by epidermis and hypodermis. *Journal of the American Society for Horticultural Science* 139 (2), 139–147.
- Khanal, B.P., Knoche, M., 2017. Mechanical properties of cuticles and their primary determinants. *Journal of Experimental Botany* 68 (19), 5351–5367, doi: 10.1093/jxb/erx265.
- Khanal, B.P., Knoche, M., Bußler, S., Schlüter, O., 2014. Evidence for a radial strain gradient in apple fruit cuticles. *Planta* 240 (4), 891–897, doi: 10.1007/s00425-014-2132-0.
- Khanal, B.P., Le, T.L., Si, Y., Knoche, M., 2020b. Russet susceptibility in apple is associated with skin cells that are larger, more variable in size, and of reduced fracture strain. *Plants* 9 (9), doi: 10.3390/plants9091118.
- Khanal, B.P., Shrestha, R., Hückstädt, L., Knoche, M., 2013b. Russeting in apple seems unrelated to the mechanical properties of the cuticle at maturity. *HortScience* 48, 1135–1138, doi: 10.21273/HORTSCI.48.9.1135.
- Kim, D., Paggi, J.M., Park, C., Bennett, C., Salzberg, S.L., 2019. Graph-based genome alignment and genotyping with HISAT2 and HISAT-genotype. *Nature Biotechnology* 37 (8), 907–915, doi: 10.1038/s41587-019-0201-4.
- Kim, D., Pertea, G., Trapnell, C., Pimental, H., Kelley, R., Salzberg, S.L., 2013. TopHat2 accurate alignment of transcriptomes in the presence of insertions, deletions and gene fusions. *Genome biology* 14 (36), 1–13, doi: 10.1186/gb-2013-14-4-r36.
- Kim, H., Lee, S.B., Kim, H.J., Min, M.K., Hwang, I., Suh, M.C., 2012. Characterization of glycosylphosphatidylinositol-anchored lipid transfer protein 2 (LTPG2) and overlapping function between LTPG/LTPG1 and LTPG2 in cuticular wax export or accumulation in *Arabidopsis thaliana*. *Plant & Cell Physiology* 53 (8), 1391–1403, doi: 10.1093/pcp/pcs083.
- Kligman, A., Dastmalchi, K., Smith, S., John, G., Stark, R.E., 2022. Building blocks of the protective suberin plant polymer self-assemble into lamellar structures with antibacterial potential. *ACS Omega* 7 (5), 3978–3989, doi: 10.1021/acsomega.1c04709.

- Knoche, M., Beyer, M., Peschel, S., Oparlakov, B., Bukovac, M.J., 2004. Changes in strain and deposition of cuticle in developing sweet cherry fruit. *Physiologia Plantarum* 120 (4), 667–677, doi: 10.1111/j.0031-9317.2004.0285.x.
- Knoche, M., Grimm, E., 2008. Surface moisture induces microcracks in the cuticle of ‘Golden Delicious’ apple. *HortScience* 43 (6), 1929–1931, doi: 10.21273/HORTSCI.43.6.1929.
- Knoche, M., Khanal, B.P., Brüggewirth, M., Thapa, S., 2018. Patterns of microcracking in apple fruit skin reflect those of the cuticular ridges and of the epidermal cell walls. *Planta* 248 (2), 293–306, doi: 10.1007/s00425-018-2904-z.
- Knoche, M., Khanal, B.P., Stopar, M., 2011. Russetting and microcracking of ‘Golden Delicious’ apple fruit concomitantly decline due to gibberellin A₄₊₇ application. *Journal of the American Society for Horticultural Science* 136 (3), 159–164, doi: 10.21273/JASHS.136.3.159.
- Knoche, M., Lang, A., 2017. Ongoing growth challenges fruit skin integrity. *Critical Reviews in Plant Sciences* 36 (3), 190–215, doi: 10.1080/07352689.2017.1369333.
- Knoche, M., Peschel, S., 2006. Water on the surface aggravates microscopic cracking of the sweet cherry fruit cuticle. *Journal of the American Society for Horticultural Science* 131 (2), 192–200.
- Knollenberg, B.J., Liu, J., Yu, S., Lin, H., Li Tian, 2018. Cloning and functional characterization of a p-coumaroyl quinate/shikimate 3'-hydroxylase from potato (*Solanum tuberosum*). *Biochemical and Biophysical Research Communications* 496 (2), 462–467, doi: 10.1016/j.bbrc.2018.01.075.
- Kolattukudy, P.E., 1980. Biopolyester membranes of plants cutin and suberin. *Science* 208 (4447), 990-1000, doi: 10.1126/science.208.4447.990.
- Kolattukudy, P.E., 1981. Structure, biosynthesis, and biodegradation of cutin and suberin. *Annual Review of Plant Biology* 32, 539–567, doi: 10.1146/annurev.pp.32.060181.002543.
- Kolattukudy, P.E., 1996. Biosynthetic pathways of cutin and waxes, and their sensitivity to environmental stresses. G. Kerstiens (Ed.), *Plant Cuticles: An Integrated Functional Approach*, BIOS Scientific Publishers, Oxford, 83–108.
- Kolattukudy, P.E., 2001. Polyester in higher plants. *Advances in Biochemical Engineering* 71, 1–49, doi: 10.1007/3-540-40021-4_1.
- Kolattukudy, P.E., Walton, T.J., 1972. The biochemistry of plant cuticular lipids. *Progress in the Chemistry of Fats and other Lipids* 13 (3), 119–175, doi: 10.1016/0079-6832(73)90006-2.
- Kolde, R., 2019. Pheatmap: pretty heatmap.

- Kosma, D.K., Murmu, J., Razeq, F.M., Santos, P., Bourgault, R., Molina, I., Rowland, O., 2014. AtMYB41 activates ectopic suberin synthesis and assembly in multiple plant species and cell types. *The Plant Journal* 80 (2), 216–229, doi: 10.1111/tpj.12624.
- Kost, T.D., Gessler, C., Jänsch, M., Flachowsky, H., Patocchi, A., Broggini, G.A.L., 2015. Development of the first cisgenic apple with increased resistance to fire blight. *PLOS ONE* 10 (12), e0143980, doi: 10.1371/journal.pone.0143980.
- Krauss, P., Markstädter, C., Riederer, M., 1997. Attenuation of UV radiation by plant cuticles from woody species. *Plant, Cell & Environment* 20 (8), 1079–1085, doi: 10.1111/j.1365-3040.1997.tb00684.x.
- Krishnamurthy, P., Vishal, B., Bhal, A., Kumar, P.P., 2021. WRKY9 transcription factor regulates cytochrome P450 genes *CYP94B3* and *CYP86B1*, leading to increased root suberin and salt tolerance in *Arabidopsis*. *Physiologia Plantarum* 172 (3), 1673–1687, doi: 10.1111/ppl.13371.
- Krishnamurthy, P., Vishal, B., Ho, W.J., Lok, F.C.J., Lee, F.S.M., Kumar, P.P., 2020. Regulation of a cytochrome P450 gene *CYP94B1* by WRKY33 transcription factor controls apoplastic barrier formation in roots to confer salt tolerance. *Plant Physiology* 184 (4), 2199–2215, doi: 10.1104/pp.20.01054.
- Kucukoglu, M., Nilsson, J., Zheng, B., Chaabouni, S., Nilsson, O., 2017. *WUSCHEL-RELATED HOMEODOMAIN4 (WOX4)*-like genes regulate cambial cell division activity and secondary growth in *Populus* trees. *The New Phytologist* 215 (2), 642–657, doi: 10.1111/nph.14631.
- Kulkarni, A., Anderson, A.G., Merullo, D.P., Konopka, G., 2019. Beyond bulk: a review of single cell transcriptomics methodologies and applications. *Current Opinion in Biotechnology* 58, 129–136, doi: 10.1016/j.copbio.2019.03.001.
- Kunst, L., Samuels, A.L., 2003. Biosynthesis and secretion of plant cuticular wax. *Progress in Lipid Research* 42 (1), 51–80, doi: 10.1016/s0163-7827(02)00045-0.
- Kunst, L., Samuels, L., 2009. Plant cuticles shine: advances in wax biosynthesis and export. *Current Opinion in Plant Biology* 12 (6), 721–727, doi: 10.1016/j.pbi.2009.09.009.
- Kurdyukov, S., Faust, A., Nawrath, C., Bär, S., Voisin, D., Efremova, N., Franke, R., Schreiber, L., Saedler, H., Métraux, J.-P., Yephremov, A., 2006a. The epidermis-specific extracellular BODYGUARD controls cuticle development and morphogenesis in *Arabidopsis*. *The Plant Cell* 18 (2), 321–339, doi: 10.1105/tpc.105.036079.
- Kurdyukov, S., Faust, A., Trenkamp, S., Bär, S., Franke, R., Efremova, N., Tietjen, K., Schreiber, L., Saedler, H., Yephremov, A., 2006b. Genetic and biochemical evidence for involvement of HOTHEAD in the biosynthesis of long-chain alpha-,omega-dicarboxylic fatty acids and formation of extracellular matrix. *Planta* 224 (2), 315–329, doi: 10.1007/s00425-005-0215-7.

- Lai, X., Khanal, B.P., Knoche, M., 2016. Mismatch between cuticle deposition and area expansion in fruit skins allows potentially catastrophic buildup of elastic strain. *Planta* 244 (5), 1145–1156, doi: 10.1007/s00425-016-2572-9.
- Landgraf, R., Smolka, U., Altmann, S., Eschen-Lippold, L., Senning, M., Sonnewald, S., Weigel, B., Frolova, N., Strehmel, N., Hause, G., Scheel, D., Böttcher, C., Rosahl, S., 2014. The ABC transporter ABCG1 is required for suberin formation in potato tuber periderm. *The Plant Cell* 26 (8), 3403–3415, doi: 10.1105/tpc.114.124776.
- Langfelder, P., Horvath, S., 2008. WGCNA: an R package for weighted correlation network analysis. *BMC Bioinformatics* 9, 559, doi: 10.1186/1471-2105-9-559.
- Lara, I., Belge, B., Goulao, L.F., 2014. The fruit cuticle as a modulator of postharvest quality. *Postharvest Biology and Technology* 87, 103–112, doi: 10.1016/j.postharvbio.2013.08.012.
- Lara, I., Heredia, A., Domínguez, E., 2019. Shelf life potential and the fruit cuticle: The unexpected player. *Frontiers in Plant Science* 10, 770, doi: 10.3389/fpls.2019.00770.
- Lashbrooke, J., Aharoni, A., Costa, F., 2015. Genome investigation suggests *MdSHN3*, an APETALA2-domain transcription factor gene, to be a positive regulator of apple fruit cuticle formation and an inhibitor of russet development. *Journal of Experimental Botany* 66 (21), 6579–6589, doi: 10.1093/jxb/erv366.
- Lashbrooke, J., Cohen, H., Levy-Samocho, D., Tzfadia, O., Panizel, I., Zeisler, V., Massalha, H., Stern, A., Trainotti, L., Schreiber, L., Costa, F., Aharoni, A., 2016. *MYB107* and *MYB9* homologs regulate suberin deposition in angiosperms. *The Plant Cell* 28 (9), 2097–2116, doi: 10.1105/tpc.16.00490.
- Leal, A.R., Barros, P.M., Parizot, B., Sapeta, H., Vangheluwe, N., Andersen, T.G., Beeckman, T., Oliveira, M.M., 2022. Translational profile of developing phellem cells in *Arabidopsis thaliana* roots. *The Plant Journal* 110 (3), 899–915, doi: 10.1111/tpj.15691.
- Lee, S.B., Go, Y.S., Bae, H.-J., Park, J.H., Cho, S.H., Cho, H.J., Lee, D.S., Park, O.K., Hwang, I., Suh, M.C., 2009a. Disruption of glycosylphosphatidylinositol-anchored lipid transfer protein gene altered cuticular lipid composition, increased plastoglobules, and enhanced susceptibility to infection by the fungal pathogen *Alternaria brassicicola*. *Plant Physiology* 150 (1), 42–54, doi: 10.1104/pp.109.137745.
- Lee, S.B., Kim, H.U., Suh, M.C., 2016. MYB94 and MYB96 additively activate cuticular wax biosynthesis in *Arabidopsis*. *Plant & Cell Physiology* 57 (11), 2300–2311, doi: 10.1093/pcp/pcw147.
- Lee, S.B., Suh, M.C., 2015. Cuticular wax biosynthesis is up-regulated by the MYB94 transcription factor in *Arabidopsis*. *Plant & Cell Physiology* 56 (1), 48–60, doi: 10.1093/pcp/pcu142.

- Lee, S.B., Suh, M.-C., 2018. Disruption of glycosylphosphatidylinositol-anchored lipid transfer protein 15 affects seed coat permeability in *Arabidopsis*. *The Plant Journal* 96 (6), 1206–1217, doi: 10.1111/tpj.14101.
- Lee, S.-B., Jung, S.-J., Go, Y.-S., Kim, H.-U., Kim, J.-K., Cho, H.-J., Park, O.K., Suh, M.-C., 2009b. Two *Arabidopsis* 3-ketoacyl CoA synthase genes, *KCS20* and *KCS2/DA/SY*, are functionally redundant in cuticular wax and root suberin biosynthesis, but differentially controlled by osmotic stress. *The Plant Journal* 60 (3), 462–475, doi: 10.1111/j.1365-313X.2009.03973.x.
- Lee, Y., Rubio, M.C., Alassimone, J., Geldner, N., 2013. A mechanism for localized lignin deposition in the endodermis. *Cell* 153 (2), 402–412, doi: 10.1016/j.cell.2013.02.045.
- Legay, S., Cocco, E., André, C.M., Guignard, C., Hausman, J.-F., Guerriero, G., 2017. Differential lipid composition and gene expression in the semi-russeted "Cox Orange Pippin" apple variety. *Frontiers in Plant Science* 8, 1656, doi: 10.3389/fpls.2017.01656.
- Legay, S., Guerriero, G., André, C., Guignard, C., Cocco, E., Charton, S., Boutry, M., Rowland, O., Hausman, J.-F., 2016. MdMyb93 is a regulator of suberin deposition in russeted apple fruit skins. *The New Phytologist* 212 (4), 977–991, doi: 10.1111/nph.14170.
- Legay, S., Guerriero, G., Deleruelle, A., Lateur, M., Evers, D., André, C.M., Hausman, J.-F., 2015. Apple russeting as seen through the RNA-seq lens: strong alterations in the exocarp cell wall. *Plant Molecular Biology* 88 (1-2), 21–40, doi: 10.1007/s11103-015-0303-4.
- Lenzian, K.J., 2006. Survival strategies of plants during secondary growth: barrier properties of phellements and lenticels towards water, oxygen, and carbon dioxide. *Journal of Experimental Botany* 57 (11), 2535–2546, doi: 10.1093/jxb/erl014.
- Li, C., Yaegashi, H., Kishigami, R., Kawakubo, A., Yamagishi, N., Ito, T., Yoshikawa, N., 2020. Apple russet ring and apple green crinkle diseases: Fulfillment of Koch's postulates by virome analysis, amplification of full-length cDNA of viral genomes, *in vitro* transcription of infectious viral RNAs, and reproduction of symptoms on fruits of apple trees inoculated with viral RNAs. *Frontiers in microbiology* 11, 1627, doi: 10.3389/fmicb.2020.01627.
- Li, F., Min, D., Song, B., Shao, S., Zhang, X., 2017. Ethylene effects on apple fruit cuticular wax composition and content during cold storage. *Postharvest Biology and Technology* 134, 98–105, doi: 10.1016/j.postharvbio.2017.08.011.
- Li, F., Wu, X., Lam, P., Bird, D., Zhen, H., Samueles, L., Jetter, R., Kunst, L., 2008. Identification of the wax ester synthase/acyl-coenzyme A:diacylglycerol acyltransferase WSD1 required for stem wax ester biosynthesis in *Arabidopsis*. *Plant Physiology* (148), 97–107, doi: 10.1104/pp.108.123471.

- Li, Y., Beisson, F., Koo, A.J.K., Molina, I., Pollard, M., Ohlrogge, J., 2007. Identification of acyltransferases required for cutin biosynthesis and production of cutin with suberin-like monomers. *Proceedings of the National Academy of Sciences* 104 (46), 18339–18344, doi: 10.1073/pnas.0706984104.
- Li, Z., Wang, L., He, J., Li, X., Hou, N., Guo, J., Niu, C., Li, C., Liu, S., Xu, J., Xie, Y., Zhang, D., Shen, X., Lu, L., Geng, D., Chen, P., Jiang, L., Wang, L., Li, H., Malnoy, M., Deng, C., Zou, Y., Li, C., Zhan, X., Dong, Y., Notaguchi, M., Ma, F., Xu, Q., Guan, Q., 2022. Chromosome-scale reference genome provides insights into the genetic origin and grafting-mediated stress tolerance of *Malus prunifolia*. *Plant Biotechnology Journal* 20 (6), 1015–1017, doi: 10.1111/pbi.13817.
- Li-Beisson, Y., Pollard, M., Sauveplane, V., Pinot, F., Ohlrogge, J., Beisson, F., 2009. Nanoridges that characterize the surface morphology of flowers require the synthesis of cutin polyester. *Proceedings of the National Academy of Sciences* 106 (51), 22008–22013, doi: 10.1073/pnas.0909090106.
- Lieberman, L.M., Sparks, E.E., Moreno-Risueno, M.A., Petricka, J.J., Benfey, P.N., 2015. MYB36 regulates the transition from proliferation to differentiation in the Arabidopsis root. *Proceedings of the National Academy of Sciences* 112 (39), 12099–12104, doi: 10.1073/pnas.1515576112.
- Lipshitz, N., Waisel, Y., 1970. Phellogen initiation in the stems of *Eucalyptus camaldulensis* Dehnh. *Australian Journal of Botany* 18 (2), 185–189, doi: 10.1071/BT9700185.
- Lipton, W.J., 1967. Some effects of low-oxygen atmospheres on potato tubers. *American Potato Journal* 44, 292–299, doi: 10.1007/BF02862531.
- Liu, C.-J., 2012. Deciphering the enigma of lignification: precursor transport, oxidation, and the topochemistry of lignin assembly. *Molecular Plant* 5 (2), 304–317, doi: 10.1093/mp/ssr121.
- Liu, C.-J., Miao, Y.-C., Zhang, K.-W., 2011. Sequestration and transport of lignin monomeric precursors. *Molecules* 16 (1), 710–727, doi: 10.3390/molecules16010710.
- Liu, D., Shi, L., Han, C., Yu, J., Li, D., Zhang, Y., 2012. Validation of reference genes for gene expression studies in virus-infected *Nicotiana benthamiana* using quantitative real-time PCR. *PLOS ONE* 7 (9), e46451, doi: 10.1371/journal.pone.0046451.
- López-Casado, G., Matas, A.J., Domínguez, E., Cuartero, J., Heredia, A., 2007. Biomechanics of isolated tomato (*Solanum lycopersicum* L.) fruit cuticles: the role of the cutin matrix and polysaccharides. *Journal of Experimental Botany* 58 (14), 3875–3883, doi: 10.1093/jxb/erm233.

- Lourenço, A., Rencoret, J., Chemetova, C., Gominho, J., Gutiérrez, A., Del Río, J.C., Pereira, H., 2016. Lignin composition and structure differs between xylem, phloem and phellem in *Quercus suber* L. *Frontiers in Plant Science* 7, 1612, doi: 10.3389/fpls.2016.01612.
- Love, M.I., Huber, W., Anders, S., 2014. Moderated estimation of fold change and dispersion for RNA-seq data with DESeq2. *Genome Biology* 15 (12), 550, doi: 10.1186/s13059-014-0550-8.
- Lu, H.-P., Gao, Q., Han, J.-P., Guo, X.-H., Wang, Q., Altosaar, I., Barberon, M., Liu, J.-X., Gatehouse, A.M.R., Shu, Q.-Y., 2022. An ABA-serotonin module regulates root suberization and salinity tolerance. *The New Phytologist*, doi: 10.1111/nph.18397.
- Luo, F., van de Weg, E., Vanderzande, S., Norelli, J.L., Flachowsky, H., Hanke, V., Peace, C., 2019. Elucidating the genetic background of the early-flowering transgenic genetic stock T1190 with a high-density SNP array. *Molecular Breeding* 39 (2), doi: 10.1007/s11032-019-0929-z.
- Macnee, N., Hilario, E., Tahir, J., Currie, A., Warren, B., Rebstock, R., Hallett, I.C., Chagné, D., Schaffer, R.J., Bulley, S.M., 2021. Peridermal fruit skin formation in *Actinidia* sp. (kiwifruit) is associated with genetic loci controlling russeting and cuticle formation. *BMC Plant Biology* 21 (1), 334, doi: 10.1186/s12870-021-03025-2.
- Macnee, N.C., Rebstock, R., Hallett, I.C., Schaffer, R.J., Bulley, S.M., 2020. A review of current knowledge about the formation of native peridermal exocarp in fruit. *Functional Plant Biology* 47 (12), 1019–1031, doi: 10.1071/FP19135.
- Mahmood, K., Zeisler-Diehl, V.V., Schreiber, L., Bi, Y.-M., Rothstein, S.J., Ranathunge, K., 2019. Overexpression of *ANAC046* Promotes Suberin Biosynthesis in Roots of *Arabidopsis thaliana*. *International Journal of Molecular Sciences* 20 (24), doi: 10.3390/ijms20246117.
- Marga, F., Pesacreta, T.C., Hasenstein, K.H., 2001. Biochemical analysis of elastic and rigid cuticles of *Cirsium horridulum*. *Planta* 213 (6), 841–848, doi: 10.1007/s004250100576.
- Marques, A.V., Pereira, H., 2013. Lignin monomeric composition of corks from the barks of *Betula pendula*, *Quercus suber* and *Quercus cerris* determined by Py–GC–MS/FID. *Journal of Analytical and Applied Pyrolysis* 100, 88–94, doi: 10.1016/j.jaap.2012.12.001.
- McCarthy, R.L., Zhong, R., Fowler, S., Lyskowski, D., Piyasena, H., Carleton, K., Spicer, C., Ye, Z.-H., 2010. The poplar MYB transcription factors, PtrMYB3 and PtrMYB20, are involved in the regulation of secondary wall biosynthesis. *Plant & Cell Physiology* 51 (6), 1084–1090, doi: 10.1093/pcp/pcq064.
- McCarthy, R.L., Zhong, R., Ye, Z.-H., 2009. MYB83 is a direct target of SND1 and acts redundantly with MYB46 in the regulation of secondary cell wall biosynthesis in *Arabidopsis*. *Plant & Cell Physiology* 50 (11), 1950–1964, doi: 10.1093/pcp/pcp139.

- McNevin, J.P., Woodward, W., Hannoufa, A., Feldmann, K.A., Lemieux, B., 1993. Isolation and characterization of *eceriferum* (*cer*) mutants induced by T-DNA insertions in *Arabidopsis thaliana*. *Genome* 36 (3), 610–618, doi: 10.1139/g93-082.
- Mele, G., Ori, N., Sato, Y., Hake, S., 2003. The knotted1-like homeobox gene *BREVIPEDICELLUS* regulates cell differentiation by modulating metabolic pathways. *Genes & Development* 17 (17), 2088–2093, doi: 10.1101/gad.1120003.
- Meyer, A., 1944a. A study of the skin structure of Golden Delicious apples. *Proceedings of the American Society for Horticultural Science* 45, 105–110.
- Meyer, K., Cusumano, J.C., Somerville, C., Chapple, C., 1996. Ferulate-5-hydroxylase from *Arabidopsis thaliana* defines a new family of cytochrome P450-dependent monooxygenases. *Proceedings of the National Academy of Sciences* 93, 6869–6874.
- Miao, Y.-C., Liu, C.-J., 2010. ATP-binding cassette-like transporters are involved in the transport of lignin precursors across plasma and vacuolar membranes. *Proceedings of the National Academy of Sciences* 107 (52), 22728–22733, doi: 10.1073/pnas.1007747108.
- Michailides, T.J., 1991. Russetting and russet scab of prune, an environmentally induced fruit disorder: Symptomatology, induction, and control. *Plant Disease* 75, 1114–1123, doi: 10.1094/PD-75-1114.
- Millar, A.A., Clemens, S., Zachgo, S., Giblin, E.M., Taylor, D.C., Kunst, L., 1999. *CUT1*, an *Arabidopsis* gene required for cuticular wax biosynthesis and pollen fertility, encodes a very-long-chain fatty acid condensing enzyme. *The Plant Cell* 11 (5), 825, doi: 10.2307/3870817.
- Mitsuda, N., Iwase, A., Yamamoto, H., Yoshida, M., Seki, M., Shinozaki, K., Ohme-Takagi, M., 2007. NAC transcription factors, NST1 and NST3, are key regulators of the formation of secondary walls in woody tissues of *Arabidopsis*. *The Plant Cell* 19 (1), 270–280, doi: 10.1105/tpc.106.047043.
- Mitsuda, N., Seki, M., Shinozaki, K., Ohme-Takagi, M., 2005. The NAC transcription factors NST1 and NST2 of *Arabidopsis* regulate secondary wall thickenings and are required for anther dehiscence. *The Plant Cell* 17 (11), 2993–3006, doi: 10.1105/tpc.105.036004.
- Mizutani, M., Ohta, D., Sato, R., 1997. Isolation of a cDNA and a genomic clone encoding cinnamate 4-hydroxylase from *Arabidopsis* and its expression manner in planta. *Plant Physiology* 113 (3), 755–763, doi: 10.1104/pp.113.3.755.
- Molina, I., Li-Beisson, Y., Beisson, F., Ohlrogge, J.B., Pollard, M., 2009. Identification of an *Arabidopsis* feruloyl-coenzyme A transferase required for suberin synthesis. *Plant Physiology* 151 (3), 1317–1328, doi: 10.1104/pp.109.144907.

- Morice, I.M., Shorland, F.B., 1973. Composition of the surface waxes of apple fruits and changes during storage. *Journal of the Science of Food and Agriculture* 24 (11), 1331–1339, doi: 10.1002/jsfa.2740241104.
- Newman, L.J., Perazza, D.E., Juda, L., Campbell, M.M., 2004. Involvement of the R2R3-MYB, AtMYB61, in the ectopic lignification and dark-photomorphogenic components of the *det3* mutant phenotype. *The Plant Journal* 37 (2), 239–250, doi: 10.1046/j.1365-313x.2003.01953.x.
- Nishitani, C., Hirai, N., Komori, S., Wada, M., Okada, K., Osakabe, K., Yamamoto, T., Osakabe, Y., 2016. Efficient genome editing in apple using a CRISPR/Cas9 system. *Scientific Reports* 6, 31481, doi: 10.1038/srep31481.
- Norris, R.F., Bukovac, M.J., 1968. Structure of the pear leaf cuticle with special reference to cuticular penetration. *American Journal of Botany* 55 (8), 975–983, doi: 10.2307/2440563.
- Öhman, D., Demedts, B., Kumar, M., Gerber, L., Gorzsás, A., Goeminne, G., Hedenström, M., Ellis, B., Boerjan, W., Sundberg, B., 2013. MYB103 is required for *FERULATE-5-HYDROXYLASE* expression and syringyl lignin biosynthesis in *Arabidopsis* stems. *The Plant Journal* 73 (1), 63–76, doi: 10.1111/tpj.12018.
- Onik, J.C., Hu, X., Lin, Q., Wang, Z., 2018. Comparative transcriptomic profiling to understand pre- and post-ripening hormonal regulations and anthocyanin biosynthesis in early ripening apple fruit. *Molecules* 23 (8), doi: 10.3390/molecules23081908.
- Osakabe, Y., Liang, Z., Ren, C., Nishitani, C., Osakabe, K., Wada, M., Komori, S., Malnoy, M., Velasco, R., Poli, M., Jung, M.-H., Koo, O.-J., Viola, R., Nagamangala Kanchiswamy, C., 2018. CRISPR-Cas9-mediated genome editing in apple and grapevine. *Nature Protocols* 13 (12), 2844–2863, doi: 10.1038/s41596-018-0067-9.
- Oshima, Y., Mitsuda, N., 2013. The MIXTA-like transcription factor *MYB16* is a major regulator of cuticle formation in vegetative organs. *Plant Signaling & Behavior* 8 (11), e26826, doi: 10.4161/psb.26826.
- Oshima, Y., Shikata, M., Koyama, T., Ohtsubo, N., Mitsuda, N., Ohme-Takagi, M., 2013. MIXTA-like transcription factors and WAX INDUCER1/SHINE1 coordinately regulate cuticle development in *Arabidopsis* and *Torenia fournieri*. *The Plant Cell* 25 (5), 1609–1624, doi: 10.1105/tpc.113.110783.
- Panikashvili, D., Shi, J.X., Bocobza, S., Franke, R.B., Schreiber, L., Aharoni, A., 2010. The *Arabidopsis* DSO/ABCG11 transporter affects cutin metabolism in reproductive organs and suberin in roots. *Molecular Plant* 3 (3), 563–575, doi: 10.1093/mp/ssp103.
- Panikashvili, D., Shi, J.X., Schreiber, L., Aharoni, A., 2011. The *Arabidopsis* ABCG13 transporter is required for flower cuticle secretion and patterning of the petal epidermis. *The New Phytologist* 190 (1), 113–124, doi: 10.1111/j.1469-8137.2010.03608.x.

- Patzlaff, A., McInnis, S., Courtenay, A., Surman, C., Newman, L.J., Smith, C., Bevan, M.W., Mansfield, S., Whetten, R.W., Sederoff, R.R., Campbell, M.M., 2003a. Characterisation of a pine MYB that regulates lignification. *The Plant Journal* 36 (6), 743–754, doi: 10.1046/j.1365-313x.2003.01916.x.
- Patzlaff, A., Newman, L.J., Dubos, C., Whetten, R.W., Smith, C., McInnis, S., Bevan, M.W., Sederoff, R.R., Campbell, M.M., 2003b. Characterisation of PtMYB1, an R2R3-MYB from pine xylem. *Plant Molecular Biology* 53, 597–608, doi: 10.1023/B:PLAN.0000019066.07933.d6.
- Perkins, M., Smith, R.A., Samuels, L., 2019. The transport of monomers during lignification in plants: anything goes but how? *Current Opinion in Biotechnology* 56, 69–74, doi: 10.1016/j.copbio.2018.09.011.
- Pertea, M., Pertea, G.M., Antonescu, C.M., Chang, T.-C., Mendell, J.T., Salzberg, S.L., 2015. StringTie enables improved reconstruction of a transcriptome from RNA-seq reads. *Nature Biotechnology* 33 (3), 290–295, doi: 10.1038/nbt.3122.
- Peschel, S., Knoche, M., 2005. Characterization of microcracks in the cuticle of developing sweet cherry fruit. *Journal of the American Society for Horticultural Science* 130 (4), 487–495, doi: 10.21273/JASHS.130.4.487.
- Petit, J., Bres, C., Mauxion, J.P., Tai, F., Martin, L.B., Fich, E.A., Joubès, J., Rose, J.K., Domergue, F., Rothan, C., 2016. The glycerol-3-phosphate acyltransferase GPAT6 from tomato plays a central role in fruit cutin biosynthesis. *Plant Physiology* (171), 894–913.
- Pfaffl, M.W., 2001. A new mathematical model for relative quantification in real-time RT-PCR. *Nucleic acids research* 29, E45, doi: 10.1093/nar/29.9.e45.
- Powell, A.A., Kostick, S.A., Howard, N.P., Luby, J.J., 2023. Elucidation and characterization of QTLs for russet formation on apple fruit in 'Honeycrisp'-derived breeding germplasm. *Tree Genetics & Genomes* 19 (1), doi: 10.1007/s11295-022-01582-7.
- Pratt, C., 1972. Periderm development and radiation stability of russet fruited sports of apple. *Hort. Res.* 12, 5–12.
- Preston, J., Wheeler, J., Heazlewood, J., Li, S.F., Parish, R.W., 2004. AtMYB32 is required for normal pollen development in *Arabidopsis thaliana*. *The Plant Journal* 40 (6), 979–995, doi: 10.1111/j.1365-313X.2004.02280.x.
- Priestly, J.H., Woffenden, L.M., 1923. The healing of wounds in potato tubers and their propagation by cut sets. *Annals of Applied Biology* 10 (1), 96–115, doi: 10.1111/j.1744-7348.1923.tb05656.x
- Pruitt, R.E., Vielle-Calzada, J.P., Ploense, S.E., Grossniklaus, U., Lolle, S.J., 2000. *FIDDLEHEAD*, a gene required to suppress epidermal cell interactions in *Arabidopsis*, encodes a putative lipid biosynthetic enzyme. *Proceedings of the National Academy of Sciences* 97 (3), 1311–1316, doi: 10.1073/pnas.97.3.1311.

- Putney, S.D., Herlihy, W.C., Schimmel, P., 1983. A new troponin T and cDNA clones for 13 different muscle proteins, found by shotgun sequencing. *Nature* 302, 718–721, doi: doi.org/10.1038/302718a0.
- Quiroga, M., Guerrero, C., Botella, M.A., Barceló, A., Amaya, I., Medina, M.I., Alonso, F.J., Forchetti, S.M. de, Tigier, H., Valpuesta, V., 2000. A tomato peroxidase involved in the synthesis of lignin and suberin. *Plant Physiology* 122, 1119–1128, doi: 10.1104%2Fpp.122.4.1119.
- Randall, R.S., Miyashima, S., Blomster, T., Zhang, J., Elo, A., Karlberg, A., Immanen, J., Nieminen, K., Lee, J.-Y., Kakimoto, T., Blajicka, K., Melnyk, C.W., Alcasabas, A., Forzani, C., Matsumoto-Kitano, M., Mähönen, A.P., Bhalerao, R., Dewitte, W., Helariutta, Y., Murray, J.A.H., 2015. AINTEGUMENTA and the D-type cyclin CYCD3;1 regulate root secondary growth and respond to cytokinins. *Biology Open* 4 (10), 1229–1236, doi: 10.1242/bio.013128.
- Ravisankar, V., Mathew, D., 2022. Multiomics bioinformatics approaches in horticultural crops. G. Rout, K.V. Peter (Ed.), *Omics in horticultural crops*, (Elsevier, Amsterdam), 27–54.
- Renard, J., Martínez-Almonacid, I., Queralta Castillo, I., Sonntag, A., Hashim, A., Bissoli, G., Campos, L., Muñoz-Bertomeu, J., Niñoles, R., Roach, T., Sánchez-León, S., Ozuna, C.V., Gadea, J., Lisón, P., Kranner, I., Barro, F., Serrano, R., Molina, I., Bueso, E., 2021. Apoplastic lipid barriers regulated by conserved homeobox transcription factors extend seed longevity in multiple plant species. *The New Phytologist* 231 (2), 679–694, doi: 10.1111/nph.17399.
- Riederer, M., Schreiber, L., 2001. Protecting against water loss: analysis of the barrier properties of plant cuticles. *Journal of Experimental Botany* 52 (363), 2023–2032, doi: 10.1093/jexbot/52.363.2023.
- Robinson, M.D., McCarthy, D.J., Smyth, G.K., 2010. edgeR: a Bioconductor package for differential expression analysis of digital gene expression data. *Bioinformatics* 26 (1), 139–140, doi: 10.1093/bioinformatics/btp616.
- Rojas-Murcia, N., Hématy, K., Lee, Y., Emonet, A., Ursache, R., Fujita, S., Bellis, D. de, Geldner, N., 2020. High-order mutants reveal an essential requirement for peroxidases but not laccases in Casparian strip lignification. *Proceedings of the National Academy of Sciences* 117 (46), 29166–29177, doi: 10.1073/pnas.2012728117.
- Russell, D.W., 1971. The metabolism of aromatic compounds in higher plants. *Journal of Biological Chemistry* 246 (12), 3870–3878, doi: 10.1016/S0021-9258(18)62115-5.
- Russell, D.W., Conn, E.E., 1967. The cinnamic acid 4-hydroxylase of pea seedlings. *Archives of Biochemistry and Biophysics* 122 (1), 256–258, doi: https://doi.org/10.1016/0003-9861(67)90150-6.

- Sato, H., Takasaki, H., Takahashi, F., Suzuki, T., Iuchi, S., Mitsuda, N., Ohme-Takagi, M., Ikeda, M., Seo, M., Yamaguchi-Shinozaki, K., Shinozaki, K., 2018. *Arabidopsis thaliana* NGATHA1 transcription factor induces ABA biosynthesis by activating *NCED3* gene during dehydration stress. *Proceedings of the National Academy of Sciences* 115 (47), E11178-E11187, doi: 10.1073/pnas.1811491115.
- Sauveplane, V., Kandel, S., Kastner, P.-E., Ehrling, J., Compagnon, V., Werck-Reichhart, D., Pinot, F., 2009. *Arabidopsis thaliana* CYP77A4 is the first cytochrome P450 able to catalyze the epoxidation of free fatty acids in plants. *The FEBS Journal* 276 (3), 719–735, doi: 10.1111/j.1742-4658.2008.06819.x.
- Scharwies, J.D., Grimm, E., Knoche, M., 2014a. Russeting and relative growth rate are positively related in ‘Conference’ and ‘Condo’ pear. *HortScience* 49 (6), 746–749, doi: 10.21273/HORTSCI.49.6.746.
- Schena, M., Shalon, D., Davis, R.W., Brown, P.O., 1995. Quantitative monitoring of gene expression patterns with a complementary DNA microarray. *Science* 270 (5235), 467–470, doi: 10.1126/science.270.5235.467.
- Schneider, K., Hövel, K., Witzel, K., Hamberger, B., Schomburg, D., Kombrink, E., Stuible, H.-P., 2003. The substrate specificity-determining amino acid code of 4-coumarate:CoA ligase. *Proceedings of the National Academy of Sciences* 100 (14), 8601–8606, doi: 10.1073/pnas.1430550100.
- Scholl, R.L., May, S.T., Ware, D.H., 2000. Seed and molecular resources for *Arabidopsis*. *Plant Physiology* 124 (4), 1477–1480, doi: 10.1104/pp.124.4.1477.
- Schönherr, J., 1976. Water permeability of isolated cuticular membranes: The effect of cuticular waxes on diffusion of water. *Planta* 131 (2), 159–164, doi: 10.1007/BF00389989.
- Schouten, S., Moerkerken, P., Gelin, F., Baas, M., Leeuw, J.W. de, Sinnighe Damasté, J.S., 1998. Structural characterization of aliphatic, non-hydrolyzable biopolymers in freshwater algae and a leaf cuticle using ruthenium tetroxide degradation. *Phytochemistry* 49 (4), 987–993, doi: 10.1016/S0031-9422(97)00942-4.
- Schreiber, L., 2010. Transport barriers made of cutin, suberin and associated waxes. *Trends in Plant Science* 15 (10), 546–553, doi: 10.1016/j.tplants.2010.06.004.
- Schreiber, L., Hartmann, K., Skrabs, M., Zeier, J., 1999. Apoplastic barriers in roots: chemical composition of endodermal and hypodermal cell walls. *Journal of Experimental Botany* 50 (337), 1267–1280, doi: 10.1093/jxb/50.337.1267.
- Segado, P., Heredia-Guerrero, J.A., Heredia, A., Domínguez, E., 2020. Cutinsomes and CUTIN SYNTHASE1 function sequentially in tomato fruit cutin deposition. *Plant Physiology* 183 (4), 1622–1637, doi: 10.1104/pp.20.00516.
- Serra, O., Geldner, N., 2022. The making of suberin. *The New Phytologist* 235 (3), 848–866, doi: 10.1111/nph.18202.

- Serra, O., Hohn, C., Franke, R., Prat, S., Molinas, M., Figueras, M., 2010. A feruloyl transferase involved in the biosynthesis of suberin and suberin-associated wax is required for maturation and sealing properties of potato periderm. *The Plant Journal* 62 (2), 277–290, doi: 10.1111/j.1365-313X.2010.04144.x.
- Serra, O., Mähönen, A.P., Hetherington, A.J., Ragni, L., 2022. The making of plant armor: The periderm. *Annual Review of Plant Biology* 73, 405–432, doi: 10.1146/annurev-arplant-102720-031405.
- Serra, O., Soler, M., Hohn, C., Franke, R., Schreiber, L., Prat, S., Molinas, M., Figueras, M., 2009a. Silencing of *StKCS6* in potato periderm leads to reduced chain lengths of suberin and wax compounds and increased peridermal transpiration. *Journal of Experimental Botany* 60 (2), 697–707, doi: 10.1093/jxb/ern314.
- Serra, O., Soler, M., Hohn, C., Sauveplane, V., Pinot, F., Franke, R., Schreiber, L., Prat, S., Molinas, M., Figueras, M., 2009b. *CYP86A33*-targeted gene silencing in potato tuber alters suberin composition, distorts suberin lamellae, and impairs the periderm's water barrier function. *Plant Physiology* 149 (2), 1050–1060, doi: 10.1104/pp.108.127183.
- Serrano, M., Coluccia, F., Torres, M., L'Haridon, F., Métraux, J.-P., 2014. The cuticle and plant defense to pathogens. *Frontiers in Plant Science* 5, 274, doi: 10.3389/fpls.2014.00274.
- Shanmugarajah, K., Linka, N., Gräfe, K., Smits, S.H.J., Weber, A.P.M., Zeier, J., Schmitt, L., 2019. *ABCG1* contributes to suberin formation in *Arabidopsis thaliana* roots. *Scientific Reports* 9 (1), 11381, doi: 10.1038/s41598-019-47916-9.
- Shi, C.-H., Wang, X.-Q., Xu, J.-F., Zhang, Y.-X., Qi, B., Jun, L., 2021. Dissecting the molecular mechanism of russeting in sand pear (*Pyrus pyrifolia* Nakai) by metabolomics, transcriptomics, and proteomics. *The Plant Journal* 108 (6), 1644–1661, doi: 10.1111/tpj.15532.
- Shi, D., Ren, A., Tang, X., Qi, G., Xu, Z., Chai, G., Hu, R., Zhou, G., Kong, Y., 2018. MYB52 negatively regulates pectin demethylesterification in seed coat mucilage. *Plant Physiology* 176, 2737–2749, doi: 10.1104/pp.17.01771.
- Shi, J.X., Adato, A., Alkan, N., He, Y., Lashbrooke, J., Matas, A.J., Meir, S., Malitsky, S., Isaacson, T., Prusky, D., Leshkowitz, D., Schreiber, L., Granell, A.R., Widemann, E., Grausem, B., Pinot, F., Rose, J.K.C., Rogachev, I., Rothan, C., Aharoni, A., 2013. The tomato SISHINE3 transcription factor regulates fruit cuticle formation and epidermal patterning. *The New Phytologist* 197 (2), 468–480, doi: 10.1111/nph.12032.
- Shi, J.X., Malitsky, S., Oliveira, S. de, Branigan, C., Franke, R.B., Schreiber, L., Aharoni, A., 2011. SHINE transcription factors act redundantly to pattern the archetypal surface of *Arabidopsis* flower organs. *PLoS Genetics* 7 (5), e1001388, doi: 10.1371/journal.pgen.1001388.

- Shiono, K., Ando, M., Nishiuchi, S., Takahashi, H., Watanabe, K., Nakamura, M., Matsuo, Y., Yasuno, N., Yamanouchi, U., Fujimoto, M., Takanashi, H., Ranathunge, K., Franke, R.B., Shitan, N., Nishizawa, N.K., Takamura, I., Yano, M., Tsutsumi, N., Schreiber, L., Yazaki, K., Nakazono, M., Kato, K., 2014. RCN1/OsABCG5, an ATP-binding cassette (ABC) transporter, is required for hypodermal suberization of roots in rice (*Oryza sativa*). *The Plant Journal* 80 (1), 40–51, doi: 10.1111/tpj.12614.
- Shukla, V., Han, J.-P., Cléard, F., Lefebvre-Legendre, L., Gully, K., Flis, P., Berhin, A., Andersen, T.G., Salt, D.E., Nawrath, C., Barberon, M., 2021. Suberin plasticity to developmental and exogenous cues is regulated by a set of MYB transcription factors. *Proceedings of the National Academy of Sciences* 118 (39), doi: 10.1073/pnas.2101730118.
- Si, Y., Khanal, B.P., Schlüter, O.K., Knoche, M., 2021. Direct evidence for a radial gradient in age of the apple fruit cuticle. *Frontiers in Plant Science* 12, 730837, doi: 10.3389/fpls.2021.730837.
- Sieber, P., Schorderet, M., Ryser, U., Buchala, A., Kolattukudy, P., Metraux, J.-P., Nawrath, C., 2000. Transgenic Arabidopsis plants expressing a fungal cutinase show alterations in the structure and properties of the cuticle and postgenital organ fusions. *The Plant Cell* 12 (5), 721, doi: 10.2307/3870997.
- Silva, S.P., Sabino, M.A., Fernandes, E.M., Correlo, V.M., Boesel, L.F., Reis, R.L., 2005. Cork: properties, capabilities and applications. *International Materials Reviews* 50 (6), 345–365, doi: 10.1179/174328005X41168.
- Simons, R.K., Aubertin, M., 1959. Development of epidermal, hypodermal and cortical tissues in the Golden Delicious apple as influenced by induced mechanical injury. *Proceedings of the American Society for Horticultural Science* 74, 1–9.
- Simons, R.K., Chu, M.C., 1978. Periderm morphology of mature 'Golden Delicious' apple with special reference to russeting. *Scientia Horticulturae* 8 (4), 333–340, doi: 10.1016/0304-4238(78)90055-9.
- Skene, D.S., 1982. The development of russet, rough russet and cracks on the fruit of the apple Cox's Orange Pippin during the course of the season. *Journal of Horticultural Science* 57 (2), 165–174, doi: 10.1080/00221589.1982.11515037.
- Smetana, O., Mäkilä, R., Lyu, M., Amiryousefi, A., Sánchez Rodríguez, F., Wu, M.-F., Solé-Gil, A., Leal Gavarrón, M., Siligato, R., Miyashima, S., Roszak, P., Blomster, T., Reed, J.W., Broholm, S., Mähönen, A.P., 2019. High levels of auxin signalling define the stem-cell organizer of the vascular cambium. *Nature* 565 (7740), 485–489, doi: 10.1038/s41586-018-0837-0.
- Soliday, C.L., Kolattukudy, P.E., Davis, R.W., 1979. Chemical and ultrastructural evidence that waxes associated with the suberin polymer constitute the major diffusion barrier to

- water vapor in potato tuber (*Solanum tuberosum* L.). *Planta* 146 (5), 607–614, doi: 10.1007/BF00388840.
- Sonbol, F.-M., Fornalé, S., Capellades, M., Encina, A., Touriño, S., Torres, J.-L., Rovira, P., Ruel, K., Puigdomènech, P., Rigau, J., Caparrós-Ruiz, D., 2009. The maize ZmMYB42 represses the phenylpropanoid pathway and affects the cell wall structure, composition and degradability in *Arabidopsis thaliana*. *Plant Molecular Biology* 70 (3), 283–296, doi: 10.1007/s11103-009-9473-2.
- Stanišić, M., Ćosić, T., Savić, J., Krstić-Milošević, D., Mišić, D., Smigocki, A., Ninković, S., Banjac, N., 2019. Hairy root culture as a valuable tool for allelopathic studies in apple. *Tree Physiology* 39 (5), 888–905, doi: 10.1093/treephys/tpz006.
- Storch, T.T., Pegoraro, C., Finatto, T., Quecini, V., Rombaldi, C.V., Girardi, C.L., 2015. Identification of a novel reference gene for apple transcriptional profiling under postharvest conditions. *PLOS ONE* 10 (3), e0120599, doi: 10.1371/journal.pone.0120599.
- Stowe, E., Dhingra, A., 2021. Development of the Arctic apple. *Plant Breeding Reviews* 44, 273–296, doi: 10.1002/9781119717003.ch8.
- Straube, J., Chen, Y.-H., Khanal, B.P., Shumbusho, A., Zeisler-Diehl, V., Suresh, K., Schreiber, L., Knoche, M., Debener, T., 2020. Russeting in apple is initiated after exposure to moisture ends: Molecular and biochemical evidence. *Plants* 10 (1), doi: 10.3390/plants10010065.
- Suer, S., Agusti, J., Sanchez, P., Schwarz, M., Greb, T., 2011. WOX4 imparts auxin responsiveness to cambium cells in *Arabidopsis*. *The Plant Cell* 23 (9), 3247–3259, doi: 10.1105/tpc.111.087874.
- Sun, X., Jiao, C., Schwaninger, H., Chao, C.T., Ma, Y., Duan, N., Khan, A., Ban, S., Xu, K., Cheng, L., Zhong, G.-Y., Fei, Z., 2020. Phased diploid genome assemblies and pan-genomes provide insights into the genetic history of apple domestication. *Nature Genetics* 52 (12), 1423–1432, doi: 10.1038/s41588-020-00723-9.
- Sutcliffe, J.G., Milner, R.J., Bloom, F.E., Lerner, R.A., 1982. Common 82-nucleotide sequence unique to brain RNA. *Proceedings of the National Academy of Sciences* 79 (16), 4942–4946, doi: 10.1073/pnas.79.16.4942.
- Szczuka and Szczuka, 2003. Cuticle fluorescence during embryogenesis of *Arabidopsis thaliana* (L.) Heynh. *Acta Biologica Cracoviensia Series Botanica* 45 (1), 63–67.
- Takahashi, K., Shimada, T., Kondo, M., Tamai, A., Mori, M., Nishimura, M., Hara-Nishimura, I., 2010. Ectopic expression of an esterase, which is a candidate for the unidentified plant cutinase, causes cuticular defects in *Arabidopsis thaliana*. *Plant & Cell Physiology* 51 (1), 123–131, doi: 10.1093/pcp/pcp173.
- Tamagnone, L., Meria, A., Parr, A., Mackay, S., Culiñez-Macia, F. A., Roberts, K., Martin, C., 1998. The AmMYB308 and AmMYB330 transcription factors from *Antirrhinum*

- regulate phenylpropanoid and lignin biosynthesis in transgenic tobacco. *The Plant Cell* 10, 135–154.
- Taylor, B.K., 1975. Reduction of apple skin russeting by gibberellin A₄₊₇. *Journal of Horticultural Science* 50 (2), 169–172, doi: 10.1080/00221589.1975.11514619.
- Taylor, B.K., 1978. Effects of gibberellin sprays on fruit russet and tree performance of Golden Delicious apple. *Journal of Horticultural Science* 53 (3), 167–169, doi: 10.1080/00221589.1978.11514814.
- Thangavel, T., Tegg, R.S., Wilson, C.R., 2016. Toughing it out—Disease-resistant potato mutants have enhanced tuber skin defenses. *Phytopathology* 106 (5), 474–483, doi: 10.1094/PHYTO-08-15-0191-R.
- Tian, T., Liu, Y., Yan, H., You, Q., Yi, X., Du, Z., Xu, W., Su, Z., 2017. agriGO v2.0: a GO analysis toolkit for the agricultural community, 2017 update. *Nucleic Acids Research* 45 (W1), W122–W129, doi: 10.1093/nar/gkx382.
- Todd, J., Post-Beittenmiller, D., Jaworski, J.G., 1999. *KCS1* encodes a fatty acid elongase 3-ketoacyl-CoA synthase affecting wax biosynthesis in *Arabidopsis thaliana*. *The Plant Journal* 17 (2), 119–130, doi: 10.1046/j.1365-313x.1999.00352.x.
- Tukey, L.D., 1959. Observations on the russeting of apples growing in plastic bags. *Proceedings of the American Society for Horticultural Science* 74, 30–39.
- Ursache, R., Jesus Vieira Teixeira, C. de, Dénervaud Tendon, V., Gully, K., Bellis, D. de, Schmid-Siegert, E., Grube Andersen, T., Shekhar, V., Calderon, S., Pradervand, S., Nawrath, C., Geldner, N., Vermeer, J.E.M., 2021. GDSL-domain proteins have key roles in suberin polymerization and degradation. *Nature Plants* 7 (3), 353–364, doi: 10.1038/s41477-021-00862-9.
- van Bergen, P.F., Blokker, P., Collinson, M.E., Sinnighe Damsté, J.S., Leeuw, J.W. de (Eds.), 2004. Structural biomacromolecules in plants: what can be learnt from the fossil record?: The evolution of plant physiology—from whole plants to ecosystems. *Linnean Society symposium series*, vol. 21. Elsevier Academic Press, Amsterdam.
- Vanblaere, T., Szankowski, I., Schaart, J., Schouten, H., Flachowsky, H., Broggini, G.A.L., Gessler, C., 2011. The development of a cisgenic apple plant. *Journal of Biotechnology* 154 (4), 304–311, doi: 10.1016/j.jbiotec.2011.05.013.
- Velasco, R., Zharkikh, A., Affourtit, J., Dhingra, A., Cestaro, A., Kalyanaraman, A., Fontana, P., Bhatnagar, S.K., Troggio, M., Pruss, D., Salvi, S., Pindo, M., Baldi, P., Castelletti, S., Cavaiuolo, M., Coppola, G., Costa, F., Cova, V., Dal Ri, A., Goremykin, V., Komjanc, M., Longhi, S., Magnago, P., Malacarne, G., Malnoy, M., Micheletti, D., Moretto, M., Perazzolli, M., Si-Ammour, A., Vezzulli, S., Zini, E., Eldredge, G., Fitzgerald, L.M., Gutin, N., Lanchbury, J., Macalma, T., Mitchell, J.T., Reid, J., Wardell, B., Kodira, C., Chen, Z., Desany, B., Niazi, F., Palmer, M., Koepke, T., Jiwan, D., Schaeffer, S., Krishnan, V., Wu,

- C., Chu, V.T., King, S.T., Vick, J., Tao, Q., Mraz, A., Stormo, A., Stormo, K., Bogden, R., Ederle, D., Stella, A., Vecchiatti, A., Kater, M.M., Masiero, S., Lasserre, P., Lespinasse, Y., Allan, A.C., Bus, V., Chagné, D., Crowhurst, R.N., Gleave, A.P., Lavezzo, E., Fawcett, J.A., Proost, S., Rouzé, P., Sterck, L., Toppo, S., Lazzari, B., Hellens, R.P., Durel, C.-E., Gutin, A., Bumgarner, R.E., Gardiner, S.E., Skolnick, M., Egholm, M., van de Peer, Y., Salamini, F., Viola, R., 2010. The genome of the domesticated apple (*Malus × domestica* Borkh.). *Nature Genetics* 42 (10), 833–839, doi: 10.1038/ng.654.
- Vélez-Bermúdez, I.-C., Salazar-Henao, J.E., Fornalé, S., López-Vidriero, I., Franco-Zorrilla, J.-M., Grotewold, E., Gray, J., Solano, R., Schmidt, W., Pagés, M., Riera, M., Caparros-Ruiz, D., 2015. A MYB/ZML complex regulates wound-induced lignin genes in maize. *The Plant Cell* 27 (11), 3245–3259, doi: 10.1105/tpc.15.00545.
- Verdaguer, R., Soler, M., Serra, O., Garrote, A., Fernández, S., Company-Arumí, D., Anticó, E., Molinas, M., Figueras, M., 2016. Silencing of the potato *StNAC103* gene enhances the accumulation of suberin polyester and associated wax in tuber skin. *Journal of Experimental Botany* 67 (18), 5415–5427, doi: 10.1093/jxb/erw305.
- Vermaas, J.V., Dixon, R.A., Chen, F., Mansfield, S.D., Boerjan, W., Ralph, J., Crowley, M.F., Beckham, G.T., 2019. Passive membrane transport of lignin-related compounds. *Proceedings of the National Academy of Sciences* 116 (46), 23117–23123, doi: 10.1073/pnas.1904643116.
- Vilaine, F., Kerchev, P., Clément, G., Batailler, B., Cayla, T., Bill, L., Gissot, L., Dinant, S., 2013. Increased expression of a phloem membrane protein encoded by *NHL26* alters phloem export and sugar partitioning in Arabidopsis. *The Plant Cell* 25 (5), 1689–1708, doi: 10.1105/tpc.113.111849.
- Villena, J.F., Domínguez, E., Stewart, D., Heredia, A., 1999. Characterization and biosynthesis of non-degradable polymers in plant cuticles. *Planta* 208 (2), 181–187, doi: 10.1007/s004250050548.
- Vishwanath, S.J., Kosma, D.K., Pulsifer, I.P., Scandola, S., Pascal, S., Joubès, J., Dittrich-Domergue, F., Lessire, R., Rowland, O., Domergue, F., 2013. Suberin-associated fatty alcohols in Arabidopsis: distributions in roots and contributions to seed coat barrier properties. *Plant Physiology* 163 (3), 1118–1132, doi: 10.1104/pp.113.224410.
- Visser, T., 1964. Juvenile phase and growth of apple and pear seedlings. *Euphytica* 13, 119–129, doi: 10.1007/BF00033299.
- Vulavala, V.K.R., Fogelman, E., Faigenboim, A., Shoseyov, O., Ginzberg, I., 2019. The transcriptome of potato tuber phellogen reveals cellular functions of cork cambium and genes involved in periderm formation and maturation. *Scientific Reports* 9 (1), 10216, doi: 10.1038/s41598-019-46681-z.

- Wahrenburg, Z., Benesch, E., Lowe, C., Jimenez, J., Vulavala, V.K.R., Lü, S., Hammerschmidt, R., Douches, D., Yim, W.C., Santos, P., Kosma, D.K., 2021. Transcriptional regulation of wound suberin deposition in potato cultivars with differential wound healing capacity. *The Plant Journal* 107 (1), 77–99, doi: 10.1111/tpj.15275.
- Wan, J., Wang, R., Zhang, P., Sun, L., Ju, Q., Huang, H., Lü, S., Tran, L.-S., Xu, J., 2021. MYB70 modulates seed germination and root system development in *Arabidopsis*. *iScience* 24 (11), 103228, doi: 10.1016/j.isci.2021.103228.
- Wang, H., Zhang, S., Fu, Q., Wang, Z., Liu, X., Sun, L., Zhao, Z., 2023. Transcriptomic and metabolomic analysis reveals a protein module involved in pre-harvest apple peel browning. *Plant Physiology*, kiad064, doi: 10.1093/plphys/kiad064.
- Wang, J., Sun, L., Xie, L., He, Y., Luo, T., Sheng, L., Luo, Y., Zeng, Y., Xu, J., Deng, X., Cheng, Y., 2016. Regulation of cuticle formation during fruit development and ripening in 'Newhall' navel orange (*Citrus sinensis* Osbeck) revealed by transcriptomic and metabolomic profiling. *Plant Science* 243, 131–144, doi: 10.1016/j.plantsci.2015.12.010.
- Wang, L., Li, J., Gao, J., Feng, X., Shi, Z., Gao, F., Xu, X., Yang, L., 2014. Inhibitory effect of chlorogenic acid on fruit russetting in 'Golden Delicious' apple. *Scientia Horticulturae* 178, 14–22, doi: 10.1016/j.scienta.2014.07.038.
- Wang, N., Zheng, Y., Duan, N., Zhang, Z., Ji, X., Jiang, S., Sun, S., Yang, L., Bai, Y., Fei, Z., Chen, X., 2015. Comparative transcriptomes analysis of red- and white-fleshed apples in an F₁ population of *Malus sieversii* f. *niedzwetzkyana* crossed with *M. domestica* 'Fuji'. *PloS one* 10 (7), e0133468, doi: 10.1371/journal.pone.0133468.
- Wang, W., Liu, X., Gai, X., Ren, J., Liu, X., Cai, Y., Wang, Q., Ren, H., 2015a. *Cucumis sativus* L. WAX2 plays a pivotal role in wax biosynthesis, influencing pollen fertility and plant biotic and abiotic stress responses. *Plant & Cell Physiology* 56 (7), 1339–1354, doi: 10.1093/pcp/pcv052.
- Wang, W., Wang, S., Li, M., Hou, L., 2018. Cloning and expression analysis of *Cucumis sativus* L. *CER4* involved in cuticular wax biosynthesis in cucumber. *Biotechnology & Biotechnological Equipment* 32 (5), 1113–1118, doi: 10.1080/13102818.2018.1499444.
- Wang, W., Zhang, Y., Xu, C., Ren, J., Liu, X., Black, K., Gai, X., Wang, Q., Ren, H., 2015b. Cucumber *ECERIFERUM1* (*CsCER1*), which influences the cuticle properties and drought tolerance of cucumber, plays a key role in VLC alkanes biosynthesis. *Plant Molecular Biology* 87 (3), 219–233, doi: 10.1007/s11103-014-0271-0.
- Wang, Y., Dai, M., Wu, X., Zhang, S., Shi, Z., Cai, D., Miao, L., 2022. An ARF1-binding factor triggering programmed cell death and periderm development in pear russet fruit skin. *Horticulture Research* 9, 1–14, doi: 10.1093/hr/uhab061.
- Wang, Y., Xu, J., He, Z., Hu, N., Luo, W., Liu, X., Shi, X., Liu, T., Jiang, Q., An, P., Le Liu, Sun, Y., Jetter, R., Li, C., Wang, Z., 2021. BdFAR4, a root-specific fatty acyl-coenzyme A

- reductase, is involved in fatty alcohol synthesis of root suberin polyester in *Brachypodium distachyon*. *The Plant Journal* 106 (5), 1468–1483, doi: 10.1111/tpj.15249.
- Wang, Z., Liu, S., Huo, W., Chen, M., Zhang, Y., Jiang, S., 2022. Transcriptome and metabolome analyses reveal phenotype formation differences between russet and non-russet apples. *Frontiers in Plant Science* 13, 1057226, doi: 10.3389/fpls.2022.1057226.
- Wei, X., Mao, L., Wei, X., Xia, M., Xu, C., 2020. MYB41, MYB107, and MYC2 promote ABA-mediated primary fatty alcohol accumulation via activation of *AchnFAR* in wound suberization in kiwifruit. *Horticulture Research* 7 (1), 86, doi: 10.1038/s41438-020-0309-1.
- Wellesen, K., Durst, F., Pinot, F., Benveniste, I., Nettesheim, K., Wisman, E., Steiner-Lange, S., Saedler, H., Yephremov, A., 2001. Functional analysis of the *LACERATA* gene of *Arabidopsis* provides evidence for different roles of fatty acid ω -hydroxylation in development. *Proceedings of the National Academy of Sciences* 98 (17), 9694–9699.
- Welsh, M.F., May, J., 1967. Virus etiology of foliar vein-flecking or ring pattern and fruit russetting or blotch on apple. *Canadian Journal of Plant Science* 47, 703–708.
- Wertheim, S.J., 1982. Fruit russetting in apple as affected by various gibberellins. *Journal of Horticultural Science* 57 (3), 283–288, doi: 10.1080/00221589.1982.11515054.
- Winkler, A., Athoo, T., Knoche, M., 2022. Russetting of fruits: Etiology and management. *Horticulturae* 8 (3), 231, doi: 10.3390/horticulturae8030231.
- Winkler, A., Grimm, E., Knoche, M., Lindstaedt, J., Köpcke, D., 2014. Late-season surface water induces skin spot in apple. *HortScience* 49 (10), 1324–1327, doi: 10.21273/HORTSCI.49.10.1324.
- Wood, G.A., 1972. Russet ring and some associated virus disorders of apple (*Malus sylvestris* (L.) Mill.) in New Zealand. *New Zealand Journal of Agricultural Research* 15 (2), 405–412, doi: 10.1080/00288233.1972.10421269.
- Woolfson, K.N., Esfandiari, M., Bernards, M.A., 2022. Suberin biosynthesis, assembly, and regulation. *Plants* 11 (4), doi: 10.3390/plants11040555.
- Wu, J., Wang, Y., Zhang, L.-X., Zhang, X.-Z., Kong, J., Lu, J., Han, Z.-H., 2012. High-efficiency regeneration of *Agrobacterium rhizogenes*-induced hairy root in apple rootstock *Malus baccata* (L.) Borkh. *Plant Cell, Tissue and Organ Culture* 111 (2), 183–189, doi: 10.1007/s11240-012-0182-1.
- Wunderling, A., Ripper, D., Barra-Jimenez, A., Mahn, S., Sajak, K., Targem, M.B., Ragni, L., 2018. A molecular framework to study periderm formation in *Arabidopsis*. *The New Phytologist* 219 (1), 216–229, doi: 10.1111/nph.15128.
- Xiao, F., Goodwin, S.M., Xiao, Y., Sun, Z., Baker, D., Tang, X., Jenks, M.A., Zhou, J.-M., 2004. *Arabidopsis* CYP86A2 represses *Pseudomonas syringae* type III genes and is required for cuticle development. *The EMBO Journal* 23 (14), 2903–2913, doi: 10.1038/sj.emboj.7600290.

- Xiao, W., Molina, D., Wunderling, A., Ripper, D., Vermeer, J.E.M., Ragni, L., 2020. Pluripotent pericycle cells trigger different growth outputs by integrating developmental cues into distinct regulatory modules. *Current biology* 30 (22), 4384-4398.e5, doi: 10.1016/j.cub.2020.08.053.
- Xu, B., Sathitsuksanoh, N., Tang, Y., Udvardi, M.K., Zhang, J.-Y., Shen, Z., Balota, M., Harich, K., Zhang, P.Y.-H., Zhao, B., 2012. Overexpression of *AtLOV1* in Switchgrass alters plant architecture, lignin content, and flowering time. *PLOS ONE* 7 (12), e47399, doi: 10.1371/journal.pone.0047399.
- Xu, H., Liu, P., Wang, C., Wu, S., Dong, C., Lin, Q., Sun, W., Huang, B., Xu, M., Tauqeer, A., Wu, S., 2022. Transcriptional networks regulating suberin and lignin in endodermis link development and ABA response. *Plant Physiology* 190 (2), 1165–1181, doi: 10.1093/plphys/kiac298.
- Xu, X., Guerriero, G., Berni, R., Sergeant, K., Guignard, C., Lenouvel, A., Hausman, J.-F., Legay, S., 2022. MdMYB52 regulates lignin biosynthesis upon the suberization process in apple. *Frontiers in Plant Science* 13, 1039014, doi: 10.3389/fpls.2022.1039014.
- Xu, X., Guerriero, G., Domergue, F., Beine-Golovchuk, O., Cocco, E., Berni, R., Sergeant, K., Hausman, J.-F., Legay, S., 2023. Characterization of MdMYB68, a suberin master regulator in russeted apples. *Frontiers in Plant Science* 14 (1143961), 1–20.
- Yadav, V., Molina, I., Ranathunge, K., Castillo, I.Q., Rothstein, S.J., Reed, J.W., 2014. ABCG transporters are required for suberin and pollen wall extracellular barriers in *Arabidopsis*. *The Plant Cell* 26 (9), 3569–3588, doi: 10.1105/tpc.114.129049.
- Yang, C., Xu, Z., Song, J., Conner, K., Vizcay Barrena, G., Wilson, Z.A., 2007. *Arabidopsis* MYB26/MALE STERILE35 regulates secondary thickening in the endothecium and is essential for anther dehiscence. *The Plant Cell* 19 (2), 534–548, doi: 10.1105/tpc.106.046391.
- Yang, L., Zhao, X., Lingyu, R., Li, C., Di Fan, Luo, K., 2017. PtoMYB156 is involved in negative regulation of phenylpropanoid metabolism and secondary cell wall biosynthesis during wood formation in poplar. *Scientific Reports* 7, 41209, doi: 10.1038/srep41209.
- Yang, T., Ma, H., Zhang, J., Wu, T., Song, T., Tian, J., Yao, Y., 2019. Systematic identification of long noncoding RNAs expressed during light-induced anthocyanin accumulation in apple fruit. *The Plant Journal* 100 (3), 572–590, doi: 10.1111/tpj.14470.
- Yang, W., Simpson, J.P., Li-Beisson, Y., Beisson, F., Pollard, M., Ohlrogge, J.B., 2012. A land-plant-specific glycerol-3-phosphate acyltransferase family in *Arabidopsis*: substrate specificity, *sn-2* preference, and evolution. *Plant Physiology* 160 (2), 638–652, doi: 10.1104/pp.112.201996.

- Ye, Y., Zhou, L., Liu, X., Hao, L., Li, D., Cao, M., Chen, H., Xu, L., Zhu, J., Zhao, Y., 2017. A novel chemical inhibitor of ABA signaling targets all ABA receptors. *Plant Physiology* 173, 2356–2369, doi: 10.1104/pp.16.01862.
- Yeats, T.H., Huang, W., Chatterjee, S., Viart, H.M.-F., Clausen, M.H., Stark, R.E., Rose, J.K.C., 2014. Tomato Cutin Deficient 1 (CD1) and putative orthologs comprise an ancient family of cutin synthase-like (CUS) proteins that are conserved among land plants. *The Plant Journal* 77 (5), 667–675, doi: 10.1111/tpj.12422.
- Yeats, T.H., Martin, L.B.B., Viart, H.M.-F., Isaacson, T., He, Y., Zhao, L., Matas, A.J., Buda, G.J., Domozych, D.S., Clausen, M.H., Rose, J.K.C., 2012. The identification of cutin synthase: formation of the plant polyester cutin. *Nature Chemical Biology* 8 (7), 609–611, doi: 10.1038/nchembio.960.
- Yeats, T.H., Rose, J.K.C., 2013. The formation and function of plant cuticles. *Plant Physiology* 163 (1), 5–20, doi: 10.1104/pp.113.222737.
- Yogendra, K.N., Kumar, A., Sarkar, K., Li, Y., Pushpa, D., Mosa, K.A., Duggavathi, R., Kushalappa, A.C., 2015. Transcription factor StWRKY1 regulates phenylpropanoid metabolites conferring late blight resistance in potato. *Journal of Experimental Botany* 66 (22), 7377–7389, doi: 10.1093/jxb/erv434.
- Yuan, G., Bian, S., Han, X., He, S., Liu, K., Zhang, C., Cong, P., 2019. An integrated transcriptome and proteome analysis reveals new insights into russetting of bagging and non-bagging "Golden Delicious" apple. *International Journal of Molecular Sciences* 20 (18), doi: 10.3390/ijms20184462.
- Zhang, B., Yang, H.-J., Qu, D., Zhu, Z.-Z., Yang, Y.-Z., Zhao, Z.-Y., 2022. The MdBBX22-miR858-MdMYB9/11/12 module regulates proanthocyanidin biosynthesis in apple peel. *Plant Biotechnology Journal* 20 (9), 1683–1700, doi: 10.1111/pbi.13839.
- Zhang, J., Eswaran, G., Alonso-Serra, J., Kucukoglu, M., Xiang, J., Yang, W., Elo, A., Nieminen, K., Damén, T., Joung, J.-G., Yun, J.-Y., Lee, J.-H., Ragni, L., Barbier de Reuille, P., Ahnert, S.E., Lee, J.-Y., Mähönen, A.P., Helariutta, Y., 2019. Transcriptional regulatory framework for vascular cambium development in *Arabidopsis* roots. *Nature Plants* 5 (10), 1033–1042, doi: 10.1038/s41477-019-0522-9.
- Zhang, L., Hu, J., Han, X., Li, J., Gao, Y., Richards, C.M., Zhang, C., Tian, Y., Liu, G., Gul, H., Wang, D., Tian, Y., Yang, C., Meng, M., Yuan, G., Kang, G., Wu, Y., Wang, K., Zhang, H., Wang, D., Cong, P., 2019. A high-quality apple genome assembly reveals the association of a retrotransposon and red fruit colour. *Nature Communications* 10 (1), 1494, doi: 10.1038/s41467-019-09518-x.
- Zhang, X., Henriques, R., Lin, S.-S., Niu, Q.-W., Chua, N.-H., 2006. Agrobacterium-mediated transformation of *Arabidopsis thaliana* using the floral dip method. *Nature Protocols* 1 (2), 641–646, doi: 10.1038/nprot.2006.97.

-
- Zhong, R., Lee, C., Zhou, J., McCarthy, R.L., Ye, Z.-H., 2008. A battery of transcription factors involved in the regulation of secondary cell wall biosynthesis in Arabidopsis. *The Plant Cell* 20 (10), 2763–2782, doi: 10.1105/tpc.108.061325.
- Zhong, R., Richardson, E.A., Ye, Z.-H., 2007. The MYB46 transcription factor is a direct target of SND1 and regulates secondary wall biosynthesis in Arabidopsis. *The Plant Cell* 19 (9), 2776–2792, doi: 10.1105/tpc.107.053678.
- Zhou, H., Bai, S., Wang, N., Sun, X., Zhang, Y., Zhu, J., Dong, C., 2022. CRISPR/Cas9-mediated mutagenesis of *MdCNGC2* in apple callus and VIGS-mediated silencing of *MdCNGC2* in fruits improve resistance to *Botryosphaeria dothidea*. *Frontiers in Plant Science* 11, 1–11, doi: <https://doi.org/10.3389/fpls.2020.575477>
- Zhou, J., Lee, C., Zhong, R., Ye, Z.-H., 2009. MYB58 and MYB63 are transcriptional activators of the lignin biosynthetic pathway during secondary cell wall formation in Arabidopsis. *The Plant Cell* 21 (1), 248–266, doi: 10.1105/tpc.108.063321.

Electronic appendix

Chapter 3 - Russeting in apple is initiated after exposure to moisture ends—I. Histological evidence

Electronical File E1. Meteorological data (XLSX)

Chapter 5 - Apple fruit periderms (russeting) induced by wounding or by moisture have the same histologies, chemistries and gene expressions

Electronical File E2. Data produced in figures (XLSX)

Chapter 6 - Time course of changes in the transcriptome during russet induction in apple fruit

Electronical File E3. Data S1 List of DEGs at corresponding timepoints in 2018 and 2019.
(Spreadsheet in .xlsx file)

Electronical File E4. Data S2 Results GO terms season 2018 (Spreadsheet in .xlsx file)

Electronical File E5. Data S3 Results GO terms season 2019 (Spreadsheet in .xlsx file)

Electronical File E6. Data S4 GOterms at corresponding time points the seasons 2018 and
2019 (Spreadsheet in .xlsx file)

Electronical File E7. Data S5 Results GO terms season 2018 12 d wet + 0 d dry $\log_2FC \leq -1$
(Spreadsheet in .xlsx file)

Electronical File E8. Data S6 List of DEGs during season 2018 (Spreadsheet in .xlsx file)

Electronical File E9. Data S7 List of DEGs during season 2019 (Spreadsheet in .xlsx file)

Chapter 7 - Functional analysis of candidate genes potentially involved in russetting of apple fruit

Electronical File E10. Sequence and alignment of *WRKY56* (HF14837) used in this study.

Electronical File E11. Sequence and alignment of *WOX4* (HF13050) used in this study.

Electronical File E12. Sequence and alignment of *MYB17* (HF15264) used in this study.

Electronical File E13. Sequence and alignment of *MYB52* (HF24488) used in this study. Comparison between the *MYB52* identified by Xu, X. et al. (2022) and the *MYB52* presented in this study.

Electronical File E14. Sequence and alignment of *MYB67* (HF11445) used in this study.

Electronical File E15. Sequence and alignment of *MYB93* (MDP0000320772) used in this study.

Acknowledgements

First of all, I would like to thank Prof. Dr. Thomas Debener and Prof. Dr. Moritz Knoche for their guidance and support throughout my research, which enabled me to complete my dissertation. Their advice on structuring the manuscripts and collaborative projects was invaluable.

I would like to express my gratitude to Yun-Hao Chen, whose participation in this project was crucial to the generation of the data obtained in this project. Without your support, I would not have been able to overcome the major workload phases. Thank you very much!

I would like to thank Bishnu P. Khanal for his helpful comments during my research. In addition, I would like to acknowledge the great work done by Shreya Suvarna and Julia Goldberg during their master's thesis in the lab, which provided me with additional information.

I would like to thank Julia Schröter, Ingrid Robotta, Birigit Milde, and Simon Sitzenstock for their technical support during my research and their help in solving problems that arose in the lab. I am also grateful for the assistance of Klaus Dreier, Franz Hoppe, Alexander Bock, Peter Grimm-Wetzel, Hannah Weiß, and Marcel Pastwa in caring for the plants necessary to conduct the experiments for my research.

It was a pleasure to work closely in the Molecular Plant Breeding group and I would like to thank my colleagues Dietmar F. Schulz, Marcus Linde, Helgard Kaufmann, Marian Uhe, Laurine Patzer, Ina Röhrs, Vinicius Vilperte, Helena Domes, Emma, and Hai Ninh Ho for the pleasant time we spent together. I was also welcomed into the Fruit Science Section and learned a lot from Andreas Winkler during my Ph.D. work.

I am grateful for the opportunity to gain additional knowledge through the WeGa PhD program. In particular, I would like to thank Prof. Dr. Traud Winkelmann for giving me the opportunity to learn about project management and coordination as a representative of the PhD students in this program.

I would like to thank Prof. Dr. Lukas Schreiber and the Department of Ecophysiology (IZMB) for their close cooperation and help with the analytical work.

I would also like to thank my colleagues and friends for their company and support, especially during the difficult times: David Wamhoff, Max Mensen, Marco Herde, Markus Niehaus, Katharina Wellpott, Diana Aria Lopez, Denise, Jelco, Michel, Lara, Daniel, Henno, Pia, Jonathan, Andreas, Kevin, Kira, Raphael, Lena, Rebecca, Oliver and Daniel Ivert, and Elia.

Finally, I would like to express my infinite gratitude to my family for their unwavering support throughout my studies. In particular, it has been a pleasure to spend these years studying and completing my Ph.D. with my brother Henryk.

Curriculum vitae**Personal information**

Name: Jannis Straube

Date of birth: 11.06.1994

Education

03/2018 – present **Ph.D. student at the Institute of Plant Genetics – Section I: Molecular Plant Breeding**
Leibniz University Hannover

- Dissertation: Transcriptomic and functional genomics of russetting on apple

10/2015 – 11/2017 **Master of Science (M. Sc.) – Plant Biotechnology**
Institute of Plant Genetics – Section I: Molecular Plant Breeding,
Leibniz University Hannover

- Thesis: Genetic analysis of *Rdr1* in different rose genomes

10/2012 – 10/2015 **Bachelor of Science (B. Sc.) – Plant Biotechnology**
Institute of Plant Genetics – Section I: Molecular Plant Breeding,
Leibniz University Hannover

- Thesis: Histological and histochemical analysis of the *Rdr1* resistance

2004 – 2012 **University Entrance Qualification (Abitur) KGS Schneverdingen**

Additional activities

10/2020 – present **Representative for the scientific assistants of study commission**
Plant science

09/2018 – 10/2022 **Member of the Ph.D. program “Kompetenznetzwerk**
Wertschöpfungsketten im Gartenbau” (WeGa Ph.D.)

10/2019 – 10/2020 **Representative of the Ph.D. students in the Ph.D. program**
“Kompetenznetzwerk Wertschöpfungsketten im Gartenbau”
(WeGa Ph.D.)

List of publications

Straube, Jannis; Suvarna, Shreya; Chen, Yun-Hao; Khanal, Bishnu P.; Knoche, Moritz; Debener, Thomas (2023): Time course of changes in the transcriptome during russet induction in apple fruit. **BMC Plant Biology** 23 (457), 1-19, doi 10.1186/s12870-023-04483-6

Wellpott, Katharina; **Straube, Jannis**; Winkelmann, Traud; Bündig, Christin (2023): Expression analysis of candidate genes as indicator for commencing drought stress in starch potatoes. **Journal of Agronomy and Crop Science** 00, 1-14, doi: 10.1111/jac.12666

Straube, Henryk; **Straube, Jannis**; Rinne, Jannis; Fischer, Lisa; Niehaus, Markus; Witte, Claus-Peter; Herde, Marco (2022): An inosine triphosphatase safeguards nucleic acids in plants from incorporation of aberrant purine nucleotides. **New Phytologist** 237 (5), 1759-1775, doi: 10.1111/nph.18656

Chen, Yun-Hao; **Straube, Jannis**; Khanal, Bishnu P.; Viktoria; Suresh, Kiran; Schreiber, Lukas; Debener, Thomas; Knoche, Moritz (2022): Apple fruit periderms (russeting) induced by wounding or by moisture have the same histologies, chemistries and gene expressions. **PLOS ONE** 17 (9), e0274733, doi: 10.1371/journal.pone.0274733

Straube, Jannis; Chen, Yun-Hao; Khanal, Bishnu P.; Shumbusho, Alain; Zeisler-Diehl, Viktoria; Suresh, Kiran; Schreiber, Lukas; Knoche, Moritz; Debener, Thomas (2020): Russeting in apple is initiated after exposure to moisture ends: Molecular and biochemical evidence. **Plants** 10 (1), doi: 10.3390/plants10010065

Chen, Yun-Hao; **Straube, Jannis**; Khanal, Bishnu P.; Knoche, Moritz; Debener, Thomas (2020): Russeting in apple is initiated after exposure to moisture ends—I. Histological evidence. **Plants** 9 (10), doi: 10.3390/plants9101293

Khanal, Bishnu P.; Imoro, Yahaya; Chen Yun-Hao; **Straube, Jannis**; Knoche, Moritz (2020): Surface moisture increases microcracking and water vapour permeance of Apple fruit skin. **Plant Biology** 23 (1), 74–82, doi: 10.1111/plb.13178

Menz, Ina; **Straube, Jannis**; Linde, Marcus; Debener, Thomas (2017): The TNL gene *Rdr1* confers broad-spectrum resistance to *Diplocarpon rosae*: *Rdr1* mediated disease resistance in roses. **Molecular Plant Pathology** 19 (5), doi: 10.1111/mpp.12589